# IJBM

*International Journal of*

**BIOMEDICINE**

ISSN 2158-0510

Available online at
www.ijbm.org

# INTERNATIONAL JOURNAL OF BIOMEDICINE

**Aims and Scope:** *International Journal of Biomedicine (IJBM)* publishes peer-reviewed articles on the topics of basic, applied, and translational research on biology and medicine. Original research studies, reviews, hypotheses, editorial commentary, and special reports spanning the spectrum of human and experimental and tissue research will be considered. All research studies involving animals must have been conducted following animal welfare guidelines such as the National Institutes of Health (NIH) Guide for the Care and Use of Laboratory Animals, or equivalent documents. Studies involving human subjects or tissues must adhere to the Declaration of Helsinki and Title 45, US Code of Federal Regulations, Part 46, Protection of Human Subjects, and must have received approval of the appropriate institutional committee charged with oversight of human studies. Informed consent must be obtained.

---

**International Journal of Biomedicine** endorses and behaves in accordance with the codes of conduct and international standards established by the Committee on Publication Ethics (COPE).

**International Journal of Biomedicine** (ISSN 2158-0510) is published four times a year by International Medical Research and Development Corp. (IMRDC), 6308, 12 Avenue, Brooklyn, NY 11219 USA

**Customer Service**: International Journal of Biomedicine, 6308, 12 Avenue, Brooklyn, NY 11219 USA; Tel: 1-917-740-3053; E-mail: editor@ijbm.org



**Manuscript Submission:** Original works will be accepted with the understanding that they are contributed solely to the Journal, are not under review by another publication, and have not previously been published except in abstract form. Accepted manuscripts become the sole property of the Journal and may not be published elsewhere without the consent of the Journal. A form stating that the authors transfer all copyright ownership to the Journal will be sent from the Publisher when the manuscript is accepted; this form must be signed by all authors of the article. All manuscripts must be submitted through the International Journal of Biomedicine`s online submission and review website. Authors who are unable to provide an electronic version or have other circumstances that prevent online submission must contact the Editorial Office prior to submission to discuss alternate options (editor@ijbm.org).

# IJBM

## INTERNATIONAL JOURNAL OF BIOMEDICINE

# SAVE THE DATE

5th Annual

# HEART iN DIABETES


## Live CME Conference

## June 18-20, 2021

## Grand Hyatt • New York City

www.heartindiabetes.com

IJBM

INTERNATIONAL JOURNAL OF BIOMEDICINE

www.ijbm.org

*Volume 11 Issue 1 March 2021*

## CONTENTS

# CONTENTS

CONTINUED

# essfn 2021

**XXIV Congress** of the European Society for Stereotactic and Functional Neurosurgery

## MARSEILLE

## INDIVIDUAL BRAIN PREDICTION

France

PALAIS DU PHARO

www.essfncongress.org

**08>11 September**


mco congrès

GENERAL ORGANISATION :
MCO Congrès - Villa Gaby
285 Corniche JF. Kennedy
13007 Marseille
T.: +33(0)4 95 09 38 00
natalie.ruston@mcocongres.com


PROVENCE | alpes | CÔTE d'AZUR

RÉGION SUD | Marseille | VILLE DE MARSEILLE

# The 66th ANNUAL CONGRESS of INTERNATIONAL COLLEGE of SURGEONS JAPAN SECTION

2021.6.26[SAT]

Venue **KURUME CITY PLAZA**

Chairman **YOSHITO AKAGI**

Department of Surgery, Kurume University School of Medicine

https://www.c-linkage.co.jp/icsj66

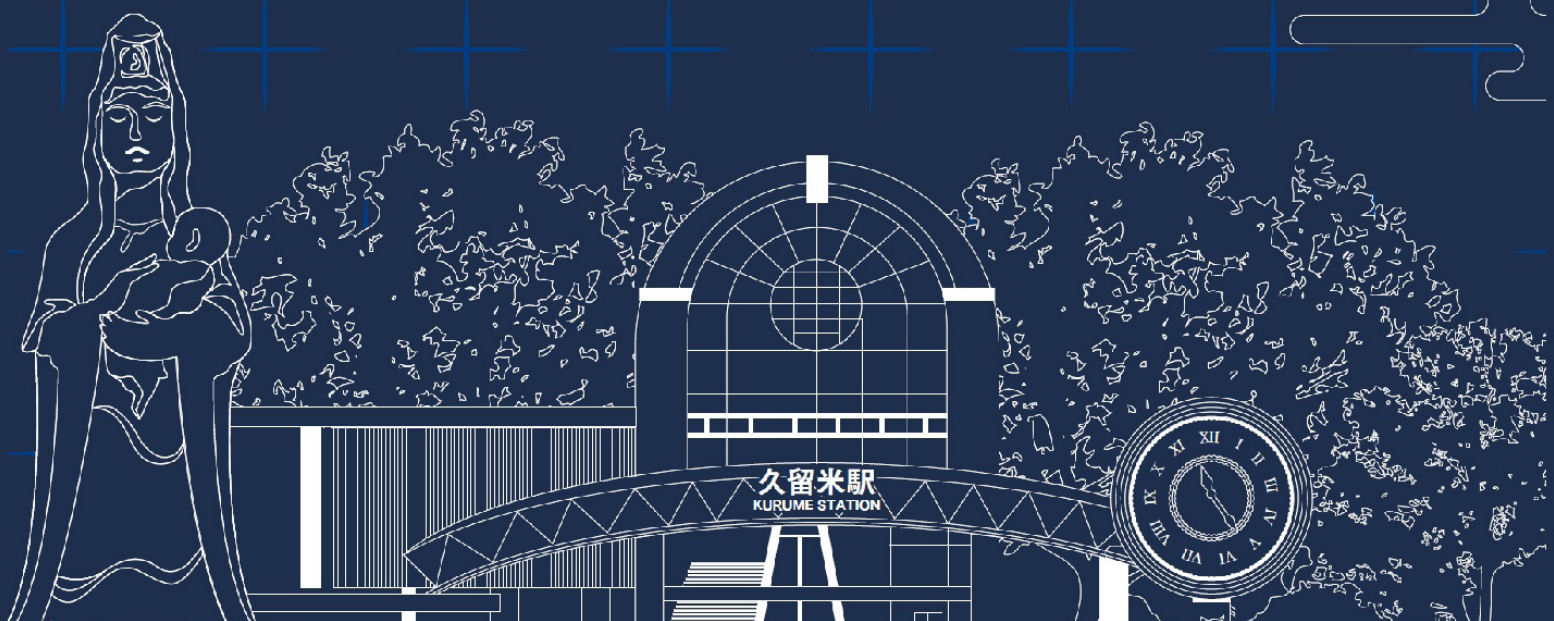

International Journal of Biomedicine 11(1) (2021) 9-13
http://dx.doi.org/10.21103/Article11(1)_OA1

ORIGINAL ARTICLE

Cardiology

INTERNATIONAL JOURNAL OF BIOMEDICINE

# Features of the Functional Status and Cytokine Profile of Patients with Chronic Heart Failure in Combination with Chronic Obstructive Pulmonary Disease

Roman E. Tokmachev, PhD; Andrey Ya. Kravchenko, PhD, ScD; Andrey V. Budnevsky, PhD, ScD; Evgeniy S. Ovsyannikov, PhD, ScD*; Evgeniy V. Tokmachev, PhD; Tatiana A. Chernik

*Voronezh State Medical University named after N.N. Burdenko*
*Voronezh, the Russian Federation*

## Abstract

***The purpose*** of this research was to study the effect of COPD on the functional status and cytokine profile of patients with chronic heart failure (CHF) with different ejection fraction (EF).

***Methods and Results:*** The study involved 240 patients diagnosed with CHF (mean age of 72.4±8.7 years). Among them, 80 patients were diagnosed with CHF and COPD. Depending on the presence of COPD, the patients were divided into two groups: Group 1 included 160 patients with CHF without COPD; Group 2 included CHF 80 patients with COPD. According to the value of LVEF, each of the two groups was divided into two more subgroups: In Group 1, CHFpEF (EF≥50%) was recorded in 69 patients (Subgroup 1) and CHFrFV (EF<50%) in 91 patients (Subgroup 2). In Group 2, CHFpEF was observed in 36 patients (Subgroup 3) and CHFrEF in 44 patients (Subgroup 4). The 6-minute walk distance (6MWD) was measured in meters and compared with the proper 6MWD(i). All patients included in the study underwent the Borg test to assess dyspnea after 6MWT. The serum levels of NT-proBNP, hs-CRP, IL-1β, IL-6, and TNF-α were determined using an automatic analyzer IMMULITE 2000 (Siemens Diagnostics, USA) and quantitative ELISA kits. The patients with CHFpEF had higher levels of hs-CRP, pro-inflammatory cytokines than patients with CHFrEF. The combination of COPD and CHF amplifies systemic inflammation (hs-CRP, proinflammatory cytokines) and myocardial remodeling processes (NT-proBNP) in comparison with the isolated course of CHF. COPD negatively affects the functional status of patients with CHF with different EF by lower values of 6MWD, 6MWD/6MWD(i) ratio, and higher results on the Borg dyspnea test. **International Journal of Biomedicine. 2021;11(1):9-13.**)

**Key Words:** chronic heart failure • ejection fraction • COPD • cytokines

**For citation**: Tokmachev RE, Kravchenko AYa, Budnevsky AV, Ovsyannikov ES, Tokmachev EV, Chernik TA. Features of the Functional Status and Cytokine Profile of Patients with Chronic Heart Failure in Combination with Chronic Obstructive Pulmonary Disease. International Journal of Biomedicine. 2021;11(1):9-13. doi:10.21103/Article11(1)_OA1

## Abbreviations

**6MWT**, the 6-minute walking test; **6MWD**, the 6-minute walk distance; **CHF**, chronic heart failure; **COPD**, chronic obstructive pulmonary disease; **CHFrEF**, CHF with reduced EF, **CHFpEF**, CHF with preserved EF; **EF**, ejection fraction; **hs-CRP**, high-sensitivity C-reactive protein; **HR**, heart rate; **IL**, interleukin; **LVEF**, left ventricular EF; **NT-proBNP**, N-terminal pro-brain natriuretic peptide.

## Introduction

With the increase in life expectancy (both of patients with cardiovascular disease and people in general), chronic heart failure (CHF) is becoming more widespread. CHF decompensation plays a dominant role among the reasons for hospitalization in cardiology departments, especially among patients over 65 years of age.[1] In the USA and European countries, more than 1 million patients are hospitalized annually for CHF. The annual mortality rate of outpatients

with CHF is 7%, and of those hospitalized - 17%.[2] The prognosis for such patients is significantly worsened when CHF is combined with other diseases.[3,4]

Difficulties in diagnosing CHF in patients with COPD, and the choice of tactics and methods of therapy in recent years, determine the increased scientific interest in the study of the cardiorespiratory continuum. It is believed that COPD affects from 25% to 42% of CHF patients.[5-7] The comorbid course of these pathologies is associated with an increased risk of readmission and death.

Respiratory failure is traditionally considered the leading cause of death in COPD patients, but this judgment is valid only for the severe course of the disease. In patients with mild and moderate forms of COPD, patients with cardiovascular disease come first in the structure of mortality. The risk of cardiovascular death in COPD patients is 2-3 times higher than in the population. Thus, Sin et al.[8] found that for every 10% decrease in $FEV_1$, the risk of developing a non-fatal coronary event increases by almost 20%, overall mortality by 14%, and cardiovascular mortality by 28%. According to the TORCH study, the causes of death of COPD patients can be represented as follows: 27% of deaths are due to cardiovascular complications, 35% to respiratory causes, 21% are associated with malignant neoplasms, and 10% for a number of other reasons.[9] In the remaining 7% of cases, the cause of death was not established.

The relationship between the mechanisms of the development of COPD and patients with cardiovascular disease is studied from every angle. The general mechanisms of etiopathogenesis include systemic inflammation, oxidative stress, and endothelial dysfunction.[10-12] The development of systemic inflammation is associated with the release of pro-inflammatory cytokines into the bloodstream, products of lipid peroxidation that induce overproduction of a number of other mediators. Thus, in the development of CHFpEF, a special role is assigned to excessive activation of the sympathetic-adrenal system and the subsequent increase in the synthesis of pro-inflammatory cytokines (TNF-α, IL-1). This, in turn, leads to an increase in the activity of nitric oxide synthases and production of NO in tissues, which has negative effects on the cardiovascular system (apoptosis and fibrosis of cardiomyocytes, direct toxic effect on the myocardium). In this regard, identifying three categories of patients with HF (with preserved, borderline and reduced LVEF) is of particular relevance to study the effect of systemic inflammation on the clinical course, functional status and prognosis of patients with comorbid COPD and CHF with different LVEF. Thus, the high comorbidity of CHF and COPD and the increased risk of unfavorable outcomes in this combination of pathologies suggest further study of the mechanisms of CHF progression, and improvement of diagnostic methods and treatment principles for this category of patients.

The purpose of this research was to study the effect of COPD on the functional status and cytokine profile of patients with CHF with different EF.

## Materials and Methods

The study involved 240 patients diagnosed with CHF (134 men and 106 women, mean age of 72.4±8.7 years), included in the regional register of CHF patients in the Voronezh region. Among them, 80 patients (48[60%] men and 32[40%] women) aged between 40 and 80 years were diagnosed with CHF and COPD (GOLD 2, group D) without exacerbation. Depending on the presence of COPD, the patients were divided into two groups: Group 1 included 160 patients with CHF who had no signs of COPD; Group 2 included 80 patients with a comorbid course of CHF and COPD. All patients with COPD corresponded to the "phenotype with frequent exacerbations" (2 or more per year) and required antibiotic therapy and/or glucocorticosteroids. The diagnosis of COPD was made on the basis of an integral assessment of symptoms, history, objective status, and spirometry data, according to GOLD, revision 2019. According to the value of LVEF, each of the two groups was divided into two more subgroups: In Group 1, CHFpEF (EF≥50%) was recorded in 69 patients (Subgroup 1) and CHFrFV (EF<50%) in 91 patients (Subgroup 2). In Group 2, CHFpEF was observed in 36 patients (Subgroup 3) and CHFrEF in 44 patients (Subgroup 4). The diagnosis of CHF was established according to 2016 ESC Guidelines for the diagnosis and treatment of acute and chronic heart failure. The functional class (FC) of CHF was determined according to the NYHA classification (1994), based on the results of the 6MWT.

The non-inclusion criteria for Groups 1 and 2 were the presence of chronic kidney disease (3b stages and higher), diabetes mellitus or taking hypoglycemic drugs, permanent atrial fibrillation, anemia, diseases of musculoskeletal system (coxarthrosis, gonarthrosis, etc., reducing motor activity), obesity (2-3 classes) and other severe somatic pathologies.

From the moment of inclusion in the study, patients were examined weekly by researchers—a cardiologist and a pulmonologist—to make sure there were no symptoms of CHF decompensation and exacerbation of COPD. After 12 weeks, the study participants underwent a standard examination, which included clinical, laboratory and instrumental methods. Exercise tolerance was determined using a complex of cardiorespiratory analysis and register of patients with CHF [13,14]) and 6MWT.

The 6MWD was measured in meters and compared with the proper 6MWD(i). The 6MWD(i) value was calculated using the formulas below, which take into account age and BMI. The formula for calculating 6MWD(i) for men: 6MWD(i)=1140-5.61×BMI-6.94×age. The 6MWD (i) value for women was defined as: 6MWD(i)=(1017-6.24×BMI-5.83×age.[1]

The serum levels of NT-proBNP, hs-CRP, IL-1β, IL-6, and TNF-α were determined using an automatic analyzer IMMULITE 2000 (Siemens Diagnostics, USA) and quantitative ELISA kits: NT-proBNP - using the Biomedica human NT-proBNP Sandwich ELISA kit (Austria), hs-CRP - using the SRB-IFA-BEST highly sensitive kit (Vector-Best, Russia), IL-1β using the Interleukin-1 beta - ELISA-BEST kit (Vector-Best, Russia), IL-6 using the Interleukin-6- ELISA-BEST kit (Vector-Best, Russia), and TNF-α using the alpha-TNF-ELISA-BEST (Vector-Best, Russia). Comprehensive two-dimensional and Doppler echocardiography were performed using an EPIQ5 ultrasound system (Phillips, USA) equipped with S5-1 Pure-Wave Cardiac Transducer. All patients included in the study underwent the Borg test to assess dyspnea after 6MWT.

All patients received treatment according to the standards for the treatment of CHF and COPD.

The study was approved by the Ethics Committee of Voronezh State Medical University named after N.N. Burdenko. Written informed consent was obtained from each patient.

All data was evaluated with STATGRAPHICS Plus 5.1. Baseline characteristics were summarized as frequencies and percentages for categorical variables and as mean±SD, median (Me) and interquartile range (IQR; 25th to 75th percentiles) for continuous variables. Student's unpaired t-test was used to compare two groups for data with normal distribution. Mann-Whitney U test was used to compare means of 2 groups of variables not normally distributed. A probability value of $P<0.05$ was considered statistically significant.

## Results

The median NT-proBNP value in Subgroup 2 was 1804(608-4908) ng/L, which significantly exceeded its value in Subgroup 1 - 980(301;2677) ng/L ($P<0.001$). The median NT-proBNP level in Subgroup 4 was 2046(1103;2806) ng/L, which also exceeded its value in Subgroup 3 - 1280(601;3150) ng/L ($P<0.001$) (Fig. 1). This result allows us to conclude that the NT-proBNP biomarker does not lose its sensitivity in the case of a combined course of COPD and CHF.

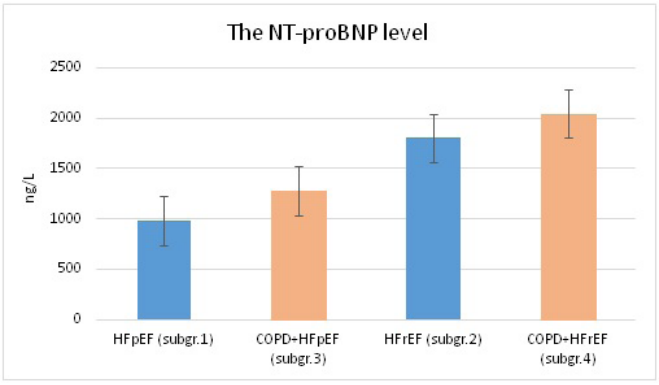


***Fig. 1.*** *The NT-proBNP level in the study subgroups.*

It was also noted that in patients of Group 2 who had a combination of COPD and CHF, the NT-proBNP level, equal to 1593(601;3150) ng/L, was higher than in Group 1 patients with isolated CHF - 1064(301;4908) ng/L ($P=0.049$).

The level of hs-CRP, known as a biomarker of endogenous inflammatory processes, in patients with CHFpEF was 3.4(1.2; 8.1) mg/L, while in patients with CHFrEF it was statistically significantly lower - 2.9(1.6;5.4) mg/l ($P<0.001$). The level of hs-CRP in Subgroup 4 was 4.1(2.3;15.6) mg/L, which was also lower than in patients of Subgroup 3 - 4.8(1.9;13.5) ng/L ($P<0.001$). The hs-CRP levels obtained in the study in isolated cardiac pathology in patients with various NYHA FC indicate an increase comparable to that in patients with FCII (3.2[1.2;7.1] mg/l), a more pronounced FCIII (3.3[1.4;7.8] mg/l) and severe FCIV (3.5[1.8;8.1] mg/l) ($P=0.06$) (Fig. 2).

We found an increase in the level of pro-inflammatory cytokines in all studied subgroups (Table 1). At the same time, the content of IL-1β, IL-6, and TNF-α was significantly higher in Group 2.

A higher level of IL-1β, IL-6, and TNF-α, hs-CRP (Table 1) in Subgroups 1 and 3 compared with Subgroups 2 and 4 reflects how important the contribution of systemic inflammation is to the development and progression of heart failure. At the same time, a higher level of pro-inflammatory cytokines was observed in Group 2 than in Group 1, which demonstrates a close pathogenetic relationship between the two pathologies.

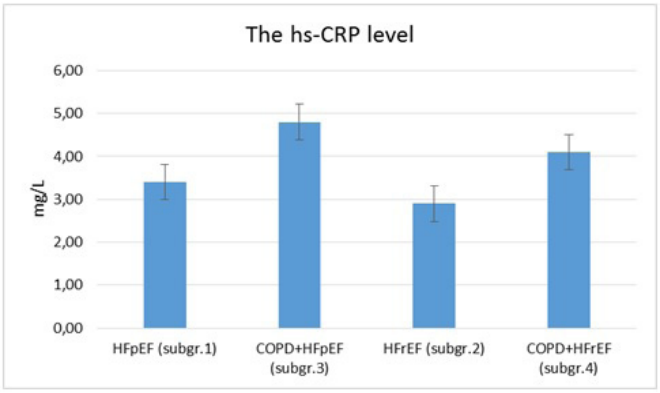


***Fig. 2.*** *The Hs-CRP level in the study subgroups.*

***Table 1.***

***Cytokine profile in study subgroups***

| Subgroup | IL-1β | *P*-value | IL-6 | *P*-value | TNF-α | P-value |
|---|---|---|---|---|---|---|
| 1 | 121.9±25.4 | 0.03 | 298.2±35.8 | 0.006 | 163.4± 27.2 | 0.04 |
| 2 | 103.1± 21.0 | | 186.5± 29.6 | | 143.0± 24.9 | |
| 3 | 139.3± 26.1* | 0.04 | 408.3± 61.3* | 0.005 | 256.8± 33.7* | 0.02 |
| 4 | 122.1± 24.8^ | | 312.7 ± 41.1^ | | 198.4± 28.1^ | |

** - P<0.05 between Subgroups 1 and 3; ^- P<0.01 between Subgroups 2 and 4.*

The 6MWD level (Table 2) in patients with comorbid COPD and CHF, regardless of EF, was less than in CHF without COPD ($P<0.05$ in both cases). This fact can be explained by a combination of obstructive and restrictive breathing disorders.

Assessment of the 6MWD/6MWD(i) ratio showed that in Group 2, the average value of this indicator was significantly less than in Group 1, regardless of EF ($P<0.05$ in both cases). In previous studies, we found that in patients with COPD, a decrease in physical activity was apparently associated not only with lung dysfunction at rest, but also depends on a number of other factors. Thus, in COPD patients, a decrease in lean body mass is often observed, which is a

consequence of systemic inflammation and muscle atrophy due to low physical activity. In turn, this study showed that the comorbid course of CHF and COPD is accompanied by a higher activity of pro-inflammatory cytokines than with isolated CHF. Therefore, it can be assumed that one of the components that reduce exercise tolerance in such patients is the activation of systemic subclinical inflammation, leading, among other things, to a decrease in lean body mass.

The values of heart rate both before and immediately after performing 6MWT in patients in the study groups did not differ significantly. At the same time, in the process of performing 6MWT, the device did not record any excess of the submaximal values of this parameter in any of the subjects.

Before the start of the test, the studied subgroups did not differ in the level of $SpO_2$. However, this parameter was significantly lower in patients with CHF and COPD immediately after 6MWT, regardless of EF (Table 2). In turn, in patients in Subgroups 3 and 4 (CHF patients with COPD), higher scores on the Borg test, reflecting the degree of dyspnea after 6MWT, compared with Subgroups 1 and 2 (CHF patients without COPD), indicate a lower tolerance to physical activity (Table 2).

***Table 2.***

***Comparative characteristics of 6MWT parameters, dynamic pulse oximetry in patients in the studied subgroups***

| Indicator | Subgr. 1 | Subgr. 3 | $P_{1-3}$ | Subgr. 2 | Subgr. 4 | $P_{2-4}$ |
|---|---|---|---|---|---|---|
| 6MWD, m | 301.5 ±153.5 | 264.6 ±120.6 | 0.04 | 251.5 ±183.5 | 202.4 ±130.2 | 0.03 |
| 6MWD(i), % | 53.0 ±29.2 | 47.2 ±25.6 | 0.01 | 48.1 ±30.5 | 42.8 ±22.4 | 0.02 |
| HR before test, bpm | 76.1 ±15.2 | 77.8 ±17.3 | 0.18 | 86.1 ±15.2 | 87.8 ±17.3 | 0.16 |
| HR after test, bpm | 102.4 ±17.5 | 107.3 ±18.8 | 0.15 | 109.4 ±17.2 | 115.1 ±14.8 | 0.15 |
| SpO2 before test, % | 97.9 ±2.0 | 97.5 ±2.1 | 0.12 | 95.2 ±2.4 | 94.9 ±2.6 | 0.26 |
| SpO2 after test, % | 95.5 ±3.0 | 93.3 ±3.1 | 0.001 | 94.1 ±3.3 | 91.2 ±2.5 | 0.001 |
| Borg test, points | 2.41 ±0.17 | 3.22 ±0.29 | 0.01 | 3.83 ±0.32 | 5.19 ±0.37 | 0.001 |

## Conclusion

The patients with CHFpEF have higher levels of hs-CRP, pro-inflammatory cytokines than patients with CHFrEF. This reflects more pronounced subclinical inflammation. The combination of COPD and CHF amplifies systemic inflammation(hs-CRP, proinflammatory cytokines) and myocardial remodeling processes (NT-proBNP) in comparison with the isolated course of CHF. COPD negatively affects the functional status of patients with CHF with different EF by lower values of 6MWD, 6MWD/6MWD(i) ratio, and higher results on the Borg dyspnea test.

## Sources of Funding

The reported study was supported by the Russian Federation President Council on Grants (Grant No. MK-1776.2020.7).

## Competing Interests

The authors declare that they have no competing interests.

## References

1. Roger VL, Go AS, Lloyd-Jones DM, Benjamin EJ, Berry JD, Borden WB, Bravata DM, Dai S, Ford ES, Fox CS, Fullerton HJ, Gillespie C, Hailpern SM, Heit JA, Howard VJ, Kissela BM, Kittner SJ, Lackland DT, Lichtman JH, Lisabeth LD, Makuc DM, Marcus GM, Marelli A, Matchar DB, Moy CS, Mozaffarian D, Mussolino ME, Nichol G, Paynter NP, Soliman EZ, Sorlie PD, Sotoodehnia N, Turan TN, Virani SS, Wong ND, Woo D, Turner MB; American Heart Association Statistics Committee and Stroke Statistics Subcommittee. Executive summary: heart disease and stroke statistics--2012 update: a report from the American Heart Association. Circulation. 2012 Jan 3;125(1):188-97. doi: 10.1161/CIR.0b013e3182456d46. Erratum in: Circulation. 2012 Jun 5;125(22):e1001.

2. Maggioni AP, Dahlström U, Filippatos G, Chioncel O, Crespo Leiro M, Drozdz J, Fruhwald F, Gullestad L, Logeart D, Fabbri G, Urso R, Metra M, Parissis J, Persson H, Ponikowski P, Rauchhaus M, Voors AA, Nielsen OW, Zannad F, Tavazzi L; Heart Failure Association of the European Society of Cardiology (HFA). EURObservational Research Programme: regional differences and 1-year follow-up results of the Heart Failure Pilot Survey (ESC-HF Pilot). Eur J Heart Fail. 2013 Jul;15(7):808-17. doi: 10.1093/eurjhf/hft050.3.

3. Budnevsky AV, Malysh EY. [Clinico-Pathogenetic Relationship of Cardiovascular Diseases and Chronic Obstructive Pulmonary Disease]. Kardiologiia. 2017 Apr;57(4):89-93. [Article in Russian].

4. Drobysheva ES, Tokmachev RE, Budnevsky AV, Kravchenko AYa. [Predictive value of biomarkers of heart cachexia in chronic heart failure]. Kardiovaskulyarnaya Terapiya i Profilaktika. 2016; 15(4):80-83. [Article in Russian].

5. Flu WJ, van Gestel YR, van Kuijk JP, Hoeks SE, Kuiper R, Verhagen HJ, Bax JJ, Sin DD, Poldermans D. Co-existence of COPD and left ventricular dysfunction in vascular surgery patients. Respir Med. 2010 May;104(5):690-6. doi: 10.1016/j.rmed.2009.11.013.

6. Cazzola M, Bettoncelli G, Sessa E, Cricelli C, Biscione G. Prevalence of comorbidities in patients with chronic obstructive pulmonary disease. Respiration. 2010;80(2):112-9. doi: 10.1159/000281880.

7. Hawkins NM, Wang D, Petrie MC, Pfeffer MA, Swedberg K, Granger CB, Yusuf S, Solomon SD, Ostergren J, Michelson EL, Pocock SJ, Maggioni AP, McMurray JJ; CHARM Investigators and Committees. Baseline characteristics

***Corresponding author**: Evgeniy S. Ovsyannikov, PhD, ScD. Department of faculty therapy, Voronezh State Medical University named after N.N. Burdenko. Voronezh, Russia. E-mail: ovses@yandex.ru*

and outcomes of patients with heart failure receiving bronchodilators in the CHARM programme. Eur J Heart Fail. 2010 Jun;12(6):557-65. doi: 10.1093/eurjhf/hfq040.
8. Sin DD, Man SF. Chronic obstructive pulmonary disease as a risk factor for cardiovascular morbidity and mortality. Proc Am Thorac Soc. 2005;2(1):8-11. doi: 10.1513/pats.200404-032MS.
9. McGarvey LP, John M, Anderson JA, Zvarich M, Wise RA; TORCH Clinical Endpoint Committee. Ascertainment of cause-specific mortality in COPD: operations of the TORCH Clinical Endpoint Committee. Thorax. 2007 May;62(5):411-5. doi: 10.1136/thx.2006.072348.
10. Budnevsky AV, Ovsyannikov ES, Labzhania NB. [Chronic obstructive pulmonary disease concurrent with metabolic syndrome: Pathophysiological and clinical features]. Ter Arkh. 2017;89(1):123-127. doi: 10.17116/terarkh2017891123-127. [Article in Russian].
11. Tokmachev RE, Kravchenko AYa, Budnevsky AV, et al. [Activation of pro-inflammatory cytokines in patients with chronic heart failure comorbid with metabolic syndrome]. Kardiovaskulyarnaya Terapiya i Profilaktika. 2015;14(2):116-117. [Article in Russian].
12. Budnevsky AV, Shurupova AD, Kravchenko AY, Tokmachev RE. [Clinical efficacy of acute respiratory viral infections prevention in patients with chronic heart failure]. Ter Arkh. 2019 Mar 30;91(3):36-41. doi: 10.26442/00403660.2019.03.000111. [Article in Russian].
13. Tokmachev RE, Maksimov AV, Budnevsky AV. Device for cardiorespiratory analysis and method for assessing cardiorespiratory state. Invention patent RU 2637917 C, 07.12.2017. Application No. 2016148274. [In Russian].
14. Budnevsky AV, Pronin SS, Kontsevaya AV. Register of patients with chronic heart failure. Certificate of registration of the computer program RU 2019667733, 26.12.2019. Application No.2019666660. [In Russian].

International Journal of Biomedicine 11(1) (2021) 14-17
http://dx.doi.org/10.21103/Article11(1)_OA2

ORIGINAL ARTICLE

Radiology

INTERNATIONAL JOURNAL OF BIOMEDICINE

# Iatrogenic Injuries During Puncture Procedures Applied To Breast

Tamara V. Pavlova, MD, PhD[1,2]; Aleksandr Yu. Vasilyev, MD, PhD, ScD[1,3*]

[1]*Central Research Institute of Radiation Diagnostics*
[2]*City Clinical Hospital named after V. M. Buyanov*
[3]*Moscow State University of Medicine and Dentistry named after A. I. Evdokimov*
*Moscow, Russia*

## Abstract

***Background:*** This article analyzes iatrogenic injuries of the breast that happen during puncture procedures.

***Methods and Results***: We have analyzed the data of 2075 invasive diagnostic procedures related to both benign and malignant breast neoplasms, conducted in various healthcare facilities in the Russian Federation. There were 1943(93.6%) cases of ultrasound-guided biopsies in our study. RG-guided biopsies were rather less frequent—132(6.4%) cases. A subcutaneous hematoma is the primary iatrogenic injury that occurs during breast puncture procedures conducted in Russian healthcare facilities. This is the most common complication during an ultrasound-guided CB (44.4%). The likelihood that this complication will occur is impossible to predict.

***Conclusion*:** The proper arrangements and patient follow-up before and after the biopsy, along with the selection of a proper invasive procedure for a pathologic neoplasm, will minimize the number of diagnostic iatrogenic injuries and improve the quality of medical care. (**International Journal of Biomedicine. 2021;11(1):14-17.**)

**Key Words:** breast cancer • fine-needle biopsy • core-biopsy • iatrogeny

**For citation**: Pavlova TV, Vasilyev AYu. Iatrogenic Injuries During Puncture Procedures Applied To Breast. International Journal of Biomedicine. 2021;11(1):14-17. doi:10.21103/Article11(1)_OA2

## Abbreviations

**FNB**, fine-needle biopsy; **CB**, core-biopsy; **US**, ultrasound; **BC**, breast cancer

## Introduction

An early diagnosis and effective treatment of breast cancer (BC) are still the key priorities for public healthcare systems in many countries.[1] As BC screening programs have been significantly improved, now the specialists are able to identify the malignant tumors in this area at early stages more often.[2,3] It is worth mentioning that most of the detected pathologic changes in the breast are benign; malignant tumors account only for 3%–6% of all cases.[4]

The X-ray picture for breast neoplasms is quite variable, which is why any "suspicious" finding, detected by a physical examination, mammography or an ultrasound scan must be confirmed.[5] A pathomorphological study is the most accurate way to determine the nature of a pathologic area. The methodology for breast biopsy has been dramatically changed in recent decades. The methods have become more injurious, from fine-needle aspiration biopsy to a vacuum suction type.[6] Regardless of the way biomaterial is obtained, the interventional methods used the for breast may result in such complications as hematomas, Mondor's disease, and acute suppurative mastitis.[7] L.L.Y. Lin et al.[8] state that the total amount of complications after breast biopsy does not exceed 6.7%. The most frequent complications are bleedings or hematomas (89.3%); breast ache is less frequent (6.9%), and dizziness is rare (0.9%). A team of scientists supervised by Bick stated that apart from the primary complication, which is a hematoma, in 2%-10% of cases, there may appear the following iatrogenic injuries: infection at a biopsy site

[*]***Corresponding author:*** *Prof. Alexander Yu. Vasilyev, MD, PhD, ScD. Department of Radiology, Moscow State University of Medicine and Dentistry named after A. I. Evdokimov, Moscow, Russia. E-mail: auv62@mail.ru*

(4%-6%) and abscesses (2%); the recurrent biopsies are taken as a separate category (4%).[9] Some scientists suppose that a biopsy may increase the risks of a metastatic spread and influence long-term treatment results.[10]

All the above-mentioned confirm that it is crucial to study the nature of diagnostic iatrogenic injuries that appear during breast puncture procedures. This study will facilitate further prevention and elimination of such injuries.

## Materials and Methods

We have analyzed the data of 2075 invasive diagnostic procedures related to both benign and malignant breast neoplasms, conducted in various healthcare facilities in the Russian Federation. As for 1784(86.1%) identified breast pathologies, the biopsies were conducted for medical reasons only (typical semeiotic signs), and in 288(13.9%) cases female patients were worried and insisted on having a biopsy. In most cases, the patients insisted on having one when the benignant neoplasms under 1.5cm (a fibroadenoma or a cyst) were detected for the first time in their lives. During most physical examinations (75.6%), pathologies of breast and regional lymph nodes were detected manually. In our data, there were 503(24.4%) non-palpable breast neoplasms. Preliminary statements, depending on the results of breast radial examination, conducted before biopsy, are presented in Table 1.

***Table 1.***

***Classification of preliminary statements, depending on the results of a radial examination, conducted before a biopsy (n=2075)***

| Pathology | Abs. | % |
|---|---|---|
| A suspected breast cancer | 348 | 16.8 |
| A cyst (including an inflammatory cyst) | 902 | 43.4 |
| A fibroadenoma (including a leaf-like fibroadenoma) | 425 | 20.5 |
| Fibrocyatic breast changes | 49 | 2.4 |
| Clustered microcalcifications | 102 | 4.9 |
| Lymphoadenopathy (regional lymph nodes) | 199 | 9.6 |
| Other | 50 | 2.4 |

*"Other" included hematomas, oleogranulomas, fibrolipomas, local fibrosis areas, and tissue architectonic damages.*

There were 1943(93.6%) cases of ultrasound-guided biopsies in our study. G-guided biopsies were rather less frequent—132(6.4%) cases. The data for the biomaterial sampling method are the following: 1471(70.9%) pathologic findings were confirmed by a fine-needle aspiration biopsy, 604(29.1%) cases were confirmed by a needle pistol system that was used to take tissue samples to conduct a histologic or an IHC test, if necessary. These tests can provide more diagnostic data about a pathologic area. The classification of performed puncture procedures, depending on biomaterial sampling and guidance methods, is shown in Fig. 1. Thus, the ultrasound-guided FNB was the most common method of sampling diagnostic material. It was performed in 1455(70.1%) cases. For 488(23.5%) cases, an ultrasound-guided CB was chosen. There were 116(5.6%) stereotaxic CBs, and 16(0.8%) female patients had to undergo an RG-guided procedure.

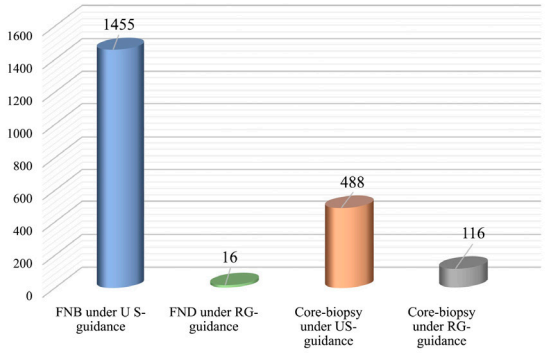


***Fig. 1.*** *Classification of performed puncture procedures, depending on biomaterial sampling and guidance methods.*

FNB was performed by a "free-hand method" using a standard skewed-ended injection needle with a diameter of 20G, which was connected to a 20 ml syringe. The specialists used to an automatic needle pistol and needles of a guillotine type with a diameter of 14G to perform a CB. The needle's length varied from 10 cm to 16 cm, depending on the location of a pathologic area.

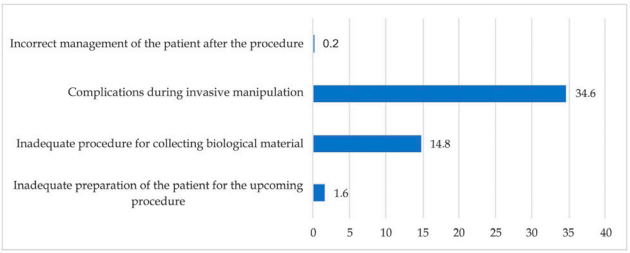


***Fig. 2.*** *Classification of faults in medical care provided by radiologists during interventional radiology procedures.*

## Results and Discussion

Fig. 2 presents the main faults in medical care provided by radiologists during interventional radiology procedures.

Improper preparation of patients for a biopsy

We were unable to analyze the preparations for all 2075 punctures because 852 procedures had been conducted in other institutions. We have analyzed the data of 1223 puncture biopsies and concluded that patient preparation errors account for 1.6% of all cases. Seven patients experienced allergic reactions during CB due to local anesthesia: 5 had hives, and 2 had bronchial spasms. Twelve patients fainted because their blood sugar level was low (they were hungry and stressed).

Improper patient follow-up after the procedure

Three (0.2%) patients had complications after an invasive procedure. Two of them had inflammation at the site where the

biopsy had been taken, and 1 had a chemical skin burn (Fig.3) because the doctor had given her improper instructions regarding the antiseptic treatment of a biopsy needle induction site.

***Fig. 3.*** *A female patient's appearance a week after the core biopsy of a neoplasm in the left breast: in the plane where a biopsy needle has been introduced, there is a chemical skin burn, due to iodine solution overuse during wound handling.*

Improper biomaterial sampling

A total of 902(61.3%) FNBs were conducted because cysts had formed and the diagnostic material had been obtained properly. Although the information value of FNB is not very high in terms of tissue neoplasms, in the rest of the cases (569 [38.7%]) this biopsy type was used to confirm a significant pathologic area. The conclusion drawn from 274(482%) cytologic statements was that the obtained material was not informative and that additional invasive procedures were required. As for CBs, 34 out of 604 procedures (5.6%) were not informative. The tissue "strips" obtained during this invasive procedure had no diagnostic value, so the procedure had to be repeated. Thus, the total amount of cases in which the initial diagnostic material was not informative grew to 308(14.8 %).

Invasive procedure complications

Hematomas were the primary complications during invasive diagnostic procedures. They appeared in different time periods after the procedure was conducted (Fig.4). In this study, there were 718(34.6%) cases with such complications. Table 2 presents the classification of complications, depending on the employed visual control and diagnostic material sampling methods. Thus, subcutaneous hematomas were the most common complications for an ultrasound-guided biopsy (44.4%). As for an RG-FNB, such complications had the lowest frequency.

***Table 2.***

***Classification of hematomas, detected after breast biopsy, depending on material sampling and guidance methods (n=718)***

| Biopsy type | Abs. | % |
|---|---|---|
| An ultrasound-guided FNB | 293 | 40.8 |
| A RG-guided FNB | 5 | 0.7 |
| An ultrasound-guided CB | 319 | 44.4 |
| A RG-guided CB | 101 | 14.1 |
| Total | 718 | 100.0 |

## Conclusion

A subcutaneous hematoma is the primary iatrogenic injury that occurs during breast puncture procedures conducted in Russian healthcare facilities. This is the most common complication during an ultrasound-guided CB (44.4%). The likelihood that this complication will occur is impossible to predict. However, proper arrangements and patient follow-up before and after the biopsy, along with the selection of a proper invasive procedure for a pathologic neoplasm, will minimize the number of diagnostic iatrogenic injuries and improve the quality of medical care.

***Fig. 4.*** *The appearance of a female patient, who had hematomas after a core biopsy: a) 8 days after an ultrasound–guided CB of a neoplasm in the left breast: at the border of upper quadrants, there is a subcutaneous hematoma; b) 12 days after a RG-guided CB of clustered calcifications in the right breast, there is a spread subcutaneous hematoma, which occupies most of the gland.*

## Competing Interests

The authors declare that they have no competing interests.

## References

1. Bray F, Ferlay J, Soerjomataram I, Siegel RL, Torre LA, Jemal A. Global cancer statistics 2018: GLOBOCAN estimates of incidence and mortality worldwide for 36 cancers in 185 countries. CA Cancer J Clin. 2018 Nov;68(6):394-424. doi: 10.3322/caac.21492.
2. Rana C, Ramakant P, Babu S, Singh K, Mishra A, Mouli S. Unusual Breast Neoplasm with Diagnostic and Management Challenges. Indian J Surg Oncol. 2018 Sep;9(3):328-335. doi: 10.1007/s13193-018-0781-3.
3. Yaffe MJ, Mittmann N, Alagoz O, Trentham-Dietz A, Tosteson AN, Stout NK. The effect of mammography screening regimen on incidence-based breast cancer mortality. J Med Screen. 2018 Dec;25(4):197-204. doi: 10.1177/0969141318780152.
4. Stachs A, Stubert J, Reimer T, Hartmann S. Benign Breast Disease in Women. Dtsch Arztebl Int. 2019 Aug 9;116(33-34):565-574. doi: 10.3238/arztebl.2019.0565.
5. Salzman B, Collins E, Hersh L. Common Breast Problems. Am Fam Physician. 2019 Apr 15;99(8):505-514. PMID: 30990294.
6. Bennett IC, Saboo A. The Evolving Role of Vacuum Assisted Biopsy of the Breast: A Progression from Fine-Needle Aspiration Biopsy. World J Surg. 2019 Apr;43(4):1054-1061. doi: 10.1007/s00268-018-04892-x.
7. Suganthan N, Ratnasamy V. Mondor's disease - a rare cause of chest pain: a case report. J Med Case Rep. 2018 Jan 9;12(1):4. doi: 10.1186/s13256-017-1530-x.
8. Lin LLY, Gao Y, Lewin AA, Toth HK, Heller SL, Moy L. Overstated Harms of Breast Cancer Screening? A Large Outcomes Analysis of Complications Associated With 9-Gauge Stereotactic Vacuum-Assisted Breast Biopsy. AJR Am J Roentgenol. 2019 Apr;212(4):925-932. doi: 10.2214/AJR.18.20421.
9. Bick U, Trimboli RM, Athanasiou A, Balleyguier C, Baltzer PAT, Bernathova M, et al.; European Society of Breast Imaging (EUSOBI), with language review by Europa Donna–The European Breast Cancer Coalition. Image-guided breast biopsy and localisation: recommendations for information to women and referring physicians by the European Society of Breast Imaging. Insights Imaging. 2020 Feb 5;11(1):12. doi: 10.1186/s13244-019-0803-x.
10. Kong YC, Bhoo-Pathy N, O'Rorke M, Subramaniam S, Bhoo-Pathy NT, See MH, Jamaris S, Teoh KH, Bustam AZ, Looi LM, Taib NA, Yip CH. The association between methods of biopsy and survival following breast cancer: A hospital registry based cohort study. Medicine (Baltimore). 2020 Feb;99(6):e19093. doi: 10.1097/MD.0000000000019093.

International Journal of Biomedicine 11(1) (2021) 18-23
http://dx.doi.org/10.21103/Article11(1)_OA3

ORIGINAL ARTICLE

Radiology

INTERNATIONAL JOURNAL OF BIOMEDICINE

# Detection of Midline Shift from CT Scans to Predict Outcome in Patients with Head Injuries

Ikhlas Abdelaziz, PhD[1, 2]; Rowa Aljondi, PhD[1]; Ali B Alhailiy, PhD[3]; Mustafa Z. Mahmoud, PhD[3*]

[1]*Department of Medical Imaging and Radiation Sciences, College of Applied Medical Sciences, University of Jeddah, Jeddah, Saudi Arabia*
[2]*Diagnostic Radiology Department, College of Medical Radiological Science, Sudan University of Science and Technology, Khartoum, Sudan*
[3]*Radiology and Medical Imaging Department, College of Applied Medical Sciences, Prince Sattam bin Abdulaziz University, Al-Kharj, Saudi Arabia*

## Abstract

***Background***: The present study aimed to detect the degree of midline shift from CT scans and the clinical status of the patient, to evaluate the relationship between the degree of midline shift found by the CT scan and Glasgow Coma Scale (GCS) score as a predictor of clinical outcome in head injury patients. Furthermore, we aimed to assess the relationship between midline shift and age, sex, and causes.

***Methods and Results***: The study included 50 subjects (36 males and 14 females). The age range of the patients in this study was 18–95 years old (mean age of 48.34±17.02 years). The inclusion criteria were patients with traumatic brain injury (TBI) or patients evaluated for level of consciousness by a neurosurgeon. Toshiba 16 Slice CT Scanner (Toshiba Medical Systems, Nasu, Japan 2003) was used to scan all patients in the supine, head first position. Contiguous 2 mm slices were obtained using the Toshiba 16-slice machine spiral technique (pitch 1.25–1.5, 0.75 s rotation time, 120 KvP, 2 mm reconstruction interval).

The results indicated that the degree of midline shift in patients with brain injuries was statistically significant as a determinant of clinical outcome. It appeared that the probability of poor clinical outcome was higher when there was a combination of midline shift and other types of intracranial hemorrhage, clinical factors, such as sex, age, and GCS score, and associated injuries. The worst outcome was seen in patients with midline shift and subdural hematoma, when compared with other lesions in patients with brain injuries.

***Conclusion***: This study suggests that the degree of midline shift may be predictive of clinical outcome in patients with head injuries.(**International Journal of Biomedicine. 2021;11(1):18-23.**)

**Key Words**: brain midline shift • Glasgow Coma Scale • intracerebral hemorrhage • intracranial pressure • subdural hematoma

**For citation**: Abdelaziz I, Aljondi R, Alhailiy AB, Mahmoud MZ. Detection of Midline Shift from CT Scans to Predict Outcome in Patients with Head Injuries. International Journal of Biomedicine. 2021;11(1):18-23. doi:10.21103/Article11(1)_OA3

## Abbreviations

**CT**, computed tomography; **TBI**, traumatic brain injury; **GCS**, Glasgow Coma Scale; **SDH**, subdural hematoma; **EDH**, epidural hematoma; **ICH**, intracerebral hemorrhage; **H-MLS**, hemorrhage and midline deformation; **dML**, deformed midline; **iML**, ideal midline; **ICH,** intracerebral hematoma; **DAI**, diffuse axonal injury.

## Introduction

Computed tomography (CT) scans are widely used for neurological diagnosis. CT scans of the brain are useful in tracing midline shift in traumatic brain injury and intracranial pathology. In intracranial pathological examination, brain midline shift is an important diagnostic feature to evaluate the severity of brain compression due to various pathologies.[1,2] Despite the functional difference of the brain hemispheres, the normal anatomic structure of the brain is symmetric and called

the midsagittal plane, which is shown in a single CT slice as the brain midline.[3] Intracranial pathological changes, such as hemorrhage or tumor (Figures 1-3), may cause midline shift.[1,3]

***Fig. 1.*** *A 59-year-old male. SDH with midline shift of 9.9 mm, right-sided weakness, GCS score of 14.*

***Fig. 2.*** *A 36-year-old male. EDH with midline shift of 3.2 mm, GCS score of 10.*

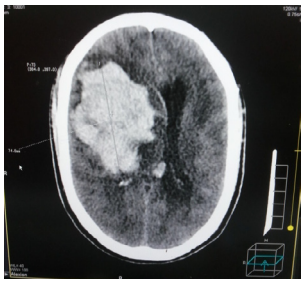

***Fig. 3.*** *A 38-year-old male. ICH with midline shift of 13.3 mm, GCS score of 3.*

Patients presenting with midline shift may suffer from continual disequilibrium. Moreover, midline shift is often associated with high intracranial pressure, which can be fatal.[4,5] Furthermore, previous studies have shown that midline shift is significant in indicating the survival probability of patients.[6] Therefore, midline shift is used as a measurement of changes in brain symmetry and is an important indicator of the severity of pathology. The degree of midline shift after traumatic brain injury (TBI) is widely recognized as an important marker of severe injury.[6] Numerous reports[7-9] have described the association between extensive midline shift on CT scans and poor outcomes or other adverse sequelae of TBI.A study by Englander et al.[10] concluded that the presence of either a midline shift greater than 5 mm or subcortical concussion on acute CT scans is associated with a greater need for assistance with ambulation, activities of daily living, and global supervision at rehabilitation discharge. In addition to midline shift, other variables, such as age, Glasgow Coma Scale (GCS) score, abnormal motor responses, other CT findings, and episodes of hypoxia and hypertension, have been subsequently introduced to build more complex and accurate prognostic models. Given the significance of midline shift in diagnosis, automated detection and computation of midline shift on brain CT images using processing techniques is an important task.[1,2] A robust and efficient algorithm to compute midline shift is an essential component of a computer-aided neurology diagnostic system.[1] There is research in the literature that focuses on automated detection and computation of midline shift.[2,11,12] A generic algorithm was used to minimize the summed score of each point of deformed midline on symmetry maps.[3,11,13] This method was proven to be effective. However, it is mainly based on symmetry of the brain structure along the image's ventricle direction, which may be lost if there is a tumor, large hemorrhage, subdural hematoma (SDH), or epidural hematoma (EDH). This shortcoming often causes failure of the method in cases of intracerebral hemorrhage (ICH). Moreover, the use of a generic algorithm makes the method time inefficient.[3] In this study, a novel method of tracing brain midline shift on CT images in TBI was used to report the cause of midline shift instead of being based on symmetry information in the image. In TBI, hemorrhage is the main cause of brain midline shift. First, we modeled the relationship between hemorrhage and midline deformation (H-MLS) caused by hemorrhage using a linear regression model. Second, using the H-MLS model, the deformed midline (dML) was determined from the hemorrhage detected on the CT images. Finally, the dML was adjusted according to the visual symmetry information. Preliminary experimental results demonstrate the effectiveness of this method.

The present study aimed to detect the degree of midline shift from CT scans and the clinical status of the patient, to evaluate the relationship between the degree of midline shift found by the CT scan and GCS score as a predictor of clinical outcome in head injury patients. Furthermore, we aimed to assess the relationship between midline shift and age, sex, and causes.

## Materials and Methods

This cross-sectional, descriptive study was performed in the department of radiology at the Al Gazira Traumatology center in Al Gazira State in Sudan during the period from February to July 2020. The study was conducted in accordance with ethical principles of the WMA Declaration of Helsinki (1964, ed. 2013). Written informed consent was obtained from all participants.

The study included 50 subjects (36 males and 14 females). The inclusion criteria were patients with TBI or patients evaluated for level of consciousness by a neurosurgeon. Adults with normal healthy brains were excluded from the study.

Toshiba 16 Slice CT Scanner (Toshiba Medical Systems, Nasu, Japan 2003) was used to scan all patients in the supine, head first position. Contiguous 2 mm slices were obtained using the Toshiba 16-slice machine spiral technique (pitch 1.25–1.5, 0.75 s rotation time, 120 KvP, 2 mm reconstruction interval).

***Methods of midline shift measurement using CT scan***

We considered revising the iML as the intersection of the CT scan and the midsagittal plane. When a large mass of pathology such as a hemorrhage emerges, the iML deforms and shifts to one side of the brain. The dML is defined as a curve that best fits the actual position of the original points on the iML, after deformation. The displacement of points from iML to dML during deformation is the amount of midline shift.

Hemorrhage is a common pathology in TBI, and it is the cause of most brain midline shifts, based on a large number of CT scans presenting with midline shifts. We have observed that, in general, the amount of midline shift caused by a hemorrhage is influenced by the following factors: the size of the hemorrhage (the larger the size, the larger the amount of midline shift), the distance between the hemorrhage and the iML (the longer the distance, the smaller the amount of midline shift), and the midline elastic property (points on the iML further apart from the skull are displaced more easily).

From these observations, a heuristic model called H-MLS was established to model the influence of the various factors on the degree of midline shift (Figure 4).

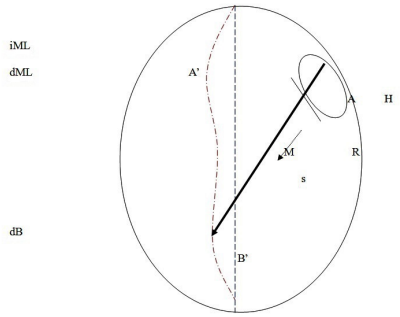


***Fig. 4.*** *The H-MLS model.*

***Tracing the deformed midline***

Based on the H-MLS model, a scheme for tracing the dML, the algorithm first computes the hemorrhage information presented in the TBI CT scan. Then, it uses the H-MLS model to predict the possible dML. The predicted dML is adjusted according to visual symmetry information.

*Step 1: Hemorrhage segmentation*: In the CT image, the intracranial hemorrhage region has a higher intensity value than normal brain tissue. The simple thresholding method is used to segment out the image regions corresponding to hemorrhage (thresholding using 160<intensity value<230).

*Step 2: Computation of hemorrhage information*: An ellipse H is fitted to the boundary of the hemorrhage, and a ray R is shot from each point A on H. For each effective ray R, the corresponding point B on iML and the corresponding r, s, and f are computed.

*Step 3: Predicting the deformed midline*: The H-MLS model is used to compute the amount of midline shift d for each point B on iML, which is also on the effective ray. Thus, there is a corresponding point B', and a simple curve-smoothing process is applied to get the predicted dML.

*Step 4: Symmetry adjusting:* In this final step, the predicted dML is adjusted to best fit the visual symmetry information.

In our H-MLS model, each hemorrhage is represented as an ellipse H that best fits the hemorrhage boundary. For each point A on H, a ray R is shot from A along the normal direction N at A.

If ray R intersects the iML at point B, it is called an effective ray, which means it affects the deformation of the midline. The intersection of the effective ray R is denoted with the dML as B'. R is back extended to let it intersect with H at A'. Therefore, the amount of midline shift of point B is the image distance between B and B'. Depicted as D = (BB').

The amount of midline shift of each point B on the iML is affected by the effective ray R passing through it. On each effective ray R, we use e = (AA') to measure the size of the hemorrhage, and we use s = (AB) to measure the distance between the hemorrhage and the iML. M is considered the middle point of the iML, then f = (BM) measures the position of B on the iML. Then, the H-MLS model is constructed as a simple linear equation: D = r + s + f

Given a number of points B on the iML, the corresponding effective ray R, and the amount of midline shift D, the linear regression method is used. Therefore, the H-MLS model is a linear regression model that reveals the relationship between intracranial hemorrhage and the midline shift caused by it.

***Data collection and analysis***

The data collected in this study were obtained directly from CT images, and the information was sorted using data sheets for each patient. The ethics and research committee approved the study, and consent forms were obtained from all patients prior to procedures.

Statistical analysis was performed using the statistical software package SPSS version 22.0 (IBM Corp., Armonk, N.Y., USA). Continuous variables were presented as mean±standard deviation (SD). Student's unpaired t-test was used to compare two groups for data with normal distribution. The frequencies of categorical variables were compared using Pearson's chi-squared test. A value of $P<0.05$ was considered significant.

# Results

In this study, males accounted for 72% (n=36) of the study population, and females accounted for 28% (n=14) (Figure 5). The age range of the patients in this study was 18–95 years old (mean age of 48.34±17.02 years). Most of the patients affected by brain injuries were between 36 and 75 years of age (Table 1).

We found that 28 patients with mild GCS scores had midline shifts up to 10mm, and only five patients had midline shifts greater than 10 mm (Table 2). The distribution of patients according to characteristics of brain injury includes SDH, EDH, ICH, and DAI. Midline shifts are presented in Table 3. Seventeen patients had midline shifts up to 10mm due to SDH, nine patients due to EDH, and six patients due to

ICH. Of these patients, 31 improved. In addition, the results show that 13 patients with midline shifts greater than 10mm improved and six died (Table 3).

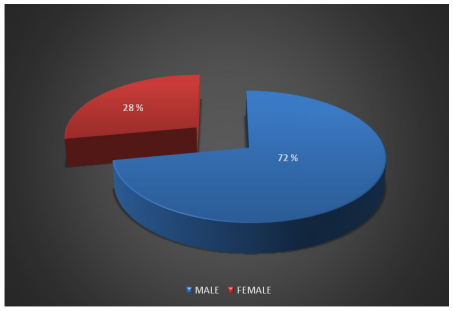


***Fig. 5.*** *Gender distribution.*

***Table 1.***

***Distribution of patients according to age***

| Age group (years) | Frequency | n (%) |
|---|---|---|
| 18–35 | 8 | 16 |
| 36–55 | 17 | 34 |
| 56–75 | 19 | 38 |
| 76–95 | 6 | 12 |
| Total | 50 | 100% |
| Mean±SD | 48.34±17.02 | |
| Age range (years) | 18–95 | |

***Table 2.***

***The distribution of patients according to midline shift severity and GCS score***

| Midline shift classification | GCS severity | | |
|---|---|---|---|
| | Mild | Moderate | Severe |
| Shift up to 10 mm | 28 | 6 | 3 |
| Shift greater than 10 mm | 5 | 3 | 5 |
| Total | 33 | 9 | 8 |

***Table 3.***

***Distribution of patients according to characteristics of brain injury with midline shift***

| Cause of midline shift | Midline shift up to 10 mm | Midline shift more than 10 mm |
|---|---|---|
| SDH | 17 | 8 |
| EDH | 9 | 6 |
| ICH | 6 | 3 |
| DAI | - | 1 |
| Final outcome | | |
| Improvement | 31 | 13 |
| Death | - | 6 |

The relationship between GCS severity and age groups is illustrated in Table 4 and Figure 6. Sixteen percent of patients were between 15 and 35 years of age, and their GCS scores—according to classification as mild, moderate, and severe—were 21.2%, 12.5%, and 0%, respectively. For patients between 36 and 55 years of age (34%), their GCS scores were 39.4%, 33.3%, and 12.5%, respectively. Thirty-eight percent of patients were aged between 56 and 75 years of age, and their GCS scores were 30.3%, 55.6%, and 50.0%, respectively. Twelve percent of patients were between 76 and 95 years of age, and their GCS scores were 9.1%, 0%, and 37.5%, respectively.

***Table 4.***

***Correlation between GCS severity and age***

| Age | GCS severity | | | | | |
|---|---|---|---|---|---|---|
| | Mild | % | Moderate | % | Severe | % |
| 18–35 | 7 | 21.2 | 1 | 11.1 | 0 | 0 |
| 36–55 | 13 | 39.4 | 3 | 33.3 | 1 | 12.5 |
| 56–75 | 10 | 30.3 | 5 | 55.6 | 4 | 50.0 |
| 76–95 | 3 | 9.1 | 0 | 0 | 3 | 37.5 |
| Total | 33 | 100% | 9 | 100% | 8 | 100% |

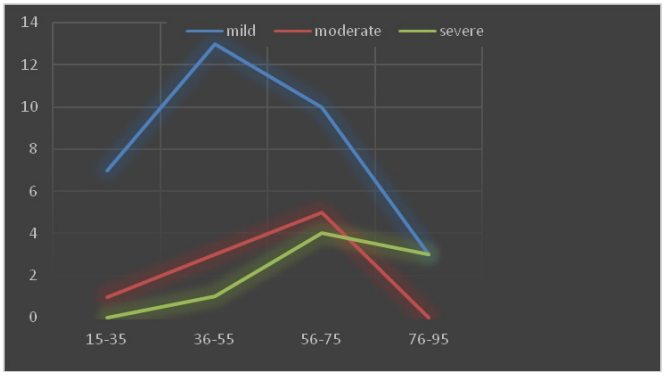


***Fig. 6.*** *Relationship between GCS severity and age group.*

Table 5 and Figure 7 illustrate a significant correlation between GCS severity and gender (P<0.05). Similarly, there was a significant relationship between midline shift and age (Table 6).

***Table 5.***

***Correlation between GCS severity and gender***

| Gender | GCS severity | | | | | | *P*-value |
|---|---|---|---|---|---|---|---|
| | Mild | % | Moderate | % | Severe | % | |
| Male | 25 | 69.4 | 6 | 16.7 | 5 | 13.9 | 0.001 |
| Female | 8 | 57.1 | 3 | 21.4 | 3 | 21.4 | 0.01 |
| Total | 33 | 66.0 | 9 | 18.0 | 8 | 16.0 | 0.01 |

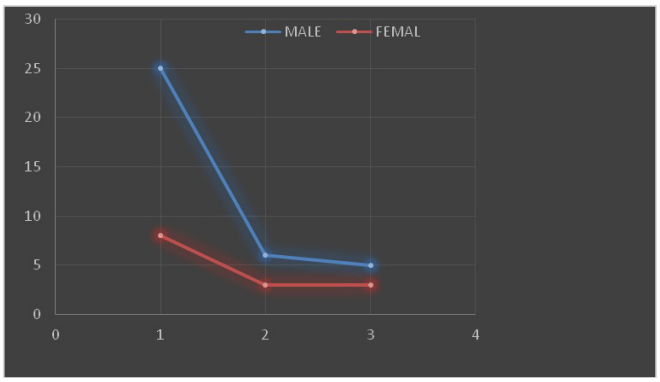


***Fig. 7.*** *Correlation between GCS severity and age (1- mild, 2 - moderate, 3 - severe).*

***Table 6.***

***Correlation between midline shift and age group***

| Midline shift | Age group (years) | | | | *P*-value |
|---|---|---|---|---|---|
| | 18–35 | 36–55 | 56–75 | 76–95 | |
| Shift up to 10 mm | 8 | 14 | 8 | 3 | 0.01 |
| Shift greater than 10 mm | 0 | 3 | 11 | 3 | 0.02 |
| Total | 8 | 17 | 19 | 6 | 0.013 |

## Discussion

This study aimed to measure the degree of midline shift using CT scan images, and to use that measurement to predict outcomes in patients with head injuries. Of the 50 patients with head injuries, 72% were male and 28% were female. GCS has been widely used to classify severity in head injury patients.

In a previous study by Chiewvit et al.,[14] which included 216 consecutive cases of traumatic head injury, 96 of 216 patients had midline shifts. Of these patients, 53 of 96 had CT scan midline shifting <10mm, whereas 37 of 96 had CT scan midline shifting >10mm. The present study revealed that lower GCS (<12), which indicates severity of head injury, was correlated with a larger degree of midline shift (shift up to 10mm and shift greater than 10mm) and poor clinical outcomes, such as death. This is consistent with previous research. They found that the greater degree of midline shift in patients with brain injuries was statistically significantly correlated with poor final clinical outcomes.[14] It appeared that the probability of a poor outcome was higher when there was a combination of midline shift and other types of intracranial hemorrhage, clinical factors, such as sex, age, and GCS score, and associated injury.

Similar results were demonstrated by Gennarelli et al.[15] and Lobato et al[16], who pointed out that the type of lesion is an important factor in determining the outcome of severity of injury assessed by GCS. In the present study, the degree of midline shift was found to be significantly correlated with GCS score, sex, and age group. This indicates that a larger midline shift tends to be associated with a lower GCS score, male sex, and advanced age.

The results of our study reveal the clinical importance of midline shift with SDH. The outcome is poorest when there is midline shift together with SDH, compared to other lesions in patients with TBI. Reviews by Valadka et al.[6] indicated that treatment of SDH with midline shift was possible in certain cases. It could be successful with smaller hematomas for patients in satisfactory clinical condition, but also for less midline shift in comatose patients where the midline shift was most likely caused by brain edema and there is minimal contribution of brain compression. Another study by Selladurai et al.[17] noticed that the degree of midline shift did not prove to be a significant predictor for all patients with midline shift. Twenty-nine patients (30%) had a GCS score between 12 and 15, while 68 patients (70%) had a GCS score <12, which was the unfavorable group. This indicates that the degree of midline shift did not prove to be of predictive significance for all patients with midline shift.

## Conclusion

The present study concluded that increased midline shift based on CT scans in patients with head injuries is related to the severity of head injury (GCS=3–12) and is significantly related to poor final clinical outcome. This is consistent with the results of previous studies. This study also found that greater midline shift tends to be associated with lower GCS scores, and the type of lesion is an important factor in determining the outcome of the severity of injury assessed by GCS. In addition, the degree of midline shift in a patient's brain injury was statistically significant as a determinant of outcome. It appears that the probability of poor outcome is higher when there is a combination of midline shift with other types of intracranial hemorrhage, clinical factors, such as sex, age, GCS score, and associated injury. Ultimately, the outcome was the poorest if there was midline shift with SDH compared to other lesions in patients with brain injuries.

## Acknowledgments

This publication was supported by the Deanship of Scientific Research at Prince Sattam bin Abdulaziz University, Alkharj, Saudi Arabia.

## Competing Interests

The authors declare that they have no competing interests.

## References

1. Liao CC, Chen YF, Xiao F. Brain Midline Shift Measurement and Its Automation: A Review of Techniques

***Corresponding author**: Professor Mustafa Z. Mahmoud, Radiology and Medical Imaging Department, College of Applied Medical Sciences, Prince Sattam bin Abdulaziz University, E-mail: m.alhassen@psau.edu.sa, PO Box: 422, Zip Code: 11942, Al-Kharj, Saudi Arabia.*

and Algorithms. Int J Biomed Imaging. 2018 Apr 12;2018:4303161. doi: 10.1155/2018/4303161.
2. Liao CC, Xiao F, Wong JM, Chiang IJ. Automatic recognition of midline shift on brain CT images. Comput Biol Med. 2010 Mar;40(3):331-9. doi: 10.1016/j.compbiomed.2010.01.004.
3. Liu R, Li S, Chew L, Boon C, Tchoyosom C, Cheng K, Tian Q, Zhang Z. From hemorrhage to midline shift: a new method of tracing the deformed midline in traumatic brain injury CT images. In: 16th IEEE International Conference on Image Processing; 2009: 2637–2640
4. Hiler M, Czosnyka M, Hutchinson P, Balestreri M, Smielewski P, Matta B, Pickard JD. Predictive value of initial computerized tomography scan, intracranial pressure, and state of autoregulation in patients with traumatic brain injury. J Neurosurg. 2006 May;104(5):731-7. doi: 10.3171/jns.2006.104.5.731.
5. Poca MA, Benejam B, Sahuquillo J, Riveiro M, Frascheri L, Merino MA, Delgado P, Alvarez-Sabin J. Monitoring intracranial pressure in patients with malignant middle cerebral artery infarction: is it useful? J Neurosurg. 2010 Mar;112(3):648-57. doi: 10.3171/2009.7.JNS081677.
6. Valadka AB, Gopinath SP, Robertson CS. Midline shift after severe head injury: pathophysiologic implications. J Trauma. 2000 Jul;49(1):1-8; discussion 8-10. doi: 10.1097/00005373-200007000-00001.
7. Jacobs B, Beems T, van der Vliet TM, Diaz-Arrastia RR, Borm GF, Vos PE. Computed tomography and outcome in moderate and severe traumatic brain injury: hematoma volume and midline shift revisited. J Neurotrauma. 2011 Feb;28(2):203-15. doi: 10.1089/neu.2010.1558.
8. Jain S, Vyvere TV, Terzopoulos V, Sima DM, Roura E, Maas A, Wilms G, Verheyden J. Automatic Quantification of Computed Tomography Features in Acute Traumatic Brain Injury. J Neurotrauma. 2019 Jun;36(11):1794-1803. doi: 10.1089/neu.2018.6183.
9. Pillai SV, Kolluri VR, Praharaj SS. Outcome prediction model for severe diffuse brain injuries: development and evaluation. Neurol India. 2003 Sep;51(3):345-9.
10. Englander J, Cifu DX, Wright JM, Black K. The association of early computed tomography scan findings and ambulation, self-care, and supervision needs at rehabilitation discharge and at 1 year after traumatic brain injury. Arch Phys Med Rehabil. 2003 Feb;84(2):214-20. doi: 10.1053/apmr.2003.50094.
11. Liu R, Li S, Su B, Tan CL, Leong TY, Pang BC, Lim CC, Lee CK. Automatic detection and quantification of brain midline shift using anatomical marker model. Comput Med Imaging Graph. 2014 Jan;38(1):1-14. doi: 10.1016/j.compmedimag.2013.11.001.
12. Xiao F, Liao CC, Huang KC, Chiang IJ, Wong JM. Automated assessment of midline shift in head injury patients. Clin Neurol Neurosurg. 2010 Nov;112(9):785-90. doi: 10.1016/j.clineuro.2010.06.020.
13. Liao CC, Chiang IJ, Xiao F, Wong JM. Tracing the deformed midline on brain CT. Biomed Eng Appl Basis Comm 2006; 18(06): 305–311. doi: 10.4015/S1016237206000452.
14. Chiewvit P, Tritakarn SO, Nanta-aree S, Suthipongchai S. Degree of midline shift from CT scan predicted outcome in patients with head injuries. J Med Assoc Thai. 2010 Jan;93(1):99-107.
15. Gennarelli TA, Spielman GM, Langfitt TW, Gildenberg PL, Harrington T, Jane JA, Marshall LF, Miller JD, Pitts LH. Influence of the type of intracranial lesion on outcome from severe head injury. J Neurosurg. 1982 Jan;56(1):26-32. doi: 10.3171/jns.1982.56.1.0026.
16. Lobato RD, Cordobes F, Rivas JJ, de la Fuente M, Montero A, Barcena A, Perez C, Cabrera A, Lamas E. Outcome from severe head injury related to the type of intracranial lesion. A computerized tomography study. J Neurosurg. 1983 Nov;59(5):762-74. doi: 10.3171/jns.1983.59.5.0762.
17. Selladurai BM, Jayakumar R, Tan YY, Low HC. Outcome prediction in early management of severe head injury: an experience in Malaysia. Br J Neurosurg. 1992;6(6):549-57. doi: 10.3109/02688699209002372.

International Journal of Biomedicine 11(1) (2021) 24-28
http://dx.doi.org/10.21103/Article11(1)_OA4

ORIGINAL ARTICLE

Surgery

INTERNATIONAL JOURNAL OF BIOMEDICINE

# Innovative Endoscopic Technologies in the Complex Treatment of Patients with Unstable Stopped Gastroduodenal Bleeding

Evgeniy F. Cherednikov, PhD, ScD[1]; Sergey V. Barannikov, PhD[1]; Igor S. Yuzefovich, PhD[1]; Galina V. Polubkova, PhD[1]; Yuri V. Maleev, PhD, ScD[2]; Irina V. Volkova[3]; Anastasiya T. Vysotskaya, PhD[1]; Oleg V. Strygin, PhD[3]; Evgeniy S. Ovsyannikov, PhD, ScD[1*]

[1]*Voronezh State Medical University named after N. N. Burdenko*
[2]*Voronezh Basic Medical College*
[3]*Voronezh City Clinical Emergency Hospital №1*
*Voronezh, the Russian Federation*

## Abstract

***Background*:** The aim of our research was to improve the results of treatment of patients with unstable bleeding gastroduodenal ulcers through the use of innovative endoscopic technologies in the complex treatment of gastroduodenal bleeding.

***Methods and results*:** The study included 132 patients with unstable ulcerative gastroduodenal bleeding. Among all patients with gastroduodenal bleeding, there were 95(71.96%) men and 37(28.04%) women. The average age of patients was 56.1±18.45 years. Among the sources of gastroduodenal ulcer bleeding, duodenal ulcers complicated by bleeding predominated were observed in 77(58.3%) patients, bleeding gastric ulcers and ulcers of gastroenteroanastomosis areas in 49(37.7%) and 6(4.6%) patients, respectively. According to the endoscopic classification (J. Forrest, 1974), continued bleeding (Forrest Ia-Ib) was observed in 44(33.3%) patients, threat of rebleeding (Forrest IIa-IIb) in 88(66.7%) patients.

All patients were divided, by random sampling, into two equivalent groups: the main group (MG, n=66) and the comparison group (CG, n=66). In the treatment of MG patients, an individual approach was applied that used the injection of ε-aminocaproic acid, argon-plasma coagulation, and the endoscopic pneumatic applications of hemostatic agents (Zhelplastan and the patient's platelet-rich auto-plasma) and granular sorbents (Aseptisorb-A, Aseptisorb-D). In CG, traditional methods of endoscopic hemostasis (injection method with ε-aminocaproic acid and vasoconstrictor drugs, argon plasma coagulation, etc.) were used without granular sorbents and innovative hemostatic agents.

In patients with the Forrest Ia-Ib bleeding, primary endoscopic hemostasis was achieved in 95.2% of cases in the MG and in 91.3% of cases in the CG ($P$>0.05). In patients with t he Forrest IIa-IIb bleeding, effectiveness of endoscopic prevention of recurrent bleeding was achieved in 95.5% of cases in the MG and in 81.4% of cases in the CG ($P$=0.047). Mortality rate was 1.5% in the MG and 4.5% in the CG ($P$>0.05). In the MG and CG, the overall frequency of recurrent bleeding from gastroduodenal ulcers, the operational activity, and the length of hospital stay were 15.2% and 4.5% ($P$=0.041), 12.1% and 1.5% ($P$=0.033), and 11.1±0.6 days and 9.2±0.4 days ($P$<0.01), respectively.

***Conclusion*:** The developed method for the complex treatment of patients with unstable gastroduodenal bleeding, based on the optimization of emergency and preventive endoscopic hemostasis, indicates that the use of therapeutic endoscopy to prevent bleeding recurrences with hemostatic agents and granular sorbents improves the reliability of endoscopic hemostasis, reduces the frequency of hemorrhage relapses and the number of emergency operations, as well as a length of hospital stay. (**International Journal of Biomedicine. 2021;11(1):24-28.**)

**Key Words:** gastroduodenal hemorrhage • endoscopic hemostasis • granular sorbents • hemostatic agents

**For citation**: Cherednikov EF, Barannikov SV, Yuzefovich IS, Polubkova GV, Maleev YuV, Volkova IV, Vysotskaya AT, Strygin OV, Ovsyannikov ES. Innovative Endoscopic Technologies in the Complex Treatment of Patients with Unstable Stopped Gastroduodenal Bleeding. International Journal of Biomedicine. 2021;11(1):24-28. doi:10.21103/Article11(1)_OA4

## Introduction

The treatment of gastroduodenal bleeding is one of the most acute problems in the practice of surgeons, endoscopists, gastroenterologists, resuscitators, etc.[1-6]

Unstable stopped gastroduodenal bleeding is associated with frequent relapses of bleeding and urgent surgery.[7-9] More than half of all cases of gastroduodenal bleeding are caused by ulcerative lesions of the stomach and duodenum.[10,11]

V.S. Savelyev notes that if the ulcer is closed with a clot (Forrest IIb), then a relapse of bleeding is possible in 20% of patients, and upon detection of a large vessel in an ulcer (Forrest IIa), recurrence of bleeding occurs in 40% of patients. When the patient has continued bleeding (Forrest Ia-Ib) or blood flow from under a clot, which was able to stop during endoscopic hemostasis, bleeding recurrence is observed in 50% of patients.[12]

In patients with unstable stopped gastroduodenal bleeding, it is important not only to stop the bleeding, but also to create conditions for reducing the risk of recurrent hemorrhage, as well as for the rapid healing of the ulcer defect as a possible source of complications.[13-16]

In this regard, the search for the new cytoprotective agents for the protection of the ulcerative defects, thrombosed vessel, and a zone of coagulation necrosis from aggressive gastric juice, as well as the development of the new methods for the prevention of the recurrent gastroduodenal ulcer bleeding are an urgent task.[17,18]

The aim of our research was to improve the results of treatment of patients with unstable bleeding gastroduodenal ulcers through the use of innovative endoscopic technologies in the complex treatment of gastroduodenal bleeding.

## Materials and Methods

A clinical study was conducted in the Voronezh City Specialized Center for the treatment of patients with gastrointestinal bleeding. The study was approved by the Ethics Committee of Voronezh State Medical University named after N.N. Burdenko. Written informed consent was obtained from each patient.

The study included 132 patients with unstable ulcerative gastroduodenal bleeding. Among all patients with gastroduodenal bleeding, there were 95(71.96%) men and 37(28.04%) women. The average age of patients was 56.1±18.45 years.

Peptic ulcer disease complicated by bleeding was observed in 72(54.5%) patients (Table 1). In 60(45.5%) patients, acute symptomatic ulcers were the cause of bleeding. Among the sources of gastroduodenal ulcer bleeding, duodenal ulcers complicated by bleeding predominated were observed in 77(58.3%) patients, bleeding gastric ulcers and ulcers of gastroenteroanastomosis areas in 49(37.7%) and 6(4.6%) patients, respectively.

According to the endoscopic classification,[19] continued bleeding (Forrest Ia-Ib) was observed in 44(33.3%) patients, threat of rebleeding (Forrest IIa-IIb) in 88(66.7%) patients.

According to the severity of blood loss (A.L.Gorbashko, 1982),[20] the patients were divided as follows: mild severity was observed in 42(31.8%), moderate in 63(47.7%) and severe in 27(20.5%).

All patients were divided, by random sampling, into two equivalent groups: the main group (MG, n=66) and the comparison group (CG, n=66). Patients were comparable in etiology of ulcerative bleeding, age, gender, degree of severity of bleeding, nature of bleeding according to endoscopic classification, and duration of observations.

***Table 1.***

***Clinical characteristics of the study groups***

| Indicator | MG (n=66) | CG (n=66) | *P* | Total (n=132) |
|---|---|---|---|---|
| Type of gastroduodenal ulcers | | | | |
| Peptic ulcer disease of the stomach and duodenum | 39(59.1%) | 33(50%) | >0.05 | 72(54.5%) |
| Acute symptomatic ulcers | 27(40.9%) | 33(50%) | >0.05 | 60(45.5%) |
| Localization of the source of bleeding | | | | |
| Duodenal ulcers | 37(56.1%) | 40(60.6%) | >0.05 | 77(58.3%) |
| Stomach ulcers | 27(40.9%) | 22(33.3%) | >0.05 | 49(37.1%) |
| Gastroentero-anastomosis ulcers | 2(3.0%) | 4(6.1%) | >0.05 | 6(4.6%) |
| Type of bleeding (J. Forrest, 1974) | | | | |
| Forrest Ia-Ib | 21(31.8%) | 23(34.8%) | >0.05 | 44(33.3%) |
| Forrest IIa-IIb | 45(68.2%) | 43(65.2%) | >0.05 | 88(66.7%) |
| The severity of blood loss (A. I. Gorbashko, 1982) | | | | |
| Mild | 22(33.3%) | 20(30.3%) | >0.05 | 42(31.8%) |
| Moderate | 32(48.5%) | 31(47.0%) | >0.05 | 63(47.7%) |
| Severe | 12(18.2%) | 15(22.7%) | >0.05 | 27(20.5%) |

In the treatment of MG patients, an individual approach was applied that used the endoscopic pneumatic applications of hemostatic agents and a granular sorbent in the complex endoscopic treatment of gastroduodenal ulcers complicated by bleeding. In particular, in patients with ongoing hemorrhage (Forrest Ia-Ib), active bleeding was stopped first by injection with ε-aminocaproic acid, then with vasoconstrictor drugs, followed by argon-plasma coagulation; and then the powder-like hemostatic agent Zhelplastan (Gelplastan) and granular sorbent Aseptisorb-D were pneumatically insufflated onto the defect area (Patent RF №2633588).[21]

In patients with the threat of rebleeding (Forrest IIa-IIb), the argon-plasma coagulation of the thrombosed vessel

(Forrest IIa) was first performed, and in Forrest IIb, the clot was first removed from the ulcer defect by washing it, then the argon-plasma coagulation of the bleeding source was also performed. After that, with the help of an insufflator, Aseptisorb-A powder was applied to the area of these ulcerative defects, followed by the application of the patient's platelet-rich auto-plasma (Patent RF № 2632771).[22]

In CG, traditional methods of endoscopic hemostasis (injection method with ε-aminocaproic acid and vasoconstrictor drugs, argon-plasma coagulation, etc.) were used without platelet-rich auto-plasma and granular sorbents. After that, the complex treatment of patients in the MG and CG did not differ.

The main criteria in assessing the results of treatment were both clinical and endoscopic indicators: the timing of the final hemostasis, the frequency of rebleeding, dynamic monitoring of the size of ulcerative defects, the quality of healing of ulcers, the presence of emergency operations, hospital length of stay, and mortality rates.

The statistical analysis was performed using the statistical software Microsoft Excel. Baseline characteristics were summarized as frequencies and percentages for categorical variables and as mean±SEM for continuous variables. For data with normal distribution, inter-group comparisons were performed using Student's t-test. Differences of continuous variables departing from the normal distribution, even after transformation, were tested by the Mann-Whitney U-test. For data with normal distribution, inter-group comparisons were performed using Student's t-test. Group comparisons with respect to categorical variables are performed using chi-square tests with Yates correction or, alternatively, Fisher's exact test when expected cell counts were less than 5. A probability value of $P<0.05$ was considered statistically significant.

## Results and Discussion

When evaluating the results of treatment of patients in the MG with unstable bleeding, it was noted that primary endoscopic hemostasis was achieved in 20(95.2%) patients with the Forrest Ia-Ib bleeding. Effectiveness of endoscopic prevention of recurrent bleeding in patients with the Forrest IIa-IIb bleeding was noted in 43(95.6%) cases. Recurrence of ulcerative bleeding was observed in 3(4.50%) cases. Repeated endoscopic hemostasis was effective in 2 cases. An 80-year-old patient was operated on urgently due to the failure of repeated endoscopic hemostasis. This patient died in the presence of severe concomitant pathology and increasing multiple organ failure in the postoperative period.

Clinical observations showed that in patients of the MG who received endoscopic treatment according to the developed technique, after pneumo-insufflation on a bleeding ulcer defect of granular sorbents in combination with hemostatic agents, followed by the application of platelet-rich auto-plasma, the granular sorbent swelled, turning into a soft elastic hydrogel that was tightly fixed in the area of the bleeding source due to its properties, protecting it from the effects of aggressive factors of the gastric and duodenal contents. This soft elastic hydrogel lay, as "a protective dressing," showed a double effect - local hemostatic and cytoprotective, preventing the resumption of bleeding and contributing to the favorable course of the reparative process.

In the CG, primary endoscopic hemostasis was achieved in 21(91.3%) patients with the Forrest Ia-Ib bleeding. Effectiveness of endoscopic prevention of recurrent bleeding in patients with the Forrest IIa-IIb bleeding was noted in 35(81.4%) cases. Among 23 patients with the Forrest Ia-Ib bleeding, 2 patients were operated on an emergency basis. Recurrence of ulcerative bleeding was observed in 10(15.2%) cases. Repeated endoscopic hemostasis was effective in 3 cases and 5 patients were operated on urgently due to recurrent profuse bleeding, of which 3 patients died in the postoperative period. One patient in the delayed order was carried out resection of the stomach.

The final results of the treatment of patients are presented in Table 2.

***Table 2.***

***Clinical effectiveness of the treatment of patients unstable bleeding gastroduodenal ulcers in the study groups***

| Indicator | MG | CG | *P*-value |
|---|---|---|---|
| The effectiveness of primary endoscopic hemostasis in Forrest Ia-Ib | 20 (95.2% in relation to n=21) | 21 (91.3% in relation to n=23) | *P*>0.05 |
| The effectiveness of endoscopic prevention of recurrent bleeding in Forrest IIa-IIb | 43 (95.5% in relation to n=45) | 35 (81.4% in relation to n=43) | *P*=0.047 |
| The frequency of recurrent bleeding | 3(4.5%) | 10(15.2%) | *P*=0.041 |
| The mean interval for recurrent bleeding, days | 3.5±0.56 | 3.27±0.27 | *P*>0.05 |
| Operations | 1(1.5%) | 8(12.1%) | *P*=0.033 |
| Mortality | 1(1.5%) | 3(4.5%) | *P*>0.05 |
| Length of hospital stay, days | 9.2±0.4 | 11.1±0.6 | *P*<0.01 |

Thus, the developed method for treatment of ulcerative gastroduodenal bleeding with the combined use of cytoprotective granular sorbents and local hemostatics in the complex therapy of patients with unstable bleeding gastroduodenal ulcers, provides reliable primary hemostasis in 95.2% of cases, increases the effectiveness of endoscopic prevention of recurrent hemorrhages from 81.4% to 95.5% ($P$=0.047), reduces the overall frequency of recurrent bleeding from gastroduodenal ulcers from 15.2% to 4.5% ($P$=0.041), decreases the operational activity from 12.1% to 1.5% ($P$=0.033) and the length of *hospital stay* from 11.1±0.6 days to 9.2±0.4 days ($P$<0.01).

## Conclusion

The developed methodology for the complex treatment of patients with unstable bleeding, based on the optimization of emergency and preventive endoscopic hemostasis indicates that the use of therapeutic endoscopy to prevent bleeding recurrences with hemostatic agents and granular sorbents improves the reliability of endoscopic hemostasis, reduces the frequency of hemorrhage relapses and the number of emergency operations, as well as a length of hospital stay.

## Acknowledgments

We gratefully acknowledge the contributions of patients to this study.

## Competing Interests

The authors declare that they have no competing interests.

## Sources of Funding

This work was supported by the Council on Grants of the President of the Russian Federation for State Support of Young Scientists and Leading Scientific Schools (Grant MK-1069.2020.7).

ClinicalTrials.gov Identifier: NCT04239118 (New Technologies for Endoscopic Treatment of Bleeding Gastroduodenal Ulcers) https://clinicaltrials.gov/ct2/show/NCT04239118

## References

1. Budnevsky AV, Cherednikov EF, Popov AV, Ovsyannikov ES, Kravchenko AY, Fursov KO. A Complex Multidisciplinary Approach to Prevention Gastro-duodenal Bleeding in Patients of General Hospital. International Journal of Biomedicine. 2017;7(3):204-207. doi: 10.21103/Article7(3)_OA8
2. Cherednikov EF, Deryaeva OG, Adianov VV, Ovchinnikov IF, Popov AV. [Modern trends of diagnosis and treatment of patients with gastrointestinal bleeding in the centre]. System Analysis and Management in Biomedical Systems. 2014;13(2):426-431. [Article in Russian].
3. Cherednikov EF, Maleev YuV, Chernyh AV, Litovkina TE, Bondarenko AA, Cherednikov EE, Popov AV. [Current views on the diagnosis, treatment, and prevention of ruptured hemorrhagic syndrome (Mallory-Weiss syndrome)]. Journal of New Medical Technologies. 2016;23(4):161-172. [Article in Russian].
4. Baev VE, Kravets BB, Cherednikov EF. [Diagnostics of ulcerative forms of stomach cancer]. Voronezh. 2003:112. [In Russian].
5. Cherednikov EF, Maleev YuV, Chernykh AV, Litovkina TE, Cherednikov EE, Shevtsov AN. [Modern views on the etiology and pathogenesis of ruptured hemorrhagic syndrome (Mallory-Weiss syndrome)]. Journal of Anatomy and Histology. 2016;(1):86-98. [Article in Russian].
6. Adianov VV, Cherednikov EF. [Optimization of treatment of gastroduodenal bleeding in patients with high surgical risk]. System Analysis and Management in Biomedical Systems. 2014;13(4):841-846. [Article in Russian].
7. Cherednikov EF, Barannikov SV, Romantsov MN, Popov AV. New aspects of preventive endoscopic hemostasis in the treatment of peptic ulcer bleeding in the experimental condition. The EPMA Journal. 2017;8(S1):45.
8. Deryaeva OG, Cherednikov EF. [Multimodality therapy of erosiveulcer gastroduodenal bleeding by patients in a multidisciplinary hospital]. System Analysis and Management in Biomedical Systems. 2014;13(3):725-730. [Article in Russian].
9. Cherednikov EF, Barannikov SV, Zhdanov AI, Moshurov IP, Polubkova GV, Maleev YuV, Ovsyannikov ES, Myachina DS. Combimed Use of biologically Active Hemostatic and Granulated Sorbent in Endoscopic Cytoprotective Hemostasis in Patients with Bleeding Gastroduodenal Ulcers. International Journal of Biomedicine. 2020;10(2):129-132. doi: 10.21103/Article10(2)_OA8
10. Cherednikov EF, Glukhov AA, Romantsov MN, Maleev YuV, Barannikov SV, Shkurina IA, Vysotskaya AT, Ovsyannikov ES. Hemostatic Agents in Combination with Diovine for Local Treatment of Simulated Bleeding Gastric Ulcers. International Journal of Biomedicine. 2020;10(2):138-141. doi: 10.21103/Article10(2)_OA10
11. Cherednikov EF., Budnevsky AV, Popov AV, Fursov KO. A new opinion on gastroduodenal bleeding preventon in patients with somatic patology. The EPMA Journal. 2017; 8(S1):46.
12. Savelyev VS. Guide to emergency surgery of abdominal organs. Moscow: Triad-X; 2004:640 pp. [In Russian].
13. Cherednikov EF, Barannikov SV, Fursov KO, Polubkova GV, Danilenko VI, Stepanov DS. [Healing of bleeding experimental defects of the stomach with topical anilovin and platelet-rich plasma]. Journal of Volgograd State Medical University. 2017;2(62):130-133. [Article in Russian].
14. Romantsov MN, Cherednikov EF, Danilenko VI, Stepanov DS, Fursov KO, Deryaeva AG. [Morphological Characteristics of Processes of Simulated Bleeding Gastric Defects Reparation in Treatment with Gelplastan and Diovin]. Journal of Anatomy and Histopathology. 2017;6(1):81-86. [Article in Russian].
15. Cherednikov EF, Barannikov SV, Maleev YuV, Fursov KO, Litovkina TE, Zakurdaev EI. [Experimental justification of the use of biologically active draining sorbent and plasma enriched by thrombocytes in treatment of bleeding defects of the stomach]. Journal of New Medical Technologies. 2017;24(2):114-118. [Article in Russian].
16. Cherednikov EF, Batkaev AR, Baev VE. The Reparative regeneration of erosive-ulcerative lesions of the stomach and duodenum in the local treatment of hydrophilic granular sorbents. System Analysis and Management in Biomedical Systems. 2005;4(2):224-225. [Article in Russian].
17. Barannikov SV, Litovkina TE, Fursov K O, Kuzmenok

***Corresponding author**: Evgeniy S. Ovsyannikov, PhD, ScD. Department of Faculty Therapy, Voronezh State Medical University named after N.N. Burdenko. Voronezh, the Russian Federation. E-mail: ovses@yandex.ru*

VA. [Experimental study of the possibility of using a biologically active draining sorbent and platelet-rich plasma in the endoscopic treatment of simulated bleeding stomach ulcers]. Postgraduate doctor. 2017;2.1(81):170-176. [Article in Russian].
18. Cherednikov EF, Barannikov SV, Maleev YuV, Fursov KO, Litovkina TE, Zakurdaev EI, Ovsyannikov ES. Experimental justification of using Aseptisorb-A and platelet-rich plasma in endoscopic treatment of mold bleeding stomach defects. International Journal of Biomedicine. 2017;7(4):298-301. doi: 10.21103/Article7(4)_OA5
19. Forrest JA, Finlayson ND, Shearman DJ. Endoscopy in gastrointestinal bleeding. Lancet. 1974 Aug 17;2(7877):394-7. doi: 10.1016/s0140-6736(74)91770-x. PMID: 4136718.
20. Gorbashko AI. Diagnostics and treatment of blood loss. Moscow: Meditsina. 1982:224 pp. [In Russian].
21. Cherednikov EF, Romantsov MN, Ovchinnikov IF, Glukhov AA, Adianov VA, Vysotskaya AT; Voronezh State Medical University named after N. N. Burdenko [Method of endoscopic treatment of ulcerative gastroduodenal bleeding]. Patent for Invention RUS No. №2633588. Application No. 2015147321 dated 03.11.15; publ. 10.05.2017; Bulletin No. 13. [In Russian].
22. Cherednikov EF, Budnevsky AV, Barannikov SV, Fursov KO, Bondarenko AA, Cherednikov EE, Volkova IV; Voronezh State Medical University named after N. N. Burdenko. [Method for endoscopic stopping of gastrointestinal bleeding]. Patent for Invention RUS No. 2632771. Application No. 2016148270 dated 09.12.2016; publ. 09.10.2017; Bulletin No. 28. [In Russian].

International Journal of Biomedicine 11(1) (2021) 29-31
http://dx.doi.org/10.21103/Article11(1)_OA5

ORIGINAL ARTICLE

Surgery

INTERNATIONAL JOURNAL OF BIOMEDICINE

# Laparoscopic Repair of Perforated Gastric Ulcer by Forming a "Covered Perforation"

Alexei I. Khripun, PhD, ScD[1]; Ilya V. Sazhin, PhD[2]; Archil S. Tsulaya[2]; Sergey N. Shurygin, PhD, ScD[2]; Leonid V. Safonov, PhD[3]; Alexey G. Vaganov[4]; Sarkis A. Asratyan, PhD[2]; Aleksandr N. Alimov, PhD, ScD[1]

*[1]Pirogov Russian National Research Medical University*
*[2]Budgetary Institution of Health «Clinical Hospital V.M. Buyanova»*
*[3]Federal Science Center of Physical Culture and Sport (VNIIFK)*
*[4]State Budgetary Institution of Healthcare of the City of Moscow «City Clinical Hospital No. 29»*
*Moscow, the Russian Federation*

## Abstract

Performing video endoscopic operations on patients with emergency surgical pathology in order to increase the efficiency and reduce the duration of surgical intervention, as well as to prevent postoperative complications, stimulates the continuous development and implementation of new minimally invasive technologies in emergency surgery. The aim of the study was to develop a new method for laparoscopic suturing of a perforated gastric ulcer (PGU) with the formation of a "covered perforation." The proposed method uses a fold-duplicator from the anterior wall of the stomach to close the perforation of the stomach wall, thus expanding the possibilities of using minimally invasive technologies for PGU.(**International Journal of Biomedicine. 2021;11(1):29-31.**)

**Key Words:** laparoscopy • perforated gastric ulcer • endoscopic techniques • abdominal cavity

**For citation**: Khripun AI, Sazhin IV, Tsulaya AS, Shurygin SN, Safonov LV, Vaganov AG, Asratyan SA, Alimov AN. Laparoscopic Repair of Perforated Gastric Ulcer by Forming a "Covered Perforation." International Journal of Biomedicine. 2021;11(1):29-31. doi:10.21103/Article11(1)_O5

## Introduction

Currently, there are several options for the surgical treatment of perforated gastric ulcer (PGU), the most common of which is suturing the perforation through its edges with interrupted, Z-shaped or continuous sutures.[1,2] The other most common way to close the perforation of the ulcer is tamponade with a strand of the greater omentum (Graham patch).[1] With the widespread introduction of minimally invasive technologies into everyday surgical practice, suturing is often performed using laparoscopy.[2,3] In some cases, the surgeon is faced with complications that limit the use of a simple interrupted suture or other suturing options. Such complications include a large size of the perforation (more than 1 cm), pronounced infiltration of the edges of the defect, the eruption of sutures on the stomach wall when tying knots, and the inability to tamponade with the omentum or other nearby tissues.[2,4]

## Method Description

In an experiment, we have developed a method of laparoscopic suturing of PGU with the formation of a "covered perforation." It assumes that the perforation is localized on the anterior wall (the pyloric or prepyloric parts) of the stomach. The anatomical basis of the method is the mobility and elasticity of the stomach wall.

The essence of the method is as follows: A 10 mm video laparoscopic trocar is inserted into the abdominal cavity through a 10 mm incision in the abdominal wall above the

***Corresponding author**: Leonid V. Safonov, PhD. Federal Science Center of Physical Culture and Sport (VNIIFK), Moscow, Russia. E-mail: lsaf@mail.ru*

navel. In the right hypochondrium, a 5 mm trocar and an endoclamp are installed, and in the left mesogastrium – a 10 mm trocar and a needle holder (Fig.1).

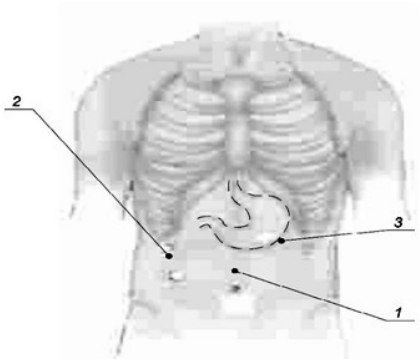


***Fig. 1.*** *Position of the trocars. 1) Umbilical 10 mm trocar for laparoscope. 2) A 5 mm trocar for endoclamping. 3) A 10 mm trocar for the needle holder.*

After insufflation of carbon dioxide until the pressure in the abdominal cavity is 12 mmHg, we perform the revision and sanitation of the abdominal cavity, and visualize the perforation on the anterior wall of the stomach.

Using a needle holder inserted through a 10 mm trocar and a clamp inserted through a 5 mm trocar, two main lines of the serous-muscular suture are applied with a polyfilament absorbable suture with a nominal diameter of 2 0 on a 25-26 mm, one-half-circle stitching needle. One is located above and the other below the perforation. The distance is 20 mm above and below from the perforation. The sutures are applied so that the needle entry is 40 mm from the proximal edge of the perforation, and needle exit is 20 mm from its distal edge. After completing the seams, at both free ends of the threads, approximately 50 mm to 80 mm long, are left (Fig.2).

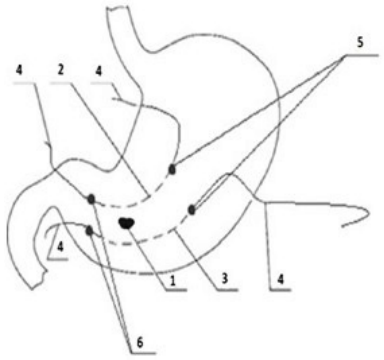


***Fig 2.*** *The imposition of the main serous-muscular sutures. 1 - Perforation hole; 2 - The upper line of the serous-muscular suture; 3 - The lower line of the serous-muscular suture; 4 - Free ends of the threads; 5 - Needle entry; 6 - Needle exit.*

The ends of the threads are tied in knots in pairs. When these nodes are tightened, the part of the stomach proximal to the perforation hole is superimposed on this hole and covers it with itself, thereby forming a fold-duplicator from the anterior wall of the stomach.

Next, two more surgical sutures, each approximately 150 mm long, are inserted into the abdominal cavity with a needle holder. In order to strengthen the previously applied sutures and create tightness between the first sutures, two additional interrupted serous-muscular sutures are equidistantly superimposed. With these sutures, the outer edge of the fold-duplicator is additionally sutured to the stomach wall (Fig. 3,4).

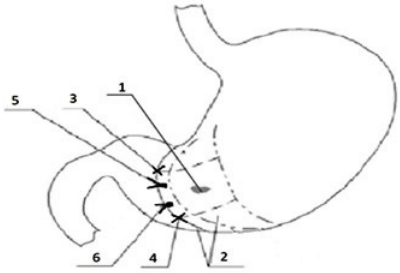


***Fig.3.*** *Strengthening the fold-duplicator of the stomach with additional interrupted sutures. 1 - Perforation hole; 2 – The formed fold-duplicator from the anterior wall of the stomach; 3, 4 - Tied knots of the main lines of the serous-muscular suture; 5, 6 - additional interrupted serous-muscular sutures to strengthen the duplicate fold.*

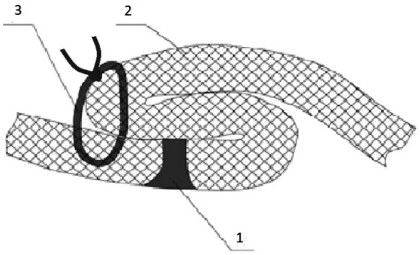


***Fig.4.*** *A schematic sectional view of the suture zone of gastric perforation. 1 - Perforation hole; 2 – A fold-duplicator from the anterior wall of the stomach; 3 - Nodal serous-muscular suture.*

We developed this method in an experiment on full-size silicone models of the human stomach from SurgiReal. The laparoscopic suturing was modeled using the LapBox Suture Pad simulator, in which we placed a silicone model of the stomach with a perforation formed on the anterior wall measuring 10x10 mm. Laparoscopic suturing was performed according to the method described above, using laparoscopic instrumentation and an endovideosurgical complex from Karl Storz. We compared the proposed method with the traditional version of PGU suturing with a two-row interrupted suture. The result was assessed using a video endoscopic complex (Olympus Exera).

## Discussion

When comparing the two laparoscopic suturing techniques for PGU, there was no clear technical advantage

of either. Studying the deformation of silicone dummies, as well as their tightness in the operation area, using endoscopic equipment and hydraulic loads, no clear differences were noted between the two methods of suturing.

The analysis of the simulation results allows us to estimate the safety of the described method of suturing. One of the key indicators of its safe use is tightness. Another important criterion is functionality. The absence of narrowing of the lumen of the stomach after applying the proposed option indicates that the normal functioning of the stomach was preserved and that there was no violation of its evacuation function.

Our proposed method of laparoscopic repair of PGU does not require special instruments, special skills of the operating surgeon, and specific equipment in the operating room. It is a simple and affordable option for suturing PGU. This makes it possible to predict its widespread use in clinical practice.

This method is not proposed to replace other widely used methods of suturing a perforated ulcer, but as an additional option for choosing an algorithm of actions for a surgeon who has encountered certain technical difficulties in closing a perforation hole. Our proposed option allows for a wider application of minimally invasive technologies for PGU, even in the case of the above complications. After the experimental part of the research, a patent application (RU, No. 2020132221) was filed.

## Competing Interests

The authors declare that they have no competing interests.

## References

1. Zatevakhina II, Kirienko AI, Sazhina AV. Emergency Abdominal Surgery: A Methodological Guide for the Practitioner. M.: LLC “Medical Information Agency”; 2018. [In Russian].
2. Sazhin VP, Bronstein PG, Zaitsev OV, Kondrus IV, Krivtsov GA, Lobankov VM et al. National clinical guidelines “Perforated ulcer.” Rostov-on-Don; 2015. [In Russian].
3. Shabunin AV, Bedin VV, Grekov DN, Yakomaskin VN, Eminov MZ, Shikov DV. Justification of the choice of surgical approach in perforated peptic ulcer. Moscow Surgical Journal. 2020;(1):7-12. doi: 10.17238/issn2072-3180.2020.1.7-12. [Article in Russian].
4. Schein M, Rogers P, Assalia A. “Common sense in an emergency abdominal surgery, 3rd edition. Russian Surzhinet, 2015. [In Russian].

International Journal of Biomedicine 11(1) (2021) 32-38
http://dx.doi.org/10.21103/Article11(1)_OA6

ORIGINAL ARTICLE

Oncology

INTERNATIONAL JOURNAL OF BIOMEDICINE

# Determination of Blood Parameters using Scanning Electron Microscopy as a Prototype Model for Evaluating the Effectiveness of Radiation Therapy for Cervical Cancer

S. N. Mamaeva, PhD[1]; I. V. Kononova, PhD[2*]; V. A. Alekseev[2]; N. A. Nikolaeva[1]; A. N. Pavlov[1]; M. N. Semenova[1.3]; G. V. Maksimov, PhD, ScD[4,5]

[1]*M.K. Ammosov North-Eastern Federal University, Medical Institute,Yakutsk, Russia*
[2]*Yakut Scientific Center of Complex Medical Problems, Yakutsk, Russia*
[3]*Republican Oncology Dispensary, Yakutsk, Russia*
[4]*Lomonosov Moscow State University, Moscow, Russia*
[5]*National University of Science and Technology MISiS, Moscow, Russia*

## Abstract

Using the method of SEM in patients with cervical cancer (CC) during radiation therapy (RT) revealed differences in the size and morphology of nanoparticles (NPs) localized on the outer surface of the erythrocyte membrane. We found that NP-V ("viruses") objects localized on the surface of the erythrocyte membrane of CC patients before RT have more distinct contours and are smaller in comparison with the number of NP-EV (extracellular vesicles) arising during RT. Our previous study showed that NP-V objects are evenly distributed not only on the surface of erythrocytes but also in blood plasma, and that during the RT the amount of NP-V decreases, while NP-EV both increases and decreases. The linear size of the NP-EV is characterized by a Gaussian distribution, while the NP-V has a normal size distribution in certain ranges with different mean values. We found that the number of NP-Vs having different linear dimensions differ significantly. Using X-ray radiation, we established characteristic elemental composition of NP. The PCR method was used to determine the HPV DNA in blood samples from CC patients. The revealed differences in the morphology and composition of NP, as well as the data of PCR analysis, possibly indicate their different nature and can be used as a criterion for assessing the effectiveness of RT and the recovery period.(**International Journal of Biomedicine. 2021;11(1):32-38.**)

**Key Words**: scanning electron microscopy • cervical cancer • extracellular vesicle • nanoparticle

**For citation**: Mamaeva SN, Kononova IV, Nikolaeva NA, Pavlov AN, Semenova MN, Maksimov GV. Determination of Blood Parameters using Scanning Electron Microscopy as a Prototype Model for Evaluating the Effectiveness of Radiation Therapy for Cervical Cancer. International Journal of Biomedicine. 2021;11(1):32-38. doi:10.21103/Article11(1)_OA6

## Abbreviations

**CC**, cervical cancer; **EV**, extracellular vesicle; **HPV**, human papillomavirus; **NP**, nanoparticle; **RT**, radiation therapy; **RBC**, red blood cell; **SEM**, scanning electron microscopy; **PCR**, polymerase chain reaction.

## Introduction

The increase in relapses or the further development of oncological diseases after a course of therapy, including a course of radiation therapy (RT), poses a challenge for researchers to develop diagnostics for the effectiveness of therapy.

In this paper, we consider the problem of analyzing a set of blood parameters of patients diagnosed with cervical cancer (CC) for a new methodology for determining the effectiveness of RT. Changes in the morphology of erythrocytes under the influence of ionizing radiation during RT were studied using a SEM.

Previously, an SEM has detected nanoparticles (NPs) on the RBC surface in the study of blood samples of CC patients during RT.[1,2] According to their size, the detected NPs probably corresponded to both V ("viruses")[1] and EV (extracellular vesicle)[2] on the cell surface. Changes were

found in the morphology of erythrocytes of CC patients, as well as in the number and size of NPs found on their surface at different stages of RT. Probably, the action of ionizing radiation affects the state of erythrocyte membranes, which is manifested in changes in their morphology and the appearance of NP-EV on the cell surface. It is important that the diameter of the erythrocytes of patients with CC is higher than in the control. The total number of poikilocytes increased by about 1% at each stage of RT. The number of NPs increased at each stage of RT and decreased after the end of RT. The SEM allowed determining erythrocyte agglutination after RT.

Obviously, the results obtained can serve as a basis for the development of indicators for the effectiveness of RT in CC. On the other hand, the nature and process of NP formation on the erythrocyte surface, the number of which changes during RT, requires further research. Our approach will allow monitoring the effectiveness of RT and explaining the causes of recurrence and further development of the disease.

Previously, we gave examples of the presence of EVs in the bodily fluids of cancer patients, including patients with CC.[2-4] EVs (exosomes, microvesicles, and apoptotic bodies), the sizes of which vary in diameter from 30nm to 2000nm, are defined as membrane particles formed on the surface by a cell of any type.[5-7] Some studies [8-9] have led to the conclusion that the presence of exosomes in the blood of cancer patients stimulates changes in the surrounding healthy cells,[10] which indicates the role of exosomes in the transmission of molecular messages from the parent cell to the target cell.[4,11,12] It is assumed that RT aggravates this process in healthy cells by increasing the EV level,[13] which in turn may be mediated by their stimulating effect.[13-16]

These studies indicate the need for a more detailed study of various blood parameters, including the EV number, as biomarkers of cancer progression. In addition, the presence of NPs on the RBC surface, not only in cancer patients, but also in patients with kidney diseases,[1] may also indicate the development of certain viral diseases.

What is the nature of these NPs? Are these NP viruses, vesicles, or are we seeing both? And if we observe both viruses and vesicles, then how to distinguish them?

In the present study, we used SEM and PCR techniques to study NPs found on the RBC surface in patients with CC receiving RT based on our assumption that they may be cellular EV or viruses.

## Materials and Methods

Blood Samples

Smears of venous blood containing K3-EDTA from 16 patients with CC were obtained. The age range was from 45 to 55 years. For 4 CC patients, analyses were taken at the beginning and at each stage of the full course of treatment, and for the remaining 12 CC patients, at the beginning and right after the first stage of RT. For the SEM examination, a thin, even layer of blood was smeared onto a clean degreased glass slide and dried.

To conduct a blood test by PCR, 20 blood samples were prepared from 6 patients with CC who did not undergo RT.

Blood fractionation

Blood samples were centrifuged at 1600 g for 10 minutes. After fractionation, samples of plasma (Pl) and buffy coat (BC) were placed into clean 1.5 ml tubes. The BC samples were further purified from erythrocytes several times using RBC lysis solution and centrifugation until a pure white precipitate was obtained. After that, a few microliters of phosphate buffer (PBS) were added to the sediment. A fraction of erythrocytes with a volume of 1ml was transferred into a 15 ml tube and 14 ml of phosphate buffer was added to it. After gentle mixing, the tubes were centrifuged for 10 minutes at 500g, draining the supernatant every time after centrifugation. The procedure for washing erythrocytes was repeated three times. After the last wash, half of the remaining suspension was transferred into a clean 1.5 ml tube. It was assumed that the bulk of the erythrocytes is associated with viral particles; therefore, the samples of the erythrocyte fraction after washing were marked as Et+.

For the dissociation of viral particles from the surface of erythrocytes, 0.25% trypsin solution was added to the remaining half of the suspension in a volume ratio of 1:3. After incubation at 37°C for 10 minutes, the suspension was vigorously stirred for 10 seconds. Next, the suspension was centrifuged at 4000rpm for 10 minutes. The resulting centrifugation top layer was transferred to a clean tube labeled V+, since this was where the virus particles were supposed to be concentrated. The erythrocyte sediment was repeatedly washed with a large volume of phosphate buffer, to remove the remainder of viral particles from the suspension, and then transferred into a clean 1.5ml tube marked Et- (erythrocytes without viral particles). All samples obtained were stored at -20°C until further use.

DNA extraction

For DNA extraction, 200µl of previously prepared samples with markings Pl, Et+, Et-, and V+ were used. Phenol and chloroform were added to each sample in an amount of 1000 µl and 200 µl, respectively. After vigorous stirring for 15 seconds, the samples were centrifuged at 13000 rpm for 10 minutes. After centrifugation, the upper liquid phase was carefully transferred to a clean tube and cold isopropanol was added to precipitate the DNA. For better precipitation, the samples were incubated at -20°C for an hour, after which they were centrifuged at 13000 rpm for 10 minutes. After centrifugation, the supernatant was carefully discarded, and the tubes were gently inverted on filter paper to remove the remaining liquid. Then the precipitates were dried in a vacuum for 2 minutes. DNA was dissolved in 50 µl TE buffer. The concentration and quality of the isolated DNA were assessed using an Implen P330 Nanophotometer.

PCR

To detect HPV particles, primers GP5+/6+(GP5+: 5'-TTTGTTACTGTGGTAGATACTAC-3' and GP6+: 5'-GAAAAATAAACTGTAAATCATATTC-3')[17,18] and MY09/11(MY09: 5'CGTCCMARRGGAWACTGATC3' and MY11: 5'-GCMCAGGGWCATAAYAATGG-3')[19-22] were used to detect a wide range of HPVs and aimed at detecting the viral gene *L1*. A region of the *β-globin* gene amplified with primers PC03/04 (PCO3: 5'-CTTCTGACACAACTGTGTTCACTAGC-3 'and PCO4: 5'-TCACCACAACTTCATCCACGTTCACC-3') was

used as an internal control and confirmation of the presence of human DNA. To check the reliability of PCR, the products of amplification were separated by electrophoresis in 2% agarose gel.

SEM images and elemental analysis

An SEM was used to study the morphology and surface of erythrocytes in patients with cervical cancer at the beginning, after the first and second (final) stages of RT (external and contact, respectively). We used a high-resolution JSM-7800F SEM(Japan Electron-Optical Laboratory, JEOL, Japan) equipped with a Schottky thermal field emission cathode and a super hybrid objective lens. The microscope is equipped with the Gentle Beam system, which reduces which reduces the speed of electron propagation of the emission beam and allows obtaining high-quality images of biological samples at low accelerating voltages. The following microscope parameters make it possible to study the morphology of the RBC surface in blood smears without spraying conductive coatings, to eliminate damage to the object, and to identify NPs (resolution of 1.2 nm): magnification range 1–100,000 at voltage of 1kV-2kV.

The maximum sample size was 20 mm. The analysis of the NP sizes was carried out using the software JMicroVision v1.2.7 (Roduit, 2007).

An additional SEM module (Oxford INCA Energy 350 energy dispersive microanalysis system) was used to conduct elemental analysis of NP on the surface of erythrocytes and on plasma. The principle of operation of the microanalyzer is based on the method of X-ray microanalysis, the essence of which is the excitation of the analyte atoms with a high-energy electron beam (probe) with simultaneous registration of the characteristic X-ray radiation of the atoms that make up this substance. The microanalyzer operates on the energy dispersive principle, according to which all sections of the X-ray spectrum are recorded simultaneously. To implement this principle, the microanalyzer is equipped with an ultra-thin SATW entrance window for registration of light elements, starting with carbon. Structurally, the microanalyzer includes a main unit with an X-max 80 detector based on an energy dispersive spectrometer and a control unit. A silicon drift detector is used to detect the characteristic X-ray radiation of the microanalyzer. The microanalyzer operation is controlled and the measurement data is processed using an IBM PC type computer and a specialized analytical software system, Aztec, while information on the mass fractions of the analyzed elements is displayed on the microanalyzer monitor.

Radiation therapy

In the Yakutsk Republican Oncological Dispensary (Yakutsk, Russia), patients received radiation therapy, which consists of two stages: first, external beam therapy using an Elekta Synergy accelerator (United Kingdom, external beam radiation therapy, 6-18 MeV), and then brachytherapy using the MultiSourse HDR device (Germany, brachytherapy with Cobalt-60 source). At the first stage, treatment was performed on a linear accelerator in the mode of working with electrons with energy of 6 MeV. The therapy was carried out as follows: 3 times for 5 days daily with a break of 2 days (i.e. at the first stage only 15 fractions of 2Gy were carried out). Then, without a break between the first and second stage, contact RT of 5Gy was performed, interspersed with distanced RT of 2Gy of 5 fractions of each type of RT. Blood samples were collected at the beginning, middle, and end of external beam therapy, then at the middle and at the end of contact radiation therapy. Multiple methods (3D CRT, IMRT, VMAT) were employed in the course of therapy to ensure precision delivery of high doses to the tumor and low doses to healthy tissue.

The study was conducted in accordance with ethical principles of the WMA Declaration of Helsinki (1964, ed. 2013) and approved by the Ethics Committee of the M.K. Ammosov North-Eastern Federal University (protocol No. 13 of April 4, 2018, decision No. 2). Written informed consent was obtained from each patient.

Primary methods for processing experimental results

To determine the elemental composition of EV and NP, as well as the RBC surface without nanosized objects, we used SEM images obtained at 40,000x magnification and at a working distance of 10 mm. Primary methods of statistical processing of experimental data were used to determine the percentage of the weight ratio of chemical elements of nanosized objects. The program displays on the monitor histograms of the weight ratio of the elements of the objects under study. Based on these histograms, the weight distribution of the elements was determined as a Gaussian normal distribution, which was verified using the Shapiro-Wilk test.

## Results and Discussion

This paper presents the results of examining blood samples of a 38-year-old female patient, who is one of the patients diagnosed with CC. To determine the elemental composition of NP-objects, which were conventionally divided into NP-EV and NP-V, we used SEM images of these objects with a magnification of 40,000x and an accelerating voltage of 1-2 kV (Fig.1).

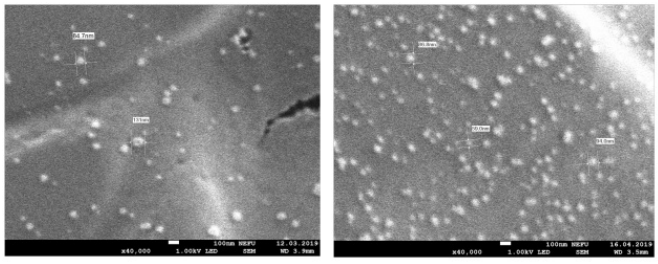

**(A)** **(B)**

***Fig. 1.*** *NP-objects on the RBC surface before (A) and during (B) RT in a blood sample from a patient with CC (magnification of 40,000x, an accelerating voltage of 1 kV).*

NP-Vs found on the surface of erythrocytes before RT have sharper contours and are much smaller than NP-Vs arising during RT. NP-EVs, that arise during RT, are evenly distributed not only on the surface of erythrocytes, but are also found in plasma. The amount of NP-Vs in some samples decreases during RT, while NP-EVs were detected precisely during RT and their number both increased and decreased during RT. The distribution of the linear dimensions of the NP-EVs corresponds to the Gaussian distribution, i.e. have a normal

distribution over one range, while NP-Vs are characterized by a discrete distribution, i.e. the linear dimensions of NP-Vs are different in several characteristic ranges, where they have the form of a Gaussian distribution. Also, the number of NP-Vs having different linear dimensions differs significantly.

To determine the elemental composition of a nanoscale object using SEM, the accelerating voltage equal to 2 kV was chosen, and the beam was directed to the nanoparticles at a magnification of 40,000x. In the course of the study, the elemental composition of 13 NP was obtained for one sample of the patient's blood before and after RT. For example, in Fig. 2, the area of aiming the beam on the NP-EV is indicated and its elemental composition is presented.

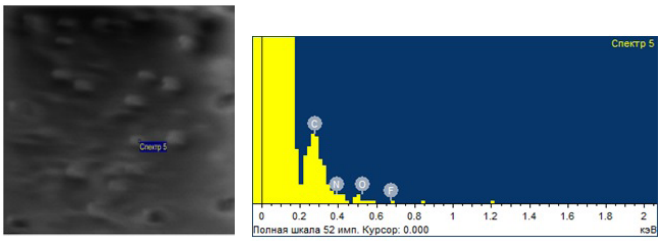


(A) (B)

***Fig. 2.*** *(A) An NP-EV is selected for the study of the elemental composition; (B) The energy spectrum of the NP specified in (A).*

In one of the samples, the spectra of 13 NPs were obtained. Figure 3 shows a histogram of the elemental weight composition of an NP-object in percent on average.

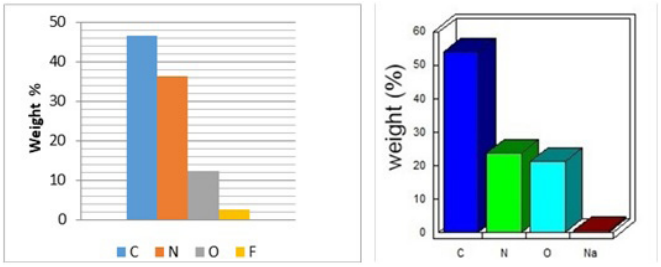


(A) (B)

***Fig. 3.*** *Histogram of the average elemental weight composition of NPs in percent: (A) - NP-VE; (B) – NP-V.*

From our data, it follows that the composition of NPs is approximately the same, which corresponds to the literature data. It is known that the atomic composition is approximately the same in cell vesicles and virus capsids, including HPV16 and HPV18, since they are composed of proteins.[23-29]

Using PCR of the erythrocyte mass of blood samples from CC patients before RT, we found that HPV DNA was detected in 41.7% of samples (16.7% in plasma, 25% in Et+), and the *β-globin* gene was found in 66,7% of samples (16.7% in plasma, 33.3% in Et+, and 16.7% in Et-). SEM studies of the same blood samples revealed the presence of NPs on the RBC surface. The number of NPs on the RBC surface was higher than in plasma. It is known[30] that some viruses trigger the formation of vesicles on the cell surface during infection. It is likely that the correlation between the number of viruses detected by SEM and vesicles on the cell surface may be the basis for the formation of new diagnostic methods and screening of vaccines. Proliferative cancer cells show an increase in cancer tissue as a result of angiogenesis, the acquisition of migratory and invasive abilities, and the acquisition of the ability to avoid attacks by immune cells and, ultimately, the formation of metastatic lesions. It is known that exosomes are involved in each of these processes.[31] In the blood, exosomes can appear from various cells; tumors are the maximum producers of exosomes ($10^9$ vesicles/mL in the blood), which correlates with their role in carcinogenesis. The relationship between circulating exosomes and tumor cells can be described as "seeds and plants." Exosomes obtained from tumor cells that carry different genetic material are released into the bloodstream. Some exosomes spread to distant organs and transform organ cells into tumor cells by transferring the bioactive component to the recipient cell. In addition to an increase in the number of circulating exosomes in the blood of cancer patients, their differences in size and morphology were revealed. For example, it was shown that the sizes of exosomes in serum obtained from patients with pancreatic adenocarcinoma were significantly smaller than those in healthy donors. Also, atomic force microscopy revealed the morphological and molecular differences between exosomes of healthy people and patients with oral cancer.[32] Based on a number of studies [30-43] that examine the relationship of viruses associated with certain cancers and exosomes it can be assumed that the observed increase in the number of vesicles in this study during RT in some patients may be triggered by the effect of radiation on tumor cells. Indeed, in the work of Mata-Rocha et al.,[44] it was found that not only exosomes obtained from HeLa cells contained HPV DNA, but also non-malignant, HPV-positive, cervical specimens with and without squamous intraepithelial lesions had HPV DNA(including E6 and E7 oncogenes). These findings point to another potential source of erythrocyte-associated EV in patients with CC: non-infectious HPV cells. Although it is likely that erythrocyte-associated EV in CC patients can be attributed to cancer cells or HPV-infected cells, the possibility that they are produced by changes in erythrocytes cannot be ruled out. This is evidenced by the fact that the diameter of the detected EV (69.91±12.15 nm)[1] closely matches the size of erythrocyte exosomes described by Huang et al..[45] Probably, erythrocytes release vesicles into the extracellular space in normal conditions, but this process is enhanced in pathology.[46]

The role of this process in the formation of pathological conditions, including CC, has not been sufficiently studied. However, exosomes have been shown to modulate the immune response by increasing the proliferation of T-cells in an antigen-presenting, cell-dependent manner.[47] In fact, the number of T-cells was increased by more than 50% compared with phytohemagglutinin stimulation alone. In addition, EVs formed on the surface of erythrocytes can be involved in inflammation and stimulate the synthesis of pro-inflammatory cytokines in peripheral blood mononuclear cells.[47]

In accordance with the literature data and the results of our studies, the number of NPs on the RBC surface increased, possibly due to the pathology of erythrocytes under the influence of viruses. The secretion of exosomes from erythrocytes, in turn, can also be enhanced by exposure to radiation.

In the course of this study, we monitored the condition of this patient, in whom the greatest increase in the number of NP-EVs was observed after RT for 1.5 years. During this period, courses of chemotherapy and drug therapy were carried out; however, during this period, in comparison with other patients, this patient underwent a relapse and a more aggressive further development of the disease with concomitant complications.

**In conclusion**, the results of this study using SEM and the PCR method indicate that the formation of NP observed before exposure to ionizing radiation can be caused by various processes, namely, the effect of viruses and the formation of vesicles on the cell surface as a result of the disease. PCR analysis of blood samples from patients with CC before RT revealed the presence of HPV DNA in some samples. An increase in the number of EV on the surface of erythrocytes and in plasma during RT indicates the formation of exosomes is activated by both cancer cells themselves and by erythrocytes under the influence of ionizing radiation. In addition, it is also assumed that viruses detected on the surface can more intensively stimulate the formation of vesicles on the surface of erythrocytes during RT.

Further observation of patients with CC after RT shows that an increase in the number of vesicles in the blood may be associated with a negative prognosis related to a relapse of the disease, i.e. about the low efficiency of RT. In addition, a slight decrease in the NP-V number during RT may also indicate a slight effect of RT on NP-V.

It is obvious that further examination of the blood of patients during RT will make it possible to reveal the quantitative ratio of these NPs before and after each stage of RT to determine the criterion (critical ratio) of the effectiveness of therapy. Thus, the complex technique for examining the blood of CC patients, considered in this work, can become the basis for developing a methodology for determining the effectiveness of RT, as well as form the basis for further studies of the role of viruses, vesicles, and erythrocytes in the development of CC.

## Acknowledgments

This study was supported by "The Fund of target capital management North-Eastern Federal University named after M. K. Ammosov"; Georgy V. Maksimov acknowledge financial support from Russian Sciences Foundation (grant RSF 19-79-30062).

## Competing Interests

The authors declare that they have no competing interests.

***Corresponding author:** Irina V. Kononova, PhD. Yakut Scientific Center of Complex Medical Problems, Yakutsk, Russia. E-mail: irinakon.07@mail.ru*

## References

1. Mamaeva SN, Maksimov GV, Antonov SR, Neustroev EP, Kononova IV, Zakharova, et al. Studying of erythrocytes of blood during radiation therapy in cases of cancer of neck of an uterus with application of methods of medical physics and nanobiotechnologies. AIP Conference Proceedings 2041, 050016 (2018); doi: 0.1063/1.5079385.
2. Mamaeva SN, Kononova IV, Ruzhansky M, Nikiforov PV, Nikolaeva NA; Pavlov AN, et al. Using Scanning Electron Microscopy and Atomic Force Microscopy to Study the Formation of Nanoparticles on Red Blood Cell Surface in Cervical Cancer Patients. International Journal of Biomedicine. 2020;10(1):70-75. doi: 10.21103/Article10(1)_OA12.
3. Kim HK, Song KS, Park YS, Kang YH, Lee YJ, Lee KR, et al. Elevated levels of circulating platelet microparticles, VEGF, IL-6 and RANTES in patients with gastric cancer: possible role of a metastasis predictor. Eur J Cancer. 2003 Jan;39(2):184-91. doi: 10.1016/s0959-8049(02)00596-8. Erratum in: Eur J Cancer. 2003 Nov;39(17):2569.
4. Liu J, Sun H, Wang X, Yu Q, Li S, Yu X, Gong W. Increased exosomal microRNA-21 and microRNA-146a levels in the cervicovaginal lavage specimens of patients with cervical cancer. Int J Mol Sci. 2014 Jan 8;15(1):758-73. doi: 10.3390/ijms15010758.
5. Jang SC, Kim SR, Yoon YJ, Park KS, Kim JH, Lee J, et al. YS. In vivo kinetic biodistribution of nano-sized outer membrane vesicles derived from bacteria. Small. 2015 Jan 27;11(4):456-61. doi: 10.1002/smll.201401803.
6. EL Andaloussi S, Mäger I, Breakefield XO, Wood MJ. Extracellular vesicles: biology and emerging therapeutic opportunities. Nat Rev Drug Discov. 2013 May;12(5):347-57. doi: 10.1038/nrd3978.
7. Mangino G, Chiantore MV, Luliano M, Capriotti L, Accardi L, Bonito PD, et al. Role of Extracellular Vesicles in Human Papillomavirus-Induced Tumorigenesis. In: Saxena SK, editor. Current Perspectives in Human Papillomavirus. IntechOpen. 2018;5:1–21. doi: 10.5772/intechopen.80654.
8. Taylor DD, Gercel-Taylor C. MicroRNA signatures of tumor-derived exosomes as diagnostic biomarkers of ovarian cancer. Gynecol Oncol. 2008 Jul;110(1):13-21. doi: 10.1016/j.ygyno.2008.04.033. Erratum in: Gynecol Oncol. 2010 Jan;116(1):153.
9. Keller S, König AK, Marmé F, Runz S, Wolterink S, Koensgen D, et al. Systemic presence and tumor-growth promoting effect of ovarian carcinoma released exosomes. Cancer Lett. 2009 Jun 8;278(1):73-81. doi: 10.1016/j.canlet.2008.12.028.
10. Chai H, Brown RE. Field effect in cancer-an update. Ann Clin Lab Sci. 2009 Fall;39(4):331-7. PMID: 19880759.
11. Honegger A, Schilling D, Bastian S, Sponagel J, Kuryshev V, Sültmann H, et al. Dependence of intracellular and exosomal microRNAs on viral E6/E7 oncogene expression in HPV-positive tumor cells. PLoS Pathog. 2015 Mar 11;11(3):e1004712. doi: 10.1371/journal.ppat.1004712.
12. Li H, Chi X, Li R, Ouyang J, Chen Y. HIV-1-infected cell-derived exosomes promote the growth and progression of cervical cancer. Int J Biol Sci. 2019 Sep 7;15(11):2438-2447. doi: 10.7150/ijbs.38146.
13. Al-Mayah A, Bright S, Chapman K, Irons S, Luo P, Carter D, Goodwin E, Kadhim M. The non-targeted effects of radiation are perpetuated by exosomes. Mutat Res. 2015

Feb;772:38-45. doi: 10.1016/j.mrfmmm.2014.12.007.
14. Arscott WT, Tandle AT, Zhao S, Shabason JE, Gordon IK, Schlaff CD, Zhang G, Tofilon PJ, Camphausen KA. Ionizing radiation and glioblastoma exosomes: implications in tumor biology and cell migration. Transl Oncol. 2013 Dec 1;6(6):638-48. doi: 10.1593/tlo.13640.
15. Mutschelknaus L, Peters C, Winkler K, Yentrapalli R, Heider T, Atkinson MJ, Moertl S. Exosomes Derived from Squamous Head and Neck Cancer Promote Cell Survival after Ionizing Radiation. PLoS One. 2016 Mar 23;11(3):e0152213. doi: 10.1371/journal.pone.0152213.
16. Mutschelknaus L, Azimzadeh O, Heider T, Winkler K, Vetter M, Kell R, Tapio S, Merl-Pham J, Huber SM, Edalat L, Radulović V, Anastasov N, Atkinson MJ, Moertl S. Radiation alters the cargo of exosomes released from squamous head and neck cancer cells to promote migration of recipient cells. Sci Rep. 2017 Sep 29;7(1):12423. doi: 10.1038/s41598-017-12403-6.
17. Snijders PJ, van den Brule AJ, Schrijnemakers HF, Snow G, Meijer CJ, Walboomers JM. The use of general primers in the polymerase chain reaction permits the detection of a broad spectrum of human papillomavirus genotypes. J Gen Virol. 1990;71 (1):173-81. doi: 10.1099/0022-1317-71-1-173. PMID: 2154534.
18. de Roda Husman AM, Walboomers JM, van den Brule AJ, Meijer CJ, Snijders PJ. The use of general primers GP5 and GP6 elongated at their 3' ends with adjacent highly conserved sequences improves human papillomavirus detection by PCR. J Gen Virol. 1995;76(4):1057-62. doi: 10.1099/0022-1317-76-4-1057. PMID: 9049358.
19. Bosch FX, Manos MM, Muñoz N, Sherman M, Jansen AM, Peto J, Schiffman MH, Moreno V, Kurman R, Shah KV. Prevalence of human papillomavirus in cervical cancer: a worldwide perspective. International biological study on cervical cancer (IBSCC) Study Group. J Natl Cancer Inst. 1995;87(11):796-802. doi: 10.1093/jnci/87.11.796. PMID: 7791229.
20. Fuessel Haws AL, He Q, Rady PL, Zhang L, Grady J, Hughes TK, Stisser K, Konig R, Tyring SK. Nested PCR with the PGMY09/11 and GP5(+)/6(+) primer sets improves detection of HPV DNA in cervical samples. J Virol Methods. 2004;122(1):87-93. doi: 10.1016/j.jviromet.2004.08.007. PMID: 15488625.
21. Cope JU, Hildesheim A, Schiffman MH, Manos MM, Lörincz AT, Burk RD, Glass AG, Greer C, Buckland J, Helgesen K, Scott DR, Sherman ME, Kurman RJ, Liaw KL. Comparison of the hybrid capture tube test and PCR for detection of human papillomavirus DNA in cervical specimens. J Clin Microbiol. 1997;35(9):2262-2265. doi:10.1128/JCM.35.9.2262-2265.1997.
22. Shah KV, Daniel RW, Simons JW, Vogelstein B. Investigation of colon cancers for human papillomavirus genomic sequences by polymerase chain reaction. J Surg Oncol. 1992;51(1):5-7. doi: 10.1002/jso.2930510104. PMID: 1325576.
23. Conway MJ, Meyers C. Replication and assembly of human papillomaviruses. J Dent Res. 2009 Apr;88(4):307-17. doi: 10.1177/0022034509333446.
24. Buck CB, Cheng N, Thompson CD, Lowy DR, Steven AC, Schiller JT, Trus BL. Arrangement of L2 within the papillomavirus capsid. J Virol. 2008 Jun;82(11):5190-7. doi: 10.1128/JVI.02726-07.
25. Schiller JT, Lowy DR. Understanding and learning from the success of prophylactic human papillomavirus vaccines. Nat Rev Microbiol. 2012 Oct;10(10):681-92. doi: 10.1038/nrmicro2872.
26. Doorbar J, Gallimore PH. Identification of proteins encoded by the L1 and L2 open reading frames of human papillomavirus 1a. J Virol. 1987 Sep;61(9):2793-9. doi: 10.1128/JVI.61.9.2793-2799.1987.
27. Klimov E, Sobolev V, Solov'ev AM, Perlamutrov Yu, Korsunskaya I. Proteins and microRNA participating in papillomavirus imfection. RUDN Journal of Medicine. 2018;22:43-49. doi:10.22363/2313-0245-2018-22-1-43-49.
28. WHO. Human papillomavirus. Available from: https://www.who.int/biologicals/vaccines/human_papillomavirus_HPV/en/
29. Cooper GM. The Cell: A Molecular Approach. 2nd edition. Sunderland (MA): Sinauer Associates; 2000. Structure of the Plasma Membrane. Available from: https://www.ncbi.nlm.nih.gov/books/NBK9898/
30. Hugel B, Martínez MC, Kunzelmann C, Freyssinet JM. Membrane microparticles: two sides of the coin. Physiology (Bethesda). 2005 Feb;20:22-7. doi: 10.1152/physiol.00029.2004.
31. Doyle LM, Wang MZ. Overview of Extracellular Vesicles, Their Origin, Composition, Purpose, and Methods for Exosome Isolation and Analysis. Cells. 2019 Jul 15;8(7):727. doi: 10.3390/cells8070727.
32. Meckes DG Jr, Raab-Traub N. Microvesicles and viral infection. J Virol. 2011 Dec;85(24):12844-54. doi: 10.1128/JVI.05853-11.
33. Osaki M, Okada F. Exosomes and Their Role in Cancer Progression. Yonago Acta Med. 2019 Jun 20;62(2):182-190. doi: 10.33160/yam.2019.06.002.
34. Meng X, Pan J, Sun S, Gon Z. Circulating exosomes and their cargos in blood as novel biomarkers for cancer. Translational Cancer Research. 2017;7(2):226-242. https://tcr.amegroups.com/article/view/16197.
35. Hood JL, Pan H, Lanza GM, Wickline SA; Consortium for Translational Research in Advanced Imaging and Nanomedicine (C-TRAIN). Paracrine induction of endothelium by tumor exosomes. Lab Invest. 2009 Nov;89(11):1317-28. doi: 10.1038/labinvest.2009.94.
36. Kalluri R. The biology and function of exosomes in cancer. J Clin Invest. 2016 Apr 1;126(4):1208-15. doi: 10.1172/JCI81135.
37. Soung YH, Ford S, Zhang V, Chung J. Exosomes in Cancer Diagnostics. Cancers (Basel). 2017 Jan 12;9(1):8. doi: 10.3390/cancers9010008.
38. Mizutani K, Terazawa R, Kameyama K, Kato T, Horie K, Tsuchiya T, et al. Isolation of prostate cancer-related exosomes. Anticancer Res. 2014 Jul;34(7):3419-23.
39. Skog J, Würdinger T, van Rijn S, Meijer DH, Gainche L, Sena-Esteves M, et al. Glioblastoma microvesicles transport RNA and proteins that promote tumour growth and provide diagnostic biomarkers. Nat Cell Biol. 2008 Dec;10(12):1470-6. doi: 10.1038/ncb1800.
40. Clayton A, Turkes A, Dewitt S, Steadman R, Mason MD, Hallett MB. Adhesion and signaling by B cell-derived exosomes: the role of integrins. FASEB J. 2004 Jun;18(9):977-9. doi: 10.1096/fj.03-1094fje.
41. Fu Q, Zhang Q, Lou Y, Yang J, Nie G, Chen Q, Chen Y, Zhang J, Wang J, Wei T, Qin H, Dang X, Bai X, Liang T. Primary tumor-derived exosomes facilitate metastasis by regulating adhesion of circulating tumor cells via SMAD3 in liver cancer. Oncogene. 2018 Nov;37(47):6105-6118. doi:

10.1038/s41388-018-0391-0. Epub 2018 Jul 10. Erratum in: Oncogene. 2019 Jul;38(28):5740-5741.
42. Fang DY, King HW, Li JY, Gleadle JM. Exosomes and the kidney: blaming the messenger. Nephrology (Carlton). 2013 Jan;18(1):1-10. doi: 10.1111/nep.12005.
43. van Doormaal FF, Kleinjan A, Di Nisio M, Büller HR, Nieuwland R. Cell-derived microvesicles and cancer. Neth J Med. 2009 Jul-Aug;67(7):266-73.
44. Mata-Rocha M, Rodríguez-Hernández RM, Chávez-Olmos P, Garrido E, Robles-Vázquez C, Aguilar-Ruiz S, et al. Presence of HPV DNA in extracellular vesicles from HeLa cells and cervical samples. Enferm Infecc Microbiol Clin. 2020 Apr;38(4):159-165. English, Spanish. doi: 10.1016/j.eimc.2019.06.011.
45. Huang H, Zhu J, Fan L, Lin Q, Fu D, Wei B, Wei S. MicroRNA Profiling of Exosomes Derived from Red Blood Cell Units: Implications in Transfusion-Related Immunomodulation. Biomed Res Int. 2019 Jun 13;2019:2045915. doi: 10.1155/2019/2045915.
46. Harisa GI, Badran MM, Alanazi FK. Erythrocyte nanovesicles: Biogenesis, biological roles and therapeutic approach: Erythrocyte nanovesicles. Saudi Pharm J. 2017 Jan;25(1):8-17. doi: 10.1016/j.jsps.2015.06.010.
47. Danesh A, Inglis HC, Jackman RP, Wu S, Deng X, Muench MO, Heitman JW, Norris PJ. Exosomes from red blood cell units bind to monocytes and induce proinflammatory cytokines, boosting T-cell responses in vitro. Blood. 2014 Jan 30;123(5):687-96. doi: 10.1182/blood-2013-10-530469.

International Journal of Biomedicine 11(1) (2021) 39-41
http://dx.doi.org/10.21103/Article11(1)_OA7

ORIGINAL ARTICLE

Obstetrics and Gynecology

INTERNATIONAL JOURNAL OF BIOMEDICINE

# Preterm Birth in Nulliparous Women

Roziya K. Kuzibaeva; Valery G. Volkov, PhD, ScD*

*Tula State University, Tula, the Russian Federation*

## Abstract

***The aim*** of this study was to assess the frequency and risk factors of Preterm birth (PB), depending on the mechanism of their occurrence in nulliparous women with singleton pregnancies.

***Methods and Results***: This retrospective, population-based cohort study included 327 nulliparous women who gave birth at 22-37 weeks gestation. Three groups of women were formed: Group 1 included 32 women with spontaneous PB, Group 2 included 115 women with preterm premature rupture of membranes (PROM), and Group 3 included 180 women with medical indication for PB. The average age of the mothers for the whole group was 29.3±6.0 years. Depending on the gestational age, PB in 22-27 weeks occurred in 23(7.4%) cases, 28-33 weeks in 110(33.6%) cases, and 34-37 weeks in 194(59%) cases. In our cohort, the frequency of PB resulting from spontaneous PB, PROM or medical indication for PB was 9.8%, 35.2%, and 55%, respectively. The main risk factors for PB were preeclampsia of varying severity, placental abruption, placental insufficiency, and fetal growth retardation. The highest number of pregnancy complications was found in Group 3.

***Conclusion***: PB in nulliparous women occurs more often in the period of 34-37 weeks, the main reason being medical indications (maternal or fetal). Attempts to analyze, interpret, and reduce the level of PB should be considered separately, depending on the mechanism of their occurrence.(**International Journal of Biomedicine. 2021;11(1):39-41.**)

**Key Words:** preterm birth • nulliparity • risk factor • preterm premature rupture of membranes • preeclampsia

**For citation**: Kuzibaeva RK, Volkov VG. Preterm Birth in Nulliparous Women. International Journal of Biomedicine. 2021;11(1):39-41. doi:10.21103/Article11(1)_OA7

## Introduction

Preterm birth (PB) is one of the medical and social problems that are relevant for most countries.[1,2] A nationwide retrospective study found that nulliparity was independently associated with an overall increased risk of spontaneous PB, compared to women during their second pregnancy.[3]

The effectiveness of PB prevention is low, despite a large number of scientific studies in this area. Early diagnosis and accurate prediction of PB and perinatal outcomes are not possible due to the large number of etiological factors and the lack of a specific diagnostic method.[4,5] PB is a complex syndrome with several obstetric precursors, including spontaneous PB with intact membranes, preterm premature rupture of membranes (PROM) with subsequent PB, and indicated or iatrogenic PB.[6,7]

The division of PB into different subtypes is important both from a clinical and epidemiological point of view, since the etiology and prevention strategies for each of them differ.

**The aim** of this study was to assess the frequency and risk factors of PB, depending on the mechanism of their occurrence in nulliparous women.

## Materials and Methods

This retrospective, population-based cohort study included nulliparous women who gave birth in the Tula Regional Perinatal Center at 22-37 weeks gestation from January 1, 2014 to December 31, 2014. The study included 327 women.

Inclusion criteria were first birth, for which the date of the last menstruation is known, confirmed gestational age, and singleton pregnancy. Exclusion criteria were multiple pregnancies and repeated births.

This study was approved by the Ethics Committee of Tula State University.

***Corresponding author**: Prof. Valery G.Volkov, PhD, ScD. Tula State University, Tula, Russia. E-mail: valvol@yandex.ru*

PB was classified into three clinical subtypes: spontaneous PB with intact fetal membranes, PROM before onset of labor, and indicated preterm birth. Thus, three groups of women were formed: Group 1 included 32 women with spontaneous PB, Group 2 included 115 women with PROM, and Group 3 included 180 women with medical indication for PB.[8]

The information relating to the PB subtypes was abstracted from the medical record.

Statistical analysis was performed using the *Statistica* 6.1 software package (Stat-Soft Inc., USA). Group comparisons with respect to categorical variables were performed using chi-square test. A probability value of $P<0.05$ was considered statistically significant.

## Results and Discussion

The average age of the mothers for the whole group was 29.3±6.0 years. Depending on the gestational age, PB in 22-27 weeks occurred in 23(7.4%) cases, 28-33 weeks in 110(33.6%) cases, and 34-37 weeks in 194(59%) cases. In our cohort, the frequency of PB resulting from spontaneous PB, PROM or medical indication for PB was 9.8%, 35.2%, and 55%, respectively.

The effect of diseases on the outcome of pregnancy is presented in Table 1. In Group 3, the leading risk factor for PB was pre-existing hypertension.

***Table 1.***
***Diseases of pregnant women, n(%)***

| Variable | Ggroup 1 (n=32) | Group 2 (n=115) | Group 3 (n=180) | Statistics |
|---|---|---|---|---|
| Anemia | 7 (21.8) | 27 (23.5) | 41 (22.8) | $\chi2$=0.042 $P$=0.9702 |
| Kidney diseases | 3 (9.3) | 11 (9.6) | 30 (16.7) | $\chi2$=3.546 $P$=0.1698 |
| Pre-existing hypertension | 1 (3.1) | 9 (7.8) | 41 (22.8) | $\chi2$=16.107 $P$=0.0003 |
| Diabetes mellitus | 1 (3.1) | 4 (3.5) | 12 (6.7) | $\chi2$=1.757 $P$=0.4154 |
| Myopia | 1 (3.1) | 4 (3.5) | 8 (4.4) | $\chi2$=0.239 $P$=0.8874 |

The effect of pregnancy complications on the delivery period is presented in Table 2. The highest number of pregnancy complications was found in Group 3. The main risk factors for PB were preeclampsia of varying severity, placental abruption, placental insufficiency, and fetal growth retardation.

The method of delivery depended on the mechanism of PB. In Group 1, vaginal delivery prevailed; in Group 2, cesarean section was performed on every third woman; in Group 3, the operation was performed in more than half of the cases.

In the world today, there is an increase in the number of iatrogenic PBs with a simultaneous decrease in the frequency of spontaneous PB.[9,10] It was found that in nulliparous women, PB is more common in the period of 22-37 weeks; the main reason is medical indications.

***Table 2.***
***Complications of pregnancy, n(%)***

| Characteristics | Group 1 (n=32) | Group 2 (n=115) | Group 3 (n=180) | Statistics |
|---|---|---|---|---|
| Polyhydramnios | - | 6 (5.2) | 21 (11.7) | $\chi2$=7.045 $P$=0.0296 |
| Placental insufficiency | 2 (6.2) | 5 (4.3) | 56 (31.1) | $\chi2$= 36.177 $P$=0.0000 |
| Fetal growth retardation | 4 (12.5) | 15 (13.0) | 57 (31.7) | $\chi2$= 15.936 $P$=0.0003 |
| Moderate preeclampsia | - | 1 (0.87) | 32 (17.8) | $\chi2$= 26.091 $P$=0.0000 |
| Severe preeclampsia | - | - | 36 (20) | $\chi2$= 33.037 $P$=0.0000 |
| Urinary tract infections | 3 (9,3) | 11 (9,6) | 30 (16,7) | $\chi2$= 3.546 $P$=0.1698 |
| Placenta previa | - | 4 (3.5) | 7 (3.9) | $\chi2$= 1.271 $P$=0.5297 |
| Placental abruption | - | 2 (1.7) | 22 (12.2) | $\chi2$= 14.148 $P$=0.0008 |
| Rh-negative blood | 1 (3.1) | 11 (9.6) | 28 (15.6) | $\chi2$= 5.086 $P$=0.0786 |
| C-Section | 1 (3.1) | 35 (30.4) | 110 (61.1) | $\chi2$= 51.466 $P$=0 |

The short cervix has been identified as a significant predictor of PB.[11] The risk of PB is inversely proportional to the length of the cervix: the shorter the cervix, the higher the risk of PB and vice versa. Transvaginal cervicometry is an effective method for assessing the risk of PB.[12-16] For this group, treatment methods include the use of progesterone or mechanical intervention, such as cerclage.[17]

For the prevention of iatrogenic PB, methods developed primarily for preeclampsia should be used. Preeclampsia is a serious pregnancy complication that not only determines maternal mortality, but is also associated with PB and prematurity.[18,19] For iatrogenic PB, which is largely mediated by preeclampsia, prophylactic low-dose aspirin reduces premature preeclampsia by 40% in women at higher risk.[20,21]

**In conclusion,** PB in nulliparous women occurs more often in the period of 34-37 weeks, the main reason being medical indications (maternal or fetal).

While greater clarity is needed, efforts to coordinate the prevention of both PB and preeclampsia, even if they are imperfect, are critical as part of any program to maximize maternal safety. Attempts to analyze, interpret, and reduce the level of PB should be considered separately, depending on the mechanism of their occurrence. These data can serve as a basis for changing health policy and clinical decisions on

the prevention of PB and related adverse outcomes. Further research is needed to determine the most effective measures, and not just progesterone, to reduce PB.

## Competing Interests

The authors declare that they have no competing interests.

## References

1. Vogel JP, Chawanpaiboon S, Moller AB, Watananirun K, Bonet M, Lumbiganon P. The global epidemiology of preterm birth. Best Pract Res Clin Obstet Gynaecol. 2018 Oct;52:3-12. doi: 10.1016/j.bpobgyn.2018.04.003.
2. Purisch SE, Gyamfi-Bannerman C. Epidemiology of preterm birth. Semin Perinatol. 2017 Nov;41(7):387-391. doi: 10.1053/j.semperi.2017.07.009.
3. Koullali B, van Zijl MD, Kazemier BM, Oudijk MA, Mol BWJ, Pajkrt E, Ravelli ACJ. The association between parity and spontaneous preterm birth: a population based study. BMC Pregnancy Childbirth. 2020 Apr 21;20(1):233. doi: 10.1186/s12884-020-02940-w.
4. Son M, Miller ES. Predicting preterm birth: Cervical length and fetal fibronectin. Semin Perinatol. 2017 Dec;41(8):445-451. doi: 10.1053/j.semperi.2017.08.002.
5. Volkov V.G., Chursina O.V. A role of comprehensive cervix assessment in the first trimester of pregnancy for predicting preterm delivery. Obstetrics, Gynecology and Reproduction. 2020;14(2):174-181. doi: 10.17749/2313-7347/ob.gyn.rep.2020.094. [Article in Russian].
6. Romero R, Dey SK, Fisher SJ. Preterm labor: one syndrome, many causes. Science. 2014 Aug 15;345(6198):760-5. doi: 10.1126/science.1251816.
7. American College of Obstetricians and Gynecologists' Committee on Practice Bulletins—Obstetrics. Practice Bulletin No. 172: Premature Rupture of Membranes. Obstet Gynecol. 2016 Oct;128(4):e165-77. doi: 10.1097/AOG.0000000000001712.
8. Cunningham FG, Leveno KJ, Bloom SL, Hauth JC, Gilstrap LC III, Wenstrom KD. Williams obstetrics. 22nd ed. New York (NY): McGraw-Hill Medical Publishing Division; 2005.
9. Grétarsdóttir ÁS, Aspelund T, Steingrímsdóttir Þ, Bjarnadóttir RI, Einarsdóttir K. Preterm births in Iceland 1997-2016: Preterm birth rates by gestational age groups and type of preterm birth. Birth. 2020 Mar;47(1):105-114. doi: 10.1111/birt.12467.
10. Lucovnik M, Bregar AT, Steblovnik L, Verdenik I, Gersak K, Blickstein I, Tul N. Changes in incidence of iatrogenic and spontaneous preterm births over time: a population-based study. J Perinat Med. 2016 Jul 1;44(5):505-9. doi: 10.1515/jpm-2015-0271.
11. Hezelgrave NL, Watson HA, Ridout A, Diab F, Seed PT, Chin-Smith E, Tribe RM, Shennan AH. Rationale and design of SuPPoRT: a multi-centre randomised controlled trial to compare three treatments: cervical cerclage, cervical pessary and vaginal progesterone, for the prevention of preterm birth in women who develop a short cervix. BMC Pregnancy Childbirth. 2016 Nov 21;16(1):358. doi: 10.1186/s12884-016-1148-9.
12. Volkov VG., Chursina OV. Ultrasound assessment of cervical length in the first trimester of pregnancy to predict preterm birth. International Journal of Biomedicine. 2018; 8(4):321-323. doi: 10.21103/Article8(4)_OA10
13. Conde-Agudelo A, Romero R, Hassan SS, Yeo L. Transvaginal sonographic cervical length for the prediction of spontaneous preterm birth in twin pregnancies: a systematic review and metaanalysis. Am J Obstet Gynecol. 2010 Aug;203(2):128.e1-12. doi: 10.1016/j.ajog.2010.02.064.
14. Lim AC, Hegeman MA, Huis In 'T Veld MA, Opmeer BC, Bruinse HW, Mol BW. Cervical length measurement for the prediction of preterm birth in multiple pregnancies: a systematic review and bivariate meta-analysis. Ultrasound Obstet Gynecol. 2011 Jul;38(1):10-7. doi: 10.1002/uog.9013.
15. Barros-Silva J, Pedrosa AC, Matias A. Sonographic measurement of cervical length as a predictor of preterm delivery: a systematic review. J Perinat Med. 2014 May;42(3):281-93. doi: 10.1515/jpm-2013-0115.
16. Conde-Agudelo A, Romero R. Predictive accuracy of changes in transvaginal sonographic cervical length over time for preterm birth: a systematic review and metaanalysis. Am J Obstet Gynecol. 2015 Dec;213(6):789-801. doi: 10.1016/j.ajog.2015.06.015.
17. Berghella V, Mackeen AD. Cervical length screening with ultrasound-indicated cerclage compared with history-indicated cerclage for prevention of preterm birth: a meta-analysis. Obstet Gynecol. 2011 Jul;118(1):148-155. doi: 10.1097/AOG.0b013e31821fd5b0.
18. Volkov VG, Granatovich NN, Survillo EV, Cherepenko OV. Retrospective analysis of maternal mortality in preeclampsia and eclampsia. Rossiyskiy Vestnik Akushera-Ginekologa. 2017;3:4-8. doi: 10.17116/rosakush20171734-8 [Article in Russian].
19. Jayaram A, Collier CH, Martin JN. Preterm parturition and pre-eclampsia: The confluence of two great gestational syndromes. Int J Gynaecol Obstet. 2020 Jul;150(1):10-16. doi: 10.1002/ijgo.13173.
20. Bramham K, Parnell B, Nelson-Piercy C, Seed PT, Poston L, Chappell LC. Chronic hypertension and pregnancy outcomes: systematic review and meta-analysis. BMJ. 2014 Apr 15;348:g2301. doi: 10.1136/bmj.g2301.
21. Hoffman MK, Goudar SS, Kodkany BS, Metgud M, Somannavar M, Okitawutshu J, Lokangaka A, Tshefu A, Bose CL, Mwapule A, Mwenechanya M, Chomba E, Carlo WA, Chicuy J, Figueroa L, Garces A, Krebs NF, Jessani S, Zehra F, Saleem S, Goldenberg RL, Kurhe K, Das P, Patel A, Hibberd PL, Achieng E, Nyongesa P, Esamai F, Liechty EA, Goco N, Hemingway-Foday J, Moore J, Nolen TL, McClure EM, Koso-Thomas M, Miodovnik M, Silver R, Derman RJ; ASPIRIN Study Group. Low-dose aspirin for the prevention of preterm delivery in nulliparous women with a singleton pregnancy (ASPIRIN): a randomised, double-blind, placebo-controlled trial. Lancet. 2020 Jan 25;395(10220):285-293. doi: 10.1016/S0140-6736(19)32973-3. Erratum in: Lancet. 2020 Mar 21;395(10228):e53.

International Journal of Biomedicine 11(1) (2021) 42-45
http://dx.doi.org/10.21103/Article11(1)_OA8

ORIGINAL ARTICLE

Obstetrics and Gynecology

INTERNATIONAL JOURNAL OF BIOMEDICINE

# Association of Polymorphisms in *PPARPGC1A, ACE*, and *DRD2* Genes with Gestational Diabetes Mellitus

Agamurad A. Orazmuradov, PhD, ScD[1]; Irina V. Bekbaeva[1*]; Gayane A. Arakelyan[1]; Marianna Z. Abitova[1]; Khalid Haddad[1]; Alexander M. Lopatin[1]; Sergey I. Kyrtikov[1]; Gulnoza K. Eldashova[1]; Ekaterina V. Mukovnikova[1]; Aleksey A. Lukaev, PhD[2]

*[1]Peoples' Friendship University of Russia (RUDN University), Moscow Russia*
*[2]Mytishchi City Clinical Hospital Mytishchi, Moscow Region, Russia*

## Abstract

***The aim*** of our research was to study the distribution of polymorphic variants of the *DRD2/ANKK1* TaqIA (rs1800497 SNP), *PPARGC1A* rs8192678 SNP, and *ACE* I/D in gestational diabetes mellitus (GDM).

**Methods and Results:** The study included 383 pregnant women (gestational age of 37.0–41.0 weeks) with GDM and 68 pregnant women without disturbed carbohydrate metabolism. This was a prospective case-control study. All patients were divided into 3 groups. Group 1 included 211 pregnant women with GDM who received diet therapy only; Group 2 included 172 pregnant women with GDM who received insulin therapy; Group 3 included 68 pregnant women without metabolic disorders. For the *DRD2/ANKK1* TaqIA (rs1800497 SNP) (A1/A2; T/C), we found that the TT homozygous genotype and T allele prevailed in Groups with GDM compared with Group without metabolic disorders.

***Conclusion***: **A** study of the *DRD2/ANKK1* TaqIA (rs1800497 SNP), *PPARGC1A* rs8192678 SNP, and *ACE* I/D revealed statistically significant increased risks for GDM in carriers of the TT genotype and T allele of the *DRD2/ANKK1* TaqIA (rs1800497 SNP).(**International Journal of Biomedicine. 2021;11(1):42-45.**)

**Key Words:** gestational diabetes mellitus • dopamine D2 receptor • PPARPGC-1A • angiotensin-converting enzyme

**For citation**: Orazmuradov AA, Bekbaeva IV, Arakelyan GA, Abitova MZ, Haddad Kh, Lopatin AM, Kyrtikov SI, Eldashova GK, Mukovnikova EV, Lukaev AA. Association of Polymorphisms in PPARPGC-1A, ACE, and DRD2 Genes with Gestational Diabetes Mellitus. International Journal of Biomedicine. 2021;11(1):42-45. doi:10.21103/Article11(1)_OA8

## Abbreviations

**DRD2**, dopamine D2 receptor; **GDM**, gestational diabetes mellitus; **PPARPGC1A**, peroxisome proliferator-activated receptor gamma coactivator 1-alpha; **ACE**, angiotensin-converting enzyme; **T2DM**, type 2 diabetes mellitus.

## Introduction

Despite the well-known role of pregestational obesity in the pathogenesis of gestational diabetes mellitus (GDM), the role of polymorphism of genes responsible for the regulation of carbohydrate and fat metabolism in GDM has been insufficiently studied.[1-3] The available data are quite contradictory. In particular, the significance of the polymorphisms in the *DRD2* gene, *PPARGC1A* gene, and *ACE* gene has been studied in most detail in relation to T2DM.[1,4,5] It should be noted that data on the role of genetic mechanisms in the formation of the complicated course of GDM are extremely few in number. However, current studies report a possible close relationship between genes responsible for the development of T2DM and of GDM.[6]

Several studies show that the Alu Insertion/Deletion (*ACE* I/D) polymorphism present on intron 16 of the *ACE* gene

[*]***Corresponding author:*** *Irina V. Bekbaeva, Peoples' Friendship University of Russia (RUDN University), Moscow, Russia. E-mail: iridescentgirl@yandex.ru*

is associated with T2DM and diabetes-related complications.[6,7] Significant associations of *ACE* SNP's, C1237T, and G2350A with GDM were observed. Haplotype analysis revealed the remarkably significant evidence of association with SNP combination ACE A240T, C1237T, G2350A, and I/D with GDM patients ($P$=0.024).[6] However, the information about the role of this gene in the development of GDM in the world scientific literature is ambiguous. There are studies that disprove the association of the *ACE* gene polymorphisms with GDM.[8]

There is also little information about the role of polymorphisms of other genes responsible for carbohydrate metabolism disorders, such as *DRD2*, *PPARGC1A* (*PGC-1 alpha*), in the pathogenesis of GDM.

SNP rs8192678 (in exon 8, G1444A/Gly482Ser) is the most important polymorphism of the *PPARGC1A* gene.[9,10] It may be a functional point mutation associated with altered gene expression. Altered gene expression might contribute to insulin resistance by impaired metabolic pathways (e.g. PPAR-mediated adipocyte differentiation, lipid oxidation, gluconeogenesis in the liver or glucose transport in the muscles).[10-13] The negative effect of the minor 482Ser allele has been described on metabolic and cardiovascular traits, such as insulin sensitivity and secretion, measures of obesity, lipid and glucose concentrations, adiponectin level, aerobic fitness.[9, 10, 13]

A widely studied SNP, the so-called DRD2/ANKK1 Taq1A polymorphism (rs1800497, C32806T, Glu713Lys) is located ~10 kb downstream from the DRD2 gene in the ankyrin repeat and kinase domain containing 1 (*ANKK1*) gene.[14] However, individuals who carry the A1 (T) allele have reduced brain D2 receptor density,[15] which has been demonstrated to increase the risk for overeating and obesity.[16, 17]

The aim of our research was to study the distribution of polymorphic variants of the *DRD2/ANKK1* TaqIA (rs1800497 SNP), *PPARGC1A* rs8192678 SNP, and *ACE* I/D in GDM.

## Materials and Methods

The study included 383 pregnant women with GDM and 68 pregnant women without disturbed carbohydrate metabolism, who gave birth between the second quarter of 2019 and the third quarter of 2020 (gestational age of 37.0–41.0 weeks). This was a prospective case-control study. Diagnosis of GDM was based on the criteria of the American College of Obstetricians and Gynecologists.[18] All patients were divided into 3 groups. Group 1 included 211 pregnant women with GDM who received diet therapy only; Group 2 included 172 pregnant women with GDM who received insulin therapy; Group 3 included 68 pregnant women without metabolic disorders.

The surveyed patients were questioned about: 1) family history of disorders of carbohydrate metabolism and obesity; 2) chronic somatic and gynecological diseases; 3) reproductive history; and 4) complications of current pregnancy, the timing of GDM detection.

After DNA extraction, the samples were subjected to a PCR-RFLP reaction to analyze the *DRD2/ANKK1* TaqIA (rs1800497 SNP), the *PPARGC1A* rs8192678 SNP, and the *ACE* I/D polymorphism.

Genomic DNA was isolated the peripheral blood leukocytes using standard extraction technique using kits from QIAmpDNABloodMiniKit» («Qiagen», Germany). Genotyping of the *ACE* I/D polymorphism was performed using a PCR method as previously described.[19] The *PPARGC1A* rs8192678 SNP was genotyped by PCR-RFLP analysis.[20] Genotyping of the *DRD2/ANKK1* TaqIA (rs1800497) polymorphism was performed by PCR-RFLP analysis.[21]

Statistical analysis was performed using the Statistica v.10 software package (*StatSoft Inc*, USA). The frequency distribution of genotypes for the studied polymorphic loci was checked for compliance with the Hardy–Weinberg equilibrium (HWE).[22] To check the statistical significance of the differences between the groups, we used Pearson $\chi 2$ test. Odds ratios (ORs) and 95% confidence intervals (CIs) were calculated. A value of $P$<0.05 was considered statistically significant.

## Results and Discussion

The genotype frequencies of all studied polymorphisms were in compliance with HWE ($P$>0.05) (Tables 1-3).

An analysis of the frequency distribution of genotypes and alleles of the *PPARGC1A* rs8192678 SNP showed no differences between groups (Table 1).

***Table 1.***

***Distribution of alleles and genotypes of the PPARGC1A rs8192678 SNP in the studied groups***

| Genotype/ allele | Group 1 (n=133) | Group 2 (n=110) | Group 3 (n=50) | Statistics |
|---|---|---|---|---|
| Ser/Ser | 15 (11.38%) | 18 (16.4%) | 4 (8%) | $\chi^2$=3.261 df=4; $P$=0.5151 |
| Gly/Ser | 72 (54.1%) | 61(55.4%) | 30 (60%) | |
| Gly/Gly | 46 (34.6%) | 31 (28.2%) | 16 (32%) | |
| Ser | 102 (38.3%) | 97 (44.1%) | 38 (38%) | $\chi^2$=1.959 df=2; $P$=0.3774 |
| Gly | 164 (61.7%) | 123 (55.9%) | 62 (62%) | |
| Compliance with HWE | $\chi^2$ =2.79 | $\chi^2$ =1.71 | $\chi^2$ =3.74 | |

For the *DRD2/ANKK1* TaqIA (rs1800497 SNP) (A1/A2; T/C), we found that the TT homozygous genotype and T allele prevailed in Groups 1 and 2 compared with Group 3 (Table 2). The carriage of the T allele of the *DRD2/ANKK1* TaqIA (rs1800497 SNP) was associated with increased *risk* of GDM (Group 1: OR=2.286; 95% CI: 1.320-3.957; $P$<0.0.1 Group 2: OR=2.436; 95% CI: 1.384-4.289; $P$<0.01)

An analysis of the frequency distribution of genotypes and alleles of the *ACE* I/D polymorphism showed no differences between groups (Table 3).

The results obtained regarding the *ACE* I/D polymorphism were not similar to a previous study conducted by Parul Aggarwal et al.[6] and Mani Mirfeizi et al.,[8] in which the researchers found the prevalence of the DD genotype in women with GDM compared to healthy women.

***Table 2.***

***Distribution of alleles and genotypes of the DRD2/ANKK1 TaqIA (rs1800497 SNP) in the studied groups***

| Genotype/ allele | Group 1 (n=72) | Group 2 (n=61) | Croup 3 (n=51) | Statistics |
|---|---|---|---|---|
| C/T | 37 (51.4%) | 27 (44.3%) | 23 (60.5%) | $\chi^2$=12.47 df=4; *P*=0.0142 |
| C/C | 21 (29.2%) | 19( 31.1%) | 26 (34.2%) | |
| T/T | 14 (19.4%) | 15 (24.6%) | 2 (5.3%) | |
| C | 79 (54.9%) | 65 (53.3%) | 75 (73.5%) | $\chi^2$=11.578 df=2; *P*=0.0031 |
| T* | 65 (45.1%) | 57 (46.7%) | 27 (26.5%) | |
| Compliance with HWE | $\chi^2$ =0.1 | $\chi^2$ =0.75 | $\chi^2$ =1.28 | |

**Group 1: OR=2.286; 95% CI: 1.320-3.957; P<0.01*
**Group 2: OR=2.436; 95% CI: 1.384-4.289; P<0.01*

***Table 3.***

***Distribution of alleles and genotypes of the ACE I/D polymorphism in the studied groups***

| Genotype/ allele | Group 1 (n=131) | Group 2 (n=123) | Group 3 (n=58) | Statistics |
|---|---|---|---|---|
| D/D | 10 (7.6%) | 15 (12.2%) | 5 (8.6%) | $\chi^2$=2.073 df=4; *P*=0.7223 |
| I/D | 47 (35.9%) | 46 (37.4%) | 23 (39.7%) | |
| I/I | 74 (56.5%) | 62 (50.4%) | 30 (51.7%) | |
| D | 67 (25.6%) | 76 (30.9%) | 33 (28.4%) | $\chi^2$=1.779 df=2; *P*=0.4109 |
| I | 195 (74.4%) | 170 (69.1%) | 83 (71.6%) | |
| Compliance with HWE | $\chi^2$ =0.43 | $\chi^2$ =1.9 | $\chi^2$ =0.04 | |

Epidemiological studies revealed inconsistent results regarding the association of the *PPARGC1A* rs8192678 SNP with the metabolic syndrome pathology. Regarding T2DM, while some studies confirmed an increased risk,[23-27] others failed to demonstrate a significant effect, or on the contrary, observed a decreased risk in the presence of the minor Ser482 allele.[28-31]

The role of the *DRD2* SNPs in the development of diabetes is not well understood. McGuire V et al.[32] demonstrated that the frequency of the *Taq1a* 'risk' allele (A1) varies according to race/ethnicity. Multiple studies have shown that the presence of at least one A1 risk (T) allele is associated with body mass index (BMI) in adults. [33] The *DRD2/ANKK1* TaqIA polymorphism could influence individual preferences for high-fat/high-sugar foods.[34] Ramos-Lopez et al.[34] suggest that the interactions between the *DRD2/ANKK1* TaqIA polymorphism and dietary factors (sugar and fats) influence triglyceride levels in diabetic patients. Barnard et al.[34] found that the A1 (T) allele appears to be highly prevalent among individuals with type 2 diabetes. Papysheva et al.[35] found that the *DRD2/ANKK1* TaqIA (rs1800497) is involved in carbohydrate and lipid metabolism disorders in pregnant women with GDM. Potential influence of the *DRD2/ANKK1* TaqIA polymorphism on GDM merits further exploration.

**In conclusion**, a study of the *DRD2/ANKK1* TaqIA (rs1800497 SNP), *PPARGC1A* rs8192678 SNP, and *ACE* I/D revealed statistically significant increased risks for GDM in carriers of the TT genotype and T allele of the *DRD2/ANKK1* TaqIA (rs1800497 SNP).

## Competing Interests

The authors declare that they have no competing interests.

## References

1. Radzinsky VE, Botasheva TL, Kotaysh GA. Obesity. Diabetes. Pregnancy. Versions and contraversions, clinical practices, prospects. M.: GEOTAR-Media, 2020.
2. Orazmuradov AA, Akhmatova AN, Savenkova IV, Arakelyan GA, Damirova KF, Haddad Kh., Orazmuradova AA. Influence of Gestational Weight Gain on the Development of Complications of Gestational Diabetes Mellitus: A Literature Review. Sys Rev Pharm. 2020;11(7):462-464.
3. Orazmuradov AA, Savenkova IV, Arakelyan GA, Damirova SF, Papysheva OV, Lukanovskaya OB. Peculiar Properties of Metabolism Women with Gestational Diabetes Mellitus. Sys Rev Pharm. 2020;11(2):237-241.
4. Orazmuradov AA, Damirova SF, Savenkova IV, Arakelyan GA, Barinova EK, Haddad Kh. Prediction and Pregravid Preparation of Women with High-Risk Development of Gestational Diabetes Mellitus. Sys Rev Pharm. 2020;11(6):175-178.
5. Orazmuradov AA, Papysheva OV, Soyunov MA, Bekbaeva IV, Arakelyan GA, Haddad Kh, Lopatin AM, et al. Peculiar Properties of Pregnancy and Childbirth in Women with Gestational Diabetes Mellitus Depending on Body Weight. Sys Rev Pharm. 2020 11(11):1338-1340.
6. Aggarwal P, Agarwal N, Das N, Dalal K. Association of polymorphisms in angiotensin-converting enzyme gene with gestational diabetes mellitus in Indian women. Int J Appl Basic Med Res. 2016 Jan-Mar;6(1):31-7. doi: 10.4103/2229-516X.174006.
7. Zhou JB, Yang JK, Lu JK, An YH. Angiotensin-converting enzyme gene polymorphism is associated with type 2 diabetes: a meta-analysis. Mol Biol Rep. 2010 Jan;37(1):67-73. doi: 10.1007/s11033-009-9648-6.
8. Mirfeizi M, Hasanzad M, Sattari M, Afshari M, Abbasi D, Ajoodani Z, Sheykheslam AB. Association of eNOS and ACE gene polymorphisms as a genetic risk factor in gestational diabetes in Iranian women. J Diabetes Metab Disord. 2018 Aug 6;17(2):123-127. doi: 10.1007/s40200-018-0348-4. Erratum in: J Diabetes Metab Disord. 2020 Jun 25;19(2):2063.
9. Wu H, Deng X, Shi Y, Su Y, Wei J, Duan H. PGC-1α, glucose metabolism and type 2 diabetes mellitus. J Endocrinol. 2016 Jun;229(3):R99-R115. doi: 10.1530/JOE-16-0021.
10. Vohl MC, Houde A, Lebel S, Hould FS, Marceau P. Effects of the peroxisome proliferator-activated receptor-gamma co-activator-1 Gly482Ser variant on features of the metabolic syndrome. Mol Genet Metab. 2005 Sep-Oct;86(1-2):300-6. doi: 10.1016/j.ymgme.2005.07.002.
11. Rodgers JT, Lerin C, Gerhart-Hines Z, Puigserver P. Metabolic adaptations through the PGC-1 alpha and SIRT1 pathways. FEBS Lett. 2008 Jan 9;582(1):46-53. doi: 10.1016/j.febslet.2007.11.034.

12. Choi YS, Hong JM, Lim S, Ko KS, Pak YK. Impaired coactivator activity of the Gly482 variant of peroxisome proliferator-activated receptor gamma coactivator-1alpha (PGC-1alpha) on mitochondrial transcription factor A (Tfam) promoter. Biochem Biophys Res Commun. 2006 Jun 9;344(3):708-12. doi: 10.1016/j.bbrc.2006.03.193.
13. Fanelli M, Filippi E, Sentinelli F, Romeo S, Fallarino M, Buzzetti R, et al. The Gly482Ser missense mutation of the peroxisome proliferator-activated receptor gamma coactivator-1 alpha (PGC-1 alpha) gene associates with reduced insulin sensitivity in normal and glucose-intolerant obese subjects. Dis Markers. 2005;21(4):175-80. doi: 10.1155/2005/576748.
14. Savitz J, Hodgkinson CA, Martin-Soelch C, Shen PH, Szczepanik J, Nugent AC, et al. DRD2/ANKK1 Taq1A polymorphism (rs1800497) has opposing effects on D2/3 receptor binding in healthy controls and patients with major depressive disorder. Int J Neuropsychopharmacol. 2013 Oct;16(9):2095-101. doi: 10.1017/S146114571300045X.
15. Noble EP, Noble RE, Ritchie T, Syndulko K, Bohlman MC, Noble LA, Zhang Y, Sparkes RS, Grandy DK. D2 dopamine receptor gene and obesity. Int J Eat Disord. 1994 Apr;15(3):205-17.
16. Stice E, Yokum S, Zald D, Dagher A. Dopamine-based reward circuitry responsivity, genetics, and overeating. Curr Top Behav Neurosci. 2011;6:81-93. doi: 10.1007/7854_2010_89.
17. Cardel MI, Lemas DJ, Lee AM, Miller DR, Huo T, Klimentidis YC, Fernandez JR. Taq1a polymorphism (rs1800497) is associated with obesity-related outcomes and dietary intake in a multi-ethnic sample of children. Pediatr Obes. 2019 Feb;14(2):e12470. doi: 10.1111/ijpo.12470.
18. ACOG Practice Bulletin No. 190: Gestational Diabetes Mellitus. Obstet Gynecol. 2018 Feb;131(2):e49-e64. doi: 10.1097/AOG.0000000000002501.
19. Cambien F, Poirier O, Lecerf L, Evans A, Cambou JP, Arveiler D, et al. Deletion polymorphism in the gene for angiotensin-converting enzyme is a potent risk factor for myocardial infarction. Nature. 1992 Oct 15;359(6396):641-4. doi: 10.1038/359641a0.
20. Ek J, Andersen G, Urhammer SA, Gaede PH, Drivsholm T, Borch-Johnsen K, Hansen T, Pedersen O. Mutation analysis of peroxisome proliferator-activated receptor-gamma coactivator-1 (PGC-1) and relationships of identified amino acid polymorphisms to Type II diabetes mellitus. Diabetologia. 2001 Dec;44(12):2220-6. doi: 10.1007/s001250100032.
21. Grandy DK, Zhang Y, Civelli O. PCR detection of the TaqA RFLP at the DRD2 locus. Hum Mol Genet. 1993 Dec;2(12):2197. doi: 10.1093/hmg/2.12.2197-a.
22. Rodriguez S, Gaunt TR, Day IN. Hardy-Weinberg equilibrium testing of biological ascertainment for Mendelian randomization studies. Am J Epidemiol. 2009 Feb 15;169(4):505-14. doi: 10.1093/aje/kwn359.
23. Andersen G, Hansen T, Gharani N, Fraiyling TM, Owen KR, Sampson M, Ellard S, Walker M, Hitman GA, Hattersley A, Mccarthy MI, Pedersen O. A common Gly482Ser polymorphism of PGC-1 is associated with type 2 diabetes mellitus in two European populations. Diabetes. 2002;51:A49–50.
24. Kunej T, Globocnik Petrovic M, Dovc P, Peterlin B, Petrovic D. A Gly482Ser polymorphism of the peroxisome proliferator-activated receptor-gamma coactivator-1 (PGC-1) gene is associated with type 2 diabetes in Caucasians. Folia Biol (Praha). 2004;50(5):157-8.
25. Shokouhi S, Haghani K, Borji P, Bakhtiyari S. Association between PGC-1alpha gene polymorphisms and type 2 diabetes risk: a case-control study of an Iranian population. Can J Diabetes. 2015 Feb;39(1):65-72. doi: 10.1016/j.jcjd.2014.05.003.
26. Jemaa Z, Kallel A, Sleimi C, Mahjoubi I, Feki M, Ftouhi B, et al. The Gly482Ser polymorphism of the peroxisome proliferator-activated receptor-g coactivator-1a (PGC-1a) is associated with type 2 diabetes in Tunisian population. Diabetes & Metabolic Syndrome: Clinical Research & Reviews. 2015;9(4):316–319.
27. Villegas R, Williams SM, Gao YT, Long J, Shi J, Cai H, et al.; AGEN-T2D Consortium, Hu F, Cai Q, Zheng W, Shu XO. Genetic variation in the peroxisome proliferator-activated receptor (PPAR) and peroxisome proliferator-activated receptor gamma co-activator 1 (PGC1) gene families and type 2 diabetes. Ann Hum Genet. 2014 Jan;78(1):23-32. doi: 10.1111/ahg.12044.
28. Lacquemant C, Chikri M, Boutin P, Samson C, Froguel P. No association between the G482S polymorphism of the proliferator-activated receptor-gamma coactivator-1 (PGC-1) gene and Type II diabetes in French Caucasians. Diabetologia. 2002 Apr;45(4):602-3; author reply 604. doi: 10.1007/s00125-002-0783-z.
29. Stumvoll M, Fritsche A, t'Hart LM, Machann J, Thamer C, Tschritter O, et al. The Gly482Ser variant in the peroxisome proliferator-activated receptor gamma coactivator-1 is not associated with diabetes-related traits in non-diabetic German and Dutch populations. Exp Clin Endocrinol Diabetes. 2004 May;112(5):253-7. doi: 10.1055/s-2004-817972.
30. Vohl MC, Houde A, Lebel S, Hould FS, Marceau P. Effects of the peroxisome proliferator-activated receptor-gamma co-activator-1 Gly482Ser variant on features of the metabolic syndrome. Mol Genet Metab. 2005 Sep-Oct;86(1-2):300-6. doi: 10.1016/j.ymgme.2005.07.002.
31. Esterbauer H, Oberkofler H, Linnemayr V, Iglseder B, Hedegger M, Wolfsgruber P, Paulweber B, Fastner G, Krempler F, Patsch W. Peroxisome proliferator-activated receptor-gamma coactivator-1 gene locus: associations with obesity indices in middle-aged women. Diabetes. 2002 Apr;51(4):1281-6. doi: 10.2337/diabetes.51.4.1281.
32. McGuire V, Van Den Eeden SK, Tanner CM, Kamel F, Umbach DM, Marder K, et al. Association of DRD2 and DRD3 polymorphisms with Parkinson's disease in a multiethnic consortium. J Neurol Sci. 2011 Aug 15;307(1-2):22-9. doi: 10.1016/j.jns.2011.05.031.
33. Barnard ND, Noble EP, Ritchie T, Cohen J, Jenkins DJ, Turner-McGrievy G, Gloede L, Green AA, Ferdowsian H. D2 dopamine receptor Taq1A polymorphism, body weight, and dietary intake in type 2 diabetes. Nutrition. 2009 Jan;25(1):58-65. doi: 10.1016/j.nut.2008.07.012.
34. Ramos-Lopez O, Mejia-Godoy R, Frías-Delgadillo KJ, Torres-Valadez R, Flores-García A, Sánchez-Enríquez S, et al. Interactions between DRD2/ANKK1 TaqIA Polymorphism and Dietary Factors Influence Plasma Triglyceride Concentrations in Diabetic Patients from Western Mexico: A Cross-sectional Study. Nutrients. 2019 Nov 22;11(12):2863. doi: 10.3390/nu11122863.
35. Papysheva OV, Nurbekov MK, Mayatskaya TA, Kotaysh GA, Kozhevnikova EN, Shchipkova ES, Morozov SG. Influence of the PGC1α, ACE and DRD2 gene polymorphisms on the development and the course of gestational diabetes. Gynecology, Obstetrics and Perinatology. 2020;19(3):63–71. doi: 10.20953/1726-1678-2020-3-63-71. [Article in Russian].

International Journal of Biomedicine 11(1) (2021) 46-49
http://dx.doi.org/10.21103/Article11(1)_OA9

ORIGINAL ARTICLE

Obstetrics and Gynecology

INTERNATIONAL JOURNAL OF BIOMEDICINE

# Cytomorphometric Analysis of Cervical Papanicolaou Smear for Females with Gynecological Clinical Complaints

Sahar Elderdiri Osman[1], Ehab Mohammed Elmadenah[2], Osman Mohammed Elmahi[3], Mubarak Elsaeed Alkarsani[3], Lienda Bashier Eltayeb[4], Hisham Ali Waggiallah[4*]

[1]*Department Histopathology and Cytology, Medical Laboratory Science Program, Alfajr College of Science and Technology, Khartoum, Sudan*
[2]*Department of Hematology, Faculty of Medical Laboratory Science, Dongola University, Aldabbah, Sudan*
[3]*Department Histopathology and Cytology, Faculty of Medical Laboratory Sciences, Karary University, Khartoum, Sudan*
[4]*Department of Medical Laboratory Science, College of Applied Medical Science, Prince Sattam bin Abdulaziz University, Al-Kharj, Saudi Arabia*

## Abstract

***Background***: Limited information is provided on the quantitative cytomorphometric study of the cervical Pap test. The cervical Pap test is an important screening program for cervical cancer. A quantitative cytomorphometric examination of cervical Pap is used to accurately identify precancerous and cancerous lesions early and to reduce the occurrence and avoidance of invasive cancer. This study was aimed to assess the cytomorphological parameters (nuclear diameter [ND], cytoplasm diameter [CD], and nuclear-to-cytoplasmic ratio [N/C ratio]) of squamous epithelial cells from a cervical Pap smear.

***Methods and Results***: A prospective study was performed on 142 consecutive cervical Pap smears from women with gynecological clinical complaints. The ND and CD were determined by the Optika optical microscope camera using a digitizer cursor in both axes. The final images were taken with an X40 magnification. The ND, CD, and the N/C ratio were then measured and expressed in micrometers.

The women were classified into 5 age groups: 5(3.5%) in the age group of <19 years, 46(32%) in the 20-29 group, 67(47.2%) in the 30-39 group, 23(16.2%) in the 40-49 group, and 1(0.7%) woman was over age 50. There were no significant differences in the N/C ratio of superficial cells between age groups. The ND, CD, and the N/C ratio were significantly higher in women with clinical complaints than in women without clinical complaints

***Conclusion***: Cytomorphometic analysis might assist in the identification of cellular alterations due to gynecological diseases and increase the sensitivity and accuracy of the Pap smear technique.(**International Journal of Biomedicine. 2021;11(1):46-49.**)

**Key Words**: cytomophometry • Pap smear • nuclear diameter • cytoplasm diameter • nuclear-to-cytoplasm ratio

**For citation**: Osman SE, Elmadenah EM, Elmahi OM, Alkarsani ME, Eltayeb LB, Waggiallah HA. Cytomorphometric Analysis of Cervical Papanicolaou Smear for Females with Gynecological Clinical Complaints. International Journal of Biomedicine. 2021;11(1):46-49. doi:10.21103/Article11(1)_OA9

## Introduction

A Pap test is an important screening procedure for cervical cancer. The identification of precancerous lesions by the Pap test decreases the occurrence of precancerous lesions and avoids the development of invasive cancer.(1) The background of the Pap test, developed by George Papanicolaou, the "father of cytology," has shown that specific cervix cells have morphological characteristics that can be used to diagnose carcinoma. Cells are obtained from the cervix, the lower part of the uterus protruding into the vagina.(2) The most mature squamous cell is considered a superficial cell, typically polygonal (45-50 μm in diameter), with a pyknotic nucleus (5-6 μm in diameter). Intermediate cells are also mature squamous

cells, typically polygonal (20-40 µm in diameter), with vesicular nucleus dimensions of 6-9 µm in diameter, and sometimes binucleated. The immature cells are named parabasal and basal cells, the parabasal cells are circular or oval rather than polygonal (15-30 µm in diameter), the nucleus is variable in size and typically larger than that of the intermediate cell. Parabasal and basal cells are not normally examined because the Pap test does not scrape off the entire thickness of the epithelium, just a few upper layers.[3] Exfoliative cytology is focused on epithelial tissue physiology. Usually, the epithelium is routinely exfoliated, and cell surface and thickness loss are permanent.[4] Ordinary epithelial cells are coherent in nature, but they shed or exfoliate as they mature. During infection and malignancies, exfoliation is excessive and epithelial cell morphology varied. [5] Cytomorphometry is a quantitative approach focused on the calculation of cytomorphological parameters, including the nuclear diameter (ND), cytoplasm diameter (CD), and the nuclear-to-cytoplasmic ratio (N/C ratio), which may improve the efficiency of the cytology.[6] Most of the published research addresses cytomorphological analysis for buccal smear[7,8] or morphometric study for histological samples of the cervix;[9] few studies discuss cytomorphological investigation for the Pap smear. The current research was therefore intended to evaluate the quantitative analysis for the cytomorphological parameters of the exfoliative, epithelial squamous cell in the cervical Pap smear.

## Materials and Methods

A prospective study was performed on 142 consecutive cervical Pap smears from women with gynecological clinical complaints. The scraped materials were taken with a cyto-spatula, smeared onto a glass slide, and immediately fixed in 95% ethyl alcohol. Subsequently, the smears were stained by the Papanicolaou staining technique.

**Papanicolaou staining method**

Slides were dehydrated by a descending concentration of alcohol (95%, 70%) and distilled water for 3 minutes each. They were treated with Mayer's Hematoxylin for 5 minutes for nuclear stain and blued for 10 minutes in flowing tap water. The smears were counterstained with orange G6 for 5 minutes, differentiated in 95% ethanol for 10 seconds, then treated with Eosin EA50 for cytoplasmic stain for 5 minutes and again differentiated in 95% ethanol for 10 seconds. Finally, the smears were dehydrated through ascending concentration of alcohol (70%, 95%, 100%) for 3 minutes each, cleared in xylene, and mounted in Distrene Polystryne Xylene. The cells were examined by using X40 objective lenses.[10]

**Cytomorphometric analysis**

Ten clearly defined cells with good staining were chosen by systematic sampling stepwise by shifting the microscope stage in a Z shape from left to right in order to avoid measuring the same cell again. Any folded, clumped, or distorted nucleus or cell was avoided in each smear. The superficial, intermediate and parabasal cells were established by morphology and staining characteristics. The ND and CD were determined by the Optika optical microscope camera using a digitizer cursor in both axes. The final images were taken with an X40 magnification. The ND, CD and N/C ratios were then measured and expressed in micrometers. Quality management measures were adopted during the collection and processing of samples.

Statistical analysis was performed using the statistical software package SPSS version 20.0 (IBM Corp., Armonk, N.Y., USA). Continuous variables were presented as mean±standard deviation (SD). Means of 2 continuous normally distributed variables were compared by independent samples Student's t-test. Multiple comparisons were performed with one-way ANOVA. The frequencies of categorical variables were compared using Pearson's chi-squared test. A value of $P \leq 0.05$ was considered significant.

The ethics and research committee approved the study, and consent forms were obtained from all patients prior to procedures.

## Results

A total of 142 smears from women aged from 16 to 49 years were examined. The women were classified into 5 age groups: 5(3.5%) in the age group of <19 years, 46(32%) in the 20-29 group, 67(47.2%) in the 30-39 group, 23(16.2%) in the 40-49 group, and 1(0.7%) woman was over age 50. Unsatisfactory smears (n=14) were excluded from the study. The quantitative cytomorphological analysis is shown in Table 1, Figure 1, and Figure 2.

***Table 1.***

***Cytomorphometric parameters (µm) in superficial (s) and intermediate (i) cells***

| Type of cells | n | Minimum | Maximum | Mean±SD |
|---|---|---|---|---|
| NDs | 128 | 2.2 | 9.00 | 4.9±1.7 |
| CDs | 128 | 17.2 | 62.00 | 37.5±10.6 |
| N/Cs | 128 | 0.05 | 0.24 | 0.1±0.03 |
| NDs | 117 | 3.0 | 18.60 | 6.9±2.6 |
| CDi | 117 | 13.6 | 57.40 | 32.2±10.1 |
| N/Ci | 117 | 0.1 | 0.57 | 0.23±0.07 |
| NDi | 5 | 6.0 | 10.00 | 8.0±1.6 |
| CDi | 5 | 23.0 | 35.00 | 29.0±5.3 |
| N/Ci | 5 | 0.9 | 0.43 | 0.9±0.1 |

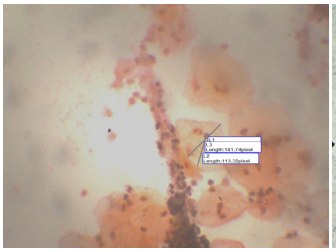

***Fig. 1.*** *Cervical Pap smear. Measuring the CD and N/C ratio using OPTIKA software.*

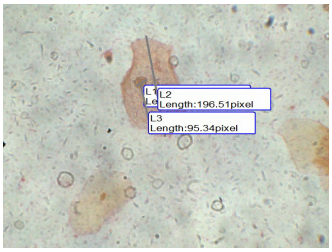


***Fig. 2.*** *Cervical Pap smear. Measuring the ND and N/C ratio using OPTIKA software.*

There were no significant differences in the N/C ratio of superficial and intermediate cells between age groups

(Table 2). The ND, CD, and the N/C ratio were significantly higher in women with clinical complaints than in women without clinical complaints (Table 3). There were significant differences in ND, CD, and N/C ratio according to type of clinical complaints (Table 4).

***Table 2.***

***The N/C ratio for superficial and intermediate cells according to the age groups***

| Type of cells | Age group (years) | n | Mean±SD | Minimum | Maximum | *P*-value |
|---|---|---|---|---|---|---|
| Superficial | < 19 | 4 | 0.1±0.02 | 0.09 | 0.14 | 0.39 |
| | 20-29 | 44 | 0.1±0.03 | 0.05 | 0.24 | |
| | 30-39 | 60 | 0.1±0.03 | 0.07 | 0.23 | |
| | 40-49 | 20 | 0.1±0.03 | 0.07 | 0.17 | |
| Intermediate | < 19 | 4 | 0.2±0.09 | 0.13 | 0.25 | 0.89 |
| | 20-29 | 38 | 0.2±0.08 | 0.12 | 0.44 | |
| | 30-39 | 58 | 0.2±0.8 | 0.14 | 0.57 | |
| | 40-49 | 17 | 0.2±0.06 | 0.14 | 0.38 | |

***Table 3.***

***Cytomorphometric parameters (CMP) according to routine Pap for women with or without clinical complaints***

| Type of cells | CMP | Clinical complaints | Mean±SD | *P*-value |
|---|---|---|---|---|
| Superficial cells | ND | Yes | 7.0±1.1 | 0.001 |
| | | No | 4.7±1.6 | |
| | CD | Yes | 41.6±6.6 | 0.081 |
| | | No | 37.1±10.8 | |
| | N/C ratio | Yes | 0.17±0.03 | 0.003 |
| | | No | 0.1±0.03 | |
| Intermediate cells | ND | Yes | 9.4±3.2 | 0.002 |
| | | No | 6.7±2.1 | |
| | CD | Yes | 35.7±5.6 | 0.306 |
| | | No | 31.96±10.27 | |
| | N/C ratio | Yes | 0.275±0.126 | 0.047 |
| | | No | 0.221±0.069 | |

***Table 4.***

***Cytomorphometric parameters for superficial cells according to type of clinical complaints***

| Superficial cell | n=128 | ND | CD | N/C |
|---|---|---|---|---|
| Lower abdominal pain with vaginal discharge | 57 | 4.5±1.5 | 36.3±11.7 | 0.1±0.03 |
| Infertility | 38 | 5.4±1.6 | 38.4±9.9 | 0.5±0.02 |
| Fistula | 3 | 5.6±0.3 | 44.1±7.9 | 0.1±0.02 |
| Uterine fibroid | 3 | 5.7±2.3 | 38.7±14.6 | 0.2±0.03 |
| Irregular cycle | 12 | 4.2±1.4 | 40.4±11.0 | 0.1±0.02 |
| Routine Pap | 9 | 7.2±0.9 | 41.9±6.9 | 0.2±0.03 |
| Oophoritis | 3 | 4.5±2.1 | 31.2±8.3 | 0.1±0.1 |
| Syphilis | 2 | 2.8± 0.0 | 24.9±1.6 | 0.1±0.02 |
| Polycystic ovaries | 1 | 3.20 | 25.8 | 0.124 |
| *P*-value | | 0.001 | 0.28 | 0.001 |

# Discussion

Cytomorphometric testing or image processing of exfoliated cells has also been proposed as a main measure to the classification and identification of cell and nuclear variations in these cytological smears, indicating that this computer-assisted analysis of microscope images can improve the susceptibility of exfoliative cytology to early detection of oral cancer, as these techniques are reliable, accurate and precise. The Pap test is the most effective cancer screening test in the world, although it has a high incidence of false-negative results due to subjective interpretation.

The current research attempted to calculate the ND, CD, and N/C ratios by computer-assisted, morphometric analysis in cervical exfoliative cytology using Optika software. In this study, there were no substantial differences in the N/C ratio of superficial cells between age groups, and this is inconsistent with previous studies conducted by Anuradha and Sivapathasundharam.[11] Patel et al.[12] observed that basal cells could only divide by a set of numbers; therefore, tissue renewal ability decreases with age, leading to aged cell accumulation. Cells that remain for a longer period of time contribute to the effects of various local environmental factors, which can be clarified by both estrogen and progesterone increase at puberty, accompanied by an increase and decrease in the uterine cycle stage. The level of these hormones declines at post-menopause. These hormones are responsible for the rise in ND, CD, and N/C ratio.[11,12]

In our research, the ND and N/C ratio were statistically significant among women at routine Pap clinics and women with clinical complaints. This finding explains that most gynecological complaints relate to fertility hormones and later promote the growth, differentiation, and maturation of the squamous epithelium of the cervix.[13]

A number of diseases, inflammation, and reactive conditions have contributed to a change in cell morphology. Many causes, such as cervicitis, have been accompanied by loss of cervical columnar cells, a typical aspect of the maturation process. As a result, sexually transmitted infections are hypothesized to encourage maturation through inflammation activation and subsequent cellular repair. In comparison, oral contraception has been associated with increased cervical ectopy (or less cervical maturation). Some have indicated that the presence of increased immaturity is due to hormonal contraception, which induces tissue edema and endocervical eversion.[13] Rani et al.[14] reported that cytomorphometry parameters were statistically significant between precancerous and cancerous Pap smears. Cigarette smoking is another potential influence because nicotine and its metabolites can be found in cervical mucus.[15] Interestingly, both hormonal contraceptives and longtime smoking have been correlated with an induced risk of cervical cancer,[16,17] and HPV infection is widespread in adolescents and young adults.[18]

**In conclusion**, it was evident that cytomorphometic analysis might assist in the identification of cellular alterations due to gynecological diseases and increase the sensitivity and accuracy of the Pap smear technique.

## Limitations of the study

Only 142 females participated in this research, so for further studies, the sample size should be expanded in order to improve the precision and accuracy of the findings by examining each of the gynecological problems and making associations with alterations in cervical squamous cells, while also taking into account age and other environmental factors.

## Acknowledgments

This publication was supported by the Deanship of Scientific Research at Prince Sattam bin Abdulaziz University, Alkharj, Saudi Arabia.

## Competing Interests

The authors declare that they have no competing interests.

## References

1. Conceição T, Braga C, Rosado L, Vasconcelos MJM. A Review of Computational Methods for Cervical Cells Segmentation and Abnormality Classification. Int J Mol Sci. 2019 Oct 15;20(20):5114. doi: 10.3390/ijms20205114.
2. Safaeian M, Solomon D, Castle PE. Cervical cancer prevention--cervical screening: science in evolution. Obstet Gynecol Clin North Am. 2007 Dec;34(4):739-60, ix. doi: 10.1016/j.ogc.2007.09.004.
3. Cibas ES, Alonzo TA, Austin RM, Bolick DR, Glant MD, Henry MR, Moriarty AT, Molina JT, Rushing L, Slowman SD, Torno R, Eisenhut CC. The MonoPrep Pap test for the detection of cervical cancer and its precursors. Part I: results of a multicenter clinical trial. Am J Clin Pathol. 2008 Feb;129(2):193-201. doi: 10.1309/E63PQJJXWCDLWNHQ.
4. Wikström I, Lindell M, Sanner K, Wilander E. Self-sampling and HPV testing or ordinary Pap-smear in women not regularly attending screening: a randomised study. Br J Cancer. 2011 Jul 26;105(3):337-9. doi: 10.1038/bjc.2011.236.
5. Varghese C, Venkataraman K, Bhagwat S. Manual for Cytology. Manuals for Training in Cancer Control. India: Ministry of helth and Family Welfare; 2005:1–44.
6. Verma R, Singh A, Badni M, Chandra A, Gupta S, Verma R. Evaluation of exfoliative cytology in the diagnosis of oral premalignant and malignant lesions: A cytomorphometric analysis. Dent Res J (Isfahan). 2015 Jan-Feb;12(1):83-8. doi: 10.4103/1735-3327.150339.
7. Elmahi OM, Alsammani NM, Mohammed Y, Eltayeb LB, Waggiallah HA. The Impact of Serum Ferritin on Exfoliated Cells Morphology from Buccal Mucosa among Iron Deficiency Anemia Patients: Morphometric Study. J Biochem Tech. 2020 May-Sep ;11(3):57-64.
8. Sankhla B, Sharma A, Shetty RS, Bolla SC, Gantha NS, Reddy P. Exfoliative cytology of buccal squames: A quantitative cytomorphometric analysis of patients with diabetes. J Int Soc Prev Community Dent. 2014 Sep;4(3):182-7. doi: 10.4103/2231-0762.142024.
9. Rahmadwati E, Naghdy G, Ross M, Todd C, Norachmawati E. Classification Cervical Cancer Using Histology Images. 2nd International Congress CACS, AISC. 2011; 145:235–243.
10. Bancroft JD, Gamble M. Theory and practice of histological techniques. 6th ed. London: Churchill Livingstone. 2008.
11. Anuradha A, Sivapathasundharam B. Image analysis of normal exfoliated gingival cells. Indian J Dent Res. 2007 Apr-Jun;18(2):63-6. doi: 10.4103/0970-9290.32422.
12. Patel PV, Kumar S, Kumar V, Vidya G. Quantitative cytomorphometric analysis of exfoliated normal gingival cells. J Cytol. 2011 Apr;28(2):66-72. doi: 10.4103/0970-9371.80745.
13. Hwang LY, Ma Y, Benningfield SM, Clayton L, Hanson EN, Jay J, Jonte J, Godwin de Medina C, Moscicki AB. Factors that influence the rate of epithelial maturation in the cervix in healthy young women. J Adolesc Health. 2009 Feb;44(2):103-110. doi: 10.1016/j.jadohealth.2008.10.006.
14. Rani M N D, Narasimha A, Kumar Ml H, Sr S. Evaluation of Pre-Malignant and Malignant Lesions in Cervico Vaginal (PAP) Smears by Nuclear Morphometry. J Clin Diagn Res. 2014 Nov;8(11):FC16-C19. doi: 10.7860/JCDR/2014/10367.5221.
15. McCann MF, Irwin DE, Walton LA, Hulka BS, Morton JL, Axelrad CM. Nicotine and cotinine in the cervical mucus of smokers, passive smokers, and nonsmokers. Cancer Epidemiol Biomarkers Prev. 1992 Jan-Feb;1(2):125-9.
16. International Collaboration of Epidemiological Studies of Cervical Cancer, Appleby P, Beral V, Berrington de González A, Colin D, Franceschi S, Goodhill A, et al. Cervical cancer and hormonal contraceptives: collaborative reanalysis of individual data for 16,573 women with cervical cancer and 35,509 women without cervical cancer from 24 epidemiological studies. Lancet. 2007 Nov 10;370(9599):1609-21. doi: 10.1016/S0140-6736(07)61684-5.
17. International Collaboration of Epidemiological Studies of Cervical Cancer, Appleby P, Beral V, Berrington de González A, Colin D, Franceschi S, Goodill A, Green J, Peto J, Plummer M, Sweetland S. Carcinoma of the cervix and tobacco smoking: collaborative reanalysis of individual data on 13,541 women with carcinoma of the cervix and 23,017 women without carcinoma of the cervix from 23 epidemiological studies. Int J Cancer. 2006 Mar 15;118(6):1481-95. doi: 10.1002/ijc.21493.
18. Dunne EF, Unger ER, Sternberg M, McQuillan G, Swan DC, Patel SS, Markowitz LE. Prevalence of HPV infection among females in the United States. JAMA. 2007 Feb 28;297(8):813-9. doi: 10.1001/jama.297.8.813.

***Corresponding author**: Dr. Hisham Ali Waggiallah. Department of Medical Laboratory Sciences, College of Applied Medical Sciences, Prince Sattam bin Abdulaziz University. E-mail: hishamwagg30@hotmail.com*

International Journal of Biomedicine 11(1) (2021) 50-52
http://dx.doi.org/10.21103/Article11(1)_OA10

ORIGINAL ARTICLE

Biotechnology

INTERNATIONAL JOURNAL OF BIOMEDICINE

# Production, Properties and Swelling of Copper-Pectic Gel Particles in an Artificial Gastroenteric Environment

Anatoly A. Shubakov, PhD; Elena A. Mikhailova*

*Institute of Physiology of Komi Science Centre of the Ural Branch of the RAS, FRC Komi SC UB RAS*
*Syktyvkar, Komi Republic, the Russian Federation*

## Abstract

***The purpose*** of the this research was to obtain and study the properties of copper-pectic gel particles (CuPGPs) obtained from aqueous solutions of apple pectin (AP) in the concentration range of 1%-5% in the presence of $Cu^{2+}$ ions.

***Methods and Results***: We used commercial AP AU701 (Herbstreith & Fox KG, Germany). CuPGPs were obtained from aqueous solutions of AP (1%, 3%, 5%) in the presence of $Cu^{2+}$ ions (1%-10%) by the method of ionotropic gelation. The diameter and density of the CuPGPs were determined. Dry CuPGPs formed from 5% AP with all tested concentrations of copper ions have the largest diameter (0.96-1.15 mm), and gel particles formed on the basis of 1% AP have the smallest diameter (0.42-0.74 mm). CuPGPs formed from 5% AP have the highest density (1.43-1.65 mg/mm$^3$), and CuPGPs formed on the basis of 1% AP have the lowest density (0.65-0.92 mg/mm$^3$). Gel particles obtained from 1% AP swelled in simulated gastric fluid (SGF) by 161% and then completely degraded immediately upon entering in simulated intestinal fluid (SIF). CuPGPs obtained from 3% AP swelled by 166% in SGF and 148% in SIF, and completely degraded in SIF after 2.5 hours of incubation in it. Gel particles obtained from 5% AP in the presence of 10% $Cu^{2+}$ swelled most strongly – by 173% in SGF and by 208% in SIF. And then, they degraded after 8 hours of incubation in simulated colonic fluid (SCF).(**International Journal of Biomedicine. 2021;11(1):50-52.**)

**Key Words**: apple pectin • cross-linking agents • copper ions • gel particles • gastroentestinal tract

**For citation**: Shubakov AA, Mikhailova EA. Production, Properties and Swelling of Copper-Pectic Gel Particles in an Artificial Gastroenteric Environment. International Journal of Biomedicine. 2021;11(1):50-52. doi:10.21103/Article11(1)_OA10

## Abbreviations

**AP**, apple pectin; **CuPGPs**, copper-pectic gel particles; **SGF**, simulated gastric fluid; **SIF**, simulated intestinal fluid; **SCF**, simulated colonic fluid.

## Introduction

Pectins are natural, biodegradable, ionic polysaccharides that are widely used in the food and pharmaceutical industries. The widespread use of pectins is based on their ability to form gels in the presence of divalent cations, such as calcium ions. Gelation occurs as a result of specific and strong interactions between calcium ions and galacturonic acid residues of pectins.[1]

Pectins differ in macromolecular structure, monosaccharide composition and degree of methyleterification of carboxyl groups of galacturonic acid residues. Pectins readily form gel particles with a wide range of physical and mechanical properties. It has been found that the key factors affecting the formation of gel particles are the degree of methyleterification of carboxyl groups, temperature, the presence of sugar, and polyvalent ions.[2]

To obtain pectic gel particles, copper ions ($Cu^{2+}$ ions) are also used instead of calcium ions as a cross-linking agent

***Corresponding author:** Elena A. Mikhailova. Institute of Physiology of Komi Science Centre of the Ural Branch of the RAS, FRC Komi SC UB RAS. Syktyvkar, the Russian Federation. E-mail: elkina@physiol.komisc.ru*

because they bind pectin more strongly than calcium ions.[3] Copper is a trace element necessary for plants and animals. The main biochemical function of copper is participation in enzymatic reactions as an activator or in the composition of copper-containing enzymes.[4]

The study of the gelation of low methyl esterified pectin (apple pectin [AP]) using $Cu^{2+}$ ions as a cross-binding agent is also relevant. In our previous article, we investigated the properties and swelling in an artificial gastroenteric environment of CuPGPs obtained from 2% and 4% AP in the presence of $Cu^{2+}$ ions.[5]

The purpose of the present work was to obtain and study the properties of CuPGPs obtained from aqueous solutions of AP in the concentration range of 1%-5% (1%, 3%, 5%) in the presence of $Cu^{2+}$ ions (1%-10%). The swelling of the obtained CuPGPs during incubation in an artificial gastroenteric environment was also investigated.

## Materials and Methods

We used commercial AP AU701 (Herbstreith & Fox KG, Germany). CuPGPs were obtained from aqueous solutions of AP (1%, 3%, 5%) in the presence of $Cu^{2+}$ ions (1%-10%) by the method of ionotropic gelation,[6,7] Certain weighed portions of AP were dissolved in corresponding volumes of distilled water by slow stirring with a magnetic stirrer MM-5 (Russia) for 2-5 hours at room temperature until complete dissolution

Gel particles of spherical shape were prepared by drop-by-drop injection of a pectin solution from a syringe through a needle with a hole diameter of 0.7 mm on the distance of 4-5 cm in the slowly stirred copper chloride solution and further stirring for 20 min at room temperature. The resulting gel particles were then washed three times in distilled water with stirring for 5 minutes and dried for 10-14 h at 37°C.

Further, the diameter and density of CuPGPs were determined using an optical microscope (Altami, Russia) with a camera and an image analysis program (ImageJ 1.46r program, National Institutes of Health, USA). For calibration, a linear scale was used; one pixel corresponded to 0.024 mm.

The swelling and degradation of CuPGPs were studied under conditions simulating the gastrointestinal environment: for these purposes, the simulated gastric fluid (SGF solution), simulated intestinal fluid (SIF solution) and simulated colonic fluid (SCF solution), as described previously.[8, 9]

To determine swelling and degradation, dry CuPGPs (1–2 mg) were placed in Petri dishes (diameter 3.5 cm) and subsequently incubated in 3 ml of SGF (2 h), SIF (4h) and SCF solutions with shaking in a shaker (Titramax 1000, Heidolph, Germany) at 100 rpm and at 37°C. The diameter and density of 100 randomly selected gel particles were measured as described above after certain time intervals. The experiments were performed in triplicate. The degree of gel swelling (SD,%) was determined by the formula[10]: $SD = (D_1\text{-}D_0)/ D_0 \times 100\%$, where $D_1$ – diameter of the particles (mm) after a certain incubation time in the medium, $D_0$ – initial diameter of the particles (mm).

The statistical analysis was performed using the statistical software BioStat (version 4.03) and Microsoft Office Excel 2007.

## Results and Discussion

CuPGPs were obtained from aqueous solutions of AP (1%, 3%, 5%) in the presence of $Cu^{2+}$ ions (1%-10%) by the method of ionotropic gelation, in which intermolecular cross-links arise between divalent $Cu^{2+}$ ions and negatively charged carboxyl groups of AP. [5,11,12] Morphological (diameter) and structural-mechanical (density) characteristics of gel particles are given.

Dry CuPGPs formed from 5% AP with all tested concentrations of copper ions have the largest diameter (0.96-1.15 mm), and gel particles formed on the basis of 1% AP have the smallest diameter (0.42-0.74 mm) (Table 1). It was shown[13] that the diameter of dry calcium-pectin gel particles formed from 1% AP in the presence of 1.0 M $CaCl_2$ solution is approximately 3 times larger – 3.56 mm. That is, $Cu^{2+}$ ions contribute to the formation of smaller pectin gel particles than $Ca^{2+}$ ions.

***Table 1.***

***Diameter of dry CuPGPs (M±SD, mm)***

| AP concentration | $CuCl_2$ concentration | | | | | |
|---|---|---|---|---|---|---|
| | 1% | 2% | 3% | 4% | 5% | 10% |
| 1% | 0.42 ± 0.05 | 0.58 ± 0.03 | 0.68 ± 0.05 | 0.71 ± 0.06 | 0.73 ± 0.07 | 0.74 ± 0.08 |
| 3% | 0.82 ± 0.02 | 0.83 ± 0.05 | 0.87 ± 0.04 | 0.89 ± 0.04 | 0.92 ± 0.06 | 0.94 ± 0.04 |
| 5% | 0.96 ± 0.08 | 0.98 ± 0.06 | 0.99 ± 0.06 | 1.00 ± 0.05 | 1.06 ± 0.05 | 1.15 ± 0.06 |

In several works,[3,14] it has been shown that $Cu^{2+}$ ions, as cross-binding agents, form denser gel particles than $Ca^{2+}$ ions. At the same time, with an increase in the concentration of AP, the density of the gel particles increases at all tested concentrations of $Cu^{2+}$ ions. CuPGPs formed from 5% AP have the highest density(1.43-1.65 mg/mm$^3$), and CuPGPs formed on the basis of 1% AP have the lowest density(0.65-0.92 mg/mm$^3$) (Table 2). $Ca^{2+}$ ions, as cross-linking agents, form gel particles from AP with a lower density(0.40 mg/mm$^3$).[13]

***Table 2.***

***Density of dry CuPGPs (M±SD, mg/mm$^3$)***

| AP concentration | $CuCl_2$ concentration | | | | | |
|---|---|---|---|---|---|---|
| | 1% | 2% | 3% | 4% | 5% | 10% |
| 1% | 0.65 ± 0.14 | 0.69 ± 0.17 | 0.75 ± 0.18 | 0.81 ± 0.14 | 0.85 ± 0.25 | 0.92 ± 0.21 |
| 3% | 1.40 ± 0.15 | 1.42 ± 0.12 | 1.46 ± 0.16 | 1.49 ± 0.12 | 1.50 ± 0.18 | 1.52 ± 0.16 |
| 5% | 1.43 ± 0.20 | 1.46 ± 0.25 | 1.51 ± 0.21 | 1.52 ± 0.18 | 1.56 ± 0.22 | 1.65 ± 0.16 |

The swelling of the obtained CuPGPs in an artificial gastroenteric environment was studied. Gel particles formed from AP (1%, 3%, 5%) with 1%-5% $Cu^{2+}$ as a cross-linking agent swelled in a simulated gastric fluid SGF by 90%-150% and degraded in a simulated intestinal fluid SIF during the first 30 minutes of incubation in it.

With an increase in AP concentration, the degree of swelling of CuPGPs increases (Fig.1). Gel particles obtained from 1% AP swelled in SGF by 161% and then completely degraded immediately upon entering in SIF. CuPGPs obtained from 3% AP swelled by 166% in SGF and 148% in SIF, and completely degraded in SIF after 2.5 hours of incubation in it.

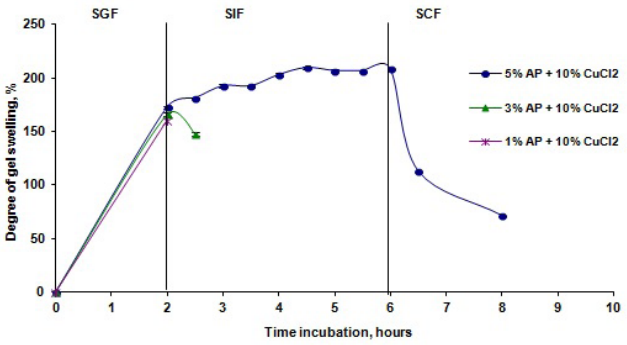


***Fig. 1.*** *Swelling and degradation of CuPGPs formed from AP (1%, 3%, 5%) and $Cu^{2+}$ ions (10% $CuCl_2$) in an artificial SGF, SIF, and SCF.*

Gel particles obtained from 5% AP in the presence of 10% $Cu^{2+}$ swelled most strongly – by 173% in SGF and by 208% in SIF. And then, they degraded after 8 hours of incubation in SCF.

Thus, we can conclude that $Cu^{2+}$ ions are stronger cross-linking agents than $Ca^{2+}$ ions. CuPGPs formed from 5% AP in the presence of 10% $Cu^{2+}$ have the highest degree of swelling and the least degradability in an artificial gastroenteric environment.

## Competing Interests

The authors declare that they have no competing interests.

## Sources of Funding

The work was performed on the theme of research work (State registration number AAAA-A17-117012310147-8).

## References

1. Braccini I, Pérez S. Molecular basis of $Ca^{2+}$-induced gelation in alginates and pectins: the egg-box model revisited. Biomacromolecules. 2001;2(4):1089-96. doi: 10.1021/bm010008g.
2. Volkova MV, Khasanshina ZR, Popov SV, Markov PA. [Gel granules from pectin callus *Lupinus angustifolius* prevent the premature release of mesalazine]. Biotechnology. 2020;36(1):53-60. doi: 10.21519/0234-2758-2020-36-1-53-60. [Article in Russian].
3. Seslija S, Veljovic D, Krusic MK, Stevanovic J, Velickovic S, Popovic I. Cross-linking of highly methoxylated pectin with copper: the specific anion influence. New J Chem. 2016;40:1618-1625. doi: 10.1039/C5NJ0332A.
4. Williams RJP. Missing information in bio-inorganic chemistry. Coord Chem Rev. 1987;79(3):175-193. doi: 10.1016 / 0010-8545 (87) 80002-4.
5. Shubakov AA, Mikhailova EA. Production, properties and transit of copper-pectic gel particles through an artificial gastroenteric environment. International Journal of Biomedicine. 2020;10(4):421-423.doi: 10.21103/Article10(4)_OA18.
6. Sriamornsak P. Effect of calcium concentration, hardening agent and drying condition on release characteristics of oral proteins from calcium pectinate gel beads. Eur J Pharm Sci. 1999 Jul;8(3):221-7. doi: 10.1016/s0928-0987(99)00010-x.
7. Sriamornsak P, Nunthanid J. Calcium pectinate gel beads for controlled release drug delivery: I. Preparation and in vitro release studies. Int J Pharm. 1998;160: 207-212. doi: PII S0378-5173 (97) 00310-4.
8. Gebara C, Chaves KS, Ribeiro MCE, Souza FN, Grosso CRF, Gigante ML. Viability of *Lactobacillus acidophilus La5* in pectin-whey protein microparticles during exposure to simulated gastrointestinal conditions. Food Res Int. 2013;51:872-878. doi: 10.1016/j.foodres.2013.02.008.
9. Shubakov AA, Mikhailova EA, Prosheva VI, Belyy VA. Swelling and degradation of calcium-pectic gel particles made of pectins of *Silene vulgaris* and *Lemna minor* callus cultures at different concentrations of pectinase in an artificial colon environment. International Journal of Biomedicine. 2018; 8(1):60-64.doi: 10.21103/Article8(1)_OA10.
10. Oliveira GF, Ferrari PC, Carvalho LQ, Evangelista RC. Chitosan-pectin multiparticulate systems associated with enteric polymers for colonic drug delivery. Carbohydr Polym. 2010;82(3):1004-1009. doi: 10.1016/j.carbpol.2010.06.041.
11. Mikhailova EA, Melekhin AK, Belyy VA, Shubakov AA. Stability of hyaluronan-pectic gel particles in the conditions of the artificial gastrointestinal environment. International Journal of Biomedicine. 2017;7(4):310-314. doi: 10.21103/Article7(4) _OA8.
12. Sriamornsak P, Kennedy RA. Swelling and diffusion studies of calcium polysaccharide gels intended for film coating. Int J Pharm. 2008 Jun 24;358(1-2):205-13. doi: 10.1016/j.ijpharm.2008.03.009.
13. Günter EA, Popeyko OV, Istomina EI. [Preparation and properties of hydrogel matrices based on pectins from callus cultures]. Biotechnology. 2020;36(3):63-72. doi: 10/21519/0234-2758-2020-36-3-63-72. [Article in Russian].
14. Rodrigues JR, Lagoa R. Copper ions binding in Cu-alginate gelation. J Carbohydr Chem. 2006;25:219-232.doi: 0.1080 / 07328300600732956.

International Journal of Biomedicine 11(1) (2021) 53-57
http://dx.doi.org/10.21103/Article11(1)_OA11

ORIGINAL ARTICLE

Dentistry

INTERNATIONAL JOURNAL OF BIOMEDICINE

# Analysis of Mineral Density of Calcified Tissues in Children with X-Linked Hypophosphatemic Rickets and Hypophosphatasia Using Cone Beam Computed Tomography Data

Dmitriy A. Lezhnev, PhD, ScD; Elena V. Vislobokova*; Larisa P. Kiselnikova, PhD, ScD; Natalia A. Sholokhova, PhD; Margarita V. Smyslenova, PhD, ScD; Viktor P. Truten, PhD, ScD

*Moscow State University of Medicine and Dentistry named after AI Evdokimov*
*Moscow, Russia*

## Abstract

***The purpose*** of the present cohort study was a quantitative assessment of the enamel, dentin, and alveolar bone mineral density (BMD) using Cone Beam Computed Tomography (CBCT) scans in patients with X-linked hypophosphatemic rickets (HLHR) and hypophosphatasia (HPP) and a comparison with the data obtained from the control group.

***Methods and Results***: The unrepresentative, non-random sample included 30 CBCT scans of children with genetically and biochemically confirmed XLHR (OMIM #307800) and HPP (OMIM: 146300, 241510, 241500, and 146300). X-ray examination and dental care were carried out in the Radiology Diagnostics Department and Pediatric Dentistry Department at Moscow State University of Medicine and Dentistry named after AI Evdokimov. The mineral density of calcified tissues (enamel, dentin, and alveolar bone) was evaluated using i-CAT Vision TM software options on reconstructed CBCT axial views.

The images of all XLHR and HPP patients visualized large pulp chambers with prominent pulp horns extending to the dentin-enamel junction. The present study revealed poor alveolar bone mineralization in patients with HPP and XLHR. Analysis of CBCT scans showed a significant dentine hypodensity in XLHR patients, which may contribute to the emergence of multiple, spontaneous, periapical abscesses spreading rapidly in the jawbone.

***Conclusion***: Data obtained could be used for planning dental treatment of patients with XLHR and HPP. (**International Journal of Biomedicine. 2021;11(1):53-57.**)

**Key Words**: X-linked hypophosphatemic rickets • hypophosphatasia • mineral density • cone beam computed tomography

**For citation**: Lezhnev DA, Vislobokova EV, Kiselnikova LP, Sholokhova NA, Smyslenova MV, Truten VP. Analysis of Mineral Density of Calcified Tissues in Children with X-Linked Hypophosphatemic Rickets and Hypophosphatasia Using Cone Beam Computed Tomography Data. International Journal of Biomedicine. 2021;11(1):53-57. doi:10.21103/Article11(1)_OA11

## Abbreviations

**BMD**, bone mineral density; **DMD**, dentin mineral density; **CBCT**, cone beam computed tomography; **XLHR**, X-linked hypophosphatemic rickets; **HPP**, hypophosphatasia.

## Introduction

Genetic disorders affecting bone mineralization cause skeleton deformities and significant bone osteoporosis. Similar problems in this cohort of patients were also identified in the maxillofacial region.[1] Disruption of the formation processes of calcified tissues (enamel, dentin, cement, and alveolar bone) causes different dental manifestations of diseases. X-linked hypophosphatemic rickets (XLHR, OMIM #307800) is a genetically determined disorder characterized by poor bone mineralization, dental abnormalities and multiple abscesses associated with caries-free teeth (Fig.1a-b). Impairment

of mineralization is the direct consequence of disrupted homeostasis of phosphate-caused mutations in the phosphate-regulating gene (*PHEX*).[2]

Hypophosphatasia HPP (HPP, OMIM 146300, 241500, 241510) is a rare, progressive, hereditary, metabolic disease caused by the lack of activity of tissue-nonspecific alkaline phosphatase resulting from mutations in the *ALPL* gene encoding enzyme.[3,4] This factor plays a crucial role in phosphate homeostasis and proper local regulation of mineralization. Poor cement mineralization leads to premature loss of primary and permanent teeth in HPP patients (Fig.1 c-d).

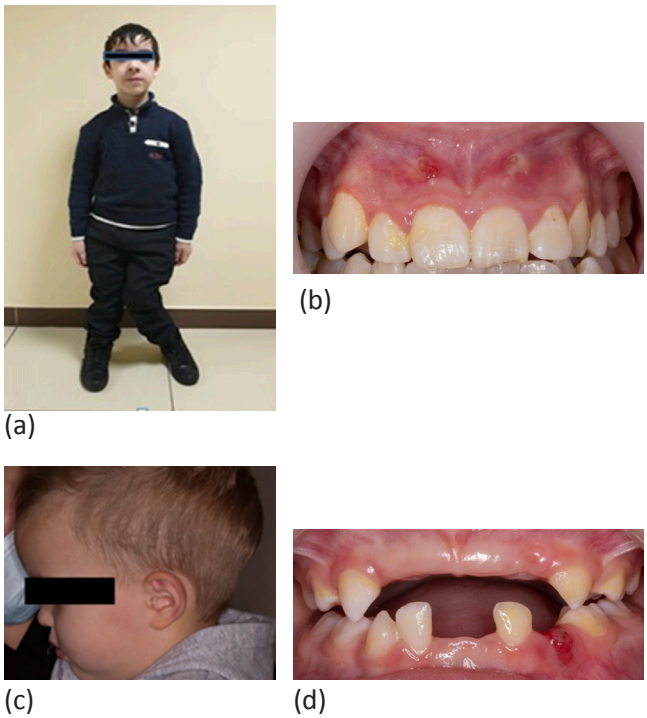


***Fig. 1.*** *Clinical features of XLHR and HPP. Skeletal pathology resulting from osteomalacia: Bowing legs in a 15-year-old patient with XLHR (a), skull deformities in a 4-year-old patient with HPP (c). Intraoral clinical picture: Periapical abscesses with sinus tracts in a 15-year-old patient with XLHR (b), premature loss of primary teeth in a 4-year-old patient with HPP (d).*

According to the literature, detection of dental manifestations in patients with XLHR and HPP was most often based on the data from traditional radiological techniques, such as panoramic tomography and intraoral periapical radiography.[5,6] With the presence of 3-D digital methods, such as cone beam computed tomography, diagnostic capabilities in dentistry have expanded significantly. CBCT has a few advantages over two-dimensional methods of examination. The high quality of diagnostic data obtained makes CBCT the method of choice for this cohort of patients.[7,8] A crucial option of CBCT is the ability to quantify the mineralization level of the studied object.

## Materials and Methods

The present study examined the results of scanning patients aged from 6 to 12 years (Group code 2_12 with mixed dentition) and from 12 to 18 years (Group code 2_18 with permanent dentition) with genetically and biochemically confirmed XLHR, and children aged from 12 to 18 years with genetically and biochemically confirmed HPP. The control groups (Group code 1_12 with mixed dentition and Group code 1_18 with permanent dentition) included CBCT data of children the same age examined for malocclusion in the Radiology Diagnostics Department at Moscow State University of Medicine and Dentistry named after AI Evdokimov. The scan protocol parameters are summarized in Table 1.

***Table 1.***
***Scanning protocol using the KaVo OP 3D Vision***

| Scanned area | FOV, cm | VD, mm | ST, sec | ET, sec | Voltage, kV | Amperage, mA | ED, E, µSv |
|---|---|---|---|---|---|---|---|
| Maxillo-facial | 16x13 | 0.25 | 26.9 | 7.4 | 120 | 5 | 0.011 |

*VD- voxel dimensions; ST- scanning time; ET- exposure time; ED- effective dose*

Data analysis was performed after constructing axial cross-sections using the software for visualizing computed tomography data i-CAT Vision. Morphometric parameters of teeth were studied, and mineral density of enamel, dentin, and alveolar bone was measured (Table 2). The presence, size and location of radiolucency, in relation to the surrounding anatomical structures, were evaluated.

***Table 2.***
***Distribution of densitometric measurements in the study groups***

| Group code | Scans (n) | Number of permanent central upper incisors/ densitometric measurements (HU) | | Number of permanent first molars/ densitometric measurements (HU) | | Alveolar BMD measure-ments (n) |
|---|---|---|---|---|---|---|
| | | enamel | dentin | enamel | dentin | |
| 1_12 (C̄ontrol group) | 24 | 48/192 | 48/192 | 96/384 | 96/384 | 96 |
| 2_12 (X̄LHR) | 10 | 20/80 | 20/80 | 40/160 | 40/160 | 40 |
| 1_18 (C̄ontrol group) | 67 | 134/536 | 134/536 | 268/1072 | 268/1072 | 268 |
| 2_18 (X̄LHR) | 17 | 34/136 | 34/136 | 68/272 | 68/272 | 68 |
| 3_18 (H̄PP) | 3 | 6/24 | 6/24 | 12/48 | 12/48 | 12 |
| Total number | 121 | 242/968 | 242/968 | 484/1936 | 484/1936 | 484 |

The mineral density of enamel and dentin was determined in Hounsfield units (HU) as the mean value of 4 areas of the tooth crown. All the first molars and upper central incisors were measured at 4 points (mesial, distal, buccal, and lingual/palatal)

encompassing as large an area as possible, but without impinging on the images corresponding to the pulp. Densitometric measurements of the alveolar bone were performed in the furcation all first molars, but without impinging on the images corresponding to the periodontal ligament. Plots with an area of 1 mm were evaluated (Figure 2).

The statistical analysis was performed using the statistical software Microsoft Excel.

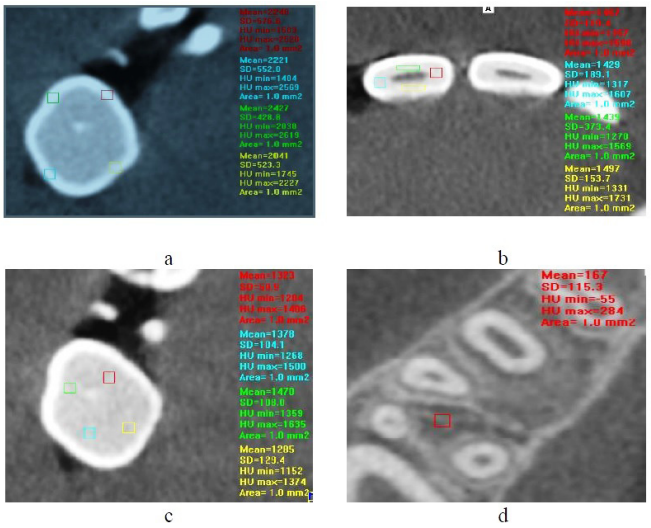


***Fig. 2.*** *CBCT. Axial cross-section. Mineral density measurements of the enamel of the first permanent molar (a); dentin of the upper central permanent incisor (b); dentin of the first permanent molar (b); alveolar bone (d) using the software for visualization of computer tomography data of the maxillofacial zone i-CATVision.*

## Results

The images of all XLHR and HPP patients visualized large pulp chambers with prominent pulp horns extending to the dentin-enamel junction (Figure 3).

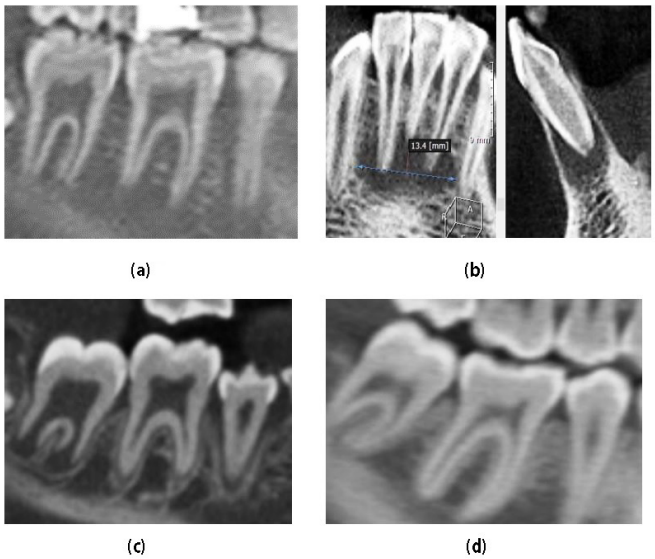


***Fig. 3.*** *CBCT. Mandible cross-sections in the lateral and frontal area: A 14-year-old HLHR patient (a, b). A 13-year-old HPP patient (c); a 14-year-old teenager of control group (d). Enlarged pulp chambers with prominent pulp horns extending to the dentin-enamel junction, alveolar bone hypodensity in XLHR and HPP patients. The large periapical lesion in the area of apparently healthy teeth in XLHR-patient (b).*

There were no statistically significant differences in the enamel mineral density of the first permanent molars and central incisors in the comparison groups (Figure 4).

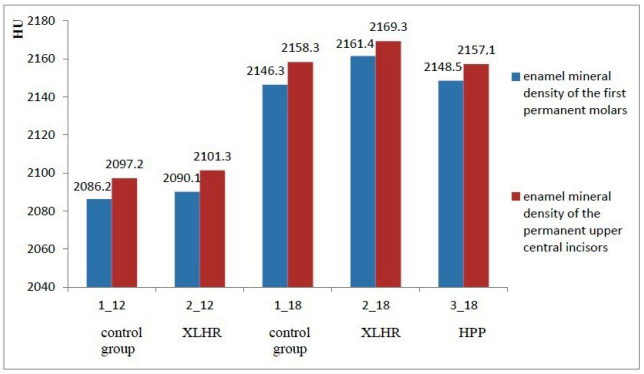


***Fig. 4.*** *Mean value of enamel mineral density in the study groups (P>0.05)*

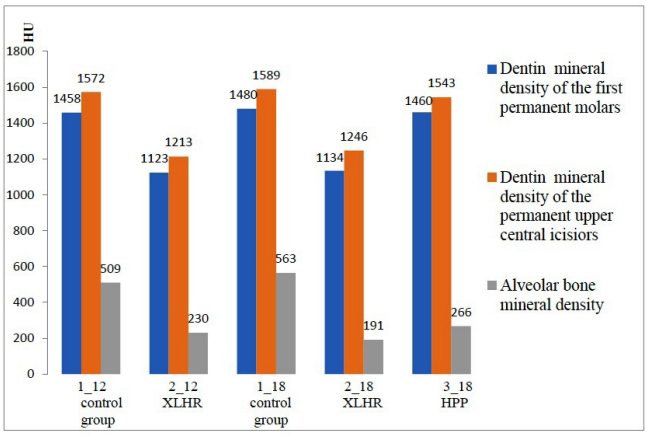


***Fig. 5.*** *Mean values of the dentin and alveolar bone mineral density in the study groups (P<0.05)*

Dentin and alveolar BMD, on the contrary, revealed a statistically significant difference in the study groups (Figure 5).

Thus, according to the results of the study, in the XLHR group of children from 6 to 12 years (Group 2_12), the mean value of dentin mineral density (DMD) of the permanent first molar and upper central incisor was 1123±108 HU and 1213±120 HU, respectively, which is significantly lower than in the control group (Group 1_12), where the corresponding indicators were 1458±148 HU and 1572±124 HU. The difference in the DMD of the first permanent molars averaged 335 HU (23%), and the difference in the DMD of the permanent upper central incisors was 359 HU (22.8%).

The same trend was observed in the XLHR group of children from 12 to 18 years (Group 2_18). The mean value of DMD of the first molar and upper central incisor was 1134±146 HU and 1346±136 HU, respectively. In the control group of the matched age (Group 1_18), indicators were 1480±144 HU and 1589±149 HU, respectively. In this age group, the average difference in the DMD of the first molars was 346 HU (23.4%), and the difference in the DMD of the permanent upper central

incisors was 343 HU (21.6%). The values of DMD in the same age group of HPP patients were almost identical to those in the control group. For the first molars, the value averaged 1460±91 HU (1.4% less), and for the upper central incisors, it averaged 1543±92 HU (2.9% less).

The alveolar BMD in the XLHR group of children from 6 to 12 years (Group 2_12) averaged 230±90HU, and in the control group of the matched age 509±89HU. The difference in alveolar BMD in these groups averaged 279HU. In the older age group, the alveolar BMD in the control group (Group 1_18), the group of XLHR children, and the group of HPP children (Group 3_18)averaged 563±100HU, 191±78HU (66.1% lower than in the control group), and 266±40HU (52.8% lower than in the control group), respectively.

It is well known that the measurements of the mineral density in Hounsfield units evaluated by CBCT data are in a significant range and depend on a number of factors: technical parameters of equipment, human factor, etc.[9] There is an objective need for additional validation of data.

To solve the above problem, it is proposed to use the option of comparing the relative mineral density indexes of different tissues for each individual scan. In a range of tissues—enamel, dentin and alveolar bone—the highest density, according to CBCT, is determined in enamel, the lowest in alveolar bone.

Literature data, which are confirmed by our results, indicate that the mineral density of enamel in patients with XLHR and HPP approximately matches the level in the group of healthy children.[10] Thus, we evaluated the dentin and alveolar bone mineralization relative to the mineral density of enamel in each individual patient scan, and then compared these indexes.

The next indexes were calculated from the CBCT data of each patient in the group:

**Ked**=mean value of enamel mineral density/mean value of DMD

**Kea**=mean value of enamel mineral density/mean value of alveolar BMD

Then the group mean indexes, Ked and Kea, were calculated. For the second version of calculating these indexes obtained earlier mean values of enamel, dentin and alveolar bone density in the groups were used (Figure 4,5). The comparison of indexes is summarized in Table 3.

***Table 3.***

***Mean values of indexes in the study groups***

| Group code | Ked mean value (version 1) | Ked mean alue (version 2) | Kea mean value (version 1) | Kea mean value (version 2) |
|---|---|---|---|---|
| 1_12 (Control group) | 1.52 | 1.38 | 4.23 | 4.11 |
| 2_12(XLHR) | 2.20 | 1.79 | 11.41 | 9.11 |
| 1_18 (Control group) | 1.53 | 1.40 | 4.21 | 3.82 |
| 2_18(XLHR) | 2.16 | 1.82 | 12.03 | 11.34 |
| 3_18 (HPP) | 1.53 | 1.43 | 10.13 | 8.09 |

Analyzing the indexes obtained by different methods, we can trace the following trend: the mineral density of dentin relative to the density of enamel in patients with hypophosphatasia and in the control group is approximately equal – 1.38-1.53 times less. At the same time, in XLHR patients, DMD is 1.79-2.20 times lower than the enamel mineral density. Alveolar BMD in patients with HPP and XLHR is 8.09-12.03 times lower than the enamel mineral density, while in control group the difference is only 3.82-4.23 times.

## Discussion

After a comparative analysis of the mineral density of calcified tissues, using different versions of calculation, we can draw the following conclusions: DMD in XLHR patients and alveolar BMD density in XLHR and HPP patients is significantly reduced, compared to healthy peers.

The present study data correlate with the results of several authors who studied the enamel and DMD of teeth in XLHR and HPP patients.[11]

R.Pauwels et al.[12] analyzed the reliability of estimating the mineral density of the studied objects in Hounsfield units according to CBCT data, compared with multi-detector computed tomography data. Van Dessel et al.[13] did not find a statistically significant difference in the assessment of the structure and quality of the alveolar bone by CBCT and computed microtomography and concluded that the CBCT method is sufficiently accurate and informative for these purposes.

The teeth of XLHR patients are characterized by enlarged pulp chambers and root canals. The layer of hard tissues-enamel, dentin and cement, on the contrary, is thinner than normal. The horns of the pulp are located extremely high and can reach the enamel-dentine junction. Skrinar reported that enlarged pulp chambers were found in 24% of children and 52% of adults.[14] According to our data, all images of XLHR and HPP patients visualized such abnormalities as large pulp chambers with prominent pulp horns extending to dentin-enamel junction.

The pathognomonic sign of the XLHR is periapical abscesses located in the area of the apparently healthy teeth with no history of trauma. Multiple, spontaneous, periapical abscesses pose special challenges to pediatric dentists, both in diagnosis and treatment, and are often the cause of primary and permanent teeth extractions in XLHR patients. Mineralization abnormalities of the dentin also may compromise the prognosis of endodontic treatment.

The cement and alveolar bone abnormal structure caused by reduced mineralization due to a lack of alkaline phosphatase activity leads to a poor tooth attachment and its subsequent premature loss in HPP patients.[15] According to our data, the alveolar BMD is reduced in adolescents with hypophosphatasia. However, there are not enough data for unambiguous conclusions. Unfortunately, it is not possible to make a correct mineral density measurement of cement using CBCT data.

The relevance of the study was due to the search for objective criteria for assessing the level of enamel, dentin, and

alveolar bone mineralization. In such cases, CBCT provides the most comprehensive amount of diagnostic information for clinicians. Data obtained could be used for planning dental treatment of patients with XLHR and HPP.

## Competing Interests

The authors declare that they have no competing interests.

## References

1. Opsahl Vital S, Gaucher C, Bardet C, Rowe PS, George A, Linglart A, Chaussain C. Tooth dentin defects reflect genetic disorders affecting bone mineralization. Bone. 2012 Apr;50(4):989-97. doi: 10.1016/j.bone.2012.01.010.
2. Lee BN, Jung HY, Chang HS, Hwang YC, Oh WM. Dental management of patients with X-linked hypophosphatemia. Restor Dent Endod. 2017 May;42(2):146-151. doi: 10.5395/rde.2017.42.2.146.
3. Bianchi ML. Hypophosphatasia: an overview of the disease and its treatment. Osteoporos Int. 2015 Dec;26(12):2743-57. doi: 10.1007/s00198-015-3272-1.
4. Whyte MP. Hypophosphatasia: An overview For 2017. Bone. 2017 Sep;102:15-25. doi: 10.1016/j.bone.2017.02.011.
5. Sabandal MM, Robotta P, Bürklein S, Schäfer E. Review of the dental implications of X-linked hypophosphataemic rickets (XLHR). Clin Oral Investig. 2015 May;19(4):759-68. doi: 10.1007/s00784-015-1425-
6. Bloch-Zupan A. Hypophosphatasia: diagnosis and clinical signs - a dental surgeon perspective. Int J Paediatr Dent. 2016 Nov;26(6):426-438. doi: 10.1111/ipd.12232.
7. de Moura PM, Hallac RR, Seaward JR, Kane AA, Aguiar M, Raggio R, Gutfilen B. Objective and subjective image evaluation of maxillary alveolar bone based on cone beam computed tomography exposure parameters. Oral Surg Oral Med Oral Pathol Oral Radiol. 2016 May;121(5):557-65. doi: 10.1016/j.oooo.2016.01.019.
8. Yeung AWK, Jacobs R, Bornstein MM. Novel low-dose protocols using cone beam computed tomography in dental medicine: a review focusing on indications, limitations, and future possibilities. Clin Oral Investig. 2019 Jun;23(6):2573-2581. doi: 10.1007/s00784-019-02907-y.
9. Zhang J, Tian Y. Liu Y, Liu Q. Alveolar mineral density measurement using CBCT images. Neuroscience and biomedical engineering. 2017;5(1): 44-49. doi : 10.2174/2213385205666170612114301
10. Ribeiro TR, Costa FW, Soares EC, Williams JR Jr, Fonteles CS. Enamel and dentin mineralization in familial hypophosphatemic rickets: a micro-CT study. Dentomaxillofac Radiol. 2015;44(5):20140347. doi: 10.1259/dmfr.20140347.
11. Hayashi-Sakai S, Sakamoto M, Hayashi T, Kondo T, Sugita K, Sakai J, Shimomura-Kuroki J, Ike M, Nikkuni Y, Nishiyama H. Evaluation of permanent and primary enamel and dentin mineral density using micro-computed tomography. Oral Radiol. 2019 Jan;35(1):29-34. doi: 10.1007/s11282-018-0315-2.
12. Pauwels R, Jacobs R, Singer SR, Mupparapu M. CBCT-based bone quality assessment: are Hounsfield units applicable? Dentomaxillofac Radiol. 2015;44(1):20140238. doi: 10.1259/dmfr.20140238.
13. Van Dessel J, Huang Y, Depypere M, Rubira-Bullen I, Maes F, Jacobs R. A comparative evaluation of cone beam CT and micro-CT on trabecular bone structures in the human mandible. Dentomaxillofac Radiol. 2013;42(8):20130145. doi: 10.1259/dmfr.20130145.
14. Skrinar A, Dvorak-Ewell M, Evins A, Macica C, Linglart A, Imel EA, Theodore-Oklota C, San Martin J. The Lifelong Impact of X-Linked Hypophosphatemia: Results From a Burden of Disease Survey. J Endocr Soc. 2019 May 7;3(7):1321-1334. doi: 10.1210/js.2018-00365.
15. Foster BL, Nociti FH Jr, Somerman MJ. The rachitic tooth. Endocr Rev. 2014 Feb;35(1):1-34. doi: 10.1210/er.2013-1009.

*__Corresponding author__: *Dr. Elena V. Vislobokova. Pediatric Dentistry Department, Moscow State University of Medicine and Dentistry named after AI Evdokimov, Moscow, Russia. E-mail: visllena@yandex.ru*

International Journal of Biomedicine 11(1) (2021) 58-60
http://dx.doi.org/10.21103/Article11(1)_CR1

CASE REPORT

INTERNATIONAL JOURNAL OF BIOMEDICINE

# Arteriovenous Malformation of the Vein of Galen: A Case Report

Vyacheslav A. Kutashov, PhD, ScD; Olga V. Ulyanova, PhD; Igor S. Protasov, PhD*; Oleg V. Zolotaryov, PhD; Elena S. Ananyeva, PhD; Anna A. Dudina, PhD; Margarita V. Uvarova, PhD

*Voronezh State Medical University named after N.N. Burdenko*
*Voronezh, the Russian Federation*

## Abstract

The article presents literature data and the authors' observations of the course of the vein of Galen aneurysmal malformation in a one-day-old newborn infant. This clinical case is of practical interest since the vein of Galen aneurysmal malformation is a rare congenital anomaly of cerebral vessels. The results of arteriovenous malformation treatment in recent years have improved considerably, but many diagnostic and curative aspects in children require the development of new approaches to addressing this problem. (**International Journal of Biomedicine. 2021;11(1):58-60.**)

**Key Words**: arteriovenous malformation • the great cerebral vein • children • diagnosis • treatment

**For citation**: Kutashov VA, Ulyanova OV, Protasov IS, Zolotaryov OV, Ananyeva ES, Dudina AA, Uvarova MV. Arteriovenous Malformation of the Vein of Galen: A Case Report. International Journal of Biomedicine. 2021;11(1):58-60. doi:10.21103/Article11(1)_CR1

## Introduction

Brain diseases caused by damage to the vascular system, are one of the major problems of modern neurology and neurosurgery. This is due to the prevalence of these pathological conditions in the population: the severity of clinical manifestations, high mortality rate, and a large percentage of disabled people. Often cerebrovascular diseases in newborns and young children are combined with congenital infections, birth hemorrhages, cerebral and non-cerebral developmental defects, and birth injuries. At the same time, in children, the defects of brain vessels, their course, treatment, and prognosis differ from those in adults, especially in very young children.

Anatomy. The great cerebral vein is a large-diameter short vein, draining the internal brain veins and two basal veins into the straight sinus. The formation of the aneurysm of the great cerebral vein occurs during the period from the sixth to the 11th weeks of intrauterine development.[1-6] At the same time, embryos first develop arteries, then veins.[7,8]

According to the angiostructural peculiarities, arteriovenous malformations (AVMs) of the vein of Galen [9] are divided into 2 types:

Choroidal type – the true AVMs of the great cerebral vein, when the feeding arteries are directly connected (have fistula) to the wall of the aneurysmally dilated great cerebral vein;

Mural type – aneurysmal dilations of the great cerebral vein caused by true cerebral AVMs or dural arteriovenous fistulas draining into the normal but dilated great cerebral vein.

Clinical manifestations of the vein of Galen aneurysmal malformation (VGAM) often depend on the child's age, his/her pathophysiological features, and the type of VGAM.[4] In newborns, VGAM can occur in the form of asymptomatic cardiomegaly and mild cyanosis to severe cardiac failure with the gradual development of hydrocephalus due to the occlusion of the cerebral aqueduct characterized by the presence of the convulsive syndrome. In children under 1 year of life, after the newborn period, the most frequent manifestation of the disease is the occlusive hydrocephalus and delay in psychomotor development.[5] In older age groups, two forms

***Corresponding author**: Igor S. Protasov, PhD. Voronezh State Medical University named after N.N. Burdenko. Voronezh, Russia. E-mail: protasovis@mail.ru*

of VGAM can be observed – apoplectic and pseudotumor-like with tumor symptoms of subtentorial localization. In the case of cranial auscultation, a pulsating noise, synchronous with the heart beat,[2] is sometimes heard. The pathological process in patients with VGAM is progradient, seldom remitting. The course of the disease should be predicted with caution.

Diagnosis and treatment. The diagnosis of VGAM in the fetus is carried out according to the ultrasound and MRI data, the latter being the method of choice. In other age groups, MRI, MRA, and CT are used. The MRA allows better visualization of the venous (venous drainage) and arterial (feeding pedicle) anatomy, as well as better assessment of the condition of the brain, which is suffering from recurrent ischemia and hemorrhage. As a rule, CT detects only pathological formations, and when the contrast agent is introduced, the image density of pathological formations significantly increases as a result of the entry of the contrast agent into the dilated vascular bed.[2,4]

Currently, the only effective method of treating VGAM in newborns and children of other age groups is surgery: endovascular occlusion of AVM feeding vessels as well as direct surgical obliteration. If hydrocephaly occurs, a shunt can be installed in the liquor system if necessary. In children, radiosurgery can also be successfully used in the treatment of VGAM. With conservative management, periodic observation (every 6-12 months) using noninvasive methods of research – MRA and X-ray CT angiography – is desirable.[3]

There is little information in the literature about the features of the VGAM clinical picture in newborns and young and older children when combined with other pathological conditions that are characteristic or common in childhood. The relevance of the problem of diagnosis and treatment of VGAM is due to the high mortality rate, disability, and frequent complications.[4]

## Case Presentation

*Patient Information*

A one-day-old newborn boy was admitted to the regional children's clinical hospital from the perinatal center for examination with the diagnosis: "The congenital anomaly of the development of cerebral vessels – the aneurism of the vein of Galen (according to ultrasonography). Cerebral ischemia of the second degree. Vesiculopustulosis."

Mother: A 31-year-old woman, gave birth to her second child with her third pregnancy, had high blood pressure starting from early pregnancy.

Father: A 39-year-old healthy man.

According to the prenatal ultrasound study, the defect of the development of cerebral vessels (aneurysm of the vein of Galen) was discovered for the first time at 39 weeks of gestation. The second delivery, at 39 weeks, by emergency cesarean section.

*Clinical Findings*

Body weight at birth – 4540g, length – 60 cm, head circumference – 35 cm, chest circumference – 36 cm. The Apgar score – 8-9 points. In the first hour of life, the infant had symptoms of respiratory failure grade 2, according to the Silverman scoring system. At 12 hours of life, a tachypnea was registered up to 60 breaths per minute, lengthening of exhalation, moderate retraction of the intercostal space (Downes scale: Grade 3). At 24 hours of age, showing stable hemodynamics, the newborn infant was transferred from the Children's Division at the Perinatal Center to the Division of Resuscitation and Intensive Care at the Regional Children's Clinical Hospital. There was no need for respiratory therapy. From the third day of life, the examination and treatment of the infant was carried out at the Division of Pathology of Newborn and Premature Babies.

*Objective Data*

The child's condition, by the nature of the disease, is severe. Consciousness and physique are correct. The skin cover is icteric and clean. No visible edemas; a moderate pastiness of tissues was noted. The ribcage is cylindrical. In the lungs, puerile respiration. The respiratory rate – 40 breaths per minute. Heart sounds are sonorous, rhythmic. The heart rate is 140 bpm. The abdomen is soft; the liver protrudes below the costal margin by 1cm, the spleen is not palpable. Urination is not disturbed. The stool is loose, regular. The child is mixed-fed; it ingests food, with no regurgitation.

Neurological status: The newborn is conscious. The head is rounded. Bregmatic fontanel is 2.0×2.0 cm, not tense. The cranial sutures are closed. Motor activity is sufficient. Reflex responses of innate automatism were evoked but quickly depleted. The cranial innervation is normal. The infant fixes his gaze and follows objects. Muscle tone is moderately reduced. Deep reflexes are lively and symmetrical. Sensitivity is not compromised. Vegetative-trophic functions are not changed.

*Diagnostic Assessment*

The blood and urine tests, biochemical analysis of blood (total protein, urea, creatinine, glucose, ALAT, ASAT, total bilirubin and its fractions, electrolytes, CRP, serum iron), are within the age normal limits. No antibodies to CMV, mycoplasma, toxoplasma, and chlamydia by the ELISA method are found. Indicators of acid-base state and coagulogram are without deviations.

Chest X-ray: no focal infiltrative changes are detected. The shadow of the mediastinum is expanded due to the lobes of the thymus gland.

Cervical spine X-ray: kyphotic deformity at the level of the C2–C4 segment. Indirect signs of natal injury are noted – dislocation of C1–C2 vertebral bodies.

ECG: sinus rhythm, heart rate of 170 bpm. The position of the electrical axis of the heart is normal. Incomplete block of the right branch of the His bundle.

Echocardiography: open oval window. The heart cavities are not enlarged. The contractility of the left ventricular myocardium is satisfactory. Data for congenital heart disease and pulmonary hypertension are not obtained.

Ultrasound of the organs of the hepatopancreatoduodenal zone and kidneys show no pathology. Neurosonography at 5 days of age: signs of aneurysm of the vein of Galen, hypoxic changes in the substance of the brain, and periventricular edema. MRI of the brain: VGAM (choroidal type).

Examination by an ophthalmologist and an ENT doctor: no pathology.

Neurologist's examination: The congenital anomaly of the development of cerebral vessels – VGAM of choroidal type. Cerebral ischemia of the second degree. Natal injury to the cervical spine.

*Treatment*

Antimicrobial and dehydration therapy and a course of energy correctors (levocarnitine) were carried out.

*Outcome and Follow-up*

During the stay in the hospital, the child's condition was satisfactory; no focal neurological symptoms were detected. The dynamics was observed by a neurosurgeon. At 16 days of age, he was discharged for outpatient care with a neurosurgeon's recommendation for surgical treatment at the age of 6-8 months.

## Discussion

This clinical case is of practical interest since the vein of Galen aneurysmal malformation is a rare congenital anomaly of cerebral vessels. The frequency of occurrence of this aneurysm in childhood is 30%.[8] In different age periods, if a child has an arteriovenous malformation, it may increase due to involving new vascular formations in the malformation; therefore, the need for expedient early detection and surgical treatment is obvious. After the surgical treatment of arteriovenous malformations in children, focal neurological symptoms, seizures, and developmental delays are often observed. These neurological disorders in children, as a rule, are more easily compensated through rehabilitation measures than in adults.[10,11] The results of arteriovenous malformation treatment in recent years (5-7 years) have improved considerably, but many diagnostic and curative aspects in children require the development of new approaches to addressing this problem.

## Competing Interests

The authors declare that they have no competing interests.

## References

1. Medvedev YuA, Matsko D.E. Aneurysms and malformations of cerebral vessels. St. Petersburg; 1993. [In Russian].
2. Petrukhin AS. Clinical Pediatric Neurology. Moscow: Meditsina; 2008. [In Russian].
3. Stakhovskaya LV, Kotov SV. Stroke: A Guide for Physicians. Moscow: Medical Information Agency; 2014. [In Russian].
4. Khachatryan VA, Samochernykh KA, Trofimova TN. Cerebrovascular pathology in children. St. Petersburg; 2006. [In Russian].
5. Brunelle F. Arteriovenous malformation of the vein of Galen in children. Pediatr Radiol. 1997 Jun;27(6):501-13. doi: 10.1007/s002470050169. PMID: 9174022.
6. Chiang V, Awad I, Berenstein A, Scott M, Spetzler R, Alexander MJ. Neonatal galenic arteriovenous malformation. Neurosurgery. 1999 Apr;44(4):847-54. doi: 10.1097/00006123-199904000-00087.
7. Girard N, Lasjaunias P, Taylor W. Reversible tonsillar prolapse in vein of Galen aneurysmal malformations: report of eight cases and pathophysiological hypothesis. Childs Nerv Syst. 1994 Apr;10(3):141-7. doi: 10.1007/BF00301078.
8. Lasjaunias PL, Alvarez H, Rodesch G, Garcia-Monaco R, Ter Brugge K, Burrows P, Taylor W. Aneurysmal Malformations of the Vein of Galen. Follow-up of 120 Children Treated between 1984 and 1994. Interv Neuroradiol. 1996 Mar 30;2(1):15-26. doi: 10.1177/159101999600200102.
9. Lasjaunias P, Terbrugge K, Piske R, Lopez Ibor L, Manelfe C. Dilatation de la veine de Galien. Formes anatomo-cliniques et traitement endovasculaire à propos de 14 cas explorés et/ou traités entre 1983 et 1986 [Dilatation of the vein of Galen. Anatomoclinical forms and endovascular treatment apropos of 14 cases explored and/or treated between 1983 and 1986]. Neurochirurgie. 1987;33(4):315-33. [Article in French].
10. Kutashov VA, Sakharov IE. Neurology and psychiatry of childhood. V.: VSMU Publishing House; 2015. [In Russian].
11. Kutashov VA, Sakharov IE, Kutashova LA, Chemordakov IA. Neurology in clinical examples. Moscow; 2019. [In Russian].

International Journal of Biomedicine 11(1) (2021) 61-64
http://dx.doi.org/10.21103/Article11(1)_CR2

CASE REPORT

INTERNATIONAL JOURNAL OF BIOMEDICINE

# Heterogeneous Neurological Disorders Associated with the SARS-CoV-2 Infection: A Case Report

Vyacheslav A. Kutashov, PhD, ScD; Olga V. Ulyanova, PhD; Igor S. Protasov, PhD*; Oleg V. Zolotaryov, PhD; Elena S. Ananyeva, PhD; Anna A. Dudina, PhD; Margarita V. Uvarova, PhD

*Voronezh State Medical University named after N.N. Burdenko*
*Voronezh, the Russian Federation*

## Abstract

The novel coronavirus SARS-CoV-2 and the disease it causes, COVID-19, along with damage to the respiratory system, can lead to disorders of the central and peripheral nervous system, as well as the muscular system. The article presents literature data and the authors' observations of the course of neurological disorders in a patient with COVID-19. This study found that there is a link between the severity of COVID-19 and the intensity and frequency of neurological disorders.(**International Journal of Biomedicine. 2021;11(1):61-64.**)

**Key Words:** SARS-CoV-2 • pandemic • status epilepticus • viral pneumonia • myasthenic syndrome

**For citation**: Kutashov VA, Ulyanova OV, Protasov IS, Zolotaryov OV, Ananyeva ES, Dudina AA, Uvarova MV. Heterogeneous Neurological Disorders Associated with the SARS-CoV-2 Infection: A Case Report. International Journal of Biomedicine. 2021;11(1):61-64. doi:10.21103/Article11(1)_CR2

## Abbreviations

**ARDS**, acute respiratory distress syndrome; **HLA**, the human leukocyte antigen; **IL**, interleukin; **IgM**, immunoglobulin M; **CPK**, creatine phosphokinase; **LDH**, lactate dehydrogenase; **ACE2**, angiotensin converting enzyme 2; **CT**, computed tomography; **CTA**, computed tomography angiography; **MRA**, magnetic resonance imaging; **ENMG**, electroneuromyography.

## Introduction

The well-functioning health systems of the developed world have been deeply shaken by the year 2019.[1-3] COVID-19 cases have been reported everywhere, and on March 11, 2020, the World Health Organization declared COVID-19 as a global pandemic. The clinical picture of the novel coronavirus SARS-CoV-2 is characterized primarily by disorders of the respiratory system (in 91.1% of the cases, the development of severe ARDS is observed as a leading complication), febrile syndrome (83%-99% of the cases), and pathology of the skin integument, gastrointestinal tract (up to 15% of the cases), urinary and nervous systems.[4]

Based on the available scientific data, the concept of a multisystem response of the body to the penetration of the SARS-CoV-2 virus has been developed. We have tried to summarize the known pathogenetic features of SARS-CoV-2 virulence.[5-8] As currently established, SARS-CoV-2 is tropic to type II alveolocytes and enterocytes of the small intestine. The virus enters the cell due to the attachment of the peplomer S-protein. Once in the cell, the virus is preactivated by serine proteases (furin and TMPRSS2); then the active phase of the viral RNA replication begins with several independent parts. After the completion of the replication phase, the vesicles containing the virion fuse with the plasmatic membrane of the cell, and the virus is released. At the moment serine

***Corresponding author**: Igor S. Protasov, PhD. Voronezh State Medical University named after N.N. Burdenko. Voronezh, Russia. E-mail: protasovis@mail.ru*

proteases are activated, cytokines and IL-2 are released, triggering the activation of CD4 lymphocytes, which in turn activate Th1 lymphocytes. However, due to the mimicry of the virus, the immune system cannot adequately recognize the amount of viral antigens, probably, among other things, due to the activation of immune control and the launch of Th-suppressors, which may be one of the causes of leukopenia. This hypothesis explains the high contagiousness of the virus during the latent period of the disease. After the virus is isolated from the "primary" cell of the type II alveocyte, it is carried out with the blood flow, and enterocytes of the small intestine become the second most important target. The mechanism of penetration into enterocytes is similar. The local response activates B-lymphocytes and triggers Th2-lymphocytes, promoting the release of IL-4 and IL-5 into the blood. The humoral response (3-8 days) begins to form; IgM is released. In response, the complement system is activated; the forming, circulating immune complexes are captured by mast cells, increasing the release of histamine and serotonin into the blood, thereby triggering a systemic inflammatory response. After a few days of the latent period, changes in metabolic processes begin in the target cells; the normal rhythm of the cell's work is disrupted, including the synthesis of the components necessary for functioning, and the process of apoptosis starts. The alveolar macrophages are activated with the release of proinflammatory agents – IL-6, IL-8, and TNF-alpha. Chemoattractants are released into the blood, stimulating the movement of monocytes and neutrophils from the blood through the endothelium and alveolar epithelium, which finally causes a violation of ventilation and perfusion processes with the accumulation of fluid in the alveoli. In turn, the leukocytes themselves are a source of leukotrienes, proteases, and platelet aggregation factor, which causes alveolar fibrin deposition, the formation of hyaline membranes, and the formation of microthrombus in the vascular bed of the lungs, forming toxic edema and acute respiratory distress syndrome. Further progression of respiratory failure is associated with the addition of bacterial flora. Thus, based on the currently available research data, it can be assumed that the rapid development, multisystem damage, rapid increase in the systemic inflammatory response syndrome, and cytokine storm are caused by the compromised states of the immune system. Since a cascade mechanism is launched, which is lightning-fast in nature, the immune system lacks time to react in a timely and adequate manner. The probable reasons for this are the following: misidentification of the virus due to mimicry of the SARS-Cov-2 S-protein to ACE2 and its presentation as an antigen by antigen-presenting cells; rapid virus replication in type II alveocytes (primary gateway for infection) with subsequent blockage of regional lymph nodes due to the peculiarities of the formation of the immune response, which contributes to an increase in local blood supply and the influx of lymphocytic cells from the recirculating pool with "inhibition" of cellular immunity; rapid migration and subsequent dissemination of replicated SARS-CoV-2 with blood flow into the small intestine; and "secondary" virus replication in enterocytes with "inhibition" of humoral immunity. Since the HLA system is responsible for the quality of antigen-presenting cells, it is logical to assume that the intensity and massiveness of the immune system response is genetically determined, especially in patients with autoimmune diseases. Thus, as a screening for the activation of the immune response (or its clearly high level in the presence of an autoimmune disease) and a high risk of developing severe forms of COVID-19 in the future, it is possible to use the levels of the so-called non-classical HLA complexes: HLA-MICA as an early signal of the immune response to the infectious damage; HLA-E as an attempt by the body to cope with a cascade of proliferative immune responses; HLA-B27 as an indicator of the number and activity of antigen-presenting cells. Taking into account the population characteristics of HLA, it is natural to assume the peculiarities of the immune response in individuals with different blood groups. Thus, it is likely that individuals with h*emagglutinins* (blood groups A (II), B (III), and AB (IV)) may have more severe forms of COVID-19 due to mimicry of the S-protein of SARS-CoV-2, but this assumption is hypothetical and requires further detailed study. However, it is clear that the presence of chronic diseases with a constant level of stimulation of the immune system contributes to hyperresponsiveness, the increased release of cytokines, and the development of severe forms of novel coronavirus infection (this is evidenced by the positive effect of the use of glucocorticosteroids). Given the features of SARS-CoV-2 replication, it is also likely to suggest in the near future the following options of treatment-blockage of virus replication: blockage of CD147 with monoclonal antibodies (mepolizumab) in the absence of signs of bacterial infection; blockage of serine proteases (furin, TMPRSS2) with Kalistat; blockage of RNA replication (Avifavir). The assumptions made are hypothetical and, of course, require further research.[4]

It is noteworthy that a number of viral infections can be accompanied by direct damage to the skeletal muscles. On the other hand, skeletal muscle damage can be secondary in severe viral infection, especially complicated by sepsis, multiple organ failure, and acute respiratory distress syndrome. L. Mao et al.,[9] on the basis of an increase in the levels of CPK and LDH, diagnosed the involvement of the muscular system in 10.7% of patients with a predominance of the severe form of the disease (19.3% and 4.8%). In groups with mild and severe cases of COVID-19, the levels of CPK and LDH were reliably higher in patients with muscle weakness than without it. At the same time, in patients with muscle symptoms, the level of CPK and LDH was significantly higher in the severe form of the disease than in the group with a mild form. This distribution suggests that the cause of damage to the muscular system could be not only a direct viral effect, but also a general severe condition with metabolic disorders. An increase in laboratory markers reflecting skeletal muscle and myocardial injury in COVID-19 has been noted by Q. Ruan et al.[10] They, as well as L. Mao et al.,[9] drew attention to the relationship between the severity of the condition and increased myoglobin content. The mechanisms of skeletal muscle damage in COVID-19 are not entirely clear. Presumably, they can be associated with ACE2 receptors, which are widely represented in skeletal muscle and myocardium; their expression increases during

viral infection and the severe condition with increased muscle tissue decay. Along with this, G. Baird and T. Montine consider the excessive production of cytokines during inflammation as a direct damaging factor of muscle tissue.[11] The role of a pathological autoimmune reaction in polyclonal stimulation of the immune system by a virus with cross-damage of skeletal muscle antigens is not excluded.[12]

Neurological disorders can be divided into 3 types:

1) Manifestations of the central nervous system (dizziness, headache, impaired consciousness, acute cerebrovascular event, ataxia, and convulsions)

2) Manifestations of the peripheral nervous system (taste, smell, and vision disorders; neuralgias)

3) Damage to the musculoskeletal system [13]

During the COVID-19 pandemic, hospitalized patients with neurological symptoms should be examined for COVID-19 to make a quick and correct diagnosis. In addition, it is essential to preserve as much as possible the quality of medical care for patients with neurological diseases, especially with acute damage to both the central and peripheral nervous systems, while taking all precautions to avoid transmission of a novel coronavirus infection to the medical personnel and patients.[14]

## Case Presentation

*Patient Information*

A 24-year-old man, on May 19, 2020, presented by ambulance to the intensive care unit of the Voronezh City Clinical Emergency Hospital No.1 with a diagnosis of "seizures of unknown genesis." Complaints: double vision, unsteadiness when walking, numbness of the lower limbs, and discomfort while swallowing.

*Clinical Findings and Diagnostic Assessment*

Status epilepticus. The patient was transferred to artificial lung ventilation (ALV) ─ mechanical ventilation, CT scan of the lungs showed a pattern characteristic of viral pneumonia caused by the novel coronavirus infection COVID-19. A COVID-19 coronavirus RNA test confirmed the diagnosis. CTA: a picture of complete trifurcation of the right internal carotid artery. The asymmetry of the vertebral arteries D>S. CT scan of the brain did not reveal any pathology. MRI of the brain revealed no pathological changes. Lumbar puncture: general analysis of cerebrospinal fluid (CSF), biochemical analysis, and polymerase chain reaction results were without pathology. CSF seeding showed no pathology either. ALV was performed for 5 days.

Clinical Diagnosis: "Status epilepticus as of May 19, 2020. Confirmed COVID-19: severe disease course, bilateral viral pneumonia."

*Treatment*

Convulex, Encorate, Sulbactam, Azithromycin, Hydroxychloroquine, Enoxaparin, Sterofundin, Omeprazole, and Tocilizumab.

*Outcome and Follow-up*

Diagnosis at discharge: "Confirmed COVID-19: severe disease course, bilateral viral pneumonia regressed, status epilepticus as of May 19, 2020."

The patient stayed at home for two days; after that, he experienced pronounced double vision, numbness of the lower limbs, dizziness, and unsteadiness when walking. The patient was readmitted to the neurological department for patients with violation of cerebral circulation at the Voronezh City Clinical Emergency Hospital No.1

*Clinical Findings and Diagnostic Assessment*

The patient's previous history also included bronchial asthma and atopic dermatitis.

Objectively: A moderate-severe condition. Skin: rash in the area of the anterior abdominal wall and shoulder joints. Heart sounds are sonorous, rhythmic. Blood pressure - 140/80 mmHg, heart rate – 76 bpm. In the lungs, breathing is vesicular. Respiratory rate – 17 per minute. The abdomen is soft, free of pain. The liver and spleen are not palpable. The stool and diuresis are without pathology. The body temperature – 36.6°C.

Neurological status: Wakefulness level – clear consciousness; there is an orientation to self, location, and time. Speech is preserved. There are no meningeal signs. Pupils D=S; direct and concomitant reaction to light is preserved. Eye slits D>S; congenital left-sided hemi-ptosis; full eyeball movement; horizontal nystagmus; diplopia when looking in all directions. The nasolabial folds are symmetrical. The tongue is on the midline. Hearing is preserved. Swallowing and phonation are not disturbed. Active pharyngeal reflexes D=S; deep reflexes D=S. No pareses. Muscle tone is not changed. There are no pathological signs. The patient performs coordination tests with misses on both sides. In the Romberg posture, swaying occurs. Sweating is normal. Dermographism is pink. There is knee-high hypoesthesia of the lower limbs.

The additional examination (brain MRI, duplex ultrasound of the brachiocephalic artery, EEG during one hour, ENMG) without pathology.

*Treatment*

Pulse therapy with glucocorticosteroids, anticholinesterase drugs, neuroprotection, and metabolic therapy. After the treatment, there was no positive dynamics; double vision did not decrease, and left-sided hemianopsia also began to appear.

Examination of the fundus revealed no pathology. Needle ENMG was repeated. The blink reflex showed an inconsistent increase in R2 component latency with stimulation on the left. The jitter from the circular muscle of the eye on the left revealed an irregular increase in the interpeak intervals without dropout of second potentials.

The ENMG picture allows us to discuss the involvement in the pathological process of the ipsilateral spinal tract of the V nerve/intercalary neurons reticular formation, mainly on the left in the brain stem. Myasthenic-type neuromuscular transmission disorder in the circular muscle of the eye was not detected; however, there were dropout units with transmission disorder. Given the data obtained, we decided to conduct 5 plasmapheresis sessions. The double vision was gone. At discharge, the patient's condition was completely stabilized with no pathology in the neurological status.

*Clinical Diagnosis: "*Encephalopolyneuropathy associated with the consequences of COVID-19; initial manifestations of myasthenic syndrome (according to ENMG data); status epilepticus as of May 19, 2020."

Thus, the damage to the nervous system in the patient appeared as a result of the COVID-19 infection and was of a heterogeneous nature.

## Discussion

Over the past few months, our understanding of the transmissivity, pathogenesis, and clinical heterogeneity of coronavirus pneumonia caused by SARS-CoV-2 has been significantly expanded and modified. The few publications devoted to the development of neurological conditions associated with COVID-19 (meningoencephalitis, acute cerebrovascular pathology, Guillain-Barré syndrome, etc.) do not give an exhaustive answer, whether those conditions are a consequence of the direct neurotropic action of the virus or are mediated by an immune response and other reactions (including pro-inflammatory and pro-thrombotic influences). Besides, like other infectious diseases, SARS-CoV-2 can lead to the clinical realization of asymptomatic comorbidities (mostly cardiovascular and endocrine disorders) and their aggravation, with a risk of a fatal outcome.

The COVID-19 pandemic poses several tasks for the neuroscience community: 1) to provide adequate therapy for patients with diseases of the nervous system (cerebrovascular diseases),[15] various forms of dementia, Parkinson's disease, amyotrophic lateral sclerosis) who are at high risk of developing complications; 2) to formulate algorithms for timely diagnostic and therapeutic care for patients with acute neurological conditions in the context of COVID-19 pandemic (acute cerebrovascular accident, exacerbation of multiple sclerosis, myasthenic crisis, status epilepticus); 3) to ensure the prevention of complications caused by coronavirus infection among patients receiving immunosuppressive therapy for various autoimmune diseases, as well as cancerous lesions of the nervous system. Despite the increasing number of publications on this topic, to date, the information on the neurological aspects of COVID-19 is incomplete and further research is required.

## Competing Interests

The authors declare that they have no competing interests.

## References

1. WHO. Coronavirus Disease (COVID-19). Situation Report – 209. Available at https://www.who.int/docs/default-source/coronaviruse/situation-reports/20200816-covid-19-sitrep-209.pdf?sfvrsn=5dde1ca2_2. Data as received by WHO from national authorities by 10:00 CEST, 16 August 2020
2. WHO. Coronavirus disease (COVID-19). Available at https://www.who.int/docs/default-source/coronaviruse/situation-reports/20200921-weekly-epi-update-6.pdf?sfvrsn=d9cf9496_4. Data as received by WHO from national authorities, as of 10 am CEST 20 September 2020
3. Cutler DM, Summers LH. The COVID-19 Pandemic and the $16 Trillion Virus. JAMA. 2020 Oct 20;324(15):1495-1496. doi: 10.1001/jama.2020.19759.
4. Karpova OV, Udalov YuD, Samoylov AS, Kudryavtsev RA. [Features of Case Management with Neuromuscular Disease During COVID-19. Clinical Impression]. Journal of Clinical Practice. 2020;11(2):107–117. doi: 10.17816/clinpract34580. [Article in Russian].
5. Rao GHR. SARS-CoV-2 Biochemistry, Transmission, Clinical Manifestations, and Prevention. International Journal of Biomedicine. 2020; 10(4):303-311. doi: 10.21103/Article10(4)_GE
6. Burki T. The origin of SARS-CoV-2. Lancet Infect Dis. 2020 Sep;20(9):1018-1019. doi: 10.1016/S1473-3099(20)30641-1.
7. Wang H, Li X, Li T, Zhang S, Wang L, Wu X, Liu J. The genetic sequence, origin, and diagnosis of SARS-CoV-2. Eur J Clin Microbiol Infect Dis. 2020 Sep;39(9):1629-1635. doi: 10.1007/s10096-020-03899-4.
8. Severe Covid-19 GWAS Group, Ellinghaus D, Degenhardt F, Bujanda L, Buti M, Albillos A, Invernizzi P, et al. Genomewide Association Study of Severe Covid-19 with Respiratory Failure. N Engl J Med. 2020 Oct 15;383(16):1522-1534. doi: 10.1056/NEJMoa2020283.
9. Mao L, Jin H, Wang M, Hu Y, Chen S, He Q, Chang J, Hong C, Zhou Y, Wang D, Miao X, Li Y, Hu B. Neurologic Manifestations of Hospitalized Patients With Coronavirus Disease 2019 in Wuhan, China. JAMA Neurol. 2020 Jun 1;77(6):683-690. doi: 10.1001/jamaneurol.2020.1127.
10. Ruan Q, Yang K, Wang W, Jiang L, Song J. Clinical predictors of mortality due to COVID-19 based on an analysis of data of 150 patients from Wuhan, China. Intensive Care Med. 2020 May;46(5):846-848. doi: 10.1007/s00134-020-05991-x.
11. Baird GS, Montine TJ. Multiplex immunoassay analysis of cytokines in idiopathic inflammatory myopathy. Arch Pathol Lab Med. 2008 Feb;132(2):232-8. doi: 10.1043/1543-2165(2008)132[232:MIAOCI]2.0.CO;2.
12. Rodionova OV, Sorokoumov VA. Neurological diseases in the context of the COVID-19 pandemic (review of the literature). The Scientific Notes of the Pavlov University. 2020;27(2):18-24. [Article in Russian].
13. Gusev EI, Martynov MY, Boyko AN, Voznyuk IA, Latsh NY, Sivertseva SA, Spirin NN, Shamalov NA. Novaya koronavirusnaya infektsiya (COVID-19) i porazhenie nervnoi sistemy: mekhanizmy nevrologicheskikh rasstroistv, klinicheskie proyavleniya, organizatsiya nevrologicheskoi pomoshchi [Novel coronavirus infection (COVID-19) and nervous system involvement: pathogenesis, clinical manifestations, organization of neurological care]. Zh Nevrol Psikhiatr Im S S Korsakova. 2020;120(6):7-16. doi: 10.17116/jnevro20201200617. [Article in Russian].
14. Tanashyan MM. Kuznetsova PI, Raskurazhev AA. [Neurological aspects of COVID-19]. Annaly Klinicheskoi i Eksperimental'noi Nevrologii. 2020;14(2):62–69. [Article in Russian].
15. Kutashov VA., Protasov IS. Recommendations for the management of patients with acute cerebrovascular accidents in the context of the COVID-19 pandemic. Voronezh State Medical University named after N.N.Burdenko; 2020. [In Russian].

International Journal of Biomedicine 11(1) (2021) 65-67
http://dx.doi.org/10.21103/Article11(1)_ShC

SHORT COMMUNICATION

INTERNATIONAL JOURNAL OF BIOMEDICINE

# Predictive Markers of Missed Miscarriage

Agamurad A. Orazmuradov, PhD, ScD[1]; Anastasiya N. Akhmatova, PhD[1]; Khalid Haddad[1]; Alexander M. Lopatin[1]; Irina V. Bekbaeva[1]; Gayane A. Arakelyan[1]; Marianna Z. Abitova[1]; Sergey I. Kyrtikov[1]; Nozimabonu M. Zokirova[1]; Aleksey A. Lukaev, PhD[2]

[1]*Peoples' Friendship University of Russia (RUDN University), Moscow Russia*
[2]*Mytishchi City Clinical Hospital Mytishchi, Moscow Region, Russia*

## Abstract

The aim of this study was to find useful the serological markers for missed miscarriage (MM) in order to predict the outcome of pregnancy. The study included 141 pregnant women aged between 18 and 45 years at gestational age under 11 weeks. All women were divided into 3 groups. Group 1 included 68 women with MM; Group 2 included 43 women with spontaneous miscarriage; Group 3 included 30 pregnant women without pathology. Proteomic analysis of the blood serum was performed using liquid chromatography-mass spectrometry. The results of our study show that immunoglobulin kappa variable 3-15 (KV315) can be considered as the most promising serologic marker for MM in early gestation. The potential role of KV315 as the serological marker is very important for predicting the course of pregnancy.(**International Journal of Biomedicine. 2021;11(1):65-67.**)

**Key Words**: missed miscarriage • serological markers • immunoglobulin kappa variable 3-15

**For citation**: Orazmuradov AA, Akhmatova AN, Haddad Kh, Lopatin AM, Bekbaeva IV, Arakelyan GA, Abitova MZ, Kyrtikov SI, Zokirova NM, Lukaev AA. Predictive Markers of Missed Miscarriage. International Journal of Biomedicine. 2021;11(1):65-67. doi:10.21103/Article11(1)_ShC

## Abbreviations

**MM**, missed miscarriage; **KV315**, immunoglobulin kappa variable 3-15; **ANA**, antinuclear antibodies; **LC**, light chain; **FLC**, free light chains: **LC-MS**, liquid chromatography-mass spectrometry; **AMBP**, alpha-1-microglobulin/bikunin precursor; **TTR**, transthyretin; **apoA-IV**, apolipoprotein A-14; **ITIH4**, inter-alpha-trypsin inhibitor heavy chain H4.

## Introduction

Missed miscarriage (MM) is one of the unsolved problems both in the Russian Federation and in the world. MM is a specific type of miscarriage and may occur in up to 50% of all women with miscarriages. There is still a lack of biomarkers with predictive value for asymptomatic patients before this event occurs, but multiple etiologic factors—including genetic risk factors, immunological factors, endocrine and blood disorders, uterine abnormalities, infections, and environmental factors—have been identified for MM.

[*]***Corresponding author:*** *Aleksey A. Lukaev, PhD. Mytishchi municipal clinical hospital, Mytishchi, Moscow Region, Russia E-mail: aleksei_lukaev@mail.ru*

It is well known that pregnancy outcome and fetal development largely depend on the state of the mother's immune system. Thus, the more pronounced the changes in the antibody content, the more often adverse pregnancy outcomes are observed.[1,2] In recent years, immunological abnormalities have begun to be considered as etiological factors of miscarriage, in particular, the circulation in the blood of ANA or anti-DNA antibodies. Increased titers of anti-DNA antibodies in various autoimmune and infectious diseases can cause inflammatory changes in the placenta and trigger a reaction of fetal rejection.[3,4]

In the modern literature, there are few data on serological markers of MM, which creates the prerequisites for conducting this study aimed at finding the prognostic serological markers for MM in order to predict the outcome of pregnancy.

## Materials and Methods

In the period from April 2020 to December 2020, a group of 141 pregnant women aged between 18 and 45 years at gestational age under 11 weeks were examined. All women were divided into 3 groups. Group 1 (Gr1) included 68 women with MM; Group 2 (Gr2) included 43 women with spontaneous miscarriage; Group 3 included 30 women without pathology (control group [CG]).

Inclusion criteria were MM, spontaneous miscarriage or physiological pregnancy at gestational age under 11 weeks. Exclusion criteria were autoimmune diseases, infectious diseases, and diseases of the thyroid gland, including thyroid dysfunction.

Examination of patients included clinical methods, questionnaire survey, analysis of case histories, laboratory tests (clinical blood test, biochemical blood test, urine test, and determination of antibody titer to the TORCH complex), and pelvic ultrasound. All women underwent an assessment of vaginal microcenosis and the quantitative and qualitative composition of the biotope of the cervical discharge. Proteomic analysis of the blood serum was performed using LC-MS.

The study was conducted in accordance with ethical principles of the WMA Declaration of Helsinki (1964, ed. 2013) and approved by the RUDN University Ethics Committee. Written informed consent was obtained from all participants.

Statistical analysis was performed using the Statistica 8.0 software package (StatSoft Inc, USA). A value of $P<0.05$ was considered statistically significant.

## Results and Discussion

For the analysis of potentially significant markers, we studied serological markers found in all 3 groups; in particular, we compared the ratios of protein concentrations in the study groups. If the concentration ratio of the investigated marker in the Gr1/CG pair was close to 1 or equal to 1, then the marker was considered nonspecific; if the concentration ratio of the investigated marker in the Gr1/Gr2 pair was close to 1 or equal to 1, then the marker was also considered non-specific; however, if the studied ratio was close to 1 or equal to 1 in the Gr1/Gr2 pair and at the same time >1 in the Gr1/CG pair, then the marker was considered potentially specific. As can be seen from Table 1, the most specific serorlogical marker of MM may be KV315, since the ratio of its concentration was 4.936 in the Gr1/CG pair, 1.243 in the Gr1/Gr2 pair, and 3.971 in the Gr2/CG pair. For all other markers, differences between groups were less pronounced.

The potential role of KV315 as the serological marker is very important for predicting the course of pregnancy. KV315 (P01624-KV315_HUMAN) (V region of the variable domain of immunoglobulin light chains that participates in the antigen recognition)[5] is involved in a number of potentially interesting pathways such as Initial triggering of complement, classical antibody-mediated complement activation, scavenging heme from plasma, FCGR activation, platelet activation, acute-phase responses, FCERI mediated NF-kB activation degranulation, signaling, aggregation, and the creation of C4 and C2 activators, regulation of complement cascade, etc[6]

***Table 1.***

***The specific serorlogical marker of MM***

| Group pair | apoA-IV | KV315 | AMBP | ITIH4 | TTR |
|---|---|---|---|---|---|
| Gr1/CG | 0.410 | 4.936 | 0.527 | 0.338 | 0.329 |
| Gr1/Gr2 | 0.565 | 1.243 | 0.530 | 0.428 | 0.332 |
| Gr2/CG | 0.728 | 3.971 | 0.993 | 0.790 | 0.993 |
| *P*-value | 0.01332 | 0.00896 | 0.00023 | -0.471 | 0.00038 |

Taking into account the results obtained, we can assume that we register a signal from the total fraction of κ-chains. According to Katzmann, the content of FLCλ slightly exceeds the content of FLCκ and amounts to 5.7-26.3 mg/ml for FLCλ and 3.3-19.4 mg/ml for FLCκ, with the diagnostic interval of 0.26-1.65 for the κ/λ ratio.[7] This indicator is often used as an auxiliary parameter for diagnosing inflammatory reactions, oncohematological diseases, rheumatoid arthritis, and systemic lupus erythematosus in the early stages of development.

There are data on the dynamics of the content of LCs and their ratio in pregnant women in the third trimester, after childbirth and in comparison with non-pregnant women. Lima et al.[6] showed that the median levels of both κ and λ FLC were significantly higher during the postpartum period than on the day of delivery. The levels of FLCκ recovered during the postpartum period were not significantly different from those of the non-pregnant women, whereas the levels of FLCλ remained low. Thus, the κ/λ ratio increased during the postpartum period, which can be related to higher activity of the adaptive immune system. According to Lima et al.,[8] this finding is an indicator of B-cell activation occurring after the systemic immunological reaction associated with childbirth. In addition, the increased κ/λ ratio may indicate polyclonal hypergammaglobulinemia, which occurs during the postpartum period and may be caused by an inflammatory state. Indirectly, polyclonal hypergammaglobulinemia is also indicated by the high level of B-cell-activating factor on the day of delivery and during the postpartum period, rather than during the third trimester of pregnancy.

Jenner et al.[9] argue that the tendency to an increase in circulating lg-LCs is not only an indicator of internal immunological processes, but also a prognostic indicator of the development of preeclampsia and various obstetric complications, including preterm birth.

**In conclusion**, the results of our study show that KV315 can be considered as the most promising serologic marker for MM in early gestation. It seems appropriate before planning a pregnancy to conduct an additional examination of women who show a high KV315 value in order to predict the outcome of pregnancy.

## Acknowledgments

This study was supported by the RUDN University Strategic Academic Leadership Program.

## Competing Interests

The authors declare that they have no competing interests.

## References

1. Radzinsky VE, Orazmuradov AA, Savenkova IV, Damirova KF, Haddad H. Preterm labour: an open problem in XXI century. Kuban Scientific Medical Bulletin. 2020;27(4):27-37. [Article in Russian].
2. Non-developing pregnancy. Chapter 14. In: Radzinsky VE, Orazmuradova AA, editors. Early pregnancy. From pregravid preparation to healthy gestation. Moscow: StatusPraesens; 2020:509-537.
3. Svyatova GS, Berezina GM, Salimbaeva DN, Kirikbaeva MS, Murtazalieva AV, Saduakasova KZ. [Genetic aspects of the idiopathic form of recurrent miscarriage. Literature review]. Science&Healthcare. 2019; 21(4):37-49. [Article in Russian].
4. Aleynik VA, Babich SM, Negmatshaeva XN, Yuldasheva OS. [Features of immunological changes in women with a miscarriage at the presence of autoantibodies]. Molodoi Uchenii. 2017;22(156):411-414. [Article in Russian].
5. Lefranc MP. Immunoglobulin and T Cell Receptor Genes: IMGT(®) and the Birth and Rise of Immunoinformatics. Front Immunol. 2014 Feb 5;5:22. doi: 10.3389/fimmu.2014.00022.
6. UniProtKB - P01624-KV315_HUMAN) https://www.uniprot.org/uniprot/P01624.
7. Klein C, Schaefer W, Regula JT. The use of CrossMAb technology for the generation of bi- and multispecific antibodies. MAbs. 2016 Aug-Sep;8(6):1010-20. doi: 10.1080/19420862.2016.1197457. Epub 2016 Jun 10. Erratum in: MAbs. 2018 Nov 13;11(1):217.
8. Lima J, Cambridge G, Vilas-Boas A, Martins C, Borrego LM, Leandro M. Serum markers of B-cell activation in pregnancy during late gestation, delivery, and the postpartum period. Am J Reprod Immunol. 2019 Mar;81(3):e13090. doi: 10.1111/aji.13090. Epub 2019 Jan 30.
9. Jenner E. Serum free light chains in clinical laboratory diagnostics. Clin Chim Acta. 2014 Jan 1;427:15-20. doi: 10.1016/j.cca.2013.08.018.

International Journal of Biomedicine 11(1) (2021) 68-72
http://dx.doi.org/10.21103/Article11(1)_PV

POINT OF VIEW

INTERNATIONAL JOURNAL OF BIOMEDICINE

# Adaptive Changes in the Psyche of Homo Sapiens during the Period of the Singularity (Part 2)

Alexander G. Kruglov, PhD, ScD*; Andrey A. Kruglov, PhD

*Central Research Institute of Radiation Diagnostics*
*Moscow, the Russian Federation*

## Abstract

Creativity, the integrative function of the psyche of Homo sapiens (HS), which arose about 50,000 years ago, allowed HS to project the image of the goal (IG), transformed into a "symbol," into the external environment. The projection constructs of the psyche have become autonomous fragments of the environment in the HS perception, not being its derivatives. Objective reality, perceived by HS, has acquired non-inherent properties: a mental product of the psyche that integrates the virtual and real components of the environment. The role of HS has evolved over the last 10,000 years, since the beginning of the agrarian revolution: from (1) a dependent subject controlled by external forces in an animated world to (2) "the crown of God's creation" in "theism" and, (3) to the status "Higher power" during the period, in which "God is Dead." Initially, HS exists in an incompletely real environment, with an increasing component of virtuality. With symbolic virtual content, HS supplemented or duplicated the entire surrounding world, creating a two-component habitat (virtual and real). The emergence and development of conceptual thinking (ConceptT) led to a partial "devirtualization" of the environment, the removal of restrictions on scientific knowledge, the rapid growth of technology and social dynamics. The result of technological development was, in the recent past, a temporary resolution of the primary frustration: the establishment of the current equilibrium in the relationships with the regulatory "dissociated symbol"—the virtual "information universe" (IU). The IU, defining as the interference of "media" with the "information body" of the Internet, we consider as a unified information space, integrated with reality and in total constituting the HS habitat. Clip thinking (ClipT), qualitatively different from ConceptT, is a new operating system of the psyche, a moderator of adaptation to a new, virtualized environment. A technological derivative of mental activity HS—the IU—without the participation of conscious forms of mental activity, transforms the algorithms of thinking, i.e. formats the psyche as a whole with adaptation to qualitative and quantitative changes in the virtual component of the environment, and to the perspectives on the development of technologies during the singularity.(**International Journal of Biomedicine. 2021;11(1):68-72.**)

**Key Words**: clip thinking • conceptual thinking • singularity • virtualization • symbol • Internet • media • information revolution

**For citation**: Kruglov AG, Kruglov AA. Adaptive Changes in the Psyche of Homo sapiens during the Period of the Singularity (Part 2). International Journal of Biomedicine. 2021;11(1):68-72. doi:10.21103/Article11(1)_PV

## Abbreviations

**CC**, creative construct; **HS**, Homo sapiens; **IG**, the image of the goal; **ClipT**, clip thinking; **ConceptT**, conceptual thinking; **DMN**, the default mode network; **IU**, information universe.

Creativity, as a specific species feature of the psyche of Homo sapiens (HS), as the ability to produce the predictive hypotheses that cannot be derived directly from the initial conditions, appeared in HS as a result of a genetic mutation, or other (exogenous or interfering) causes, about 50,000 years ago.[1] HS (Cro-Magnons), having a new feature of the species ("creativity"), compared with Homo neanderthalensis, acquired a much greater range of adaptive behaviors, as well as a strategic advantage in conditions of interspecific competition, which resulted in dominating and

***Corresponding author:** *Alexander G. Kruglov, PhD, ScD. Central Research Institute of Radiation Diagnostics. Moscow, the Russian Federation. E-mail: krag48@mail.ru*

then crowding out the competitive subspecies.[2,3] Creativity created a unique for biological species ability to form flexible forms of adaptive behavior, change behavioral tactics, create technical means of hunting and war, as well as pictorial (artistic in our understanding) plots of achieving a future result (caves of Altamira, Montespan, Chauvet, etc.[4, 5]), which do not require reactive behavior. That is, in the absence of the subject of the image, virtual images with real prototypes were created. Cro-Magnons also created complex three-dimensional models: a bear in the Montespan Cave. Such models could be used both for ritual purposes (future totem) and for practicing hunting skills.[5] The operating systems of the Cro-Magnon psyche (thinking, memory, imagination, etc.), integrated creativity, made it possible to create the abstract image of the goal (IG). In the inevitable process of additions and interpretations, the IG, which received projection model characteristics, was transformed into a "symbol" (image+sense).[6] Thus, the projection of the IG into the external environment, the virtualized or mock-up "symbol," in the perception of Cro-Magnons becomes an autonomous fragment of the habitat, not being its natural derivative.[2,7,8]

The system of primary abstract representations, transforming in generations, inevitably (already at the stage of lack of means of fixation) interferes, increasing in volume and becoming more complex in structure, increasing the degree of uncertainty. Only the person with uncertainty tolerance (priest, ideologue - divergent) is capable of systematizing an array of mythologemes,[2,7] becoming an intermediary between the population and the complex structure of ideas, beliefs, mythologemes, myths. Integration of creative constructs (CC) by priests throughout generations creates stable virtual constructions that generally reflect reality in the form of sensually-specific associations perceived as real objects of the external environment.[2,7,8]

In other words, objective reality is endowed with not inherent properties, namely a mental product that integrates fragments of objective and virtual reality. Thus, a unified information space is created with the fixation of the individual's trajectory options in this system. A possibility of prognostic assessments forms, the level of anxiety decreases, the stability of society increases, and social negentropy is produced. With the accumulation of experience in the discrepancy between the forecasts and the results, the perception of their inconsistency grows. The result is the projection of control functions onto an external object with a potential that exceeds the capabilities of a person, the delegation of regulation and control functions to the object of worship. Direct and feedback links with an external control object (an object of worship) are always channeled, mediated by the "priest." [2,3,8]

For the first time in hominid history, a new need—the relationships with a symbolic image perceived as an objective reality—created an insoluble frustration as achieving equilibrium ("current equilibrium") in the relationships with the governing virtual creative construct—the "symbol." The manager CC ("symbol") has the location of the expected result outside the achievable and creates a primary insoluble frustration, which has an inexhaustible negentropic potential for creating homomorphic socio-psychological constructions of approaching the ideal, symbolic image of the goal (IG).[2,3]

A figurative, symbolic display of reality in cases, in which reality does not fit into the framework of a formal-logical and abstract display, forms mythologemes. Mythologeme is a stable psychological construct that reflects reality in the form of sensually-specific associations that are perceived as really existing.[9,10] Mythologeme is able to direct the activity of an individual to achieve significant goals,[11] creating a sequence of elements of ideas about reality and being a conceptual basis for behavior, which allows for some forms of behavior to equalize mythologeme and "motive."[7] The most important disposition of the motive is the "need,"[12] which forms the image of the future result – IG, which is the leading link in conscious behavior. The formation of IG is a psychophysiological stimulus for purposeful behavior and a starting point for the formation of an assessment scale for the speed of achieving a result, i.e. subjective time. In other words, in the psychological (subjective) time, the expected result (IG) has the fixed coordinate characteristics (virtual): a "reference point" in the future, while the present is always a temporary interval.[9] That is, the virtual "future" (IG) determines the vector of the dynamics of the "present."

The emergence of writing, as a sign of the end of the prehistoric era (the Neolithic period), is a historical moment that determined the entire subsequent trajectory of the HS development, the beginning of the "agrarian revolution," the emergence of civilization, and the first network of horizontal structures (scribes, merchants, etc.). The dynamics of the rapid growth of technology is subordinated to the goals of the producing economy, extensive population growth (including wars as a tool), and irreversible processes of terraforming (starting with the destructive for the environment slash-and-burn agriculture). The agrarian revolution transformed animistic beliefs into theistic religions, and the scientific revolution of the 18th and 19th centuries brought "theism" to the final formula: "God is Dead."[13] In other words, the role of HS has evolved over the last 10,000 years, since the beginning of the agrarian revolution: from (1) a dependent subject controlled by external forces in an animated world to (2) "the crown of God's creation" in "theism" and, (3) to the status "Higher power" during the period, in which "God is Dead."

Throughout the history of HS, the CC (Symbol) extrapolated to the external environment has repeatedly transformed from the association of "image and meaning" to dissociation. The main forms of dissociation of the symbol: 1) the preservation of the "image" and "sense" when verbalization is taboo (some totems, the naming of "divine" emperors of China, etc.); 2) the elimination of the "image" while preserving the "sense" and verbalization (Islam, iconoclasm in Christianity, etc.); 3) the elimination of the "image" and verbalization, while maintaining the "sense" (Judaism, some forms of early Christianity), i.e. ultimate virtualization of the "symbol". In other words, HS, for most of its development, existed in an environment with an ever-increasing and increasingly complex virtuality component. We believe that it was the filling of the habitat with projection constructs of the psyche that transformed HS thinking in the following sequence: 1) concrete-objective, based on interaction with

real objects; 2) visual-figurative, with the establishment of interconnections between objects and the possibility of a close forecast; 3) abstract-logical, operating with categories that are absent in reality. An example is the oldest written epics of the first city-kingdoms, Sumerian sources: "The Epic of Gilgamesh" and others. Virtual structures filled the entire habitat. Suffice it to recall the myths of Ancient Greece, which virtualized, filled the entire world with symbolic content. In this regard, the painting of the Middle Ages is indicative: a lack of perspective, a lack of time sequence, hierarchization of the world of "symbols," in which "a symbol is not a sign of reality, but replaces it, assuming the properties of reality."[14]

Egocentrism of pre-conceptual thinking, irreversibility of mental operations, insensitivity to logical contradictions, a transductive connection of pre-conceptual structures have created a habitat supplemented and expanded by virtual constructions. In other words, creativity, symbolic thinking, the intellectual activity of HS created a new, virtualized environment at the beginning of humanity's journey, in which the projection constructs of the psyche acquired the properties of real objects of equal size to natural objects. That is, HS initially lives in an incompletely real environment, with an increasing component of virtuality.

The global spread of typography, starting in the 15th century, and the emergence of "textual" culture initiated the emergence and development of conceptual thinking (ConceptT), which became the dominant type of thinking that shapes the psyche as a whole. We consider thinking as an integral function of the psyche, a special kind of mental and practical activity, including cognitive and transformative functions. It should be noted that ConceptT does not exist outside of verbal thinking, without words, in contrast to instincts and appetence. The sequential creation of a printed text ("general, whole") from separate "signs" is an individual, personified way of creating an "image" that has semantic content, i.e. "concept." The reading process is a way of step-by-step creation of an independent "image," a "synthesis" function. An intelligent operation with the opposite vector is "analysis" ("assembly-disassembly" of the image). Comparison of synthesized "images" makes it possible to highlight common features (abstraction), with the subsequent unification of different images into one category (generalization) and integration into one system, constituting a "concept." We have simplified the description of the algorithm of an independent, individual, based on printed text, construction of an integral "image" that has semantic content and unites disparate elements, i.e. "concept."

We believe that the rapid growth of the exponential schedule of technological development [15-17] in the 18th-20th centuries is associated with a fairly high, above-threshold population level of the development of ConceptT based on textual education. Caused by the development and spread of ConceptT, the transformation of the psyche in significant population formations initiated radical changes in the structures of society, changing the categories of "possible" and "acceptable," creating new ethics.

In other words, ConceptT, which forms "independent images" based on the "sign" information of printed texts, over 300-350 years (from Gutenberg,1439), having reached quantitatively "critical population mass," initiated social dynamics and transformed the structure of society generally. The result of the changes in thinking that initiated the dynamics of society was a radical change in basic individual goals: from "service and devotion" to "independence and individualism." The spread of ConceptT in all social strata of the changed structure of society revealed the carriers of "Creativity", independent of class restrictions, who were given the opportunity to realize their potential in all types of human activity: from military spheres to scientific laboratories.

The ability to analyze, synthesize, construct, and structure the images and concepts, potentiated by the default mode network (DMN), led to the rapid development of scientific knowledge about the natural laws of the real environment, the exponential growth of scientific knowledge and technology, and a decrease in the volume and influence of the virtual component of the surrounding world.

The set of new knowledge and skills has radically rebuilt the structure of relationships with the former objects of worship of cults and confessions. An increase in the number of individuals who possessed an independent ConceptT, capable of analyzing and synthesizing, led to a bifurcation of the final target mythologemes: from theistic canons to an abstract "Supreme Being", heterogeneous "Just Societies" and so on, which shared the formula "God is Died" (Friedrich Nietzsche, 1882), the absence of a personified object of worship, and new (humanistic) ideals—symbols. These new CCs were united by humanistic IGs, which removed the limitations of scientific knowledge but are still beyond the attainable. We believe that this was the main motive (the same frustration, which has a new humanistic content) that initiated the wave of population and social dynamics of the 18-20 centuries. The result was a change in the role of HS in own perception and a transformation into a "Supreme Being" took place, accompanied for some time by a feeling of boundless power that did not have the limitations of the ethical nature of the era of theism. This period (the late nineteenth and early twentieth century) was accompanied by rapid scientific development, turbulent events in social dynamics, disastrous advances in war, and terraforming technologies. With no solutions for "primary frustration" for 50,000 years, the need of HS in equilibrium in the parametric relationships with an external control object that was beyond the reach of the attainable, received a temporary solution in the late 20th and early 21st centuries. This phenomenon made it possible for dialogue, direct contact (through the operating systems of the Internet and social media) with an external object of technological genesis, which has the properties of regulation and control, a universal virtual product of human activity - the "information universe" (IU). Generalized characteristics (the absence of the "image" with the preservation of "sense" and verbalization) allow constructively categorizing IU as a "dissociated symbol." The expanding range of regulatory functions of the technological product of the HS activity (IU) and the possibilities of satisfying the physical and mental needs of a person tends in the future to replace them with a virtual product.

An obstacle to full contact with IU is ConceptT with analytic-synthetic (critical) functions, conservative stability, and the desire (created by the specifics of textual learning) to build autonomous images by operating systems of the psyche on the basis of cause-and-effect relationships. The reciprocal relationship of perception and processing of incoming information, the structuring action of DMN that completes the phase of perception, also prevents the processing of sequences that are not interrelated. The perception of environmental images that are not in causal relationships and are not interconnected sequences form "clip thinking" (ClipT).[18,19] A 6-fold excess of the speed of ClipT compared to ConceptT is accompanied by a decrease in the activity of DMN and analytical and synthetic functions. ClipT forms the ability to perceive a larger (compared to ConceptT) amount of short volumes of information per unit of time, with an increase in the total number and range of heterogeneous units of incoming information, increasing the multitasking of thinking.[20]

Differences between ClipT and ConceptT form stable differences in the trajectories of the development of the psyche as a whole. In ClipT, the exhaustion of the role of the linear sequence of "signs" as the basis of cultural development,[21] a decrease in the criticality of thinking, insensitivity to logical contradictions, the absence of semantic completeness,[22] the destruction of the context and internal semantic connections, and the fragmentation of perceived images form a deficient view of the real environment. ClipT partially returns thinking to the pre-text era, archaizes the structure of the psyche as a whole. In perception, preference is given to multiple incoherent episodes, in contrast to completed story media models.[23,24] In ClipT, one's perceptions are taken to be equivalent to the connections of objects of perception.

Media moderates perception, creating and imposing ready-made, formed operational images, initiating purposeful behavior significant groups of the population through a variety of communicative operators. Here are just a few examples: 1) Fashion in all its manifestations, with an endless succession of replaceable "images" (without content and interconnected sequences), creating massive unified forms of imitative behavior; 2) Information and analytical programs that create suggestive logical constructions on any given topic; and many other things that form unified forms of population-level behavior with the dynamics of globalization, increasing the potential of manipulative technologies. The rapidly increasing interference of media with the information body of the Internet has formed a virtual IU: a universal information space that interferes with "reality" and, in total, makes up the HS habitat. We believe that the quantitative ratios of "reality" and the complementary IU with the constantly accelerating growth of IU are variable quantities.

ClipT, including archaic "thinking in complexes" and "paralogical thinking," accompanied by a decrease in analytical and synthetic functions, is a derivative of the IU, which is characterized by a rapid increase in the speed, density, and chaos of the information flow. It is ClipT, developing and improving, adapts the psyche as a whole to a new, more and more virtualized environment. The new integral environment is gradually leveling the ethical and moral limitations of the "theistic era," creating (first in the virtual component: computer games, communication in social networks, etc.) forms of behavior that reduce the role of moral and other psychological regulatory mechanisms. The next stage is the extrapolation of the solutions and behavior tactics familiar for the virtual environment to the environment as a whole, without taking into account the boundaries between the virtual and real components.

In other words, the present state and prospects for the development of HS have reliable signs of an adaptive transformation of the psyche as a whole towards the "pre-conceptual" level, archaization, accompanied by a decrease in restraining ethical regulators and the creation of an environment with an increasing virtual component of technological genesis—the IU.

Changing the boundaries of "acceptable" and "possible," infinitely expanding the user's virtual potential through a variety of operational modes of moderation, the IU has formed a multicomponent habitat that transforms the HS psyche. That is, the technological derivative of intellectual activity HS (the IU) determines the trajectory of the transformation of the psyche HS without the participation of conscious forms of mental activity, forming the type of thinking that is optimal for the changed structure of the living environment. The practically uncontrolled growth of technology in all areas of knowledge accelerates the adaptive transformation of the psyche, the changes of which cannot be limited to thinking.

Currently, in our opinion, we are in a transitional period of transformation of the HS psyche into a new quality, with the emergence of new operating systems, one of which, observed in development, is defined as ClipT. Without the goal of making forecasts for the development of HS, we believe that the interference of the main directions of genetic engineering, cyborgization, chipping and development (up to implantation) of interfaces with computer technology, with the subsequent qualitative transformation of the physical and mental properties of HS and a change in the role of perceived forms of mental activity, is highly probable in the near future. We believe that in the future, new physical, psychophysiological, mental properties of HS are more compatible with high-speed, easily switchable ClipT in contrast to ConceptT, which has insufficient speed characteristics, forms stable (conservative) mental constructs, and develops the ability to devirtualize the objective world.

Thus, technologies—a product of HS intellectual activity—from a certain already passed level of development, without the conscious participation of the subject, format the HS psyche, adapting it to new qualitative and quantitative levels of virtualization of the environment, the prospects for the development of the technologies themselves during the singularity. ClipT is only one registered and measurable integral indicator of the dynamics of changes in the psyche.

## Conclusion

Creativity, the integrative function of the HS psyche, which arose about 50,000 years ago, allowed HS to project IGs, transformed into a "symbol," into the external

environment. The projection constructs of the psyche have become autonomous fragments of the environment in the HS perception, not being its derivatives. Objective reality, perceived by HS, has acquired non-inherent properties: a mental product of the psyche that integrates the virtual and real components of the environment.

Initially, HS exists in an incompletely real environment, with an increasing component of virtuality. The emergence and development of ConceptT led to a partial "devirtualization" of the environment, the removal of restrictions on scientific knowledge, the rapid growth of technology and social dynamics. The result of technological development was, in the recent past, a temporary resolution of the primary frustration: the establishment of the current equilibrium in the relationships with the regulatory "dissociated symbol"—the virtual IU. The IU, defining as the interference of "media" with the "information body" of the Internet, we consider as a unified information space, integrated with reality and in total constituting the HS habitat. ClipT, qualitatively different from ConceptT, is a new operating system of the psyche, a moderator of adaptation to a new, virtualized environment. A technological derivative of mental activity HS—the IU—without the participation of conscious forms of mental activity, transforms the algorithms of thinking, i.e. formats the psyche as a whole with adaptation to qualitative and quantitative changes in the virtual component of the environment, and to the perspectives on the development of technologies during the singularity.

## Competing Interests

The authors declare that they have no competing interests.

## References

1. Klein RG. The human career. Human biological and cultural origins. Chicago: The University of Chicago Press; 1989.
2. Kruglov AG. Creativity as a Determinant of the Development of Homo Sapiens. International Journal of Biomedicine. 2016;6(4):298-302.
3. Kruglov AG. Creativity as a Determinant of Intraspecific Aggressive Properties of the Psyche of Homo Sapiens. International Journal of Biomedicine. 2017;7(2):150-154.
4. Devlet E. Altamira: at the origins of art. M.; 2004.
5. Bray W, Trump D. The penguin dictionary of archaeology. (Translated by Nikolaev GA). M.: Progress; 1990.
6. Losev AF. Essays on ancient symbolism and mythology. 1993. M.: Misl; 1993. [In Russian].
7. Kruglov AG. A Mythologem as a Determinant of Goal-Directed Behavior. International Journal of Biomedicine. 2015;5(4):231-234.
8. Frazer JG. The Golden Bough: A Study in Magic and Religion. Translated from English into Russian. Moscow: TERRA-Knizhnii Klub; 2001.
9. Rubinshtein SL. Fundamentals of general psychology. St. Petersburg; 2003. [In Russian].
10. Jung CG. Archetype and Symbol. Translated from English into Russian. M.: Kanon; 1991.
11. Toporkov AL. Myth: tradition and psychology of perception. The myth and mythology in modern Russia. Moscow; 2000. [In Russian].
12. Shvyrkov VB. Introduction to objective psychology. Neuronal basics of psychics. Moscow: Psychology Institute of the Russian Academy of Sciences; 1995. [in Russian].
13. Mozheiko MA. History of Philosophy. Encyclopedia. Minsk. 2002:987-988. [In Russian].
14. Gurevich AJ. Categories of Medieval Culture. M.; 1984. [In Russian].
15. Panov AD. Singular point of history. Social sciences and modernity. M. MSU; 2005:122-137. [In Russian].
16. Snooks GB. Uncovering the laws in Global history. Social Evolution & History. 2002;1(1):25-53.
17. Snooks GD. The dynamic society. Exploring the source of global change. London, NY, Routledge; 1996.
18. Girenok FI. Clip consciousness. M. Akademicheskii Prospect; 2014. [In Russian].
19. Girenok FI. Clip consciousness. M. Prospect; 2016. [In Russian].
20. Rosen L. Me, My Space and I: Parenting the Net Generation. NY; 2007.
21. McLuhan M. The Gutenberg Galaxy: The Making of Typographic Man. M. Academic project (Translation from English into Russian); 2005.
22. Golovin SJ. Dictionary of practical psychologist. M.: Harvest; 1998. [In Russian].
23. Toffler E. Shock of the future. M. AST; 2008. [In Russian].
24. Toffler E. The Third Wave. M. AST; 2010. [In Russian].

**Online-Only Articles**

*International Journal of Biomedicine 11(1) (2021) 73-77*
*http://dx.doi.org/10.21103/Article11(1)_OA12*

ORIGINAL ARTICLE

Neurology

INTERNATIONAL JOURNAL OF BIOMEDICINE

# Effect of Wrist Tapping on Interhemispheric Coherence in Patients with Juvenile Myoclonic Epilepsy

Ekaterina A. Narodova, PhD[1*]; Natalia A. Shnayder, PhD, ScD[1,2]; Vladislav E. Karnaukhov[1]; Olesya D. Bogomolova[3]; Kirill V. Petrov[1]; Valeriya V. Narodova, PhD, ScD[1]

[1]*V.F. Voino-Yasenetsky Krasnoyarsk State Medical University, Krasnoyarsk, Russia*
[2]*V.M. Bekhterev National Medical Research Center of Psychiatry and Neurology, St. Petersburg, Russia*
[3]*Medical Center "Health Compass", Krasnoyarsk, Russia*

## Abstract

***The aim*** of this study was to assess the dynamics of interhemispheric coherence (IC) as an indicator of integration of different areas of the brain and their participation in the performance of certain functions before and after wrist tapping (WT), using the author's method in juvenile myoclonic epilepsy (JME).

***Methods and Results:*** The study included 81 subjects of working age, including 51 clinically healthy volunteers (median age of 39[21;56] years) and 30 patients (median age of 27[23;38] years) with JME. Analysis of IC in the electrode pairs Fp1-Fp2, F3-F4, C3-C4, T3-T4 was performed using a computer encephalographic complex. A coherent EEG analysis was used to identify and evaluate the relationships between different areas of the brain. Based on the change in the coherence coefficients (CCs), the level of integrative activity of brain structures was quantified. In healthy volunteers, before and after WT, we observed a statistically significant decrease in CCs for the beta-1 band in the pairs Fp1-Fp2, F3-F4, and C3-C4 ($P<0.05$), while in the pair T3-T4, changes in CCs were not statistically significant ($P>0.05$). At the same time, a statistically significant decrease in CCs in the alpha band was found only in the frontal regions in the pairs Fp1-Fp2 and F3-F4 ($P<0.05$). No statistically significant changes were found in all the studied pairs in the theta band. When comparing CCs in JME patients in beta–1 and theta bands, before and after WT, we did not find statistically significant changes in CCs in all the studied electrode pairs. However, in the alpha band, we found a statistically significant decrease in CCs in the frontal region in the F3-F4 ($P=0.0038$) and C3-C4 electrode pairs ($P=0.034$). The results of the study of interhemispheric integration showed statistically significant differences between patients with JME and the control group.

***Conclusion***: WT according to the author's method does not provoke the occurrence of interictal epileptiform discharges on the EEG and epileptic seizures in patients with JME. Coherent analysis showed positive changes in interhemispheric integrations of neurons in the beta–1 and alpha frequency ranges, mainly in the anterior hemispheres. (**International Journal of Biomedicine. 2021;11(1):73-77.**)

**Key Words:** interhemispheric coherence • electroencephalography • epilepsy • wrist tapping

**For citation**: Narodova EA, Shnayder NA, Karnaukhov VE, Bogomolova OD, Petrov KV, Narodova VV. Effect of Wrist Tapping on Interhemispheric Coherence in Patients with Juvenile Myoclonic EpilepsyInternational Journal of Biomedicine. 2021;11(1):73-77. doi:10.21103/Article11(1)_OA12

## Introduction

The pathogenesis of epilepsy is based on the spontaneous membrane instability of neurons, which leads to the appearance of a paroxysmal depolarization shift on the cell membrane. In this case, a sudden prolonged depolarization of the neuron occurs with the resulting flash of discharges. The increased tendency to depolarization of epileptogenic neurons is due to their so-called hypersensitivity caused by damage to the membrane or neuron metabolism: violation of the regulation of the concentration of extracellular ions and (or) transmitters that determine their imbalance. The latter leads to increased excitability of neural networks due to a lack of inhibitory effects.[1] However, an epileptic focus is not yet epilepsy,

***Corresponding author:** Ekaterina A. Narodova, PhD. V.F. Voino-Yasenetsky Krasnoyarsk State Medical University, Krasnoyarsk, the Russian Federation. E-mail: katya_n2001@mail.ru*

since in the presence of an electrographically recorded focus, an epileptic attack may be absent, and the disease does not develop. On the other hand, even with clinically manifest epilepsy, epileptic seizures are repeated, as a rule, only with a certain frequency; therefore, in the pauses between them, the epileptic focus remains blocked. In patients with juvenile myoclonic epilepsy (JME), functional disconnections in thalamo-motor and thalamo-frontal networks were found.[2,3] According to the study performed by Y.Wang,[4] functional network activity at rest was shown to be higher in JME patients in several brain regions than in healthy volunteers. At the same time, the brain regions involved in primi hyperfunction are mostly located in the left hemisphere, including the dorsolateral prefrontal cortex, the middle temporal gyrus, and the dorsal part of the striatum. Patients with JME had not only higher average values of indicators over the entire study period, but also a higher level of their variations, as evidenced by standard deviations of time series.

The aim of this study was to assess the dynamics of interhemispheric coherence (IC) as an indicator of integration of different areas of the brain and their participation in the performance of certain functions before and after wrist tapping (WT), using the author's method in JME.

## Materials and Methods

The study included 81 subjects of working age, including 51 clinically healthy volunteers (median age of 39[21;56] years) and 30 patients (median age of 27[23;38] years) with JME. Analysis of IC in the electrode pairs Fp1-Fp2, F3-F4, C3-C4, T3-T4 (Figure 1) was performed using a computer encephalographic complex ("Neurocartograph", MBS, Moscow).

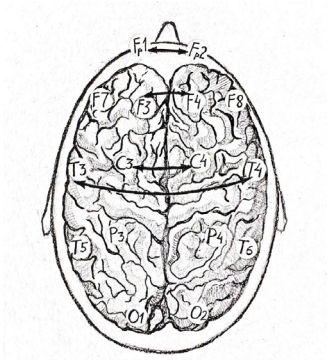


***Fig. 1.*** *Pairs of electrodes for evaluating IC: F1 – F2 (frontopolar); F3 – F4 (frontal); C3 – C4 (central); T3 – T4 and T5- T6 (temporal).*

We used coherent EEG analysis as an accessible neurophysiological technique that allows us to identify and evaluate the relationships between different areas of the brain, since the coherence coefficients (CCs) allow us to detect and evaluate the functional activity and participation of different areas of the cortex in the performance of certain functions. Based on the change in CCs,[5] it becomes possible to quantify the level of integrative activity of brain structures. At the same time, CC, being a measure of coherent EEG analysis, can vary from 0 to 1: the higher the CC, the more consistent the functional activity and integration of one area of the convexital cortex with another.

The study of the WT was carried out according to the author's modified methodology, "Method of exogenous rhythmic stimulation influence on an individual human rhythm" [RF patent №2606489 of 10.01.2017].

Inclusion criteria for the main group:

-Patients with JME

-Signed voluntary informed consent

-Male and female

-The age period: the youth (males 17-21; females 16-20 years); the first period of middle age (males 22-35 years; females 21-35 years); the second period of middle age (males 36-60 years; females 36-55 years)

-Russian-speaking Europeans

Inclusion criteria in the control group:

-Healthy adults

-Signed voluntary informed consent

-Male and female

-The age period: the youth (males 17-21; females 16-20 years); the first period of middle age (males 22-35 years; females 21-35 years); the second period of middle age (males 36-60 years; females 36-55 years)

-Russian-speaking Europeans

Exclusion criteria:

- Children and adolescents
- Refusal to participate in this study
- Participation in other studies

-Acute and chronic neurological, psychiatric and endocrinological disorders at the time of examination

- Alcohol intake (2 or more drinks during the last 2 weeks)
- Use of narcotic drugs at the time of the study and in history

Statistical processing was carried out using the STATISTICA Version 10 (StatSoft, USA). The normality of distribution of continuous variables was tested by Shapiro-Wilk test. Median (Me), interquartile range (IQR; 25th to 75th percentiles) were calculated. The Mann-Whitney U-Test was used to compare differences between two independent groups. The Wilcoxon test was used to compare differences between two dependent groups. A value of $P<0.05$ was considered significant.

## Results abd Discussion

When studying the characteristics of IC in healthy volunteers before and after WT, we found a statistically significant decrease in CCs, mainly in the fronto-central parts of the brain. The decrease was most pronounced for high-frequency rhythms, compared to low-frequency rhythms. A comparative characteristic of IC in the beta-1 band (Table 1, Figure 2) indicates a statistically significant decrease in CC in the antero-posterior direction with a predominance decrease in the fronto-central leads. In particular, we observed a statistically significant decrease in CCs in the pairs Fp1-Fp2, F3-F4, and C3-C4 ($P<0.05$), while in the pair T3-T4, changes in CCs were not statistically significant ($P>0.05$).

***Table 1.***

***Comparative characteristics of IC in healthy volunteers in the beta-1 band***

| Pairs of electrodes | Before tapping | | | After tapping | | | *P*-value |
|---|---|---|---|---|---|---|---|
| | Me | $P_{25}$ | $P_{75}$ | Me | $P_{25}$ | $P_{75}$ | |
| Fp1 - Fp2 | 0.12 | 0.09 | 0.18 | 0.11 | 0.66 | 0.16 | 0.0006 |
| F3 - F4 | 0.23 | 0.12 | 0.28 | 0.2 | 0.1 | 0.29 | 0.02 |
| C3 - C4 | 0.23 | 0.15 | 0.32 | 0.22 | 0.1 | 0.32 | 0.004 |
| T3 - T4 | 0.05 | 0.03 | 0.07 | 0.04 | 0.03 | 0.06 | 0.056 |

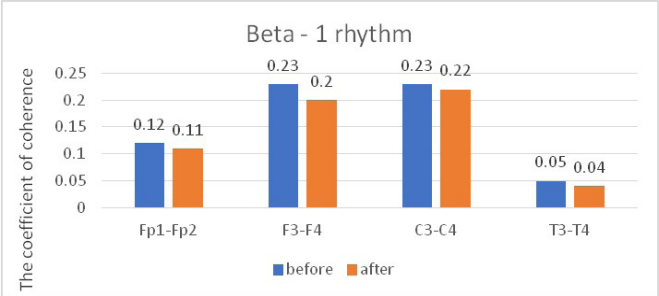


***Fig. 2.*** *Main characteristics of IC in healthy volunteers in the beta-1 band: blue column – before WT; orange column – after WT.*

Similar dynamics were observed when comparing the characteristics of IC in the alpha band (Table 2, Figure 3). However, the zonal gradient was less pronounced when we analyzed dynamics in the alpha rhythm, compared to the beta-1 band. At the same time, a statistically significant decrease in CCs in the alpha band was found only in the frontal regions in the pairs Fp1-Fp2 and F3-F4 ($P$<0.05), while changes in CCs were not statistically significant in the pairs C3-C4 and T3-T4 ($P$>0.05).

***Table 2.***

***Comparative characteristics of IC in healthy volunteers in the alpha band***

| Pairs of electrodes | Before tapping | | | After tapping | | | *P*-value |
|---|---|---|---|---|---|---|---|
| | Me | $P_{25}$ | $P_{75}$ | Me | $P_{25}$ | $P_{75}$ | |
| Fp1 - Fp2 | 0.29 | 0.17 | 0.41 | 0.25 | 0.11 | 0.4 | 0.001 |
| F3 - F4 | 0.42 | 0.26 | 0.54 | 0.38 | 0.21 | 0.56 | 0.0116 |
| C3 - C4 | 0.44 | 0.28 | 0.52 | 0.39 | 0.25 | 0.54 | 0.13 |
| T3 - T4 | 0.13 | 0.07 | 0.22 | 0.13 | 0.07 | 0.21 | 0.74 |

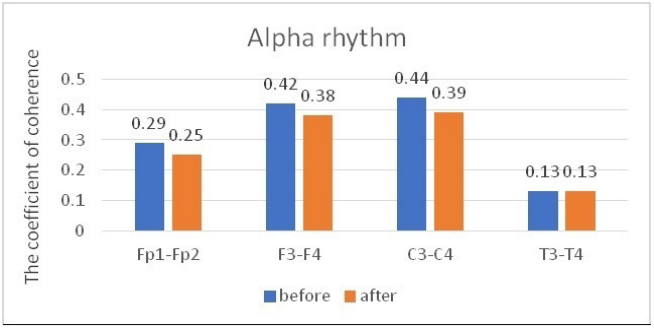


***Fig. 3.*** *Main characteristics of IC in healthy volunteers in the alpha band: blue column – before WT; orange column – after WT.*

When we analyzed the dynamics of CCs in the theta band, no statistically significant changes were found in all the studied pairs (Table 3, Figure 4).

***Table 3.***

***Comparative characteristics of IC in healthy volunteers in the theta band***

| Pairs of electrodes | Before tapping | | | After tapping | | | *P*-value |
|---|---|---|---|---|---|---|---|
| | Me | $P_{25}$ | $P_{75}$ | Me | $P_{25}$ | $P_{75}$ | |
| Fp1 - Fp2 | 0.12 | 0.07 | 0.18 | 0.1 | 0.008 | 0.25 | 0.09 |
| F3 - F4 | 0.27 | 0.15 | 0.44 | 0.27 | 0.12 | 0.37 | 0.01 |
| C3 - C4 | 0.29 | 0.16 | 0.44 | 0.27 | 0.13 | 0.38 | 0.04 |
| T3 - T4 | 0.07 | 0.04 | 0.14 | 0.07 | 0.04 | 0.11 | 0.138 |

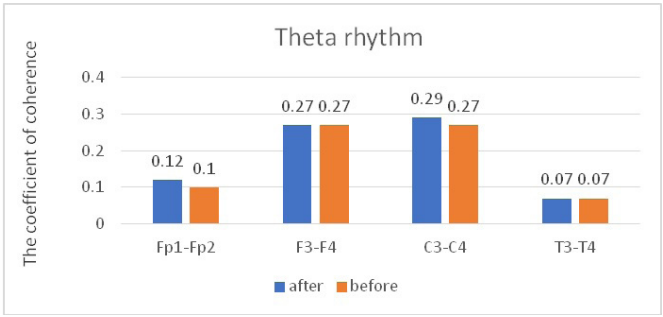


***Fig. 4.*** *Main characteristics of IC in healthy volunteers in the theta band: blue column – before WT; orange column – after WT.*

When comparing CCs in JME patients in beta–1 and theta bands, before and after WT, we did not find statistically significant changes in CCs in all the studied electrode pairs (Tables 4, 5; Figures 5, 6). However, in the alpha band, we found a statistically significant decrease in CCs in the frontal region in the F3-F4 ($P$=0.0038) and C3-C4 electrode pairs ($P$=0.034) (Table 6, Figure 7).

***Table 4.***

***Comparative characteristics of IC in JME patients in the beta-1 band***

| Pairs of electrodes | Before tapping | | | After tapping | | | *P*-value |
|---|---|---|---|---|---|---|---|
| | Me | $P_{25}$ | $P_{75}$ | Me | $P_{25}$ | $P_{75}$ | |
| Fp1 - Fp2 | 0.255 | 0.15 | 0.46 | 0.27 | 0.17 | 0.41 | 0.753 |
| F3 - F4 | 0.4 | 0.31 | 0.58 | 0.455 | 0.27 | 0.61 | 0.775 |
| C3 - C4 | 0.455 | 0.34 | 0.61 | 0.46 | 0.31 | 0.6 | 0.991 |
| T3 - T4 | 0.18 | 0.14 | 0.24 | 0.175 | 0.11 | 0.25 | 0.592 |

***Table 5.***

***Comparative characteristics of IC in JME patients in the theta band***

| Pairs of electrodes | Before tapping | | | After tapping | | | *P*-value |
|---|---|---|---|---|---|---|---|
| | Me | $P_{25}$ | $P_{75}$ | Me | $P_{25}$ | $P_{75}$ | |
| Fp1 - Fp2 | 0.39 | 0.22 | 0.52 | 0.32 | 0.2 | 0.47 | 0.477 |
| F3 - F4 | 0.45 | 0.34 | 0.6 | 0.47 | 0.3 | 0.6 | 0.837 |
| C3 - C4 | 0.47 | 0.32 | 0.61 | 0.44 | 0.32 | 0.64 | 0.573 |
| T3 - T4 | 0.24 | 0.13 | 0.4 | 0.21 | 0.11 | 0.36 | 0.362 |

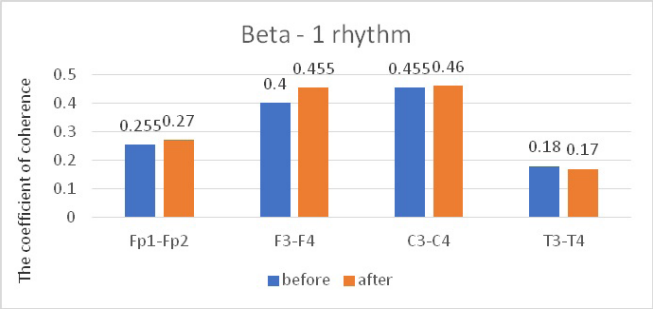


***Fig. 5.*** *Main characteristics of IC in JME patients in the beta-1 band: blue column – before WT; orange column – after WT.*

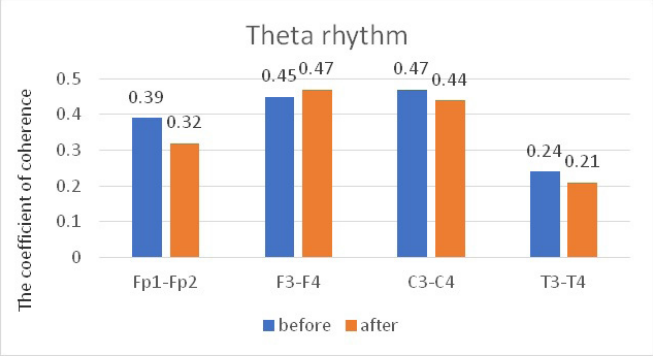


***Fig. 6.*** *Main characteristics of IC in JME patients in the theta band: blue column – before WT; orange column – after WT.*

***Table 6.***

***Comparative characteristics of IC in JME patients in the alpha band***

| Pairs of electrodes | Before tapping | | | After tapping | | | *P*-value |
|---|---|---|---|---|---|---|---|
| | Me | $P_{25}$ | $P_{75}$ | Me | $P_{25}$ | $P_{75}$ | |
| Fp1 - Fp2 | 0,51 | 0,43 | 0,61 | 0,45 | 0,35 | 0,57 | 0,17 |
| F3 - F4 | 0,66 | 0,57 | 0,73 | 0,62 | 0,51 | 0,74 | 0,038 |
| C3 - C4 | 0,68 | 0,57 | 0,76 | 0,67 | 0,48 | 0,75 | 0,034 |
| T3 - T4 | 0,41 | 0,22 | 0,47 | 0,32 | 0,18 | 0,49 | 0,158 |

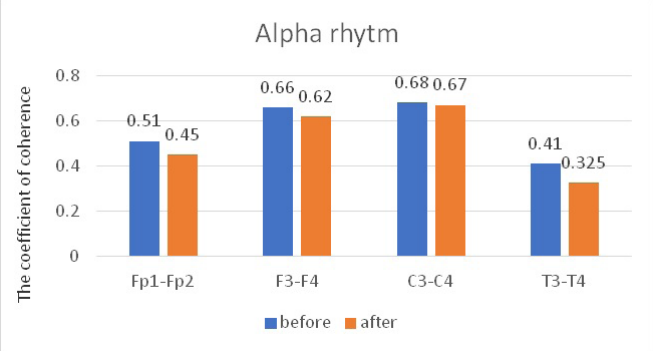


***Fig. 7.*** *Main characteristics of IC in JME patients in the alpha band: blue column – before WT; orange column – after WT.*

The data we obtained are consistent with the results of studies conducted earlier on healthy volunteers,[6,7] as well as with the results of our studies in the control group of healthy volunteers. After a session of WT according to the author's method, our control group showed a decrease in the strength of correlations between the coefficients of IC, mainly for the beta–1 band and to a lesser extent for the alpha band, in the anterior hemispheres (frontal cortex). In contrast, a comparable group of patients with JME in the interictal period experienced a statistically significant decrease in the strength of correlations between CCs, to a greater extent for the alpha band, as well as in the anterior hemispheres.

However, a comparative analysis of CCs for the beta–1 band in JME patients and in the control group showed statistically significant differences in CCs in all studied electrode pairs(Fp1-Fp2, F3-F4, C3-C4, T3-T4), consisting in higher CC indicators, both before tapping and after tapping in JME patients (Table 7), which may be due to a higher level of synchronization of cortical rhythms in epilepsy than in the norm. It is noteworthy that the greatest statistical significance of intergroup differences was noted in the mid–temporal leads (T3-T4), which is consistent with the results of a neuroradiological study on the involvement of the mediobasal parts of the temporal lobe.[8-10]

***Table 7.***

***Comparative characteristics of IC in healthy volunteers and JME patients in the beta-1 band***

| PoE | Before tapping | | *P*-value | After tapping | | *P*-value |
|---|---|---|---|---|---|---|
| | HV Me[$P_{25}$ ; $P_{75}$] | JME Me[$P_{25}$; $P_{75}$] | | HV Me[$P_{25}$ ; $P_{75}$] | JME Me[$P_{25}$ ; $P_{75}$] | |
| Fp1 - Fp2 | 0.12 [0.09; 0.18] | 0.255 [0.15; 0.46] | 0.00002 | 0.11 [0.66; 0.16] | 0.27 [0.17; 0.41] | 0.00004 |
| F3 - F4 | 0.23 [0.12; 0.28] | 0.4 [0.31; 0.58] | 0.0017 | 0.2 [0.1; 0.29] | 0.45 [0.27; 0.61] | 0.0059 |
| C3 - C4 | 0.23 [0.15; 0.32] | 0.45 [0.34; 0.61] | 0.005 | 0.22 [0.1; 0.32] | 0.46 [0.31; 0.6] | 0.007 |
| T3 - T4 | 0.05 [0.03; 0.07] | 0.18 [0.14; 0.24] | 0.0000 | 0.04 [0.03; 0.06] | 0.17 [0.1; 0.25] | 0.0000 |

*HV - healthy volunteer; PoE-pairs of electrodes*

A comparative analysis of the characteristics of IC for alpha rhythm also showed statistically significant differences due to higher values of CCs before and after WT in JME patients, compared to the control group (Table 8), while CCs in both the alpha band and the beta–1 band have the most significant intergroup differences in the mid–temporal divisions (T3-T4). A similar picture was observed when we compared the characteristics of IC in the theta band (Table 9).

Thus, the results of the study of interhemispheric integration (based on the analysis of IC coefficients in patients with JME during the interictal period of background EEG at rest and after a WT session using the author's method) showed statistically significant differences between patients with JME and the control group. However, the dynamics of CC

indicators in the JME group, compared to the control group, after a single session of WT according to the author's method was insignificant, which is probably due to the presence of a stable pathological condition in patients with epilepsy – the epileptoic system.

***Table 8.***

***Comparative characteristics of IC in healthy volunteers and JME patients in the alpha band***

| PoE | Before tapping | | *P*-value | After tapping | | *P*-value |
|---|---|---|---|---|---|---|
| | HV Me[$P_{25}$ ; $P_{75}$] | JME Me[$P_{25}$; $P_{75}$] | | HVr Me[$P_{25}$ ; $P_{75}$] | JME Me[$P_{25}$ ; $P_{75}$] | |
| Fp1 - Fp2 | 0.29 [0.17; 0.41] | 0.51 [0.43; 0.61] | 0.03 | 0.25 [0.11; 0.4] | 0.45 [0.35; 0.57] | 0. 002 |
| F3 - F4 | 0.42 [0.26; 0.54] | 0.66 [0.57; 0.73] | 0.02 | 0.38 [0.21; 0.56] | 0.62 [0.51; 0.74] | 0. 004 |
| C3 - C4 | 0.44 [0.28; 0.52] | 0.68 [0.57; 0.76] | 0.0008 | 0.39 [0.25; 0.54] | 0.67 [0.48; 0.75] | 0.007 |
| T3 - T4 | 0.13 [0.07; 0.22] | 0.41 [0.22; 0.47] | 0.0001 | 0.13 [0.07; 0.21] | 0.32 [0.18; 0.49] | 0. 0001 |

*HV - healthy volunteer; PoE-pairs of electrodes*

***Table 9.***

***Comparative characteristics of IC in healthy volunteers and JME patients in the theta band***

| PoE | Before tapping | | *P*-value | After tapping | | *P*-value |
|---|---|---|---|---|---|---|
| | HV Me[$P_{25}$ ; $P_{75}$] | JME Me[$P_{25}$; $P_{75}$] | | HV Me[$P_{25}$ ; $P_{75}$] | JME Me[$P_{25}$ ; $P_{75}$] | |
| Fp1 - Fp2 | 0.12 [0.07; 0.18] | 0.39 [0.22; 0.52] | 0.03 | 0.1 [0.008; 0.25] | 0.32 [0.2; 0.47] | 0.012 |
| F3 - F4 | 0.27 [0.15; 0.44] | 0.45 [0.34; 0.6] | 0.05 | 0.27 [0.12; 0.37] | 0.47 [0.3; 0.6] | 0.009 |
| C3 - C4 | 0.47 [0.32; 0.61] | 0.68 [0.57; 0.76] | 0.03 | 0.27 [0.13; 0.38] | 0.44 [0.32; 0.64] | 0.02 |
| T3 - T4 | 0.07 [0.04; 0.14] | 0.24 [0.13; 0.4] | 0.000 | 0.07 [0.04; 0.11] | 0.21 [0.11; 0.36] | 0.000 |

*HV - healthy volunteer; PoE-pairs of electrodes*

Thus, this result suggests that in order to obtain a stable antiepileptic effect by activating the neurons of the antiepileptic system, it is necessary to develop and implement not a single, but a course application of wrist tapping. The prospects of this approach are generally confirmed by the positive changes in the state of cortical rhythm under the influence of wrist tapping on the characteristics of the beta-1 and alpha rhythms.

## Competing Interests

The authors declare that they have no competing interests.

## References

1. Bate L, Gardiner M. Molecular genetics of human epilepsies. Expert Rev Mol Med. 1999;1999:1-22. doi: 10.1017/S1462399499001349.
2. Wang L, Wu L, Wang Y, Li H, Liu X, Du X, Dong G. Altered Brain Activities Associated with Craving and Cue Reactivity in People with Internet Gaming Disorder: Evidence from the Comparison with Recreational Internet Game Users. Front Psychol. 2017;8:1150. doi: 10.3389/fpsyg.2017.01150
3. Jiang S, Wen N, Li Z, Dube U, Del Aguila J, Budde J, et al. Integrative system biology analyses of CRISPR-edited iPSC-derived neurons and human brains reveal deficiencies of presynaptic signaling in FTLD and PSP. Transl Psychiatry. 2018;8(1):265. doi: 10.1038/s41398-018-0319-z
4. Wang Y, Berglund IS, Uppman M, Li TQ. Juvenile myoclonic epilepsy has hyper dynamic functional connectivity in the dorsolateral frontal cortex. Neuroimage Clin. 2019;21:101604. doi: 10.1016/j.nicl.2018.11.014
5. Ivanov LB. State of intra- and interhemispheric integration according to coherent EEG analysis in healthy children and in pathology. Proceedings of the international conference "Clinical neuroscience: neurophysiology, neurology, neurosurgery." 5th Eastern European Conference "Epilepsy and Clinical Neurophysiology." Yalta-Gurzuf, June 01-10, 2003. Gurzuf; 2003:32-35. [in Russian]
6. Kanda PAM, Anghinah R, Smidth MT, Silva JM. The clinical use of quantitative EEG in cognitive disorders. Dement Neuropsychol. 2009;3(3):195-203. doi: 10.1590/S1980-57642009DN30300004
7. Coan JA, Allen JJ. Frontal EEG asymmetry as a moderator and mediator of emotion. Biol Psychol. 2004;67(1-2):7-49. doi: 10.1016/j.biopsycho.2004.03.002
8. Hattingen E, Lückerath C, Pellikan S, Vronski D, Roth C, Knake S, Kieslich M, Pilatus U. Frontal and thalamic changes of GABA concentration indicate dysfunction of thalamofrontal networks in juvenile myoclonic epilepsy. Epilepsia. 2014;55(7):1030-1037. doi: 10.1111/epi.12656
9. Lin K, Jackowski AP, Carrete H Jr, de Araújo Filho GM, Silva HH, Guaranha MS, Guilhoto LM, Bressan RA, Yacubian EM. Voxel-based morphometry evaluation of patients with photosensitive juvenile myoclonic epilepsy. Epilepsy Res. 2009;86(2-3):138-145. doi: 10.1016/j.eplepsyres.2009.05.016
10. Kim SH, Lim SC, Kim W, Kwon OH, Jeon S, Lee JM, Shon YM. Extrafrontal structural changes in juvenile myoclonic epilepsy: a topographic analysis of combined structural and microstructural brain imaging. Seizure. 2015;30:124-131. doi: 10.1016/j.seizure.2015.06.009

International Journal of Biomedicine 11(1) (2021) 78-81
http://dx.doi.org/10.21103/Article11(1)_OA13

ORIGINAL ARTICLE

Radiology

INTERNATIONAL JOURNAL OF BIOMEDICINE

# A Study of Posterior Segment Pathology in Cataractous Eyes Using B-scan Ultrasonography

Mohammed Abdalla Shakour[1], Caroline E. Ayad[1], Samih Kajoak[2], Hamid Osman[2*], E. Rahim[2]

*[1]College of Medical Radiological Sciences, Sudan University of Science and Technology, Khartoum, Sudan*
*[2]Taif University, College of Medical Applied Sciences, Department of Diagnostic Radiology Sciences, Taif, Saudi Arabia*

## Abstract

***Background***: Ultrasonography (US) is a valuable diagnostic modality for detecting posterior segment eye diseases (PSEDs) in patients with cataractous eyes. This imaging modality can better facilitate planning surgery and predicting prognosis. The purpose of this study was to determine the role of B-scan US in evaluating posterior segment abnormalities of eyes in cataract patients pre-operatively to limit complications and visual impairment.

***Methods and Results***: A prospective, cross-sectional study to assess cataracts by US, as well as to detect posterior segment abnormalities of eyes in cataract patients, was conducted in Sudan at Albasar International Foundation (Makah Eye Complex in Omdurman) between December 2018 and December 2019.

All patients (n=380; 48% males and 52% females; a mean age of 63±12.57 years) with non-visualization of the fundus, regardless of age and gender, were involved and were assumed to have orbital pathologies. Patients with high-risk extrusion of intraocular contents and a previous history of ocular surgery were excluded from the present study. All patients with dense cataracts were evaluated using standard US machines (Echoscan US-4000; NIDEK CO., LTD.) equipped with a real-time high-frequency probe.

The typical age of the patients complaining of cataracts was between 61 and 70 years, which constituted 35% of cases, followed by age >70 years, which constituted 24.2% of cases. About 47.63% patients had ocular pathology in the posterior segment of the eye. The most common PSEDs were vitreous abnormalities (46.2%). Among vitreous abnormalities, most abnormal eyes had vitreous changes (36.1%), followed by vitreous detachment (3.7%); 1.3% of patients had retinal detachment.

***Conclusion***: Ocular US should be the first screening modality in the evaluation of posterior segment pathologies in cataractous eyes and should be performed in cataract patients pre-operatively for better surgical planning and predicting post-operative visual prognosis.(**International Journal of Biomedicine. 2021;11(1):78-81.**)

**Key Words**: B-scan ultrasonography • cataract • posterior segment eye diseases

**For citation**: Shakour MA, Ayad CE, Kajoak S, Osman H, Rahim E. A Study of Posterior Segment Pathology in Cataractous Eyes Using B-scan Ultrasonography. International Journal of Biomedicine. 2021;11(1):78-81. doi:10.21103/Article11(1)_OA13

## Abbreviations

**PVD**, posterior vitreous detachment; **PSEDs**, posterior segment eye diseases; **RD**, retinal detachment; **VD**, vitreous detachment; **IOFB**, intraocular foreign body.

## Introduction

A cataract (lens opacification) is a degenerative disease of the lens and represents one of the most important causes of visual impairment. The proportion of cataract blindness among all ocular diseases ranges from 5% in Western Europe, North America, and affluent countries to 50% in developing countries.[(1)] Forecasts predict that there will be almost 115 million cases of blindness and 588 million people with moderate to severe vision impairment in 2050 (up from figures

of 36 million and 217 million today, respectively).[2] There are several risk factors that may be frequently associated with cataracts, such as injury, diabetes, ultraviolet irradiation, specific ocular abnormalities (e.g., uveitis), and hypertension, but the main non-modifiable risk factor is aging. Cataract surgery and insertion of an intraocular lens are highly effective, resulting in almost immediate visual rehabilitation.[3]

Among patients with vision problems, fundoscopy and slit-lamp evaluation are the basis for diagnosis. In some cases in which cataracts change posterior segment eye diseases (PSEDs), which are defined as diseases of the retina, choroid and optic nerve,[4] Ultrasonography (US) is an indispensable diagnostic tool for evaluating and diagnosing many PSEDs. It helps the radiologist and ophthalmologist in diagnosing disease and choosing the optimal method of treatment.[4] B-scan US is a powerful, non-invasive, rapid, cost-effective, and non-ionizing real-time diagnostic tool that provides a good anatomic background, provides valuable diagnostic information for evaluating lesions of the posterior segment in eyes, and helps to rule out vitreous abnormalities, such as retinal, vitreous, and choroidal detachments, as well as tumors and other pathologic conditions that affect the posterior segment of the eye.[5] These conditions are mainly attributable to the cystic nature of the eye and its surface location, which allows high-frequency probes to demonstrate normal anatomy and pathologies accurately.[6] If the ophthalmologist and surgeon are aware of these pathologies pre-operatively, the surgical plan can be modified to better predict the visual outcome after cataract surgery and permit measures to combat anticipated complications.[7,8]

There are statistical discrepancies in previous studies with respect to the prevalence of the posterior segment of the eye among patients with cataracts. The significant variance exists among findings associated with cataracts across various populations. Vepa et al.[9] reported that in their study posterior segment lesions occurred in 54(11.02%) cases. Qureshi et al.[10] reported that the prevalence of posterior segment lesions in Pakistan was 12%; specifically, 3% of patients had retinal detachment (RD), 2% – posterior vitreous detachment (PVD), 3% – vitreous hemorrhage, 1.2% – posterior staphyloma, and 1% – intraocular foreign body (IOFB).[10] Shen et al.[11] reported vitreous detachment (VD) prevalence in a large cohort of Chinese to be 2.7%.

Cataractous eyes with posterior segment pathologies have not been the subject of comprehensive reports and few studies have reported the sonographic findings related to cataracts. The purpose of this study was to determine the role of B-scan US in evaluating posterior segment abnormalities of eyes in cataract patients pre-operatively to limit complications and visual impairment.

## Materials and Methods

We performed a prospective, cross−sectional study to assess cataracts by US, as well as to detect posterior segment abnormalities of eyes in cataract patients. The study was conducted in Sudan at Albasar International Foundation (Makah Eye Complex in Omdurman) between December 2018 and December 2019.

All patients (n=380) with non-visualization of the fundus, regardless of age and gender, were involved and were assumed to have orbital pathologies. Patients with high-risk extrusion of intraocular contents and a previous history of ocular surgery were excluded from the present study.

The data collection sheet was designed to collect demographic data. All registered patients underwent a pre-operative evaluation protocol that included intraocular pressure, posterior synechiae, visual acuity determination, pupillary reaction, biometric measurements, and a slit-lamp test. Risk factors, such as diabetes mellitus, hypertension, corneal opacities, iris coloboma, and deviated eyes, were specifically sought and noted.

After completing an ocular examination, all patients with dense cataracts were evaluated using standard US machines (Nidek Echo scan model US-4000; company, city, state, country) equipped with a real-time high-frequency probe. The procedure was explained to the patients, who were placed in a supine position and asked to flex the neck and head slightly, then rotated to the opposite side to prevent gel spreading. The ultrasonic probe accepts linear, 7.5–10MHz small footprint transducers, which are suitable for this purpose. The transducer was placed over the globe of the eye with a closed eyelid after application of the gel, then anteroposterior, transverse, and longitudinal views of the B-scan, along with A-scan, were obtained for both eyes. Low- and high-gain sensitivities were selected throughout the US. Images from the machine were collected and analyzed for evaluation. We determined that significant posterior segment pathology on the US affected the post-operative visual results. Images were diagnosed by a professional sonologist and ophthalmologist.

Statistical analysis was performed using statistical software package SPSS version 16.0 (SPSS Inc, Chicago, IL).

## Results

The sample consisted of 380 cataract patients (48% males and 52% females) with a mean age of 63±12.57 years. The patients were classified into 7 age groups. The typical age of the patients complaining of cataracts was between 61 and 70 years, which constituted 35% of cases, followed by age >70 years, which constituted 24.2% of cases; the other age groups are shown in Figure 1.

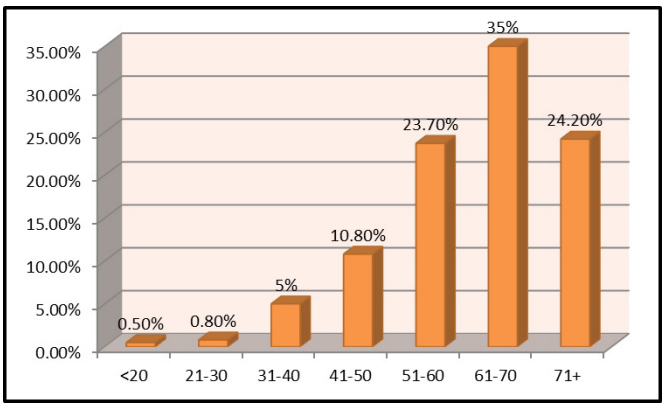


***Fig. 1.*** *Age distribution of the study sample.*

Of this total number of patients, 12.1% had diabetes mellitus and 17.9% – systemic hypertension.

About 47.63% patients had ocular pathology in the posterior segment of the eye (Table 1). The most common PSEDs were vitreous abnormalities, followed by retinal detachment.

***Table 1.***

***Frequency distribution of pathology in the posterior segment in cataractous eyes.***

| Ocular Abnormalities | No. of Abnormalities | % |
|---|---|---|
| Normal | 199 | 52.37 |
| Vitreous | 176 | 46.2 |
| Retina | 5 | 1.31 |
| Choroid | 0 | 0 |

Among vitreous abnormalities, most abnormal eyes had vitreous changes (36.1%), followed by VD (3.7%). Vitreous changes mean that vitreous volume was reduced, and the fibers were thickened, tortuous, and surrounded by liquid vitreous (Fig.2).

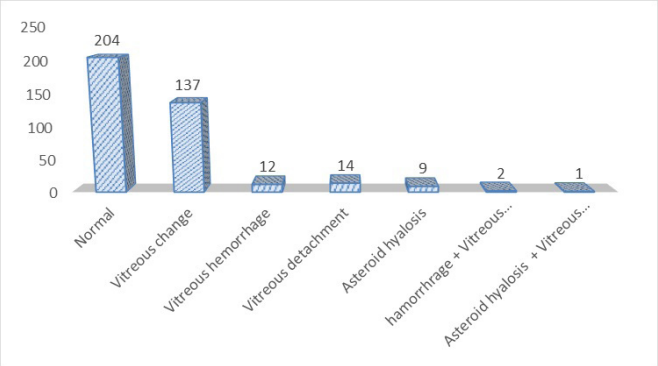


***Fig. 2.*** *Sonographic appearance of vitreous.*

## Discussion

Cataracts are among the most important causes of treatable blindness in developing countries, like Sudan, due to a lack of awareness and education, low-quality service, and high-cost treatment. Many patients present with advanced cataracts, which preclude fundus visualization and make clinical and ophthalmoscopic examinations difficult and minimally informative prior to cataract surgery. Under such circumstances, ophthalmic US has been shown to be an invaluable tool in the diagnosis and management of posterior segment pathology in patients with dense cataracts. Moreover, ophthalmic US is non-invasive, rapid, and cost-effective with no exposure to ionizing radiation. Thus, ophthalmic US enables a dynamic study and provides valuable diagnostic information of various ophthalmic diseases not obtainable by other imaging methods.[12-14]

Ocular abnormalities are believed to be more common in males than in females. In a study conducted by Sharma,[8] the gender ratio was 2:1, respectively. In another study, by Mcleod et al.,[15] male predominance was also reported. The current study, however, was not in agreement with the findings of previous studies; specifically, we demonstrated female predominance over males (52% vs. 48%.

The results of the present study demonstrated that in the 35% and 24.2% of the patients who presented in the 61–70 and >70-year age groups, respectively, age was statistically correlated with cataracts. In this study, 12.1% of patients had diabetes mellitus and 17.9% had hypertension. Richter et al.[16] have confirmed that in the elderly with a history of hypertension and diabetes, those conditions were risk factors for cataracts.

In the current study, 380 cases with advanced cataracts were examined by B-scan US, which revealed that 47.63% had PSEDs. A much lower percentage of PSEDs was recorded by Salman et al.[17] and Chanchlani et al.,[18] who reported that 9% and 8.7% of patients had PSEDs, respectively. In contrast, PSEDs were present in 77.5% of patients screened by B-mode US in cataract patients between 2005 and 2007 by Mendes et al.[18] These statistical discrepancies concerning the prevalence of PSEDs by US may be due to exclusion and inclusion criteria in each study, examination techniques used, and the expertise of examiners, because ocular US is dependent on the skill of the operator. In addition, variations between the populations scanned in different studies are also assumed to have contributed.

In the present study, RD was identified by B-scan US in 1.31% of patients, which is less than that reported by Meenakshi et al. – 2.5%,[9] Qureshi et al. – 3%,[10] and Jain et al. – 5%.[19] In addition, Salman et al.[17] reported only 0.7% patients with RD, and RD was identified in up to 9.3% of the cases evaluated by Mendes et al.[18] The sonographic ocular investigations in this study demonstrated that vitreous abnormalities were the most common finding (46.2%). This finding is in agreement with previous results published by Mcleod et al.,[15] who studied 176 eyes and found that the majority of patients had vitreous abnormalities. Sharma[8] reported similar results in another study. Vitreous changes (36.1%), followed by vitreous hemorrhage (3.2%) were most prevalent among patients with vitreous abnormalities. In previous studies, vitreous hemorrhage was reported in posterior segment B-scan US to range from 1%–3%,[20.21] which is lower than the percentage found in the present study. This disparity is assumed to be primarily attributed to the higher number of diabetic and hypertensive patients in our study, with an estimated higher prevalence of proliferative retinopathy and vitreous hemorrhage.

**In conclusion**, ocular US should be the first screening modality in the evaluation of posterior segment pathologies in cataractous eyes and should be performed in cataract patients pre-operatively for better surgical planning and predicting post-operative visual prognosis. Ocular US is cost-effective, rapid, and non-ionizing, which empowers US to provide useful diagnostic information about numerous ophthalmic diseases not obtained by other diagnostic imaging modalities.

***Corresponding author**: Hamid Osman. Taif University, College of Medical Applied Sciences, Department of Diagnostic Radiology Sciences. Taif, Saudi Arabia. E-mail: hamidsssan@yahoo.com*

## Competing Interests

The authors declare that they have no competing interests.

## References

1. Pascolini D, Mariotti SP. Global estimates of visual impairment: 2010. Br J Ophthalmol. 2012 May;96(5):614-8. doi: 10.1136/bjophthalmol-2011-300539.
2. Bourne RRA, Flaxman SR, Braithwaite T, Cicinelli MV, Das A, Jonas JB, Keeffe J, Kempen JH, Leasher J, Limburg H, Naidoo K, Pesudovs K, Resnikoff S, Silvester A, Stevens GA, Tahhan N, Wong TY, Taylor HR; Vision Loss Expert Group. Magnitude, temporal trends, and projections of the global prevalence of blindness and distance and near vision impairment: a systematic review and meta-analysis. Lancet Glob Health. 2017 Sep;5(9):e888-e897. doi: 10.1016/S2214-109X(17)30293-0.
3. World Health Organization. (2007). Global Initiative for the Elimination of Avoidable Blindness : action plan 2006-2011. Geneva: World Health Organization. https://apps.who.int/iris/handle/10665/43754
4. Sushil K, Ruchi G. Diagnostic ultrasonography of the eye. All India Ophthalmological Society. AIOS, CME series. 2011; 24:17–9.
5. Skandesh BM, Mohan Kumar, Sreenivasa Raju N. Role of high resolution sonography (B-SCAN) in the evaluation of posterior segment lesions of the eye. International Journal of Contemporary Medicine Surgery and Radiology. 2018;3(3):C11-C16.
6. Byrne SF, Green RL. Ultrasound of the eye and orbit. 2nd ed. St. Louis: Mosby; 2002
7. Agrawal D, Ahirwal D. A study of role of B scan ultrasound in posterior segment pathology of eye. Int J Med Res Rev. 2015;3(9):969–74.
8. Sharma OP. Orbital sonography with its clinicosurgical correlation. Indian J Radiol Imaging. 2005;15:537–54.
9. Meenakshi V, Jyothirmayi T, Sree B. Role of B-Scan Ultrasonography in cataract patients in a tertiary care centre. J Evol Med Dent Sci. 2015;4(83):14525–30. doi: 10.14260/jemds/2015/2066.
10. Qureshi MA, Laghari K. Role of B-scan ultrasonography in pre-operative cataract patients. Int J Health Sci (Qassim). 2010 Jan;4(1):31-7.
11. Shen Z, Duan X, Wang F, Wang N, Peng Y, Liu DT, Peng X, Li S, Liang Y. Prevalence and risk factors of posterior vitreous detachment in a Chinese adult population: the Handan eye study. BMC Ophthalmol. 2013 Jul 16;13(1):33. doi: 10.1186/1471-2415-13-33.
12. Allen D, Vasavada A. Cataract and surgery for cataract. BMJ. 2006 Jul 15;333(7559):128-32. doi: 10.1136/bmj.333.7559.128.
13. De La Hoz Polo M, Torramilans Lluís A, Pozuelo Segura O, Anguera Bosque A, Esmerado Appiani C, Caminal Mitjana JM. Ocular ultrasonography focused on the posterior eye segment: what radiologists should know. Insights Imaging. 2016 Jun;7(3):351-64. doi: 10.1007/s13244-016-0471-z.
14. Chanchlani M, Chanchlani R. A study of posterior segment evaluation by B-Scan in hyper mature cataract. J Clini Exp Ophthalmol. 2016;7:1. doi: https://doi.org/10.4172/2155-9570.1000516.
15. McLeod D, Restori M. Ultrasonic examination in severe diabetic eye disease. Br J Ophthalmol. 1979 Aug;63(8):533-8. doi: 10.1136/bjo.63.8.533.
16. Richter GM, Torres M, Choudhury F, Azen SP, Varma R; Los Angeles Latino Eye Study Group. Risk factors for cortical, nuclear, posterior subcapsular, and mixed lens opacities: the Los Angeles Latino Eye Study. Ophthalmology. 2012 Mar;119(3):547-54. doi: 10.1016/j.ophtha.2011.09.005.
17. Salman A, Parmar P, Vanila CG, Thomas PA, Jesudasan CA. Is ultrasonography essential before surgery in eyes with advanced cataracts? J Postgrad Med. 2006 Jan-Mar;52(1):19-22.
18. Mendes MH, Betinjane AJ, Cavalcante Ade S, Cheng CT, Kara-José N. Ultrasonographic findings in patients examined in cataract detection-and-treatment campaigns: a retrospective study. Clinics (Sao Paulo). 2009;64(7):637-40. doi: 10.1590/S1807-59322009000700005.
19. Jain A, Gauba N, Kaur I, Singh S, Jaswal H. Role of B-Scan in cataract patients. Indian J Appl Radiol. 2017;3(1):110.
20. Ali SI, Rehman H. Role of B-scan in preoperative detection of posterior segment pathologies in cataract patients. Pak J Ophthalmol. 1997;13:108-12.
21. Shaikh FU, Narsani AK, Jatoi SM, Shaikh ZA. Preoperative posterior segment evaluation by ultrasonography in dense cataract. Pak J Ophthalmol. 2009;25(3):135.

International Journal of Biomedicine 11(1) (2021) 82-86
http://dx.doi.org/10.21103/Article11(1)_OA14

ORIGINAL ARTICLE

Radiology

INTERNATIONAL JOURNAL OF BIOMEDICINE

# Study of Traumatic Head Injuries Using Computed Tomography

Samih Kajoak[1], H. Osman[1*], Caroline E. Ayad[2], Alamin Musa[3], Mohammed Yousef [4], Nahla L. Faizo[1], Bushra Abdel Malik[5]

[1]*Taif University, College of Applied Medical Sciences, Department of Radiological Sciences, KSA*
[2]*College of Medical Radiological Sciences, Sudan University of Science and Technology, Khartoum, Sudan*
[3]*King Khalid University, College of Applied Medical Sciences, Department of Diagnostic Radiology Sciences, KSA*
[4]*Batterji Medical College, Radiological Sciences Program, KSA*
[5]*Hail University, College of Applied Medical Sciences, Department of Diagnostic Radiology Sciences, KSA*

## Abstract

***The aim*** of this retrospective research was to study traumatic head injury (THI) using CT scan and to classify the types of head trauma fractures and types of hemorrhages.

***Methods and Results***: The current study included 53 THI patients (43/81.1%) males and 10/18.9% females) with positive and negative CT scan findings. A complete clinical history and patients' data were taken from CT reports, which included age, gender, type of trauma, associated injury, and CT findings with their percentages. The study was carried out in Taif city in King Abdelaziz Hospital and King Faisal Hospital.

The distribution of various etiologies of THI has shown that the most common etiology was road traffic accident (RTA) (45.3%). The typical age for THI was between 21 to 30 years old (26.4%). The distribution of the traumatic causes for each age group showed that the typical age for RTA was the age group of 11-20 years (33.3%), for falls – the age groups of 2-10 years (33.3%) and over 60 years of age (33.3%). The frequency of various CT findings of THI was as follows: intracranial hemorrhage (56.6%), fracture (39.6%), pneumocephalus (22.6%), contusion (22.6%), foreign body (11.3%), and proptosis (3.8%). The distribution of fracture cases, according to their types, was as follows: a linear fracture (76.2%), comminuted fracture (23.8%), basilar fracture (14.3%), and depressed fracture (9.5%). The frontal bone was the most affected site with fractures (30.7%).

***Conclusion***: CT is an appropriate clinical modality used in the management of THI patients in the emergency department. CT has the advantage of being fast, safe, available, sensitive to most acute post-traumatic injuries, accurate in identifying the head abnormalities such as fractures and hemorrhage during the first 24 hours after injury, which is beneficial in the early assessment, therapy planning, monitoring, and long-term patient care.(**International Journal of Biomedicine. 2021;11(1):82-86.**)

**Key Words:** computed tomography • traumatic head injury • road traffic accident

**For citation**: Kajoak S, Osman H, Ayad CE, Musa A, Yousef M, Faizo NL, Malik BA. Study of Traumatic Head Injuries Using Computed Tomography. International Journal of Biomedicine. 2021;11(1):82-86. doi:10.21103/Article11(1)_OA14

## Abbreviations

**CT**, computed tomography; **THI**, traumatic head injury; **TBI**, traumatic brain injury; **MRI**, magnetic resonance imaging; **RTA**, road traffic accident.

## Introduction

Traumatic head injury (THI) is one of the most common causes of death and disability in children and adults worldwide. In some literature sources,[1,2] the terms "traumatic head injury" and "traumatic brain injury" have been used interchangeably. Therefore, head injuries are characterized as brain injuries caused by external mechanical force, such as blast waves, rapid acceleration or deceleration, or projectile penetration, leading to temporary or permanent loss of brain function.[3] They account for a significant number of hospitalizations and a high degree of mortality worldwide. Statistically, the Center

for Disease Control and Prevention (CDC) has estimated that annually, about 1.5 million Americans survive a traumatic brain injury (TBI). Among these, approximately 230,000 are hospitalized. In 2000, there were 10,958 TBI diagnoses. In 2015, this number jumped to 344,030. Mortality across all TBI severities is approximately 3%, yet morbidity is more difficult to estimate.[4] The primary external cause of the head trauma, and therefore TBI, are road traffic accidents (RTAs) (accounting for approximately 60% of the cases), falls (20%-30%), violence (10%), and workplace and sports related activities (10%).[5-7] Therefore, all THIs need prompt diagnosis by a doctor with expertise in evaluating head injuries. A neurological examination will evaluate sensory and motor skills and the functioning of one or more cranial nerves. It will also check hearing and speech, coordination and balance, mental status, and behavior or mood changes, among other abilities. Subsequently, early diagnosis and correct supervision of THIs can meaningfully change their progression, especially within 48 hours of injury.[8] The severity of TBIs can be classified into mild, moderate, and severe injuries, according to the Glasgow Coma Scale (GCS), duration of loss of consciousness, and duration of posttraumatic amnesia.[9]

Health care professionals will use head scans to evaluate the severity of the primary head injuries and decide if surgery will be required to help treat any damage to the brain. Generally, conventional skull radiography was a commonly used radiological technique in head trauma situations, but currently, cross-sectional imaging generated during CT scans has become the preferred option, particularly in THI management, for a number of reasons. CT has fast examination time, wide availability, and is highly sensitive and accurate for detecting acute intra-axial and extra-axial hemorrhage. CT allows a clear presentation of the brain or bone injuries as seen in skull, temporal bone, facial, and orbital fractures, and lack of contraindications to metallic foreign bodies. It is also cheaper than MRI.[10]

CT scan is the primary modality of choice for accurate diagnosis of patients with THI, which helps in appropriate treatment and prompt intervention in surgery areas.

The aim of this retrospective research was to study THI using CT scan and to classify the types of head trauma fractures and types of hemorrhages.

## Materials and Methods

The current study included 53 THI patients (43/81.1%) males and 10/18.9% females; the age range 2-91 years.) with positive and negative CT scan findings. A complete clinical history and patients' data were taken from CT reports, which included age, gender, type of trauma, associated injury, and CT findings with their percentages. The study was carried out in Taif city in King Abdelaziz Hospital and King Faisal Hospital.

We obtained 5-mm-thick axial and 10-mm-thick axial sections using the multislice spiral CT technique. Bone algorithms with wide window settings were studied to visualize any fracture of the skull. Soft tissue and brain window were studied to visualize any hemorrhage or contusions. No contrast material was administrated (Figure 1). Statistical analysis was performed using statistical software package SPSS version 16.0 (SPSS Inc, Chicago, IL).

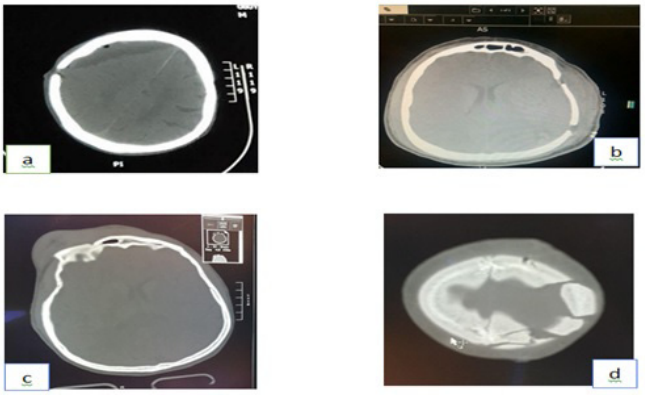


**Fig. 1.** *Various forms of skull fracture. (a) Linear fracture of the right parietal bone with chronic subdural hematoma. (b) Linear fracture of the left parietal bone with excessively soft tissue swelling. (c) Depressed fracture of the frontal bone with overlying soft tissue swelling. (d) Comminuted and displaced fracture of parietal bones.*

## Results

The distribution of various etiologies of THI has shown that the most common etiology was an RTA (45.3%), followed by falls (28.3%), an assault (18.9%), gunshot (1.88%), and other (5.7%).

The typical age for THI was between 21 to 30 years old (26.4%), followed by 11 to 20 years (16.9%), and other age groups (Figure 2).

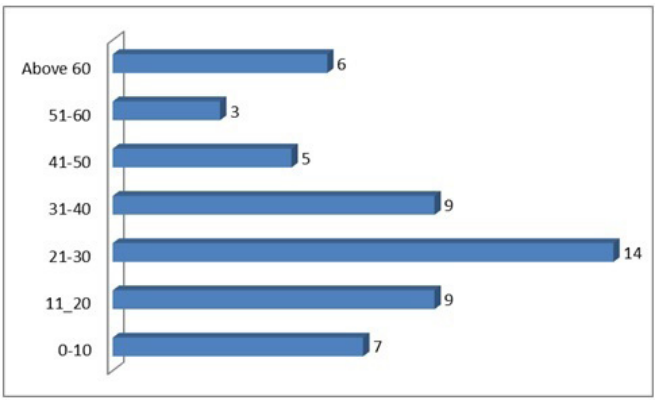


***Fig. 2.*** *Age distribution of patients*

The distribution of the traumatic causes for each age group is shown in Table 1. The typical age for RTA was the age group of 11-20 years (33.3%), for falls – the age groups of 0-10 years (33.3%) and over 60 years of age (33.3%).

Figure 3 shows the frequency of various CT findings of THI. There were 30(56.6%) patients with intracranial hemorrhage, 26(49.1%) patients with fracture, 12(22.6%) patients with pneumocephalus, 12(22.6%) patients with

contusion, 6(11.3%) patients with foreign body, and 2(3.8%) patients with proptosis. Most patients had several complications at the same time.

***Table 1.***

***The distribution of the traumatic causes for each age group***

| Age groups | Traumatic causes | | | | | n(%) |
|---|---|---|---|---|---|---|
| | RTA (n=24) | Falls (n=15) | Assault (n=10) | Gunshot (n=1) | Other (n=3) | |
| 2 – 10 | 2 | 5 | 0 | 0 | 0 | 7 (13.2%) |
| 11 - 20 | 8 | 0 | 0 | 0 | 1 | 9 (16.98%) |
| 21 - 30 | 6 | 1 | 7 | 0 | 0 | 14 (26.4%) |
| 31 - 40 | 4 | 1 | 2 | 1 | 1 | 9 (16.98%) |
| 41 - 50 | 2 | 1 | 1 | 0 | 1 | 5 (9.4%) |
| 51 - 60 | 1 | 2 | 0 | 0 | 0 | 3 (5.7%) |
| Above 60 | 1 | 5 | 0 | 0 | 0 | 6 (11.3%) |
| *P*-value | >0.05 | 0.011 | >0.05 | >0.05 | >0.05 | 53 (100%) |

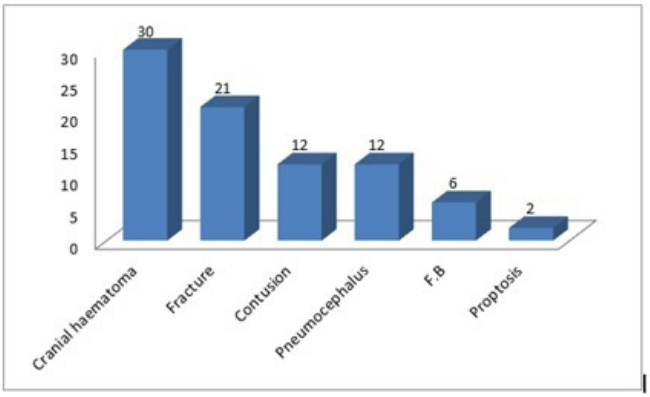


***Fig. 3.*** *The frequency of various CT findings of THI*

The distribution of cranial hemorrhage cases, according to its types, was as follows: subgaleal hematoma (SGH-40.5%), subdural hematoma (SDH-23.8%), epidural hematoma (EDH-19.0%), subarachnoid hematoma (SAH-11.9%), intracerebral hematoma (ICH-2.4%), and intraventricular hematoma (IVH-2.4%) (Fig.4).

The distribution of fracture cases, according to their types, was as follows: a linear fracture (76.2%), comminuted fracture (23.8%), basilar fracture (14.3%), and depressed fracture (9.5%). Sometimes the patient had more than one type of fracture.

The frontal bone was the most affected site with fractures (30.7%), followed by parietal bone (19.2%), nasal bone (15.3%), occipital bone (11.5%), temporal bone (11.5%), zygomatic arch (7.7%), and sphenoid bone (3.8%) (Table 2). There was no significant relationship between site and type of fracture.

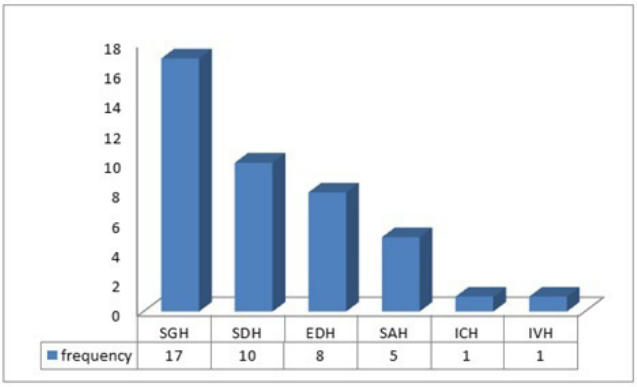


***Fig. 4.*** *The distribution of cranial hemorrhage cases, according to its types.*

***Table 2.***

***The relationship between site and type of fracture.***

| Site of fracture | Type of fracture | | | | n (%) |
|---|---|---|---|---|---|
| | linear | comminuted | basilar | depressed | |
| Frontal bone | 6 | 0 | 1 | 1 | 8 (30.7%) |
| Parietal bone | 1 | 3 | 0 | 1 | 5 (19.2%) |
| Occipital bone | 3 | 0 | 0 | 0 | 3 (11.5%) |
| Temporal bone | 2 | 0 | 1 | 0 | 3 (11.5%) |
| Zygomatic arch | 1 | 1 | 0 | 0 | 2 (7.7%_ |
| Nasal bone | 3 | 1 | 0 | 0 | 4 (15.3%) |
| Sphenoid bone | 0 | 0 | 1 | 0 | 1 (3.8%) |
| Total number | 16 | 5 | 3 | 2 | 26 (100%) |
| *P*-value >0.05 | | | | | |

## Discussion

THI is an increasingly worldwide health concern. Precise assessment of patients suffering from head trauma using a CT scan is very useful in diagnosis and treatment. In the current manuscript of 53 cases listed, 43(81.1%) are males, and only 10(18.9%) are females, showing male preponderance in THI. This may be attributed to the fact that males remain out of their homes more commonly in our local community. This result is similar to the findings in the USA.[11]

According to our study, RTA is the more common etiology of THI (45.3%). These results were close to those obtained by Bordignon et al.[12] and Agrawal et al.[13]

The majority of patients in our study were seen to be in the third decade of life (26.4%) followed by the second decade and fourth decade, which together accounted for 16.97% of cases. These age groups are the more commonly involved groups in society, which spend the majority of the day outside homes, involved in social and economic life. Therefore, they are more prone to RTA with THI. These results were similar to those obtained by other researchers.[14,15]

Falls were the most common etiological factor of THI for the age groups of 2-10 years (33.3%) and over 60 years of age (33.3%).

In our study, the cranial hemorrhage (extracranial and intracranial) was the most common finding, constituting 56.6%. Extracranial hemorrhage is composed of caput succedaneum, cephalohematoma, and subgaleal hematoma. Intracranial hemorrhage is composed of subdural hematoma, epidural hematoma, subarachnoid hematoma, intracerebral hematoma, and interventricular hematoma. In our study, the most frequent hematoma type in THI was subgaleal hematoma (56.1%). The study carried out by Zimmerman et al.[5] found that the most frequent intracranial lesion in 286 patients was hemorrhagic contusions.

The results of our study showed that fracture cases accounted for 49.1% of total THI complications. In the study conducted by Yattoo et al.,[16] the CT results in 547 patients showed a skull fracture in only 8.9% of cases. In our series, the distribution of fracture cases according to their types revealed that a linear fracture was more common (76.2%), and the frontal bone was the most affected site for fracture (30.7%). Our results showed the frequent presence of combined THI complications. For example, 61.9% of skull fractures have been associated with cranial hemorrhage and 58.3% pneumocephalus with cranial hemorrhage. About 15.1% of cases included fractures, cranial hemorrhage, and contusion.

In the time instantly after head trauma, a CT scan is most widely used to diagnose severe problems that could be life-threatening as well as to check whether there are metallic foreign bodies. MRI anatomical imaging is very effective and precise for cerebral pathology diagnosis in THI patients to determine that there are no metallic bodies involved in the injury. Nonetheless, the CT scan is the primary imaging tool of choice in the first 24 hours following injury.[17-19] MRI is mostly considered superior to CT after 48 to 72 hours. While CT scan is effective in detecting bone disease and other forms of early bleeds, the accuracy of MRI to diagnose hematomas increases with time as blood composition changes.[20]

**In conclusion**, CT is an appropriate clinical modality used in the management of THI patients in the emergency department. CT has the advantage of being fast, safe, available, sensitive to most acute post-traumatic injuries, accurate in identifying the head abnormalities such as fractures and hemorrhage during the first 24 hours after injury, which is beneficial in the early assessment, therapy planning, monitoring, and long-term patient care. Furthermore, CT should only be done when clinically indicated to help minimize costs and prevent unneeded radiation exposure.

Our study also concludes that RTA is the chief cause of THI and that head injuries are generally more frequent in males than in females and in the most active age group relative to other age groups; in addition, the most frequent fracture type for THI is a linear fracture.

## Competing Interests

The authors declare that they have no competing interests.

## References

1. Johnson KM. The hazards of stopping a brain in motion: evaluation and classification of traumatic brain injury. Virtual Mentor. 2008 Aug 1;10(8):516-20. doi: 10.1001/virtualmentor.2008.10.8.cprl1-0808.
2. Ghebrehiwet M, Quan LH, Andebirhan T. The profile of CT scan findings in acute head trauma in Orotta Hospital, Asmara, Eritrea. JEMA. 2009;4:5-8.
3. Maas AI, Stocchetti N, Bullock R. Moderate and severe traumatic brain injury in adults. Lancet Neurol. 2008 Aug;7(8):728-41. doi: 10.1016/S1474-4422(08)70164-9.
4. Georges A, Booker JG. Traumatic Brain Injury. 2020 Nov 19. In: StatPearls [Internet]. Treasure Island (FL): StatPearls Publishing; 2020 Jan–. PMID: 29083790.
5. Zimmerman RA, Bilaniuk LT, Gennarelli T, Bruce D, Dolinskas C, Uzzell B. Cranial computed tomography in diagnosis and management of acute head trauma. AJR Am J Roentgenol. 1978 Jul;131(1):27-34. doi: 10.2214/ajr.131.1.27.
6. Hyder AA, Wunderlich CA, Puvanachandra P, Gururaj G, Kobusingye OC. The impact of traumatic brain injuries: a global perspective. NeuroRehabilitation. 2007;22(5):341-53.
7. Asaleye CM, Famurewa OC, Komolafe EO, Komolafe MA, Amusa YB. The pattern of Computerized Topographic findings in moderate and severe head injuries in ILE- IFE, Nigeria. West Afr J Radiol. 2005;12:8–13.
8. Sosin DM, Sniezek JE, Waxweiler RJ. Trends in death associated with traumatic brain injury, 1979 through 1992. Success and failure. JAMA. 1995 Jun 14;273(22):1778-80.
9. Sternbach GL. The Glasgow coma scale. J Emerg Med. 2000 Jul;19(1):67-71. doi: 10.1016/s0736-4679(00)00182-7. PMID: 10863122.
10. Majdan M, Mauritz W, Brazinova A, Rusnak M, Leitgeb J, Janciak I, Wilbacher I. Severity and outcome of traumatic brain injuries (TBI) with different causes of injury. Brain Inj. 2011;25(9):797-805. doi: 10.3109/02699052.2011.581642.
11. Edelman RR, Hesselink JR, Zlatkin MB, Crues JV., III. Clinical Magnetic Resonance Imaging. New York, NY: Elsevier; 2005.
12. Bordignon KC, Arruda WO. CT scan findings in mild head trauma: a series of 2,000 patients. Arq Neuropsiquiatr. 2002 Jun;60(2-A):204-10. doi: 10.1590/s0004-282x2002000200004.
13. Agrawal A, Agrawal CS, Kumar A, Lewis O, Malla G, Khatiwada R, Rokaya P. Epidemiology and management of paediatric head injury in eastern Nepal. Afr J Paediatr Surg. 2008 Jan-Jun;5(1):15-8. doi: 10.4103/0189-6725.41630.

***Corresponding author**: Hamid Osman. Taif University, College of Medical Applied Sciences, Department of Diagnostic Radiology Sciences. Taif, Saudi Arabia. E-mail: hamidsssan@yahoo.com*

14. Norlund A, Marké LA, af Geijerstam JL, Oredsson S, Britton M; OCTOPUS Study. Immediate computed tomography or admission for observation after mild head injury: cost comparison in randomised controlled trial. BMJ. 2006 Sep 2;333(7566):469. doi: 10.1136/bmj.38918.659120.4F.
15. Jeret JS, Mandell M, Anziska B, Lipitz M, Vilceus AP, Ware JA, Zesiewicz TA. Clinical predictors of abnormality disclosed by computed tomography after mild head trauma. Neurosurgery. 1993 Jan;32(1):9-15; discussion 15-6. doi: 10.1227/00006123-199301000-00002.
16. Yattoo G, Tabish A. The profile of head injuries and traumatic brain injury deaths in Kashmir. J Trauma Manag Outcomes. 2008 Jun 21;2(1):5. doi: 10.1186/1752-2897-2-5.
17. Glauser J. Head injury: which patients need imaging? Which test is best? Cleve Clin J Med. 2004 Apr;71(4):353-7. doi: 10.3949/ccjm.71.4.353.
18. Garnett MR, Cadoux-Hudson TA, Styles P. How useful is magnetic resonance imaging in predicting severity and outcome in traumatic brain injury? Curr Opin Neurol. 2001 Dec;14(6):753-7. doi: 10.1097/00019052-200112000-00012.
19. Kampfl A, Schmutzhard E, Franz G, Pfausler B, Haring HP, Ulmer H, Felber S, Golaszewski S, Aichner F. Prediction of recovery from post-traumatic vegetative state with cerebral magnetic-resonance imaging. Lancet. 1998 Jun 13;351(9118):1763-7. doi: 10.1016/S0140-6736(97)10301-4.
20. Lee B, Newberg A. Neuroimaging in traumatic brain imaging. NeuroRx. 2005 Apr;2(2):372-83. doi: 10.1602/neurorx.2.2.372.

International Journal of Biomedicine 11(1) (2021) 87-91
http://dx.doi.org/10.21103/Article11(1)_OA15

ORIGINAL ARTICLE

Surgery

INTERNATIONAL JOURNAL OF BIOMEDICINE

# Clinical and Pathogenetic Aspects of Complex Treatment of Decompensated Forms of Chronic Venous Insufficiency of the Lower Extremities

Vladimir V. Izosimov, MD, PhD; Serhiy H. Hryvenko, MD, PhD, ScD*; Yuriy G. Baranovskiy, MD, PhD; Yuriy V. Artemov, MD, PhD; Andrej A. Dovgan MD, PhD; Elizaveta V. Izosimova

*Medical Academy named after S.I. Georgievsky of Vernadsky CFU*
*Simferopol, Crimea*

## Abstract

The article presents a clinical assessment of the effectiveness of the author's method of pharmacological correction in the complex treatment of patients with trophic ulcers of venous origin in the lower extremities. Based on the analysis of the data obtained, we found that the use of the proposed method of drug correction in the complex treatment of chronic venous ulcer ensures the effectiveness of treatment, a reduction in the duration of inpatient treatment, and the reliability of rehabilitation in the postoperative period.(**International Journal of Biomedicine. 2021;11(1):87-91.**)

**Key Words:** chronic venous insufficiency • chronic venous ulcer • chronic venous disease

**For citation**: Izosimov VV, Hryvenko SH, Baranovskiy YuG, Artemov YuV, Dovgan AA, Izosimova EV. Clinical and Pathogenetic Aspects of Complex Treatment of Decompensated Forms of Chronic Venous Insufficiency of the Lower Extremities. International Journal of Biomedicine. 2021;11(1):87-91. doi:10.21103/Article11(1)_OA15

## Abbreviations

**CVD**, chronic venous disease; **CVI**, chronic venous insufficiency; **DHS**, dioctahedral smectite; **CVU**, chronic venous ulcer

## Introduction

Chronic venous disease (CVD) of the lower extremities is one of the most prevalent disorders worldwide.[1] The steadily progressive course of CVD of the lower extremities leads to the development of complications in 15%-25% of patients with varicose veins and in more than 80% of patients with post-thrombotic disease.[2] As chronic venous insufficiency (CVI) progresses, persistent severe microcirculation disorders develop, ultimately leading to the appearance of an ulcer.[3] Trophic ulcers are a complication of CVI of the lower extremities and occur in 2% of the working-age population of industrialized countries.[4] Every year in the United States, 2.2 million cases of chronic venous ulcers (CVU) are diagnosed.[5] In Russia, from 1.5 to 5 million people suffer from this severe pathology.[1,6] The high prevalence of CVU and its tendency to recur dictate the need to use an optimal complex of various modern methods of treatment.[1]

Modern strategy and tactics to treat CVU suggest a differentiated approach and a combination of different methods of conservative and surgical interventions.[3,7] Only an integrated approach to the treatment of this category of patients—a combination of CVU sanitation, competent compression, and drug therapy in an indispensable combination with corrective operations on the venous system—makes it possible to obtain a good, persistent clinical result and subsequent

***Corresponding author:** Serhiy H. Hryvenko, MD, PhD, ScD. Medical Academy named after S.I. Georgievsky of Vernadsky CFU, Simferopol, Crimea. E-mail: hryva@mail.ru*

long-term, relapse-free course of the disease.[1] Therefore, the development and implementation of modern methods of CVU treatment, their inclusion in the complex of preoperative preparation and their combination with various methods of surgical correction of CVI is an urgent problem of modern phlebology.[7] In addition, it should be clearly remembered that even in cases of successful surgical correction, patients with CVI need a long-term and sometimes lifelong maintenance therapy aimed at leveling the known risk factors for CVI and its key pathogenetic mechanisms.[8] Unfortunately, to date a clear, comprehensive, step-by-step approach has not yet been developed for the treatment of patients with CVU.

The variety of the proposed methods for treating CVU indicates dissatisfaction with the results of each of them. In this regard, the search for new pathogenetically substantiated methods for the treatment of CVU remains relevant in order to correct general disorders and normalize the condition of tissues, enhance their regeneration, fight ischemia, normalize lymph circulation, and correct body hemostasis.[9] A number of recent studies have indicated the positive role of enterosorbents in the treatment of complicated forms of varicose veins. [10] The therapeutic effectiveness of enterosorption also depends on a number of factors, including the direction of the therapeutic effect of the sorbent that is used. In our opinion, dioctahedral smectite (DHS) is of particular interest. DHS is one of the sorbents highly standardized for the raw materials from which it is obtained. DHS has a strong polymeric organosilicon base containing aluminum and magnesium as heteroatoms coordinating OH-groups around themselves. The porous structure provides "softness" of the DHS action and compatibility in contact with biological media.[11] Magnesium contained in DHS is also important for the repair processes. The feasibility of using magnesium preparations has been confirmed in patients with varicose veins, including those who have undergone phlebectomy, from the standpoint of their influence on the level of matrix metalloproteinases and their inhibitors.[12]

The aim of this study was to improve the immediate, long-term and functional results of complex treatment of CVI patients with CVU of the lower extremities on the basis of the development and implementation of new pathogenetically substantiated methods of pharmacotherapy.

## Materials and Methods

The presented clinical study is based on a prospective analysis of the results of examination and complex treatment of 106 CVI patients with CVU who underwent surgical treatment in the period from 2012 to 2017. The study was carried out in compliance with Ethical Principles for Medical Research Involving Human Subjects, Adopted by the 18th WMA General Assembly, Helsinki, Finland, June 1964, and amended by the 59th WMA General Assembly, Seoul, Republic of Korea, October 2008. Written informed consent was obtained from all patients before inclusion in the study.

The main group (MG) consisted of 52 patients (mean age of 62.80±1.52 years), who were additionally prescribed the enterosorbent DHS and magnesium orotate [13,14] in the complex of the baseline therapy (diosmin drugs, antiplatelet agents, decongestant therapy, and compression stockings). The *prescribed dosage* of magnesium orotate was 1000 mg three times a day for seven days, then 500 mg two to three times a day. The duration of the course was at least 4-6 weeks. The possibility of a repeated course of treatment was determined based on the patient's status. As DHS, the enterosorbent "Benta" (Krymfarmed) was prescribed: 3 grams three times a day, 30 minutes before meals. The contents of the "Benta" package were dissolved in 100ml of warm drinking water, mixed thoroughly and taken orally. The course of administration was 7 days.

The comparison group (CG) consisted of 54 patients (mean age of 61.59±1.68 years) who received the above-mentioned baseline therapy.

For both groups of patients, the common clinical sign was the presence of CVU in the exudation phase (CEAP class C6S). All patients had both single and multiple CVU. The CVU duration ranged from 6 months to 5 years. CVU of the lower third of the leg was diagnosed in 97(91.5%) patients. Most often, CVUs were formed on the left leg, where they were diagnosed in 56(52.8%) patients. On the medial surface of the leg, CVUs were diagnosed in 57(53.8%) patients, on the lateral surface – in 9(8.5%) patients, on the posterior surface – in 10(9.4%) patients, and on the anterior surface – in 21(19.8%) patients. CVUs on various surfaces of the middle third of the leg were detected in 9(8.5%) patients. The CVU area ranged from 3.0 cm² to more than 20.0 cm². At the same time, in 28(26.4%) patients, the CVU area was up to 5 cm², in 74(69.8%) patients – from 6 cm² to 20 cm², in 4(3.8%) patients – exceeded 20 cm².

Demographic indicators in MG and CG did not show statistical differences. In both groups, women prevailed (58.5% versus 41.5% for men). In addition, the studied groups of patients were comparable in terms of the presence of concomitant diseases. None of the identified comorbidities at the time of treatment and at the stages of complex treatment had a pronounced manifestation and did not significantly affect the results of the presented study. The local treatment of CVUs was performed after their surgical treatment, regardless of their origin.

We used conventional slab phlebectomy to implement pathogenetically substantiated surgical correction of existing hemodynamic disorders, in order to eliminate pathological veno-venous refluxes and to exclude irreversibly transformed areas of the saphenous veins of the lower extremities from the bloodstream in 60.87% (in both groups) of patients with varicose veins,. In patients with CVUs with post-thrombotic syndrome, surgical treatment was performed on 16.2% of patients.

The clinical parameters used to assess the effectiveness of complex treatment were the timing of wound cleansing, the appearance of granulations, changes in the intensity of pain syndrome, the timing of the onset of epithelialization, the presence or absence of side effects of treatment, and the average bed-day. These parameters were also recorded.

The area of the purulent wound and CVU was assessed in both groups using the method of digital photography and

further computer calculation of the area of the defect. For this purpose, we used the LesionMeter program, which is an application for the iPhone. The LesionMeter program allows us to measure the area of neoplasms, skin lesions, or CVU of any shape without additional tools. Measurement of the CVU area began with photographing it against the background of a standard size plastic bank card. With the CVU contours outlined with a finger, the application subsequently calculated CVU area itself. A dynamic study of the wound area and CVU was performed upon admission, on Day 7 and Day 14 of treatment. The rate of CVU healing was calculated using the formula: Vs = (S-Sn) / t, according to the method of L.N. Popova (1942), where S is the CVU area before treatment, Sn is the CVU area for further measurements, t is the number of days between the measurements.[15]

The statistical analysis was performed using the statistical software Microsoft Excel 2010. The mean (M) and standard error of the mean (SEM) were calculated. Student's unpaired and paired t-tests were used to compare average values for data with normal distribution. A probability value of $P \leq 0.05$ was considered statistically significant.

## Results

All patients were examined according to the same program. In both groups, the clinical picture was characterized by a significant severity of all clinical signs. Ultrasound findings indicated a pronounced venous and functional insufficiency of the lower extremities. At the same time, in the MG patients, as a result of the application of the proposed complex treatment of CVU, the indicators of clinical effectiveness have significantly improved (Table 1).

***Table 1.***

***Therapeutic efficacy of complex treatment of CVU in CVI***

| Group | n | Timing of wound clearing (day) | Timing of the onset of granulations (day) | Timing of the onset of epithelialization (day) | Average bed-day (day) |
|---|---|---|---|---|---|
| MG | 52 | 6.17±0.24 | 9.52±0.33 | 13.06±0.37 | 16.89±0.42 |
| CG | 54 | 8.92±0.25 | 14.09±0.31 | 17.11±0.27 | 21.85±0.33 |
| *P*-value | | <0.05 | <0.05 | <0.05 | <0.05 |

We found that in MG the relief from inflammatory phenomena, reduction of edema and pain, occurred much faster. Patients subjectively noted an improvement in their well-being. The onset of the granulation phase of the wound process and wound cleansing also occurred faster in MG than in CG ($P<0.05$). In particular, in MG, the wound clearing was observed in 6.17±0.24 days versus 8.92±0.25 days in CG ($P<0.05$). The average timing of the onset of granulations in MG was 9.52±0.33 days versus 14.09±0.31 days in CG ($P<0.05$), and the average terms of the onset of epithelialization were 13.06±0.37 days and 17.11±0.27 days ($P<0.05$), respectively. All taken together, these improvements determined the possibility of reducing the average bed-day in the patients of MG to 16.89±0.42 days versus 21.85±0.33 days in CG ($P<0.05$).

The data obtained during the assessment of the repair processes correlate with the indicators of the CVU healing rate (Table 2). Thus, the average rate of CVU healing in MG during the first 14 days after the start of complex treatment using the proposed pharmacotherapy was significantly higher than in CG ($P<0.05$). In MG, the healing rate increased by more than 24.55% in comparison with CG.

***Table 2.***

***CVU healing rate during the first 14 days after the start of complex treatment***

| Group | Average rate of epithelialization ($cm^2$) in day | *P*-value |
|---|---|---|
| MG | 0.088±0.0062 | <0.05 |
| CG | 0.062±0.0043 | |

All of the above are illustrated by the following clinical case. A 64-year-old man presented to the Simferopol Central Regional Clinical Hospital for outpatient treatment with a diagnosis of "Varicose veins of the right lower extremity. CVI stage 3. Trophic ulcer of the right leg" (Fig.1). At the time of inspection, the area of the lower leg CVU was 4.10 cm². After 8 days of the treatment, the CVI area decreased to 3.59 cm². By Day 15 of treatment, a further decrease in the CVI area was noted to 2.87 cm². On Days 23, 30 and 35, the CVI area was 1.16 cm², 0.93 cm², and 0.79 cm², respectively (Fig.2).


***Fig. 1.*** *A 64-year-old man. Varicose veins of the right lower extremity. CVI stage 3. Trophic ulcer of the right leg. Day 1 of complex treatment.*

Since the compared groups of patients at the start of the study did not differ in clinical-anthropometric or biochemical parameters, or in the size of the wound surface, and since surgical treatment of CVI was a standard procedure and was

performed every other day by two surgeons, in accordance with the protocol, the differences in the rate of CVU healing can be attributed only to the effect of the proposed pharmacological correction in complex treatment.

***Fig. 2.*** *A 64-year-old man. Varicose veins of the right lower extremity. CVI stage 3. Trophic ulcer of the right leg. Day 14 of complex treatment.*

Given the diversity of the modern pharmacological market, the selection of effective combinations of drugs, as well as their use regimens for the treatment of CVU, remains relevant. Moreover, these approaches must have a high degree of safety for the patients and relative financial availability, and must also affect the maximum number of links in pathogenesis. Taking into account that under conditions of disturbed trophism in the wound the synthesis of tissue elements is extremely slowed down, it seems advisable to use medications that stimulate regeneration processes along with various methods aimed at improving trophism. From these positions, the proposed methods and methods of pharmacotherapy are optimal, effective, and safe treatment regimens in the complex treatment of complicated CVD forms.

After CVU healing, elective surgical interventions were performed, the purpose of which was to eliminate venous stasis and create hemodynamic prerequisites for the normalization of blood circulation in the tissues of the affected limbs. We used conventional slab phlebectomy to implement pathogenetically substantiated surgical correction of existing hemodynamic disorders, in order to eliminate pathological veno-venous refluxes and to exclude irreversibly transformed areas of the saphenous veins of the lower extremities from the bloodstream in 60.87% (in both groups) of patients with varicose veins.

For CVU patients with post-thrombotic syndrome, surgical treatment was performed on 16.2% of them. In this category of patients, a smooth course of the early postoperative period was observed. All patients noted an insignificant severity of pain in the operated limb, which made it possible to use only non-narcotic analgesics even on the first day after the operation and contributed to the early activation of patients. There were no wound complications in the postoperative period. Skin sutures were removed after 6-7 days. In all patients, the wounds healed by primary intention. Patients were discharged for outpatient treatment on days 7-10 under the supervision of a surgeon at the local polyclinic.

Of the 48 operated patients in MG, 14(29.16%) were examined in the late postoperative period (after 6 months and 1 year). No signs of CVU recurrence were found in any case. All patients noted a steady improvement in the quality of life.

Based on the results obtained, an algorithm for the complex treatment of patients with CVU was developed and proposed for use in clinical practice (Fig.3).

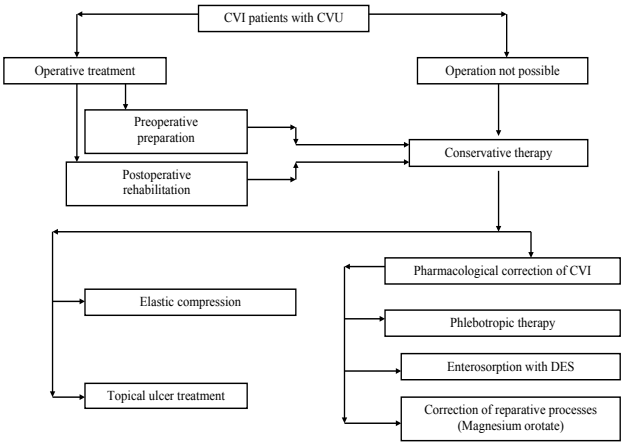


***Fig. 3.*** *Algorithm for complex treatment of CVI patients with CVU*

All of the above-mentioned therapeutic measures used in the complex allow us to effectively treat CVU and provide adequate preoperative preparation, as well as effective postoperative and medical-social rehabilitation of patients.

Thus, the complex treatment of CVU and purulent-necrotic wounds in CVI with the inclusion of the proposed methods of pharmacological correction has a sufficient clinical justification. The application of the proposed pharmacological correction may become a promising auxiliary method of treatment in patients with necrotic ulcerative lesions of the skin of venous origin. The effect of the proposed pharmacotherapy on the regeneration processes determines the possibility of additional inclusion of DHS and magnesium orotate in the treatment protocol for patients with CVU.

**In conclusion**, the use of the proposed method of drug correction in the complex treatment of CVU ensures the effectiveness of treatment, a reduction in the duration of inpatient treatment, and the reliability of rehabilitation in the postoperative period.

## Competing Interests

The authors declare that they have no competing interests.

## References

1. Shimanko A, Dibirov M, Zubritskiy V, Zemlyanoy A, Tsuranov S, Matveyev D, Shvidko V, Majorov A, Tyurin D. [Modern approach to treatment of venous trophic ulcers in patients with chronic diseases of lower extremities' veins]. Medicinskij Mestnik MVD. 2015;4(77):10-14. [Article in Russian].
2. Katorkin SE, Melnikov MA, Kravtsov PF, Zhukov

AA, Kushnarchuk MJ, Repin AA. [Efficiency of Layer Dermatolipectomy (Shave Therapy) in Complex Treatment of Patients with Lower Limbs Venous Trophic Ulcers]. Novosti Khirurgii. 2016;24(3):255-264. doi: 10.18484/2305-0047.2016.3.255. [Article in Russian].
3. Bogdanec LI, Smirnova ES, Vasil'ev IM. [Povyshenie effektivnosti lecheniya trofícheskih yazv venoznogo geneza]. Ambulatory Surgery: Hospital-Replacing Technologies. 2014;1-2:16-21. [Article in Russian].
4. Matveev SA, Stoyko YuM, Masayshvili KV, Karpyshev DS. [Ambulatory treatment of gerontological patients with venous trophic ulcers]. Bulletin of Pirogov National Medical & Surgical Center . 2014;9(3):16-19. [Article in Russian].
5. Alavi A, Sibbald RG, Phillips TJ, Miller OF, Margolis DJ, Marston W, Woo K, Romanelli M, Kirsner RS. What's new: Management of venous leg ulcers: Treating venous leg ulcers. J Am Acad Dermatol. 2016 Apr;74(4):643-64; quiz 665-6. doi: 10.1016/j.jaad.2015.03.059.
6. Sergeev NA, Shestakov MS, Fomina ED, Grishakov PI. [Venous trophic ulcers: diagnostics, conservative and complex treatment (literature review)]. Verhnevolzhskij medicinskij zhurnal. 2016;15(2):23-29. [Article in Russian].
7. Katorkin SE, Zhukov AA, Kushnarchuk MJ. [Combined treatment of vasotrophic ulcers in lower limbs chronic venous insufficiency]. Novosti Hirurgii. 2014;22(6):701-709. doi:10.18484/2305-0047.2014.6.701.[Article in Russian].
8. Wittens C, Davies AH, Bækgaard N, Broholm R, Cavezzi A, Chastanet S, de Wolf M, Eggen C, Giannoukas A, Gohel M, Kakkos S, Lawson J, Noppeney T, Onida S, Pittaluga P, Thomis S, Toonder I, Vuylsteke M, Esvs Guidelines Committee, Kolh P, de Borst GJ, Chakfé N, Debus S, Hinchliffe R, Koncar I, Lindholt J, de Ceniga MV, Vermassen F, Verzini F, Document Reviewers, De Maeseneer MG, Blomgren L, Hartung O, Kalodiki E, Korten E, Lugli M, Naylor R, Nicolini P, Rosales A. Editor's Choice - Management of Chronic Venous Disease: Clinical Practice Guidelines of the European Society for Vascular Surgery (ESVS). Eur J Vasc Endovasc Surg. 2015 Jun;49(6):678-737. doi: 10.1016/j.ejvs.2015.02.007.
9. Mikitin IL, Karapetyan GE, Kochetova LV, Yakimov SV, Pakhomova RA. [Modern view on treatment of trophic ulcers]. Kreativnaya Hirurgiya i Onkologiya. 2013;(4):108-112. doi:10.24060/2076-3093-2013-0-4-108-112. [Article in Russian].
10. Bilyayeva OO, Korzhyk NP, Myronov OM, Balinska MI, Yemets VV. [Role of enterosorpents in treatment of complicated varicose disease]. Klinichna Hirurgija. 2014;6:43-45. [Article in Ukrainian].
11. Ursova NI. [The role of enterosorbents in treatment of endogenous intoxication syndrome]. Voprosy Sovremennoi Pediatrii – Curent Pediatrics. 2012;11(6):26-31. doi: 10.15690/vsp.v11i6.489. [Article in Russian].
12. Kalinin RE, Suchkov IA, Pshennikov AS, Kamaev A.A, Isakov SA, Ryabkov AN. Application of Magnesium Drugs and Their Influence on the Indicators of Connective Tissue Dysplasia in Patients with Varicose Veins. Novosti Khirurgii. 2018;26(1):51-59. doi: 10.18484/2305-0047.2018.1.51
13. Hryvenko SH, Izosimov VV, inventors; Hryvenko SH, Izosimov VV, assignees. [The method of conservative treatment of varicose veins of the lower extremities]. Ukraine patent UA 89297. April 10, 2014. [In Ukrainian].
14. Dzjubanovs'kij IJa, Hryvenko SH, Izosimov VV, inventors; Dzjubanovs'kij IJa, Hryvenko SH, Izosimov VV, assignees. [The method of treating complicated varicose disease of the lower extremities]. Ukraine patent UA 112033. November 25, 2016 [In Ukrainian].
15. Popova LN. How the boundaries of the formed epidermis change during wound healing. Abstract of PhD Thesis. Voronezh, 1942. [In Russian].

International Journal of Biomedicine 11(1) (2021) 92-95
http://dx.doi.org/10.21103/Article11(1)_OA16

ORIGINAL ARTICLE

Population Genetics

INTERNATIONAL JOURNAL OF BIOMEDICINE

# The *FTO*, *PNPLA3* and *TM6SF2* Gene Polymorphisms and Genetic Predisposition to NAFLD in Yakut Population

Aleksandra T. Diakonova*; Khariton A. Kurtanov, PhD; Nadezhda I. Pavlova, PhD; Tuyara N. Aleksandrova

*Yakut Science Center of Complex Medical Problems*
*Yakutsk, the Republic of Sakha (Yakutia), Russia*

## Abstract

***The aim*** of our research was to study the distribution of alleles and genotypes of the *FTO* rs9939609 SNP, the *PNPLA3* rs738409 SNP, and the *TM6SF2* rs58542926 SNP in the Yakut population.

***Methods and Results***: A total of 85 DNA samples from the population were tested. An analysis of the frequency distribution of alleles and genotypes of the *FTO* rs9939609 SNP in the study group did not reveal significant differences. An analysis of the frequency distribution of alleles and genotypes of the *PNPLA3* rs738409 SNP revealed that in men and women the G allele and the homozygous GG genotype prevailed. The results of the analysis of the frequency distribution of alleles and genotypes of the *TM6SF2* rs58542926 SNP showed the predominance of individuals with the C allele (89% in men and 90% in women) with statistical significance in women.

***Conclusion***: The further studies with a larger sample size are required to detect the features of the distribution of alleles and genotypes of the *FTO* rs9939609 SNP and the *TM6SF2* rs58542926 SNP in that population. (**International Journal of Biomedicine. 2021;11(1):92-95.**)

**Key Words:** nonalcoholic fatty liver disease • single nucleotide polymorphism • genome-wide association study • Yakuts

**For citation**: Diakonova AT, Kurtanov KhA, Pavlova NI, Aleksandrova TN. The FTO, PNPLA3 and TM6SF2 Gene Polymorphisms and Genetic Predisposition to NAFLD in Yakut Population. International Journal of Biomedicine. 2021;11(1):92-95. doi:10.21103/Article11(1)_OA16

## Abbreviations

**bp**, base pairs; **NAFLD**, nonalcoholic fatty liver disease; **PNPLA3**, patatin-like phospholipase domain-containing protein 3; **SNP**, single nucleotide polymorphism; **TM6SF2**, transmembrane 6 superfamily member 2

## Introduction

A person's genetic predisposition determines the risk of developing NAFLD. However, not all at-risk individuals develop the disease, suggesting that most complex multifactorial diseases are the result of interactions between genes and the environment. The onset or severity of the disease may differ in individuals with the same genotype in different environmental conditions, or vice versa, confirming that the phenotype is a consequence of genotype-environmental interactions; diet, lifestyle, exposure to chemicals and toxins constitute the bulk of environmental risks. Most diseases of the modern lifestyle, such as diabetes, cardiovascular diseases, hypertension, and obesity, are usually transmitted by a multifactorial mode of inheritance. This term refers to a complex type of inheritance, which involves a combination of both genetic and other factors, including the environment.[1] Nonalcoholic fatty liver disease (NAFLD) is one of the most important complex and multifactorial lifestyle diseases. NAFLD initiates from extra fat storage in the liver and can advance to hepatitis, fibrosis, liver failure, and hepatocellular carcinoma. NAFLD is often associated with obesity, diabetes, and hyperlipidemia. The prevalence of the disease varies markedly in different populations. It ranges from 20% to 30% in Western countries,[2] from 20% to 30% in Europeans,[3] 8% to 9% in Japan,[4] and 25%-30% in India.[5] The overall

***Corresponding author:** Aleksandra T. Diakonova. Yakut Science Center of Complex Medical Problems. Yakutsk, the Republic of Sakha (Yakutia), Russia. E-mail: dyakonovaa@bk.ru*

prevalence of NAFLD in Asia has so far been estimated at 29.6%. Due to significant changes in lifestyle and dietary habits, NAFLD has become a major social health burden in China, with a prevalence of 18.2% in 2000-2006, 20.0% in 2007-2009, and 20.9% in 2010–2013. A recent meta-analysis found that the national prevalence of NAFLD in China reached 29.1%.[6]

Understanding genetic predisposition has been a major focus of recent research, in addition to changes in dietary habits and lifestyle modifications that have been shown to benefit patients with NAFLD and help better control the disease. [1] The GWAS identified several genes as a major genetic determinant for the predisposition to NAFLD. The association between SNPs in the fat mass and obesity-associated (*FTO*) gene and BMI and obesity has been confirmed in multiple populations.[7-13] Gerken et al.[14] showed that FTO shares sequence motifs with Fe(II)- and 2-oxoglutarate–dependent oxygenates, which allows it to alter DNA methylation and regulate gene transcription. The *FTO* gene encodes one of the lipolysis regulators, which is involved in the control of adipocyte differentiation, energy homeostasis, and leptin-independent appetite control. The FTO SNPs associated with adiposity are intronic and may exert functional effects through altered expression of FTO mRNA. According to the results of previous studies, the A allele of the *FTO* rs9939609 is associated with decreased lipolysis, impaired appetite control, and a lack of satiety after an adequate meal.[15-18] The phenotypic manifestation of the A allele of the *FTO* gene is overweight and obesity due to overeating,[18,19] which in turn is one of the most common risk factors for the development of NAFLD.

Molecular genetic studies have shown that the *PNPLA3* gene, located on the long arm of chromosome 22q13.31, is expressed in the membranes of hepatocytes and is responsible for intrahepatic lipid metabolism by coding for the synthesis of adiponutrin, a protein that regulates the activity of triacylglycerolipase in adipocytes. The most significant polymorphism in the *PNPLA3* gene is I148M (rs738409). The most prominent variant is the *PNPLA3* rs738409 [G], which is a nonsynonymous substitution of cytosine for guanine (C>G) that changes codon 148 from encoding isoleucine (I) to methionine (M) (I>M, I148M).[20,21] Wild-type (148I) *PNPLA3* has lipolytic activity towards triglycerides.[22,23] The 148M mutation leads to the development of macrovescicular steatosis.[22,23] In humans, the *PNPLA3* I148M mutation has been shown to influence not only intrahepatic remodeling but also reduces very low density lipoproteins (VLDL) secretion.[24] Recently, a study showed that carriers of the rs738409[G] allele have lower de novo lipogenesis as compared to non-carriers due to a reduction in liver SREBP1c mRNA levels.[25] However, the issue of the functional consequences of the I148M polymorphism is therefore still intensively debated.[26]

In 2014, the significance of rs58542926 in the transmembrane 6 superfamily member 2 (*TM6SF2*) gene in NAFLD was found for the first time.[27] The *TM6SF2* rs58542926 is a substitution of guanine by adenine in nucleotide 499, which leads to the replacement of glutamic acid by lysine in amino acid residue 167(E167K).[27] Recent studies have found that *TM6SF2* rs58542926 was a significant risk factor for the development of NAFLD.[28,29]

The aim of our research was to study the distribution of alleles and genotypes of the *FTO* rs9939609 SNP, the *PNPLA3* rs738409 SNP, and the *TM6SF2* rs58542926 SNP in the Yakut population.

## Materials and Methods

The study of the *FTO* rs9939609, SNP the *PNPLA3* rs738409 SNP, and the *TM6SF2* rs58542926 SNP was carried out in the Department of Molecular Genetics at YSC CMP. For the study, we used DNA samples from the collection of biomaterials of the YSC KP using the UNU "Genome of Yakutia" (reg. No. USU_507512). A total of 85 DNA samples from the population were tested.

The inclusion criteria for the study were Yakuts by ethnicity, living in Yakutia, without liver damage by chronic viral hepatitis. Exclusion criteria: autoimmune hepatitis, primary biliary cholangitis, primary sclerosing cholangitis, hereditary hemochromatosis, Wilson-Konovalov disease, and alcohol abuse (>30g/l).

Genomic DNA samples were isolated from peripheral blood lymphocytes using a commercial DNA kit, Excel Biotech (Yakutsk). The study SNPs were analyzed by PCR-RFLP reaction. The gene regions containing the polymorphic variants were amplified with standard pairs of primers produced by Biotech-Industry LLC (Moscow, Russia). The reaction mixture (25 μl) for PCR contained of forward and reverse primer (10 pmol/μl) (1μl) (Moscow, Russia), Dream Taq PCR master mix (12.5 μl), deionized water (9.5 μl), and DNA in the amount of 100μg/ml (1μl). A mixture for RFLP (20μL) consisted of amplificate (7μL), deionized water (10.9μL), restriction buffer (2μL), and restriction endunuclease Hpy188I (2 u.a.) for the *TM6SF2* gene, Zrm I (2 u.a.) for the gene *FTO,* and BstF5VI (2 e.a.) for the *PNPLA3* gene.

The temperature-time regime for PCR is optimized for amplification of this nucleotide sequence and is presented in Table 1.

***Table 1.***

***Conditions for PCR***

| Gene | Amplification | The length of the restriction fragments | PCR conditions |
|---|---|---|---|
| *TM6SF2* | 429 bp | CC–178 bp, 166 bp, 85 bp<br>TT–251, 178 bp<br>CT–251 bp, 178 bp, 166 bp, 85 bp | 1. 94 °C – 10 min<br>2. (94 °C – 1 min; 62 °C – 40 sec; 72 °C – 1 min) – 40 cycles<br>3. 72 °C – 10 min |
| *FTO* | 182 bp | AA–154 bp, 28 bp<br>AT–154 bp, 28 bp, 182 bp<br>TT–182 bp | 1. 95 °C – 4 min<br>2. (94 °C – 30 sec; 58 °C – 30 sec; 72 °C – 1 min) – 35 cycles<br>3. 72 °C – 10 min |
| *PNPLA3* | 333 bp | CC–200 bp, 133 bp<br>GC–333 bp, 200 bp, 133 bp<br>GG– 333 bp | 1. 95 °C – 5 min<br>2. (94 °C – 30 sec; 66 °C – 30 sec; 72 °C – 40 sec) – 37 cycles<br>3. 72 °C – 5 min |

PCR products were detected by horizontal electrophoresis in a 2% agarose gel plate with the addition of ethidium bromide, a specific intercalating fluorescent DNA (RNA) dye, using a standard Tris-acetate buffer at a field voltage of ~ 20V/cm for 30 minutes. RFLP products were detected by horizontal electrophoresis in 4% agarose gel stained with ethidium bromide using a standard Tris-acetate buffer at 120V for 1 hour.

Statistical analysis was performed using the Statistica 8.0 software package (Stat-Soft Inc., USA). The correspondence of the distributions of genotypes to the expected values at HWE and comparison of the frequencies of allelic variants/genotypes were performed using the chi-square test. A probability value of $P<0.05$ was considered statistically significant.

## Results and Discussion

An analysis of the frequency distribution of alleles and genotypes of the FTO rs9939609 SNP in the study group did not reveal significant differences (Table 2). An analysis of the frequency distribution of alleles and genotypes of the PNPLA3 rs738409 SNP revealed that in men and women the G allele and the homozygous GG genotype prevailed (Table 3). The results of the analysis of the frequency distribution of alleles and genotypes of the TM6SF2 rs58542926 SNP showed the predominance of individuals with the C allele (89% in men and 90% in women) with statistical significance in women (Table 4).

***Table 2.***

***Frequency distribution of alleles and genotypes of the FTO rs9939609 SNP in the study group***

| FTO | n | | Genotype, % | | | Allele, % | | $\chi^2$ | *P* |
|---|---|---|---|---|---|---|---|---|---|
| | | | AA | AT | TT | A | T | | |
| All | 85 | O | 4 | 30 | 66 | 19 | 81 | 0.012 | 0.912 |
| | | E | 4 | 30,5 | 65,5 | | | | |
| Woman | 63 | E | 13 | 27 | 60 | 26 | 74 | 5.748 | 0.0165 |
| | | E | 7 | 39 | 54 | | | | |
| Man | 22 | O | 4 | 32 | 64 | 20 | 80 | 0.011 | 0.917 |
| | | E | 4 | 32 | 64 | | | | |

*Note: O - observed; E - expected.*

***Table 3.***

***Frequency distribution of alleles and genotypes of the PNPLA3 rs738409 SNP in the study group***

| PNPLA3 | n | | Genotype, % | | | Allele, % | | $\chi^2$ | *P* |
|---|---|---|---|---|---|---|---|---|---|
| | | | CC | CG | GG | C | G | | |
| All | 85 | O | 14 | 33 | 53 | 31 | 69 | 4.274 | 0.0387 |
| | | E | 9 | 43 | 48 | | | | |
| Woman | 63 | O | 13 | 32 | 55 | 29 | 71 | 3.11 | 0.0778 |
| | | E | 8 | 41 | 51 | | | | |
| Man | 22 | O | 18 | 36 | 45 | 36 | 64 | 1.01 | 0.3149 |
| | | E | 13 | 46 | 40 | | | | |

The frequency of occurrence of the mutant alleles of the study SNPs in various populations, according to Ensembl.org, is presented in Table 5.

***Table 4.***

***Frequency distribution of alleles and genotypes of the TM6SF2 rs58542926 SNP in the study group***

| TM6SF2 | n | | Genotype, % | | | Allele, % | | $\chi^2$ | *P* |
|---|---|---|---|---|---|---|---|---|---|
| | | | CC | CT | TT | C | T | | |
| All | 85 | O | 84 | 12 | 4 | 89 | 11 | 12.187 | 0.0005 |
| | | E | 80 | 19 | 1 | | | | |
| Woman | 63 | O | 84 | 11 | 5 | 90 | 10 | 10.059 | 0.0015 |
| | | E | 80 | 18 | 1 | | | | |
| Man | 22 | O | 82 | 14 | 4 | 89 | 11 | 2.296 | 0.1297 |
| | | E | 79 | 20 | 1 | | | | |

***Table 5.***

***The frequency of occurrence of the mutant alleles (%) of the study SNPs in various populations, according to Ensembl.org***

| SNP | Mutant allele | Yakuts | Puerto Ricans | Peruvians | Finns | South Han Chinese |
|---|---|---|---|---|---|---|
| rs9939609 *FTO* | A | 19 | 36 | 8 | 39 | 14 |
| rs738409 *PNPLA3* | G | 69 | 32 | 72 | 17 | 38 |
| rs58542926 *TM6SF2* | T | 11 | 9 | 5 | 6 | 11 |

We previously found a high frequency of the *PNPLA3* (rs738409) [G] allele in the Yakut population (72%-73%).[30,31] The accumulation of triglycerides in hepatocytes, associated with the *PNPLA3* p.I148M variant, was probably an adaptation to a cold climate; this accumulation is not needed in the modern world, but leads to NAFLD among the Yakut population. As noted by many domestic and foreign researchers, carriers of the *PNPLA3* G allele are more susceptible to liver diseases (NAFLD, NASH) with a high risk of developing cirrhosis and hepatocellular carcinoma.[20]

Undoubtedly, further studies with a larger sample size are required to detect the features of the distribution of alleles and genotypes of the FTO rs9939609 SNP and the TM6SF2 rs58542926 SNP in that population.

## Competing Interests

The authors declare that they have no competing interests.

## References

1. Kumar A, Shalimar, Walia GK, Gupta V, Sachdeva MP. Genetics of nonalcoholic fatty liver disease in Asian populations. J Genet. 2019 Mar;98:29. PMID: 30945694.
2. Bellentani S, Scaglioni F, Marino M, Bedogni G. Epidemiology of non-alcoholic fatty liver disease. Dig Dis. 2010;28(1):155-61. doi: 10.1159/000282080.
3. Blachier M, Leleu H, Peck-Radosavljevic M, Valla DC, Roudot-Thoraval F. The burden of liver disease in Europe: a review of available epidemiological data. J Hepatol. 2013 Mar;58(3):593-608. doi: 10.1016/j.jhep.2012.12.005.
4. Kawaguchi T, Sumida Y, Umemura A, Matsuo K, Takahashi M, Takamura T, et al.; Japan Study Group of Nonalcoholic Fatty Liver Disease. Genetic polymorphisms of

the human PNPLA3 gene are strongly associated with severity of non-alcoholic fatty liver disease in Japanese. PLoS One. 2012;7(6):e38322. doi: 10.1371/journal.pone.0038322.
5. Amarapurkar D, Kamani P, Patel N, Gupte P, Kumar P, Agal S, et al. Prevalence of non-alcoholic fatty liver disease: population based study. Ann Hepatol. 2007 Jul-Sep;6(3):161-3.
6. Gu Z, Bi Y, Yuan F, Wang R, Li D, Wang J, et al. *FTO* Polymorphisms are Associated with Metabolic Dysfunction-Associated Fatty Liver Disease (MAFLD) Susceptibility in the Older Chinese Han Population. Clin Interv Aging. 2020 Aug 11;15:1333-1341. doi: 10.2147/CIA.S254740.
7. Scuteri A, Sanna S, Chen WM, Uda M, Albai G, Strait J, et al. Genome-wide association scan shows genetic variants in the FTO gene are associated with obesity-related traits. PLoS Genet. 2007l;3(7):e115. doi: 10.1371/journal.pgen.0030115.
8. Andreasen CH, Stender-Petersen KL, Mogensen MS, Torekov SS, Wegner L, Andersen G, et al. Low physical activity accentuates the effect of the FTO rs9939609 polymorphism on body fat accumulation. Diabetes. 2008 Jan;57(1):95-101. doi: 10.2337/db07-0910.
9. Do R, Bailey SD, Desbiens K, Belisle A, Montpetit A, Bouchard C, et al. Genetic variants of FTO influence adiposity, insulin sensitivity, leptin levels, and resting metabolic rate in the Quebec Family Study. Diabetes. 2008 Apr;57(4):1147-50. doi: 10.2337/db07-1267.
10. Grant SF, Li M, Bradfield JP, Kim CE, Annaiah K, Santa E, et al. Association analysis of the FTO gene with obesity in children of Caucasian and African ancestry reveals a common tagging SNP. PLoS One. 2008;3(3):e1746. doi: 10.1371/journal.pone.0001746.
11. Hinney A, Nguyen TT, Scherag A, Friedel S, Brönner G, Müller TD, et al. Genome wide association (GWA) study for early onset extreme obesity supports the role of fat mass and obesity associated gene (FTO) variants. PLoS One. 2007 Dec 26;2(12):e1361. doi: 10.1371/journal.pone.0001361.
12. Hubacek JA, Bohuslavova R, Kuthanova L, Kubinova R, Peasey A, Pikhart H, Marmot MG, Bobak M. The FTO gene and obesity in a large Eastern European population sample: the HAPIEE study. Obesity (Silver Spring). 2008 Dec;16(12):2764-6. doi: 10.1038/oby.2008.421.
13. Hunt SC, Stone S, Xin Y, Scherer CA, Magness CL, Iadonato SP, Hopkins PN, Adams TD. Association of the FTO gene with BMI. Obesity (Silver Spring). 2008 Apr;16(4):902-4. doi: 10.1038/oby.2007.126.
14. Gerken T, Girard CA, Tung YC, Webby CJ, Saudek V, Hewitson KS, et al. The obesity-associated FTO gene encodes a 2-oxoglutarate-dependent nucleic acid demethylase. Science. 2007;318(5855):1469-72. doi: 10.1126/science.1151710.
15. Speakman JR, Rance KA, Johnstone AM. Polymorphisms of the FTO gene are associated with variation in energy intake, but not energy expenditure. Obesity (Silver Spring). 2008 Aug;16(8):1961-5. doi: 10.1038/oby.2008.318.
16. Wardle J, Llewellyn C, Sanderson S, Plomin R. The FTO gene and measured food intake in children. Int J Obes (Lond). 2009 Jan;33(1):42-5. doi: 10.1038/ijo.2008.174.
17. den Hoed M, Westerterp-Plantenga MS, Bouwman FG, Mariman EC, Westerterp KR. Postprandial responses in hunger and satiety are associated with the rs9939609 single nucleotide polymorphism in FTO. Am J Clin Nutr. 2009 Nov;90(5):1426-32. doi: 10.3945/ajcn.2009.28053.
18. Tanofsky-Kraff M, Han JC, Anandalingam K, Shomaker LB, Columbo KM, Wolkoff LE, et al. The FTO gene rs9939609 obesity-risk allele and loss of control over eating. Am J Clin Nutr. 2009 Dec;90(6):1483-8. doi: 10.3945/ajcn.2009.28439.
19. Cecil JE, Tavendale R, Watt P, Hetherington MM, Palmer CN. An obesity-associated FTO gene variant and increased energy intake in children. N Engl J Med. 2008 Dec 11;359(24):2558-66. doi: 10.1056/NEJMoa0803839.
20. Romeo S, Kozlitina J, Xing C, Pertsemlidis A, Cox D, Pennacchio LA, et al. Genetic variation in PNPLA3 confers susceptibility to nonalcoholic fatty liver disease. Nat Genet. 2008 Dec;40(12):1461-5. doi: 10.1038/ng.257.
21. Xu R, Tao A, Zhang S, Deng Y, Chen G. Association between patatin-like phospholipase domain containing 3 gene (PNPLA3) polymorphisms and nonalcoholic fatty liver disease: a HuGE review and meta-analysis. Sci Rep. 2015 Mar 20;5:9284. doi: 10.1038/srep09284.
22. He S, McPhaul C, Li JZ, Garuti R, Kinch L, Grishin NV, Cohen JC, Hobbs HH. A sequence variation (I148M) in PNPLA3 associated with nonalcoholic fatty liver disease disrupts triglyceride hydrolysis. J Biol Chem. 2010 Feb 26;285(9):6706-15. doi: 10.1074/jbc.M109.064501.
23. Pirazzi C, Adiels M, Burza MA, Mancina RM, Levin M, Ståhlman M, et al. Patatin-like phospholipase domain-containing 3 (PNPLA3) I148M (rs738409) affects hepatic VLDL secretion in humans and in vitro. J Hepatol. 2012 Dec;57(6):1276-82. doi: 10.1016/j.jhep.2012.07.030.
24. Petit JM, Guiu B, Masson D, Duvillard L, Jooste V, Buffier P, et al. Specifically PNPLA3-mediated accumulation of liver fat in obese patients with type 2 diabetes. J Clin Endocrinol Metab. 2010 Dec;95(12):E430-6. doi: 10.1210/jc.2010-0814.
25. Cox AJ, Wing MR, Carr JJ, Hightower RC, Smith SC, Xu J, et al. Association of PNPLA3 SNP rs738409 with liver density in African Americans with type 2 diabetes mellitus. Diabetes Metab. 2011;37(5):452-5. doi: 10.1016/j.diabet.2011.05.001.
26. Dongiovanni P, Donati B, Fares R, Lombardi R, Mancina RM, Romeo S, Valenti L. PNPLA3 I148M polymorphism and progressive liver disease. World J Gastroenterol. 2013 Nov 7;19(41):6969-78. doi: 10.3748/wjg.v19.i41.6969.
27. Kozlitina J, Smagris E, Stender S, Nordestgaard BG, Zhou HH, Tybjærg-Hansen A, et al. Exome-wide association study identifies a TM6SF2 variant that confers susceptibility to nonalcoholic fatty liver disease. Nat Genet. 2014 Apr;46(4):352-6. doi: 10.1038/ng.2901.
28. Chen LZ, Xia HH, Xin YN, Lin ZH, Xuan SY. TM6SF2 E167K Variant, a Novel Genetic Susceptibility Variant, Contributing to Nonalcoholic Fatty Liver Disease. J Clin Transl Hepatol. 2015;3(4):265-70. doi: 10.14218/JCTH.2015.00023.
29. Li Y, Liu S, Gao Y, Ma H, Zhan S, Yang Y, Xin Y, Xuan S. Association of TM6SF2 rs58542926 gene polymorphism with the risk of non-alcoholic fatty liver disease and colorectal adenoma in Chinese Han population. BMC Biochem. 2019 Feb 6;20(1):3. doi: 10.1186/s12858-019-0106-3.
30. Kurtanov KA, Sydykova LA, Pavlova NI, Filippova NP, Dodokhov VV, Apsolikhova GA,et al. [Polymorphism of the adiponutrin gene (PNPLA3) in the indigenous inhabitants of the Republic of Sakha (Yakutia) with type 2 diabetes mellitus]. Almanac of Clinical Medicine. 2018;46(3):258-263. doi: 10.18786/2072-0505-2018-46-3-258-263. [Article in Russian].
31. Kurtanov KA, Pavlova NI, Diakonova AT, Sydykova LA, Aleksandrova TN, Borisova YP, Dodokhov VV. The structure of Haplotypes and Diplotypes in the *PNPLA3* gene in the Yakut Population International Journal of Biomedicine. 2020; 10(4):433-437.

International Journal of Biomedicine 11(1) (2021) 96-98
http://dx.doi.org/10.21103/Article11(1)_OA17

ORIGINAL ARTICLE

Histology and Cytology

INTERNATIONAL JOURNAL OF BIOMEDICINE

# Morphological Approach to the Study of the Dynamics of Changes in the Fibrous Structures of the Dermis in Dermotension

Lyubov A. Kopteva[1], Ekaterina S. Mishina[1*], Maria A. Zatolokina[1], Maxim V. Mnichovich[2], Elena S. Chernomortseva[1]

[1]*Kursk State Medical University, Kursk, Russia*
[2]*Research Institute of Human Morphology, Moscow, Russia*

## Abstract

***Background***: The method of dermotension is successfully used in surgical practice to close extensive defects or as a result of treating fractures using the Ilizarov apparatus. However, to obtain the desired result, surgeons often neglect the condition of the skin flap itself. In this regard, the purpose of our study was to study the dynamics of changes in fibrous structures in the dermis of the skin during dermotension.

***Methods and Results***: The material for the 14-day study was a skin flap of Wistar rats obtained after distraction with the Ilizarov apparatus. Analyzing the morphological picture of the state of the dermis after the study, we found a decrease in the thickness of both the epidermis and the dermis by 2.3 and 3.3 times, respectively. A decrease in the density of collagen structures of both types I and III was also noted.

***Conclusion***: The results obtained indicate the restructuring, first of all, of the fibrous component of the dermis, which consists in reparative-restorative processes, which must be taken into account when choosing the rate and duration of dermotension. **International Journal of Biomedicine. 2021;11(1):96-98.**)

**Key Words:** dermotension • fibrous skeleton • Ilizarov apparatus • skin • adaptive rearrangements

**For citation**: Kopteva LA, Mishina ES, Zatolokina MA, Mnichovich MV, Chernomortseva ES. Morphological Approach to the Study of the Dynamics of Changes in the Fibrous Structures of the Dermis in Dermotension. International Journal of Biomedicine. 2021;11(1):96-98. doi:10.21103/Article11(1)_OA17

## Introduction

As a material for alloplasty, skin is widely used in the treatment of various surgical pathologies. In such cases, the most widespread methods of dermotension are the Ilizarov apparatus or balloon methods.[1-5] The literature available to us contains mainly the results observed in clinical practice, and there are no data on morphological changes as a result of stretching.[6-9] In this regard, the aim of the work was to study the adaptive rearrangement of the fibrous skeleton of the rat dermis under conditions of dermotension.

***Corresponding author**: Ekaterina S. Mishina, PhD. Department of Histology, Embryology, and Cytology. Kursk State Medical University. Kursk, Russia. E-mail: katusha100390@list.ru*

## Materials and Methods

The material for this study was the skin of the anterior surface of the tibia of 30 laboratory animals, male Wistar rats, which 5 days after flexion osteoclasia of the tibia underwent tibia lengthening using the Ilizarov apparatus at a daily rate of 0.5 mm in 4 doses. The animals were removed from the experiment after 14 days of distraction. The skin of intact animals was examined as a control.

The experiments were performed in accordance with the norms for the humane treatment of animals, which are regulated by the International Guidelines of the Association for the Assessment and Accreditation of Laboratory Animal Care, and approved by the Regional Ethics Committee of Kursk State Medical University (Protocol No. 4 dated June 10, 2019).

A fragment of skin, 1×1cm in size, after fixation, was studied using light-optical microscopy (staining by the Mallory method) and a scanning electron microscopy (SEM). To determine the types of collagen, the preparations were stained with Sirius Red, and then examined in polarized light using an Altami Polar 2 polarizing microscope, at a magnification of ×100.

Statistical analysis was performed using the statistical software Microsoft Excel-2003. The normality of distribution of continuous variables was tested by the Kolmogorov-Smirnov test with the Lilliefors correction and Shapiro-Wilk test. For descriptive analysis, results are presented as mean±standard deviation (SD). The Mann-Whitney U-test was used to compare the differences between the two independent groups. A probability value of $P \leq 0.05$ was considered statistically significant.

## Results

The middle layer was stretched parallel to the direction of the tensile forces. Figure 1 presents the orientation of collagen and elastic fibers. In the papillary layer, there are mostly thin, branched collagen fibers that form delicate reticular structures. In the mesh layer, the fibers have a larger diameter. Along with large bundles of fibers, thinner reticular structures and a microfibrillar component were found around fibroblasts. At the border of the reticular layer and the hypodermis, destruction of the fibrous skeleton was observed. At the same time, active neocollagenesis was not observed. A significant number of microvessels, mainly of the capillary type, were observed in the papillary and outer part of the reticular dermis.

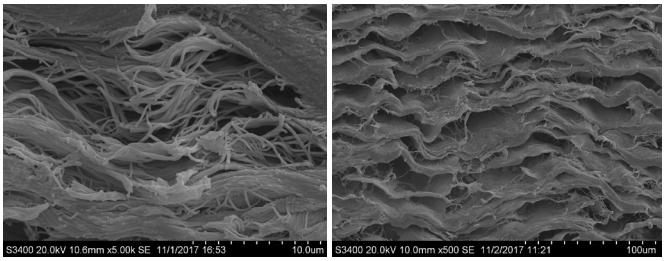


*A* *B*

***Fig. 1.*** *Micrograph of the skin after dermotension. A - Subepidermal layer of the dermis, SEM ×5000; B - Fibrous structures of the dermis with predominant anisotropy, SEM ×500*

When studying the cellular component, we determined the stimulating effect of mechanical action on the activation and proliferative activity of fibroblastic diferon. By the end of the period of distraction in the dermis, there was a significant increase in the number and density of all types of cells found in it, with the exception of fibrocytes. At the same time, under the conditions created during the period of distraction, both pronounced heteromorphism of the cells of the leading fibroblastic population and changes in the ratio of macrophages and mast cells were noted. An active macrophage reaction was observed in the papillary layer, less pronounced in the reticular layer of the skin. Mast cell accumulations were observed near microvessels (Table 1).

***Table 1.***

***Quantitative characteristics of the structural components of the skin***

| Parameters | Control | Dermotension | *P*-value |
|---|---|---|---|
| Thickness of epidermis | 30.5±0.3 μm | 12.90±0.10 μm | ≤ 0.05 |
| Thickness of dermis | 2.47±0.04 mm | 0.73±0.11 mm | ≤ 0.05 |
| Numerical density of cells per 1 $mm^2$ of the dermis | | | |
| Fibrocytes | 37.6±1.2 | 19.5±0.9 | ≤ 0.05 |
| Fibroblasts | 15.3±0.8 | 41.7±1.1 | ≤ 0.05 |
| Macrophages | 6.70±0.21 | 33.0±1.9 | ≤ 0.05 |
| Mast cells | 7.03±0.18 | 10.23±0.2 | ≤ 0.05 |

When studying photomicrographs of the skin of control animals after polarizing microscopy, we observed a large number of collagen fibers, predominantly type I, in the dermis (Figure 2A) and a fairly, uniformly high density of fibrous structures (Table 2).

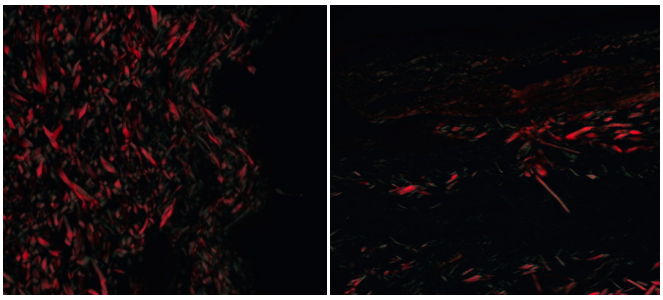

*A* *B*

***Fig. 2.*** *Micrograph of the dermis of rats. Polarizing microscopy. Sirius Red coloring, ×100; A - in the control group. B - with distraction.*

***Table 2.***

***Distribution of collagen types in the dermis of the skin***

| Group | Field area in 1000 pixels | Red PD (TIC) | Green PD (TIIIC) | Collagen ratio (I/III) |
|---|---|---|---|---|
| Control | 235.2±1.7 | 25.1±1.1 | 7.6±1.1 | 3.3±0.32 |
| Dermotension | 348.2±2.1* | 8.62±0.76* | 11.9±1.3 | 0.72±0.1* |
| *P*-value | ≤ 0.05 | ≤ 0.05 | > 0.05 | ≤ 0.05 |

*PD - pixel density; TIC- type I collagen; TIIIC- type III collagen*

In the study of sections stained with hematoxylin and eosin in the experimental animals with skin distraction, the density of collagen in the dermis had decreased sharply. When staining with Sirius Red in the dermis, we noted a sharp decrease in the density of collagen fibers (Figure 2B). Moreover, the main decrease in density occurred in the surface

layers of the dermis. When studying the same skin fragment in polarized light, we noted a very weak red glow and a slight green glow, which indicates a decrease in the density of type I collagen by 2.9 times and an increase in type III collagen by 1.5 times.

**In conclusion,** the revealed structural features of the dermis and analysis of reactive changes in various cell populations can serve as criteria for assessing the phasing of reparative processes developing under the created conditions, and can be taken into account when developing the staging and rate of stretching to justify their introduction into clinical practice.

## Competing interests

The authors declare that they have no competing interests.

## References

1. Martel II, Grebenyuk LA, Dolganova TI. [Elimination of an extensive femoral soft-tissue defect using dermotension according to Ilizarov technology]. ORTHOPAEDIC GENIUS. 2016;(4):109-113. [Article in Russian].
2. Bogosyan RA. [Expander dermotension – a new method for surgical filling of skin defects. Modern Technologies in Medicine]. 2011;2:31-34. [Article in Russian].
3. Filippova OV, Baindurashvili AG, Afonichev KA, Vashetko RV. [Surgical treatment of children with scars on the lower leg and in the area of Achilles tendon using expander dermatension]. Traumatology and Orthopaedics of Russia. 2015; 1 (75): 74-82. [Article in Russian].
4. Grebenyuk LA, Kobyzev AE, Grebenyuk EB, Ivliev DS. [The technique of determining plastic reserves of the skin in patients with orthopedic pathology]. Medical Science and Education of Ural. 2013; 14(4): 11-17. [Article in Russian].
5. Mishina ES, Omelyanenko NP, Kovalev AV, Volkov AV, Smorchkov MM. [Structural dynamics of the skin when modeling dermotension]. Annals of Plastic, Reconstructive, and Aesthetic Surgery. 2018;4:10. [Article in Russian].
6. Dąbrowska AK, Spano F, Derler S, Adlhart C, Spencer ND, Rossi RM. The relationship between skin function, barrier properties, and body-dependent factors. Skin Res Technol. 2018 May;24(2):165-174. doi: 10.1111/srt.12424.
7. Maiti R, Gerhardt LC, Lee ZS, Byers RA, Woods D, Sanz-Herrera JA, Franklin SE, Lewis R, Matcher SJ, Carré MJ. In vivo measurement of skin surface strain and sub-surface layer deformation induced by natural tissue stretching. J Mech Behav Biomed Mater. 2016 Sep;62:556-569. doi: 10.1016/j.jmbbm.2016.05.035.
8. Svoboda M, Bílková Z, Muthný T. Could tight junctions regulate the barrier function of the aged skin? J Dermatol Sci. 2016 Mar;81(3):147-52. doi: 10.1016/j.jdermsci.2015.11.009.
9. Dibirov M, Gadzhimuradov R, Koreiba K, Minabutdinov A, Biomedical Technologies in the Treatment of Skin and Soft Tissue. Defects in Patients with Diabetic Foot Syndrome. International Journal of Biomedicine. 2016;6(1):41-45.

IJBM

INTERNATIONAL JOURNAL OF BIOMEDICINE

# Instructions for Authors

**International Journal of Biomedicine (IJBM)** publishes peer-reviewed articles on the topics of basic, applied, and translational research on biology and medicine. International Journal of Biomedicine welcomes submissions of the following types of paper: Original articles, Reviews, Perspectives, Viewpoints, and Case Reports.

All research studies involving animals must have been conducted following animal welfare guidelines such as *the National Institutes of Health (NIH) Guide for the Care and Use of Laboratory Animals*, or equivalent documents. Studies involving human subjects or tissues must adhere to the *Declaration of Helsinki and Title 45, US Code of Federal Regulations, Part 46, Protection of Human Subjects*, and must have received approval of the appropriate institutional committee charged with oversight of human studies. Informed consent must be obtained.

**Pre-submissions**

Authors are welcome to send an abstract or draft manuscript to obtain a view from the Editor about the suitability of their paper. Our Editors will do a quick review of your paper and advise if they believe it is appropriate for submission to our journal. It will not be a full review of your manuscript.

**Manuscript Submission**

Manuscript submissions should conform to the guidelines set forth in the Recommendations for the Conduct, Reporting, Editing and Publication of Scholarly Work in Medical Journals (ICMJE Recommendations), available from www.ICMJE.org.

Original works will be accepted with the understanding that they are contributed solely to the Journal, are not under review by another publication, and have not previously been published except in abstract form.

All manuscripts must be submitted through the International Journal of Biomedicine`s online submission system (www.ijbm.org/submission.php). Manuscripts must be typed, double-spaced using a 14-point font, including references, figure legends, and tables. Leave 1-inch margins on all sides. Assemble the manuscript in this order: Title Page, Abstract, Key Words, Text (Introduction, Methods, Results, and Discussion), Acknowledgments, Sources of Funding, Disclosures, References, Tables, Figures, and Figure Legends. References, figures, and tables should be cited in numerical order according to first mention in the text.

The preferred order for uploading files is as follows: Cover letter, Full Manuscript PDF (PDF containing all parts of the manuscript including references, legends, figures and tables), Manuscript Text File (MS Word), Figures (each figure and its corresponding legend should be presented together), and Tables. Files should be labeled with appropriate and descriptive file names (e.g., SmithText.doc, Fig1.eps, Table3.doc). Text, Tables, and Figures should be uploaded as separate files. (Multiple figure files can be compressed into a Zip file and uploaded in one step; the system will then unpack the files and prompt the naming of each figure. See www.WinZip.com for a free trial.)

Authors who are unable to provide an electronic version or have other circumstances that prevent online submission must contact the Editorial Office prior to submission to discuss alternate options (editor@ijbm.org).

**Cover Letter**

The cover letter should be saved as a separate file for upload. In it, the authors should (1) state that the manuscript, or parts of it, have not been and will not be submitted elsewhere for publication; (2) state that all authors have read and approved the manuscript; and (3) disclose any financial or other relations that could lead to a conflict of interest. If a potential conflict exists, its nature should be stated for each author. When there is a stated potential conflict of interest a footnote will be added indicating the author's equity interest in or other affiliation with the identified commercial firms.

The corresponding author should be specified in the cover letter. All editorial communications will be sent to this author. A short paragraph telling the editors why the authors think their paper merits publication priority may be included in the cover letter.

**Types of articles**

Original articles

Original articles present the results of original research. These manuscripts should present well-rounded studies reporting innovative advances that further knowledge about a topic of importance to the fields of biology or medicine. These can be submitted as either a full-length article (no more than 6,000 words, 4 figures, 4 tables) or a Short Communication (no more than 2,500 words, 2 figures, 2 tables). An original

article may be Randomized Control Trial, Controlled Clinical Trial, Experiment, Survey, and Case-control or Cohort study.

Case Reports

Case reports describe an unusual disease presentation, a new treatment, a new diagnostic method, or a difficult diagnosis. The author must make it clear what the case adds to the field of medicine and include an up-to-date review of all previous cases in the field. These articles should be no more than 5,000 words with no more than 6 figures and 3 tables. Case Reports should consist of the following headings: Abstract (no more than 100 words), Introduction, Case Presentation (clinical presentation, observations, test results, and accompanying figures), Discussion, and Conclusions.

Reviews

Reviews analyze the current state of understanding on a particular subject of research in biology or medicine, the limitations of current knowledge, future directions to be pursued in research, and the overall importance of the topic. Reviews could be non-systematic (narrative) or systematic. Reviews can be submitted as a Mini-Review (no more than 2,500 words, 3 figures, and 1 table) or a long review (no more than 6,000 words, 6 figures, and 3 tables). Reviews should contain four sections: Abstract, Introduction, Topics (with headings and subheadings, and Conclusions and Outlook.

Perspectives

Perspectives are brief, evidenced-based and formally structured essays covering a wide variety of timely topics of relevance to biomedicine. Perspective articles are limited to 2,500 words and usually include ≤10 references, one figure or table. Perspectives contain four sections: Abstract, Introduction, Topics (with headings and subheadings), Conclusions and Outlook.

Viewpoints

Viewpoint articles include academic papers, which address any important topic in biomedicine from a personal perspective than standard academic writing. Maximum length is 1,200 words, ≤70 references, and 1 small table or figure.

## Manuscript Preparation

### Title Page

The first page of the manuscript (title page) should include (1) a full title of the article, (2) a short title of less than 60 characters with spaces, (3) the authors' names, academic degrees, and affiliations, (4) the total word count of the manuscript (including Abstract, Text, References, Tables, Figure Legends), (5) the number of figures and tables, and (6) the name, email address, and complete address of corresponding author.

Disclaimers. An example of a disclaimer is an author's statement that the views expressed in the submitted article are his or her own and not an official position of the institution or funder.

### Abstract

The article should include a brief abstract of no more than 200 words. Limit use of acronyms and abbreviations. Define at first use with acronym or abbreviation in parentheses. The abstract should be structured with the following headings: Background, Methods and Results, and Conclusions. The Background section should describe the rationale for the study. Methods and Results should briefly describe the methods and present the significant results. Conclusions should succinctly state the interpretation of the data. Authors should supply a list of up to four key words not appearing in the title, which will be used for indexing. The key words should be listed immediately after the Abstract. Use terms from the Medical Subject Headings (MeSH) list of Index Medicus when possible.

### Main text in the IMRaD format

Introduction should describe the purpose of the study and its relation to previous work in the field; it should not include an extensive literature review.

Methods should be concise but sufficiently detailed to permit repetition by other investigators. Previously published methods and modifications should be cited by reference. A subsection on statistics should be included in the Methods section.

Results should present positive and relevant negative findings of the study, supported when necessary by reference to Tables and Figures.

Discussion should interpret the results of the study, with emphasis on their relation to the original hypotheses and to previous studies. The importance of the study and its limitations should also be discussed.

The IMRaD format does not include a separate Conclusion section. The conclusion is built into the Discussion. More information on the structure and content of these sections can be found in the Recommendations for the Conduct, Reporting, Editing and Publication of Scholarly Work in Medical Journals (ICMJE Recommendations), available from www.ICMJE.org.

### Acknowledgments, Sources of Funding, and Disclosures

***Acknowledgments*** : All contributors who do not meet the criteria for authorship should be listed in an acknowledgments section. Examples of those who might be acknowledged include a person who provided purely technical help, writing assistance, or a department chairperson who provided only general support. Authors should declare whether they had assistance with study design, data collection, data analysis, or manuscript preparation. If such assistance was available, the authors should disclose the identity of the individuals who provided this assistance and the entity that supported it in the published article.

***Sources of Funding:*** All sources of financial support for the study should be cited on the title page, including federal or state agencies, nonprofit organizations, and pharmaceutical or other commercial sources.

***Disclosure and conflicts of interest:*** All authors must disclose any financial or other relations that could lead to a conflict of interest. If a potential conflict exists, its nature should be stated for each author. All sources of financial support for the study should be cited, including federal or state agencies, nonprofit organizations, and pharmaceutical or other commercial sources. Please use ICMJE Form for Disclosure of Potential Conflicts of Interest (http://www.icmje.org/conflicts-of-interest/).

### References

References should follow the standards summarized in the NLM's International Committee of Medical Journal Editors (ICMJE) Recommendations for the Conduct, Reporting,

Editing and Publication of Scholarly Work in Medical Journals: Sample References webpage (www.nlm.nih.gov/bsd/uniform_requirements.html) and detailed in the NLM's Citing Medicine, available from www.ncbi.nlm.nih.gov/books/NBK7256/. MEDLINE abbreviations for journal titles (www.ncbi.nlm.nih.gov/nlmcatalog/journals) should be used. The first six authors should be listed in each reference citation (if there are more than six authors, "et al" should be used following the sixth). Periods are not used in authors' initials or journal abbreviations. Examples of journal reference style:

*Journal Article:* Serruys PW, Ormiston J, van Geuns RJ, de Bruyne B, Dudek D, Christiansen E, et al. A Polylactide Bioresorbable Scaffold Eluting Everolimus for Treatment of Coronary Stenosis: 5-Year Follow-Up. J Am Coll Cardiol. 2016;67(7):766-76. doi: 10.1016/j.jacc.2015.11.060.

*Book:* Murray PR, Rosenthal KS, Kobayashi GS, Pfaller MA. Medical Microbiology. 4th ed. St. Louis: Mosby; 2002.

*Chapter in Edited Book:* Meltzer PS, Kallioniemi A, Trent JM. Chromosome alterations in human solid tumors. In: Vogelstein B, Kinzler KW, editors. The Genetic Basis of Human Cancer. New York: McGraw-Hill; 2002:93–113.

References should be numbered consecutively in the order in which they are first mentioned in the text. Identify references in text, tables, and legends by Arabic numerals in parentheses and listed at the end of the article in citation order.

**Tables**

Tables should be comprehensible without reference to the text and should not be repetitive of descriptions in the text. Every table should consist of two or more columns; tables with only one column will be treated as lists and incorporated into the text. All tables must be cited in the text and numbered in order of appearance. Tables should include a short title. Place explanatory matter in footnotes, not in the heading. Explain all nonstandard abbreviations in footnotes, and use symbols to explain information if needed. Each table submitted should be double-spaced, each on its own page. Each table should be saved as its own file as a Word Document. Explanatory matter and source notations for borrowed tables should be placed in the table footnote.

**Figures and Legends**

All illustrations (line drawings and photographs) are classified as figures. All figures should be cited in the text and numbered in order of appearance. Figures should be provided in .tiff, .jpeg or .eps formats. Color images must be at least 300 dpi. Gray scale images should be at least 300 dpi. Line art (black and white or color) and combinations of gray scale images and line art should be at least 1,000 dpi. The optimal size of lettering is 12 points. Symbols should be of a similar size. Figures should be sized to fit within the column (86 mm) or the full text width (180 mm). Line figures must be sharp, black and white graphs or diagrams, drawn professionally or with a computer graphics package. Legends should be supplied for each figure and should be brief and not repetitive of the text. Any source notation for borrowed figures should appear at the end of the legend. Figures should be uploaded as individual files.

**Units of Measurement**

Measurements of length, height, weight, and volume should be reported in metric units (meter, kilogram, or liter) or their decimal multiples. Temperatures should be in degrees Celsius. Blood pressures should be in millimeters of mercury. All measurements must be given in SI or SI-derived units. Drug concentrations may be reported in either SI or mass units, but the alternative should be provided in parentheses where appropriate.

**Style and Language**

The journal accepts manuscripts written in English. Spelling should be US English only. The language of the manuscript must meet the requirements of academic publishing. Reviewers may advise rejection of a manuscript compromised by grammatical errors. Non-native speakers of English may choose to use a copyediting service.

**Abbreviations and Symbols**

Use only standard abbreviations; use of nonstandard abbreviations can be confusing to readers. Avoid abbreviations in the title of the manuscript. The spelled-out abbreviation followed by the abbreviation in parenthesis should be used on first mention unless the abbreviation is a standard unit of measurement.

Drugs should be referred to by their generic names. If proprietary drugs have been used in the study, refer to these by their generic name, mentioning the proprietary name, and the name and location of the manufacturer, in parentheses.

**Permissions**

To use tables or figures borrowed from another source, permission must be obtained from the copyright holder, usually the publisher. Authors are responsible for applying for permission for both print and electronic rights for all borrowed materials and are responsible for paying any fees related to the applications of these permissions. This is necessary even if you are an author of the borrowed material. It is essential to begin the process of obtaining permission early, as a delay may require removing the copyrighted material from the article. The source of a borrowed table should be noted in a footnote and of a borrowed figure in the legend. It is essential to use the exact wording required by the copyright holder. A copy of the letter granting permission, identified by table or figure number, should be sent along with the manuscript. A permission request form is provided for the authors use in requesting permission from copyright holders.

**Open Access Policy**

All articles published by International Journal of Biomedicine are made freely and permanently accessible online immediately upon publication, without subscription charges or registration barriers. Articles published under an IMRDC user license are protected by copyright and may be used for non-commercial purposes. A copy of the full text of each Open Access article is archived in an online repository separate from the journal. The International Journal of Biomedicine's articles are archived in Scientific Electronic Library (Russian Science Citation Index). The authors can also self-archive the final publisher's version/PDF on personal website, departmental website, institutional repository with a link to publisher version.

Users may access, download, copy, translate, text and data mine (but may not redistribute, display or adapt) the articles for non-commercial purposes provided that users cite the article using an appropriate bibliographic citation (i.e. author(s), journal, article title, volume, issue, page numbers, DOI and the link to the definitive published PDF version on www.ijbm.org).

**Article Processing Charges**

When a paper is accepted for publication, the author is issued an invoice for payment of Article Processing Charge (APC). APC can be paid by the author or on their behalf, for example, by their institution or funding body.

APC helps IMRDC recover the costs of publication—including peer review management, production of the journal printed version, and online hosting and archiving, as well as inclusion in citation databases, enabling electronic citation in other journals that are available electronically. IJBM publishes all content Open Access and makes the content freely available online for researchers and readers.

IJBM charges a processing fee of $100 per printed black and white journal page and $200 per printed page of color illustrations. IJBM charges a processing fee of $85 per page in the case of online-only publications. For online-only publications, all illustrations submitted in color will be published in color online, at no cost to the author.

Under IJBM's existing policy, certain categories of authors are eligible for a discount. The amount of discount depends on factors such as country of origin, position of the author in the institute and quality and originality of the work. Young researchers and first time authors may also qualify for a discount. To apply for a discount, please contact our office using the 'Contact Us' page or send email to the Publisher (editor@ijbm.org) with the following information:

- Your name and institution with full address details
- Reason for applying for a waiver
- Title of your paper
- Country of residence of any co-authors.

**Page Proofs**

Page proofs are sent from the Publisher electronically and must be returned within 72 hours to avoid delay of publication. Generally, peer review is completed within 3-4 weeks and the editor's decision within 7-10 days of this. It is therefore very rare to have to wait more than 6 weeks for a final decision.

**IMRDC Author Services**

If you need help preparing a manuscript for submission, our publisher, IMRDC, offers a range of editorial services for a fee, including Advanced Editing and Translation with Editing. Please note that use of IMRDC Author Services does not guarantee acceptance of your manuscript.

It is important to note that when citing an article from IJBM, the correct citation format is **International Journal of Biomedicine.**